

**THE ROLE OF HYPOXIA INDUCIBLE FACTORS 1 AND 2 IN COBALT-INDUCED LUNG
INFLAMMATION AND DEVELOPMENT OF LUNG IMMUNITY**

By

Steven Paul Proper

A DISSERTATION

**Submitted to
Michigan State University
in partial fulfillment of the requirements
for the degree of**

**Biochemistry & Molecular Biology - Environmental Toxicology - Doctor of
Philosophy**

2013

ABSTRACT

THE ROLE OF HYPOXIA INDUCIBLE FACTORS 1 AND 2 IN COBALT-INDUCED LUNG INFLAMMATION AND DEVELOPMENT OF LUNG IMMUNITY

By

Steven Paul Proper

Cobalt is a transition metal utilized frequently in industry for the production of alloys, such as tungsten carbide. Human exposures to cobalt result mostly from workers inhaling cobalt-containing dusts. Many of these workers develop hard metal lung disease (HMLD or “cobalt lung”). Cobalt has been shown to be the necessary component in tungsten carbide dust to cause HMLD, though the mechanism is largely unknown. Interestingly, cobalt is a well-known hypoxia mimic and activates hypoxia-inducible factor (HIF)-mediated signaling. Our previous studies using a doxycycline inducible, lung epithelial-specific knockout of HIF1 α showed a switch from neutrophilic to eosinophilic recruitment during cobalt-induced inflammation, suggesting a role for epithelial HIF1 α in modulating the immune response of the lung. Little is known, however, about the role of HIF2 α in cobalt-induced lung injury or the possible overlap of HIF1 α and HIF2 α in this context. With this in mind, several experiments have been performed to elucidate the mechanism of HIF1 α -deficient induced eosinophilia and the role of HIF1 α and HIF2 α in cobalt-induced lung inflammation.

To characterize the mechanism of change in cobalt-induced inflammatory response in the HIF1 α -deficient mice, several experiments were performed, including flow cytometry of

resident lung immune cells, different temporal HIF1 α deletions, use of specific pharmacologic inhibitors of the suspected effector pathway of NF- κ B and the protective pathway of adenosine receptor A2B (Adora2b). These studies revealed that cobalt-treated HIF1 α -deficient mice produced more GATA3+ T-helper cells, confirming that the eosinophilia involved a T-helper type 2 (T_H2) response. Also, inducing the HIF1 α deletion in the early postnatal time period (P4-14), and not the adult (P32 onward) was required in establishing a predisposition for eosinophilic inflammation. Adora2b exerts protective effects on inflamed tissues, and inhibition of this receptor prior to cobalt dosing decreased the eosinophilia seen in HIF1 α -deficient mice to control levels, suggesting a role for adenosine signaling in promoting eosinophilic inflammation. Use of the proteasome inhibitor TCH013, thought to selectively inhibit NF- κ B, immediately prior to cobalt dosing, was ineffective in altering the expected eosinophilia. Overall these data imply that HIF1 α in alveolar epithelial type II and Club (Clara) cells plays a vital role in establishing the lung's immune environment early in postnatal lung development.

HIF2 α -deficient mice treated with cobalt display eosinophilia which peaks at the 14 day time point, later than eosinophilia observed at 2-5 days in HIF1 α -deficient mice. When mice lose both HIF1 α and HIF2 α by recombination, results are similar to the HIF1 α -deficient mice at 5 days, suggesting that the effects of HIF1 α loss are more important in driving earlier eosinophilia. Gene expression, histopathological analyses and cytokine profiling of lungs showed increases in classic T_H2 markers correlated with eosinophilic inflammation. All together these data show that both HIF1 α and HIF2 α are likely involved in post-natal development of proper immune responses to cobalt-induced lung inflammation.

Copyright by
STEVEN PAUL PROPER
2013

ACKNOWLEDGEMENTS

I would first like to thank my mentor, Dr. John J. LaPres. When I arrived at MSU in 2006 I was very interested in his lab's research, and after a rotation I was relieved that he was willing to take me as his first DO-PhD student. Over the years he has been incredibly understanding when medical school, clinical rotations, commuting or major life events demanded my time. John has provided a supportive learning environment while challenging me to expand my skill set and has taught me to think more clearly about the literature, my experiments, writing and presentations. His door was always open, and I have enjoyed our many chats over a quick lunch in his office during an incubation step. Sometimes it was research, other times music and movie quotes. I am eternally grateful for the guidance he has provided me.

I am immensely appreciative for my committee members Dr. Jack R. Harkema, Dr. Timothy Zacharewski, Dr. Eric Hegg, and Dr. William (Bill) Henry who have all played a significant role in my research by providing valuable guidance and insightful comments during our meetings and discussions. I would especially like to thank Jack Harkema for providing a wealth of knowledge and collaboration regarding toxicologic pathology and the art of histopathology, his incredibly helpful manuscript reviews and also for providing additional mentorship to me during conferences.

A huge debt of gratitude is owed to the DO-PhD Program, especially Dr. J. Justin McCormick and Bethany Heinlen for their unwavering support, advocacy and guidance since I joined the program in 2006. I have enjoyed watching them advance the profile of the DO-PhD Program at MSU by enhanced programming, training, and communication among the many

involved departments at MSU, all for the benefit of the students. I am grateful and proud to have been given an opportunity to be in this program.

I would like to thank the Biochemistry & Molecular Biology (BMB) Program, especially Dr. Tom Sharkey (Dept. Chair), Dr. John L. Wang (Graduate Recruitment Director) and Dr. Jon M. Kaguni (Graduate Student Director) for accepting me into their program and their years of support and guidance afterwards. They have been especially helpful for me as I navigated the unique schedule of the DO-PhD Program through the BMB Department. Sincere thanks go out to all BMB Department staff for their assistance over the years, especially Jessica Lawrence, Teresa Vollmer, Melinda Kochenderfer, Pappan (Kaillathe) Padmanabhan, Laurie Secord, Billy Yang, Carol Vanderjagt, Ron Norris and Joyce Robinson. I must also thank Joe Leykam and all the past members of the RTSF for their assistance.

Furthermore, I would like to thank the Center for Integrative Toxicology and the Environmental and Integrative Toxicological Sciences (EITS) Program, especially Dr. Robert Roth and Dr. Norbert Kaminski for allowing me the opportunity to gain expertise in the area of Toxicology as a second PhD major while at MSU. Their support has been instrumental in my training in toxicology, and has definitively set the course of my research interests in the future. I am also grateful for the help of Amy Swagart, Kasey Baldwin and Lauren St John during my time in the EITS Program.

Importantly, I owe a huge debt of gratitude to all the members of the LaPres Lab who have helped directly with my research, especially Krista K. Greenwood for her immense amount of time spent on animal work, as well as Nathan Downing, Corey Cook and Christian Merrill. I

also must thank Dr. Yogesh Saini for creating the mouse strains that I have used and for his excellent training in animal techniques and collaboration since his graduation from MSU. I also want to thank current and past LaPres lab members for their friendship and creating a fun atmosphere in the lab, including Hye Jin Hwang, Dr. Dorothy Tappenden, Dr. Scott G. Lynn, Dr. Kyunghye Burkitt, Dr. Ajith Vengellur and Dr. KangAe Lee.

I especially would like to thank all the members of the Harkema lab for their countless contributions to my studies and pathological analyses, especially Lori Bramble, Ryan Lewandowski, Dennis Shubitowski and Dr. Christina Brandenberger. I also would like to thank Dr. James Wagner and Dr. Daven Jackson-Humbles for their assistance in functional airway analyses and expertise. I wish to thank members of the Schutte lab including Youssef Kousa, Arianna Smith and Tamer Mansour for assistance and training in immunofluorescence and mouse techniques. I also want to thank Dr. Stephen Carey for his mentorship these last few years. I am indebted to the MSU Histopathology lab, especially Amy Porter and Kathy Joseph for all their help over the years with my histology, teaching me new skills and helping with all my puzzles. Further, I am very thankful to ULAR, especially Don Herrington and Ken Ledford for all their work in caring for our mice.

I wish to express my sincerest gratitude to my former mentors Dr. Deborah Keil and Dr. Ray Wells for encouraging me to pursue and continue research, and to all the teachers over the years who have inspired in me the wonder of science and the satisfaction of learning, especially Dr. Ali Zand, Dr. Stacey Seeley, Dr. Pat Atkinson, Dr. Daryl Doyle and Dr. Judy Harwood.

I sincerely wish to thank all of my fellow graduate students and close friends – I appreciate your empathy, humor and support during the stressful times, and I value deeply the friendships we have made. Of special note are Nick Tebeau, Cherie and Sean Kifer, Tyler and Lisa Voss, Michelle Manente Angrish and Krishan Angrish, Noshir Amaria, Nathan and Christina Schuldt, Tony Brandau and Shanti Virupannavar Brandau, Eric Carter and Julie Brownell Carter, Dustin and Maria Carver, Chad Shultz, Eric Schauburger, Josph Prinsen, Igor Korolev, Hae Young Hawong, Youssef Kousa, Dionisia Quiroga, Tyrell Simkins, Darin Quach, Paul Beach, Ania Kopec, Agnes Forgacs, Peer Karmaus and Rupinder Sayal.

I wish to thank my family for all their love and support, especially my parents, Doug and Linda, for always believing in me. I want to thank my brother Chris and his wife Deb, my parents-in-law John and Jeannine Bauer, my brothers-in-law Ryan and Zach Bauer, John and Keri Reigger and Wayne Proper for all their support as well.

Most importantly, I wish to thank my wife Alexis for her constant support, patience and understanding these many years. She has always been there for me, and I could not have done this without her. This is a special year for us because we welcomed our son Jamie Russell into the world November 30th. His smiles and laughter are a bright spot in our life, and we are very happy that he is here with us.

No meaningful work in life is done (or possible) alone. Thank you all!

TABLE OF CONTENTS

LIST OF TABLES	xii
LIST OF FIGURES	xiii
KEY TO ABBREVIATIONS AND SYMBOLS	xvii
CHAPTER 1 - INTRODUCTION AND SPECIFIC AIMS	1
Oxygen – historical and biological significance	2
Review of lung anatomy, physiology and development	4
Premature birth, supplemental O ₂ , bronchopulmonary dysplasia and asthma	14
Immune mechanisms in the lung	16
Innate immunity	16
Adaptive immunity	23
Role of T cells in lung defense	23
T-helper type 1 (T _H 1) response	24
T-helper type 2 (T _H 2) response	26
Other T-cell responses	27
Mechanisms of lung neutrophilia and eosinophilia	27
Epithelial-immune crosstalk in inflammatory responses	30
Alveolar epithelial type II (A ₂ TEC) cells and immunity	31
The Hygiene Hypothesis	31
Normoxia, hypoxia and oxygen sensing mechanisms	33
Hypoxia Signaling	36
Hypoxia inducible factors	36
HIFs in lung inflammation	43
Other hypoxia-responsive signaling pathways in lung inflammation	45
Table 2. Non-HIF hypoxia-responsive transcription factors (modified from [216]).	46
Nuclear factor kappa B (NF-κB)	47
Purinergic (adenosine) receptors	48
Cobalt	52
Occurrence and uses	52
Toxicity	53
Hard metal lung disease	53
Role of HIFs in cobalt toxicity	55
Hypotheses and Specific Aims	56
CHAPTER 2 – MATERIALS AND METHODS	57
Description of mice	58
Doxycycline treatment and animal husbandry	62
Cobalt exposure	65

PSB1115 exposure	65
TCH013 exposure	66
LPS exposure	66
Hyperoxia exposure	66
Necropsy, tissue harvesting and processing	68
Histopathology and immunohistochemistry	68
Gene expression analysis by qRT-PCR	69
Cytokine bead array	72
Flow cytometry of lung immune cells	72
Statistical analytical methods	73
CHAPTER 3 – MECHANISTIC INVESTIGATIONS OF THE EOSINOPHILIC PHENOTYPE OF MICE DEFICIENT IN HIF1α IN LUNG EPITHELIUM TREATED WITH COBALT	74
Results	75
Timing of HIF1 α Deletion and Eosinophilia	75
Determination of T _H 2 Inflammation by Flow Cytometry	78
PSB1115 and Adora2b in Cobalt-Induced lung injury	83
NF- κ B in Cobalt-induced lung injury	89
TCH013	89
LPS	93
Hyperoxia during early postnatal phase	97
Discussion	103
CHAPTER 4 – COMPARATIVE PHENOTYPES OF COBALT-INDUCED RESPIRATORY INFLAMMATION IN MICE DEFICIENT FOR HIF1α, HIF2α or HIF1α/2α IN LUNG EPITHELIUM. 112	112
Results	113
HIF2 α ^{Δ/Δ} mice 60 μ g CoCl ₂ time course	113
HIF2 α IHC	113
BAL Cellularity	113
Histopathology and Immunohistochemistry	118
Cytokine analysis	125
HIF1 α /2 α mice treated at 5 days	129
HIF1 α and HIF2 α IHC	129
BAL Cellularity	129
Histopathology and Immunohistochemistry	133
Cytokine analysis of whole lung lysate by bead array	135
Gene expression analyses	135
Discussion	142
CHAPTER 5 – SUMMARY AND CONCLUSIONS	148
Summary of Research	149
Major findings and implications	149
Proposed Working Model	150
Knowledge gaps and future studies	153

REFERENCES 157

LIST OF TABLES

Table 1. Partial summary of cytokine/chemokine-mediated recruitment of cellular effectors in the lung.....	28
Table 2. Non-HIF hypoxia-responsive transcription factors (modified from [216]).....	46
Table 3. List of primers for mouse genotyping and qRT-PCR.....	70

LIST OF FIGURES

Figure 1. Comparative epithelial constituents across regions of mouse and human lungs.....	8
Figure 2. Comparison of human and mouse lung development.	13
Figure 3. Overview of pulmonary epithelial cell influence in immunity.	18
Figure 4. T-Helper (T _H) cell Subtypes.....	25
Figure 5. Cartoon of HIF α and HIF β subunit domains and functions	37
Figure 6. Review of HIF signaling	39
Figure 7. Possible crosstalk of HIF1 α with Adora2b and NF- κ B in CTL and HIF1 $\alpha^{\Delta/\Delta}$ cells	50
Figure 8. Inducible, lung epithelium-specific transgenic knockout mouse model.....	59
Figure 9. Eosinophilia in HIF1 $\alpha^{fl/fl}$ mice by genotype and DOX treatment.....	60
Figure 10. Mouse experiment treatment and dosing schemes	64
Figure 11. BAL total cells and macrophages from various DOX regimens in HIF1 α mice treated with 5d cobalt	76
Figure 12. BAL eosinophils and neutrophils (PMNs) from various DOX regimens in HIF1 α mice treated with 5d cobalt.....	77
Figure 13. BAL lymphocytes from various DOX regimens in HIF1 α mice treated with 5d cobalt.	78
Figure 14. T _H 2 immune cell populations in HIF1 α mice with 5d cobalt.....	80
Figure 15. T _H 1 immune cell populations in HIF1 α mice with 5d cobalt.....	81
Figure 16. T _C immune cell populations in HIF1 α mice with 5d cobalt	82
Figure 17. IHC for Adora2b in lungs of cobalt treated CTL and HIF1 $\alpha^{\Delta/\Delta}$ mice.....	84

Figure 18. BAL total cells and macrophages from HIF1 α mice treated with cobalt for 5 days +/- PSB1115.....	87
Figure 19. BAL eosinophils and PMNs from HIF1 α mice treated with cobalt for 5 days +/- PSB1115	88
Figure 20. BAL lymphocytes from HIF1 α mice treated with cobalt for 5 days +/- PSB1115	89
Figure 21. Structural schematic of TCH013	90
Figure 22. BAL total cells and macrophages from HIF1 α mice treated with cobalt for 5 days +/- TCH013	91
Figure 23. BAL eosinophils and PMNs from HIF1 α mice treated with cobalt for 5 days +/- TCH013.....	92
Figure 24. BAL lymphocytes from HIF1 α mice treated with cobalt for 5 days +/- TCH013	93
Figure 25. BAL total cells and macrophages from HIF1 α mice in P4-30 and P32-42 DOX groups treated +/- LPS	95
Figure 26. BAL eosinophils and PMNs from HIF1 α mice in P4-30 and P32-42 DOX groups treated +/- LPS	96
Figure 27. BAL lymphocytes from HIF1 α mice in P4-30 and P32-42 DOX groups treated +/- LPS	97
Figure 28. H&E Staining for P0-14 mice exposed to 75% O ₂	99
Figure 29. HIF1 α IHC for mice exposed to 75% O ₂ from P0-14.....	100
Figure 30. BAL total cells and macrophages from CTL mice exposed to 75% O ₂ from P0-14 and 5d cobalt as adults	101
Figure 31. BAL eosinophils and PMNs from CTL mice exposed to 75% O ₂ from P0-14 and 5d cobalt as adults.	102
Figure 32. BAL lymphocytes from CTL mice exposed to 75% O ₂ from P0-14 and 5d cobalt as adults	103
Figure 33. HIF2 α IHC for CTL and P4-30 DOX treated mice.....	114

Figure 34. BAL total cells and macrophages from HIF2 α mice treated with cobalt for 1, 5 and 14 days	116
Figure 35. BAL eosinophils and PMNs from HIF2 α mice treated with cobalt for 1, 5 and 14 days	117
Figure 36. BAL lymphocytes from HIF2 α mice treated with cobalt for 1, 5 and 14 days.....	118
Figure 37. HIF2 α strain H&E stain for mice with 1, 5 and 14 days cobalt	120
Figure 38. HIF2 α strain major basic protein IHC for mice with 1, 5 and 14 days cobalt	122
Figure 39. AB-PAS stain for HIF2 α mice with 1, 5 and 14 days cobalt.....	124
Figure 40. IL-4 and IL-5 cytokine levels from bead array in HIF2 α mice.	126
Figure 41. IL-6 and KC cytokine levels from bead array in HIF2 α mice	127
Figure 42. IFN γ and IL-10 cytokine levels from bead array in HIF2 α mice	128
Figure 43. HIF1 α and HIF2 α IHC for HIF1 α /2 α mice	130
Figure 44. BAL total cells and macrophages from HIF1 α , HIF2 α and HIF1 α /2 α mice at 5 days cobalt exposure	131
Figure 45. BAL eosinophils and PMNs from HIF1 α , HIF2 α and HIF1 α /2 α mice at 5 days cobalt exposure.....	132
Figure 46. BAL lymphocytes from HIF1 α , HIF2 α and HIF1 α /2 α mice at 5 days cobalt exposure.....	133
Figure 47. H&E stain from HIF2 α and HIF1 α /2 α mice at 5 days cobalt exposure.....	134
Figure 48. MBP IHC from HIF2 α and HIF1 α /2 α mice at 5 days cobalt exposure	136
Figure 49. AB-PAS stain from HIF2 α and HIF1 α /2 α mice at 5 days cobalt exposure	137
Figure 50. IL-4 and IL-5 cytokines from WLL of HIF1 α , HIF2 α and HIF1 α /2 α mice after 5 days cobalt exposure	138
Figure 51. IL-6 and IL-17 cytokines from WLL of HIF1 α , HIF2 α and HIF1 α /2 α mice after 5 days cobalt exposure	139
Figure 52. IFN γ and TNF α cytokines from WLL of HIF1 α , HIF2 α and HIF1 α /2 α mice after 5 days cobalt exposure	140

Figure 53. WLL gene expression profiles of HIF1 α , HIF2 α and HIF1 α /2 α mice with 5 days cobalt exposure..... 141

Figure 54. Working model of WT and HIF $\alpha^{\Delta/\Delta}$ lung epithelial cells exposed to cobalt 151

KEY TO ABBREVIATIONS AND SYMBOLS

2-OG	2-oxoglutarate (α -keto glutarate)
A2BR	see Adora2b
AB-PAS	Alcian blue – periodic acid Schiff (stain)
ADP	adenosine diphosphate
Adora2b	adenosine receptor A2B (aka A2BR)
ALI	acute lung injury
AM	alveolar macrophage
APC	antigen presenting cell
ARNT	aryl hydrocarbon receptor nuclear translocator
ATI	alveolar epithelial type I
ATII	alveolar epithelial type II
ATP	adenosine triphosphate
BAL	bronchoalveolar lavage
bHLH	basic helix loop helix
BPD	bronchopulmonary dysplasia
cAMP	cyclic adenosine monophosphate
CC	cysteine-cysteine family of chemokines (β chemokines)
CD	cluster of differentiation (cell surface marker)
CD40L	cluster of differentiation 40 ligand
CO ₂	carbon dioxide
CoCl ₂	cobalt (II) chloride
Cre	cre recombinase
CTAD	carboxy terminal trans activation domain
CTL	control
CXC	cysteine-x-cysteine family of chemokines (α chemokines)
DC	dendritic cell

pDC	plasmacytoid dendritic cell
mDC	myeloid dendritic cell
cDC	conventional dendritic cell
DOX	doxycycline
Δ/Δ	deficiency via recombination
EDHB	ethyl 3,4-dihydroxybenzoic acid
Eos	eosinophils
Epas1	endothelial PAS-domain protein 1 (aka HIF2 α)
Epo	erythropoietin
ETC	electron transport chain
FADH ₂	flavin adenine dinucleotide (reduced and hydroquinone form)
FIH	factor inhibiting HIF
GA	gestational age
GATA3	GATA binding protein 3
G _i	G alpha inhibitory protein
GOE	Great oxygenation event
GPCR	G-protein coupled receptor
G _q	G alpha q/11 protein
G _s	G alpha stimulatory protein
H&E	hematoxylin & eosin (stain)
HIF	hypoxia inducible factor
HMLD	hard metal lung disease
HRE	hypoxia response element
IFN γ	interferon gamma
IHC	immunohistochemistry (antibody labeling of tissues)
I κ B	inhibitor of kappa B protein
IKK	I κ B kinase (complex)
IL	interleukin

iNOS	inducible nitric oxide synthase
Io	ionomycin
i.p.	intra-peritoneal (injection)
KC	keratinocyte-derived chemokine (aka CXCL1 or GRO α)
LPS	lipopolysaccharide
LT α	lymphotoxin alpha (aka tumor necrosis factor beta)
MBP	major basic protein
MCE	mucociliary escalator
MEF	mouse embryonic fibroblast
MHCII	major histocompatibility complex II
NADH	nicotinamide adenine dinucleotide (reduced form)
NF- κ B	nuclear factor kappa B
NO	nitric oxide
NTAD	amino terminal trans activation domain
ODD	oxygen dependent degradation domain
OVA	ovalbumin (usually refers to model of sensitization/challenge of ovalbumin)
PAS	Per-Arnt-Sim
P _i	inorganic phosphate
PHD	prolyl hydroxylase domain-containing enzyme
PKC	protein kinase C
PMA	phorbolmyristate acetate
PMN	neutrophil, or polymorphonuclear leukocyte
PNEC	pulmonary neuroendocrine cell
PRR	pattern recognition receptor
pVHL	protein product of Von Hippel Lindau tumor suppressor gene
RBC	red blood cell (erythrocyte)
ROP	retinopathy of prematurity
ROS	reactive oxygen species
rtTA	reverse tetracycline transactivator

Stat	signal transducer and activator of transcription
SP-C	surfactant protein C
T ₀	naïve T lymphocyte
TAD	trans activation domain
T-bet	T-box expressed in T cells (aka T-box 21)
T _C	cytotoxic T lymphocyte
TCA	tricarboxylic acid
TCR	T cell receptor
TGFβ	transforming growth factor beta
T _H	T helper lymphocyte
T _{H1}	T helper type 1 lymphocyte
T _{H2}	T helper type 2 lymphocyte
T _{H17}	T helper type 2 lymphocyte
T _{REG}	T regulatory cell
TLR	Toll-like receptor
TNFα	tumor necrosis factor alpha
TSLP	thymic stromal lymphopietin
Vegf	vascular endothelial growth factor
WLL	whole lung lysate
Ym1	chitinase 3-like 3
Ym2	chitinase 3-like 4

CHAPTER 1 - INTRODUCTION AND SPECIFIC AIMS

Oxygen – historical and biological significance

The discovery of oxygen resulted from the early study of air, combustion and respiration in 17th and 18th centuries [1-5]. As modern science took root and the age of alchemy gave way to chemistry and beyond, decades of further experimentation has revealed the fundamental role oxygen has played in the evolution of almost all multicellular life. Oxygen is the third most abundant element in the universe based on spectroscopic analysis behind hydrogen and helium [6], and the most abundant element in the Earth's crust by mass [4]. Molecular oxygen (dioxygen; O₂) accounts for 20.9% of the atmosphere, the presence of which can be almost entirely attributed to photosynthetic organisms. Geologic evidence to date suggests that nearly 2.4 billion years ago there was a Great Oxygenation Event (GOE) which brought the oxygen concentrations above 0.001% [7, 8]. The rate of O₂ increase from the GOE to more current levels (>20%) seems to be gradual, but is still an area of debate among geologists and paleobiologists [9]. A more detailed timeline of atmospheric O₂ concentrations from the last 550 million years shows great variation, and claims that oceanic and atmospheric O₂ levels have driven evolution of multicellular life are supported not just by the fossil record and geochemistry, but also through evolutionary and systems biology [10-13].

Biologically, oxygen's most fundamental role is to be the final electron acceptor in the mitochondrial electron transport chain (ETC). The proton gradient produced by the ETC is used for production of adenosine triphosphate (ATP), the energy currency of nearly all eukaryotic

and multicellular life. Reducing equivalents, in the form of NADH and FADH₂ produced by the tricarboxylic acid (TCA) cycle and β-oxidation of fatty acids are donated to the ETC. The ETC uses the transfer of electrons to drive a proton (H⁺) gradient across the inner mitochondrial membrane. This gradient is utilized by ATP synthase (Complex V), producing ATP from ADP and P_i using the energy inherent in the process of the protons leaking back into the matrix [14].

NADH donates electrons to Complex I (NADH dehydrogenase), and FADH₂ donates electrons to Complex II (succinate dehydrogenase). Both Complex I and II donate electrons to Coenzyme Q (ubiquinone), which in turn donates electrons to Complex III (cytochrome *b/c*₁). Cytochrome *c* accepts electrons from Complex III and donates them to Complex IV (cytochrome *a/a*₃ or cytochrome *c* oxidase). Oxygen is utilized as the final electron acceptor in the ETC, as Complex IV donates four electrons to O₂ to form two molecules of water. This entire process of utilizing O₂ to accept electrons for ATP production is referred to as oxidative phosphorylation or aerobic respiration.

Review of lung anatomy, physiology and development

Due to oxygen's central role in energy production, multicellular animals (metazoans) have evolved systems to ensure adequate transport of O₂ to the cells of the body. The energy demand of cells and body size represent key drivers for the resulting respiratory systems and their complexity [15]. Respiratory systems are concerned primarily with gas exchange. Simple tubular structures that diffuse oxygen directly to tissues are seen with insect tracheal systems [16], whereas larger animals such as birds and mammals require a highly specialized centralized gas exchange organ (lung) to transfer of O₂ into a nutrient-rich fluid (blood) which is then pumped by the heart to the tissues [17].

Mammals utilize a diaphragm, a thin muscle that horizontally separates the thoracic and abdominal cavities, which when contracted creates negative pressure in the pleural space (between the inner wall of the thorax (parietal pleura) and the outer wall of the lung (visceral pleura)). This negative pressure, in addition to accessory muscles and the movements of the rib cage, forces the expansion of lung tissue, filling the airway and lungs. Inhaled air is humidified, heated and mixed with residual air in the lung. To maximize the efficiency of gas exchange with blood, air is brought past a large surface area (approximately 75 m² in adult humans) and also within close proximity to the red blood cells (within 1 μm). Blood contains erythrocytes (red blood cells or RBCs) which house large amounts of hemoglobin, the proteins which carry oxygen to the tissues and return carbon dioxide (CO₂) from the tissues to the lungs to be

exhaled as waste. Relaxation of the diaphragm creates positive pressure in the pleural space which condenses lung tissue and causes air to be expelled from the lungs [18-20].

The airway is divided into two main compartments: the conducting regions and respiratory (gas exchange) regions. As implied, the conducting regions are concerned with conducting and conditioning air from the external environment to the respiratory regions. For humans, the conducting airway includes everything from the nose to the terminal bronchiole; more specifically, the nasal cavity, nasopharynx, glottis/larynx, trachea, bronchi, bronchioles and terminal bronchioles. The respiratory regions are located entirely within the deep lung, which begins at the respiratory bronchiole, and then to the alveolar ducts and alveoli. Beginning in the trachea, several divisions (up to approximately 23) of branching occur which increase the surface area for gas exchange. Bronchi occupy the first 3 divisions, and divisions 4-16 represent the journey of bronchioles to terminal bronchioles. Respiratory bronchioles occupy divisions 17-19, alveolar ducts 20-22, and finally the alveolus itself at 22-23. The journey from terminal bronchiole to alveolus is on average 5 mm [21].

As mice are used as the model organism in my studies in this dissertation, it is worth noting some important differences between murine and human airways to put the results of my experiments into context. Mice are obligate nose breathers which humans are not. Additionally, in humans inspired air has to bend 90° to move into line with the trachea, which rodent airways do not require. Though the nasal airway will not be discussed here, the mouse has highly developed and complex nasal turbinates and olfactory system that differs from humans. Regarding the gross anatomy of the lung, one major difference in gross architecture is

that the human lung contains 3 right lobes and 2 left lobes (with a small cardiac lingula), to make room for the heart. Mouse lungs, in contrast, have 4 right lobes and a single large left lobe. Mice have approximately 13-17 airway divisions before reaching alveoli (compared to approx. 17-21 in humans). Bronchi in the lungs of humans have several generations of cartilaginous walls, while mice have none within the lung proper. Submucosal glands are also not present in the airways distal to the larynx in mice, whereas humans contain submucosal glands through the 2nd division of pulmonary bronchi. Another major difference in mice is that they do not have respiratory bronchioles – terminal bronchioles give way directly to alveolar ducts and “skip” the respiratory bronchiole structure seen in humans and other mammals. Mice also have much thinner pleura (outer lining of lung) with less connective tissue than humans, probably due to size [22].

In regards to cells lining the airway, the trachea and proximal bronchi are initially composed of pseudostratified columnar epithelium, primarily of ciliated cells and goblet cells, with a few serous and neuroendocrine cells, and many basal cells. Human lungs maintain this epithelial cell architecture through most of the bronchial tree, whereas mice switch at the first bronchial branch to a simple columnar epithelium where Club cells are the majority cell type with ciliated cells. Upon reaching the terminal bronchiole, human lungs transition to a respiratory bronchiole, where some outpockets of alveoli appear, with sporadic re-introduction of the bronchial epithelium until reaching the alveolar duct. In mice, the terminal bronchiole leads abruptly to the alveolar duct, where the only epithelial cells that are observed are alveolar type I (ATI) cell and the occasional alveolar type II (ATII) cell. Alveolar macrophages are

also seen throughout the alveolar regions. Figure 1 shows a summary of the cellular components of both mouse and human lung epithelium [23].

Figure 1

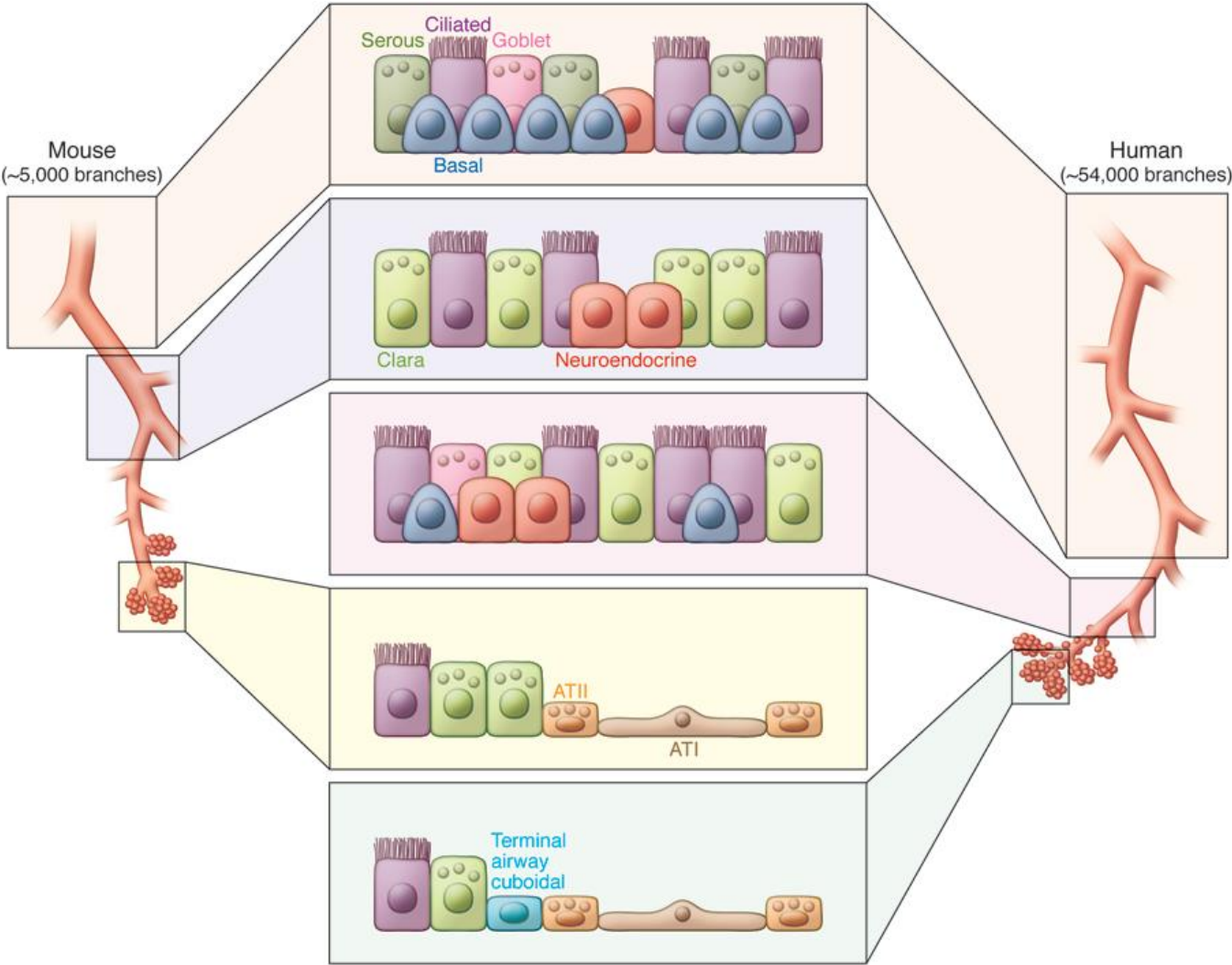


Figure 1. Comparative epithelial constituents across regions of mouse and human lungs. Epithelial cells of airways in mouse lungs (left side, says “Mouse ~5,000 branches”) and human lungs (right side, says “Human ~54,000 branches”) are compared. Major

Figure 1 (cont'd)

differences include the presence of basal cells and goblet cells in human airways all the way to the respiratory bronchioles, whereas in mice they end at roughly the main stem bronchi. Serous cells in mice are only present in the proximal tracheal airway and submucosal glands. In mice, Club cells and ciliated epithelium dominate the bronchi and bronchioles, leading the Club cell to occupy a higher percentage of total airway surface in mice than is seen in humans. Serous cells = dark green; ciliated cells = purple; goblet cells = pink; basal cells = blue; neuroendocrine cells = salmon; Club cells = light green; ATII cells = light orange; ATI cells = brown [23]. For interpretation of the references to color in this and all other figures, the reader is referred to the electronic version of this thesis (or dissertation).

Reproduced with permission of the copyright owner. Further reproduction prohibited without permission.

Lungs represent one of the most complex organs both because of the vast structural complexity required for effective gas exchange, and also for the specificity their cells display to defend the lung from injury. There are approximately 40 unique cell types in the respiratory tract, their distribution reflecting the function of the local airway in which they reside [24]. In the bronchial tree we find many epithelial cells, including ciliated cells, goblet (mucous) cells, serous cells, basal cells, neuroendocrine cells, dendritic cells and Club cells. The primary function of the ciliated epithelial cells is to operate the mucociliary escalator (MCE), a hygiene and protective apparatus where cilia beat in unison to flow a mucous layer (contributed by the mucous cells and containing any unwanted particles) on top of a periciliary layer (contributed by the serous cells) back toward the oropharynx. This process is described in more detail in the following section. Goblet cells function to provide the protective mucous which forms the mucous layer of the MCE and also defense from chemical injury. Serous cells have a non-mucous role, which includes the production and secretion of many protective and antimicrobial proteins such as lysozyme, IgA, peroxidase and lactoferrin [25]. Basal cells act as stem cells for the bronchial epithelium, showing self-renewal and ability to differentiate into ciliated and non-ciliated cell types [26, 27]. Pulmonary neuroendocrine cells (PNECs) are innervated basally and contain many granules filled with neuroactive peptides. Of all lung cell types, PNECs have the most varied putative functions including oxygen sensing & regulating pulmonary blood flow, bronchial tone, and provide a stem cell niche for ciliated and Club cells after injury [28, 29].

Toward the more distal end of the bronchial tree we find Club cells, which are cuboidal non-ciliated, non-mucous secretory cells of the distal bronchioles that perform many functions. They secrete protective molecules such as Club cell secretory protein (CCSP) (member of the

secretoglobin family), surfactant proteins A, B and D, antimicrobial peptides, proteases and mucins to the extracellular fluid. Club cells also function to metabolically detoxify xenobiotic substances and can act as a stem cell population for damaged epithelial cell types such as ciliated and mucous goblet cells [30]. Recent controversy surrounding Max Clara, major contributor of initial characterization of the cell type that bore his name, and his use of tissue samples from executed prisoners in Nazi Germany and outspoken involvement in the Nazi Party have resulted in the renaming of the Clara cell to the “Club” cell [31, 32].

In the alveolar compartment we find ATI and ATII cells, and alveolar macrophages (AMs). ATI cells are the thin, flat, gas-exchanging epithelial cells, while ATII cells are cuboidal, producing surfactants which not only hold the alveolus open by reducing surface tension, but can also act as an antimicrobial [33]. ATII cells also regulate fluid levels in the alveolar compartment, and act as stem cells for the alveolus, reproducing and differentiating into ATI cells after these cells have been lost to injury [34]. AMs play a key function of housekeeping and innate defense, phagocytosing any used surfactant or particulates and patrolling the airway for harmful microbes. Additionally, AMs play a role in adaptive immunity with the ability to act as antigen-presenting cells (APCs) and by modulating many inflammatory responses [35-37].

Development of the lung in mammals is absolutely essential for transitioning to air breathing from the previous placental source of O₂. Some mammals, however, do not finish (or even start) the process of alveolarization, the final stage of lung development, until sometime after birth. Lung development occurs in 5 major stages: embryonic, pseudoglandular, canalicular, saccular and alveolar, which differ in timing across species [23]. For example, the

embryonic stage in humans begins around weeks 3-4 post-conception, whereas in mice this stage doesn't start until embryonic day 9.5 (E9.5), considered mid-gestation (Figure 2). Lungs originate as buds from the ventral primitive foregut (future esophagus), regulated primarily by thyroid transcription factor 1. Branching morphogenesis, directed by a plethora of transcription factors, including fibroblast growth factor, transforming growth factor β , epidermal growth factor, bone morphogenic protein, wingless-related integration site, retinoic acid, hedgehog and Notch signaling, follows in order to give the basic shape of the bronchial tree [23, 38, 39]. The canalicular stage is characterized by thinning mesenchyme along the airway branches, finishing the bronchial tree shape and differentiation of ciliated, secretory and neuroendocrine cells. The sacular stage is defined by expansion of the distal lung into saccules, larger versions of alveoli, as ATI and ATII cells start to differentiate [40, 41]. Finally, alveolarization occurs until about P30 in mice, and in humans concludes anywhere between 2-21 years, depending on the source. Modern techniques have indicated that alveolarization continues much later than initially thought [42]. This is not surprising when one considers body length and thoracic size does not plateau until age 17 for girls and 20 for boys [43].

Figure 2

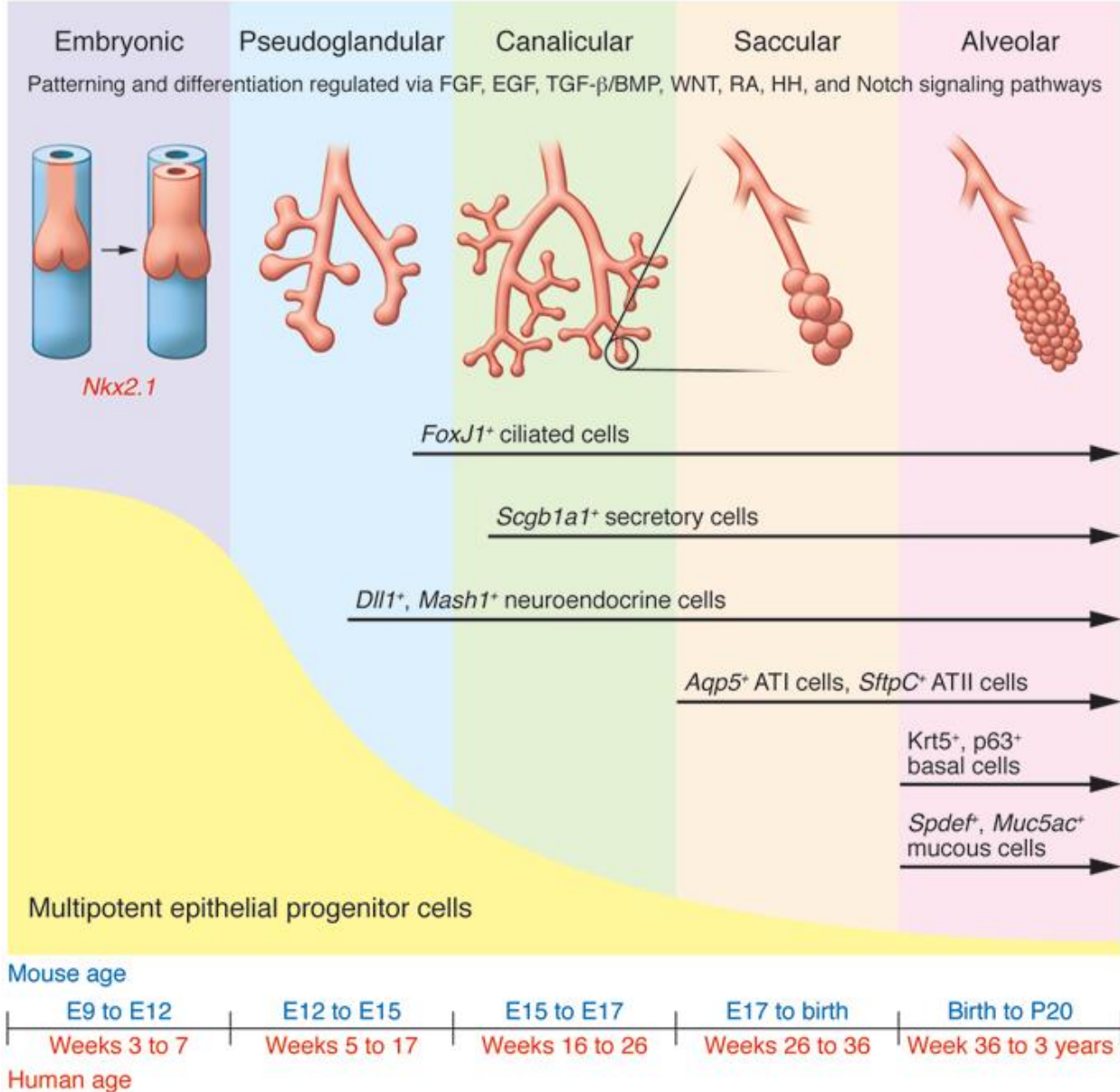


Figure 2. Comparison of human and mouse lung development. The five stages of lung development are overlaid with their gestational ages, dominant transcriptional networks and appearance of major cell types. Note that birth of mice (usually E19) places them in the saccular stage, whereas humans brought to term (37 weeks) are farther along into the alveolar stage [23]. Also note that text underneath the developmental stages (Embryonic, Pseudoglandular, etc.) is: “Patterning and differentiation regulated via FGF, EGF, TGF- β /BMP, WNT, RA, HH, and Notch signaling pathways.”

Reproduced with permission of the copyright owner. Further reproduction prohibited without permission.

Premature birth, supplemental O₂, bronchopulmonary dysplasia and asthma

Babies born prematurely have had higher rates of survival the last 30 years, thanks in no small part to the availability of exogenous surfactants and improved supportive care. The gestational age (GA) at which babies can expect to survive is between 23-26 weeks, which is during the canalicular stage of lung development, before any of the terminal saccules (precursors to alveoli) are formed. The exogenous surfactants supplement the endogenous ones still developing in ATII cells from babies born before GA 26 weeks, and help maintain airway patency during exhalation. Another supportive measure is supplemental O₂, though the baby's O₂-saturation of hemoglobin (O₂sat) is kept below 95% to avoid retinopathy of prematurity (ROP), a complication discovered in the 1950s [44]. The pathogenesis of ROP is dysfunctional vascular development in the retina, thought to be from high O₂ which negatively impacts hypoxia signaling (discussed later) [45].

Bronchopulmonary dysplasia (BPD) is the primary pulmonary manifestation of survivors of severe premature birth (GA <28 weeks) and low birth weight (<1500 grams), and is thus associated with prematurity and supplemental O₂. BPD is a disease characterized by underdeveloped lungs, specifically fewer and larger ("simplified") alveoli, which limits the amount of gas exchange. Individuals with BPD have many sequelae later in life, most prominently asthma and wheezing disorders [46]. Some wheeze can be attributed structurally to loss of parenchymal tissue (alveolar simplification) which reduces tethering of bronchi (holds these airways open during exhalation), leading to obstructed airflow. Whether there are other

molecular contributors to allergic airway disease in patients with immature lungs or BPD remains to be demonstrated, but several large cohort studies have solidified the increased incidence of asthma in premature infants. Infants born in the extremely premature range of 24 to 28 weeks have higher incidence of asthma both in childhood and in early adulthood (age 25-35) [47-49].

While no causative relationships between BPD or asthma and hypoxia signaling have been proven to date, hypoxia signaling is known to significantly affect lung development. It is tempting to speculate that the halted development seen in BPD is a result of a normally hypoxic environment of the developing lungs being interrupted by premature birth, exposing the lungs to higher amounts of oxygen than would be expected for this developmental period [50]. Perhaps changes in oxygen exposure can affect hypoxia signaling, and thus alter lung development in such a way that increases the likelihood of developing allergic disease and altering lung immunity. Recent studies by our lab have supported this notion, and have shown that loss of HIF1 α in lung epithelial cells causes an exacerbated response using the ovalbumin sensitization/challenge model of asthma in mice [51]. Further investigation of hypoxia signaling and its relationship to premature birth, supplemental O₂, BPD and asthma are needed to determine whether these associations are pathophysiologically meaningful.

Immune mechanisms in the lung

With an epithelial surface of $>70\text{m}^2$, the airway represents the second largest surface on the human body, requiring a proportionate defense effort. As a result, several mechanisms have emerged that protect the airway from chemical, particulate and other environmental stresses, such as microbial pathogens. Broadly, these mechanisms of immunity fall into two categories: innate and adaptive. Innate mechanisms are less specific, protect from a wide range of threats, act quickly (or continuously) and the machinery required to recognize threats does not require further adaptation for function. These mechanisms are in sharp contrast to adaptive immunity which, while being much more specific, requires more time to act. Presentation and matching of pathogenic antigens as well as expansion of the effector cell populations and their specific antibodies are required before adaptive immunity can begin. These immune mechanisms are executed by the lung epithelium and immune cells, including alveolar macrophages, dendritic cells, bone-marrow derived granulocytes and monocytes, as well as B and T cells. An understanding of innate and adaptive immune mechanisms in the airway, and their overlap, is essential to putting any toxicological investigation of the airway into the proper context.

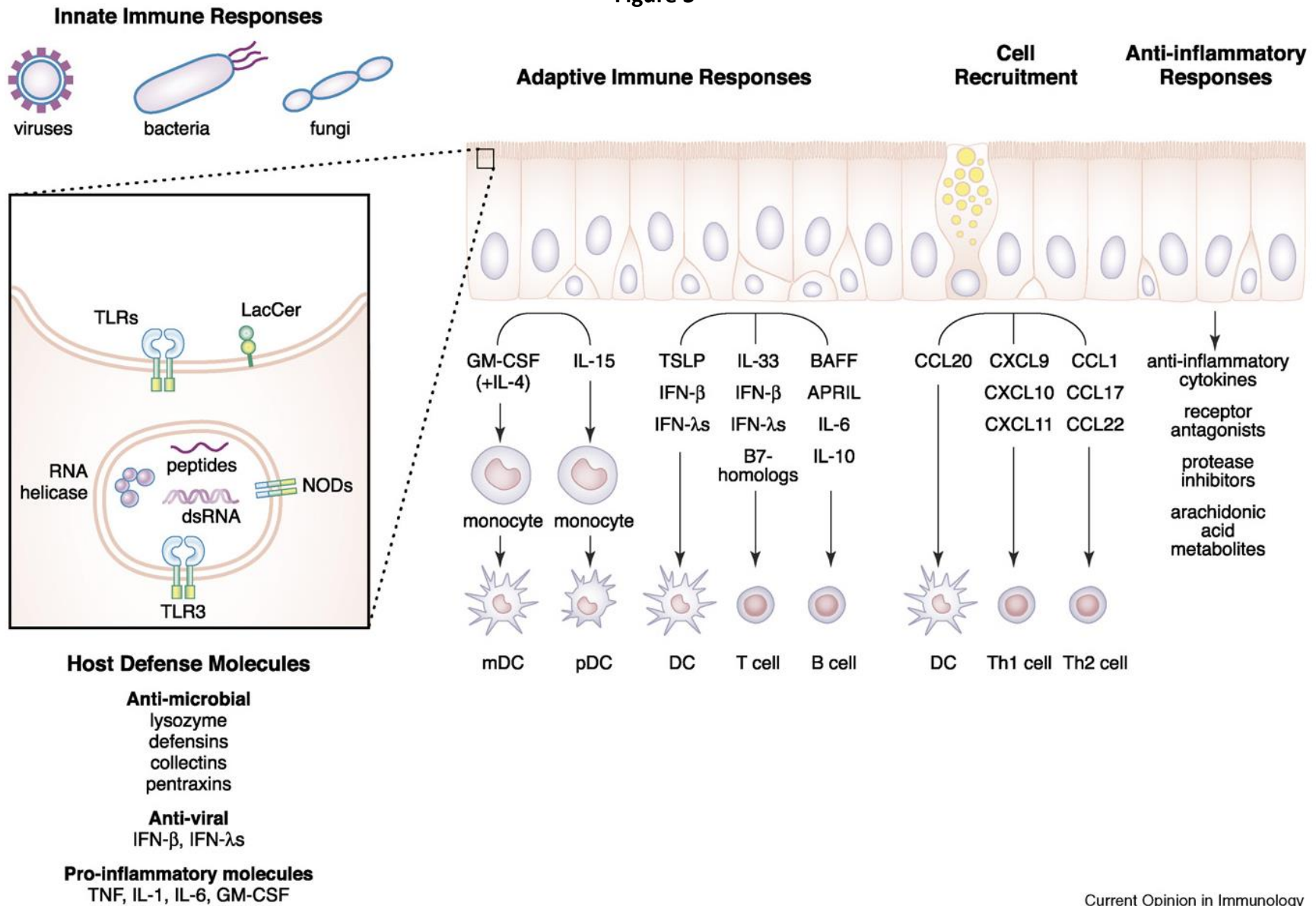
Innate immunity

Innate mechanisms begin with the basics of mechanical and chemical barriers. One of the most effective examples of this in the airway is the MCE of the tracheobronchial tree, which has three functions: clearance of particulates, chemical protection and biological protection. The surface fluid of the MCE in the airway, aided by turbulent air flow, traps inhaled

particulates, which are then carried out of the lung by the action of millions of synchronously beating cilia to the glottis where they can be coughed and swallowed. The surface fluid also provides chemical protection by providing a physical layer to trap certain compounds and provides antioxidant potential through peroxidases [52]. Other secretory products in the airway lining fluid of the MCE, as well as elsewhere along the bronchial epithelium, provide biological protection by targeting common microbial pathogens. Compounds such as IgA and IgG, lysozyme, lactoferrin, fibronectin, cathelicidin, β -defensins and antiproteases, such as secretory leukoprotease inhibitor, are secreted by epithelial cells to protect the airway [53, 54]. Antimicrobial action of these compounds assists the action of macrophages and other immune effector cells, fulfilling the biological protective function of the MCE [55, 56].

Epithelial cells provide far more protection than simply a physical and chemical barrier of the MCE. Along with macrophages and dendritic cells, epithelial cells contain an array of pattern recognition receptors (PRRs). PRRs recognize conserved molecular moieties of microbes and alert immune effector cells of danger via specific downstream signaling [57]. One classic family of PRRs are the toll-like receptors (TLRs) [58]. TLRs recognize many different types of pathogen-associated molecules. For example, recognition of lipopolysaccharide (LPS), a key constituent of the outer membrane of gram-negative bacterial cell walls, is mediated through surface receptors CD14 and TLR4 [59]. Epithelial cells use these and other systems to alert the immune system in several ways, usually through activation of the nuclear factor kappa B (NF- κ B pathway) (Figure 3) [60, 61]. Recent focus on the epithelial role in allergic airway disease has revealed that these cells can control the nature of the ensuing immune response directly [62, 63].

Figure 3



Current Opinion in Immunology

Figure 3. Overview of pulmonary epithelial cell influence in immunity. Epithelial cells function both as effectors of innate

Figure 3 (cont'd)

immunity, but also in modulating adaptive immune responses, recruitment of immune cells, and production of anti-inflammatory mediators. Epithelial secretion of cytokines and chemokines influence a variety of different cell types. (mDC and pDC indicate myeloid and plasmacytoid dendritic cells, respectively) [60]. *Note that text underneath "Innate Immune Responses" (top left) is: "viruses, bacteria, fungi". Note that text underneath the "Host Defense Molecules" (left bottom) is: "Anti-microbial, lysozyme, defensins, collectins, pentraxins" and "Anti-viral, IFN- β , IFN- γ " and "Pro-inflammatory molecules, TNF, IL-1, IL-6, GM-CSF". Text underneath "Anti-Inflammatory Responses"(right side) is: "anti-inflammatory cytokines, receptor antagonists, protease inhibitors, arachidonic acid metabolites". Note that text underneath "Adaptive Immune Responses" (middle) is: "GM-CSF (+ IL-4), monocyte, mDC; IL-15, monocyte, pDC; TSLP, IFN- β , IFN γ s, DC; IL-33, IFN- β , IFN γ s, B7-homologs, T cell; BAFF, APRIL, IL-6, IL-10, B cell". Note that text underneath "Cell Recruitment"(middle right) is: "CCL20, DC; CXCL9, CXCL10, CXCL11, Th1 cell; CCL1, CCL17, CCL22, Th2 cell".*

Reproduced with permission of the copyright owner. Further reproduction prohibited without permission.

Macrophages are derived from hematopoietic tissues such as bone marrow and circulate as monocytes in the peripheral blood until they are called upon by tissues to fill roles as resident macrophages or to replace resident macrophages that have died. Macrophages patrol all of the portals of entry to the body, and while they can participate in direct killing of microbes, their primary function in the body is cleanup of cellular debris via phagocytosis and to signal infections to the rest of the immune system. This signaling is usually through antigen presentation and secretion of cytokines and chemokines. Armed with an array of PRRs, macrophages can become activated upon exposure to microbes (usually through interferon gamma (IFN- γ) and tumor necrosis factor alpha (TNF α)) and can amplify signals to the rest of the immune system [64, 65]. Recently it has been appreciated that activation of macrophages can occur in several different ways, based on the stimulus, to affect one type of response over others. Initially these were referred to as either “classically activated, M1” macrophages or “alternatively activated, M2” macrophages. M1 macrophages are induced through IFN- γ and TNF α /LPS and stimulate the production of inducible nitric oxide synthase (iNOS) and secretion of interleukin (IL)-1 β , IL-12 and TNF α with microbicidal activity. In contrast, “alternatively activated, M2” macrophages are activated by IL-4, which stimulates the production of arginase. Further research has clarified that macrophages can exhibit different phenotypical markers simultaneously and also retain a large amount of plasticity, which has led to the suggestion that the ‘M1 vs. M2 axis’ be considered more like a continuum [66-71]. Regardless of the name of the macrophage, it is clear that they play a vital role in almost every level of immunity.

Neutrophils (polymorphonuclear cells or PMNs) are also derived from hematopoietic stem cells, and are the primary cell type responsible for phagocytosis and killing of microbes,

being far more efficient at phagocytosis and bacterial killing than macrophages [72]. PMNs play a central role in innate host defense, and circulate the peripheral blood until called upon by chemokines and other signals to migrate into affected tissues and become activated [73]. One key feature of PMNs are their azurophilic (colored strongly with azure stain) granules which are filled with several antimicrobial peptides and oxidases. Upon fusion, either with phagosomes or the plasma membrane (a process referred to as “degranulation”), these granules increase the concentration of antimicrobial peptides and produce large amounts of reactive oxygen species (ROS) in what is called a “respiratory burst”, unleashing superoxide, hydroxyl radical, hydrogen peroxide, hypochlorous acid and chloramines [54, 74, 75]. In humans, the lung is reported to house roughly 40% of circulating PMNs at any time, allowing them close access to affected airway tissues [76]. PMNs are activated by several signals, including Toll-like receptors. Administration of LPS to the lung of animals can rapidly recruit PMNs so much that in 3-4 hours post-administration, 60-80% of cells in bronchoalveolar lavage (BAL) are PMNs [77]. Defects in several aspects of PMN function leave humans susceptible to many infections, further verifying the central role of PMNs in host defense [78, 79].

Eosinophils, like neutrophils, are derived from granulocyte precursors in the bone marrow and patrol in peripheral blood until called to specific tissues. Unlike PMNs, eosinophils have classically been attributed with defense against parasitic infections (e.g. helminthes or “worms”) and associated with allergic responses and asthma. Several recent reviews have challenged this classical view of eosinophils as damaging effector cells in these limited contexts and have outlined more broad roles for these cells as immune modulators and orchestrators of tissue repair and regeneration [80-82]. Eosinophils’ namesake derives from their cationic

granules which hold Eosin stain. These granules contain many cytotoxic cationic proteins including Major Basic Protein (MBP) which makes up roughly 50% of the protein contained in these granules [83-85]. Other proteins in these granules include eosinophilic cationic protein, eosinophil peroxidase, and eosinophil-derived neurotoxin, which, along with MBP have cytotoxic properties. Granules may also contain cytokines and other immunomodulators such as IL-2, -3, -4, -5, -6, -8, -10, -12, -13, -16, -18, TGF α/β , GM-CSF, TNF α and IFN γ , among others [86]. Interestingly, degranulation of eosinophils has been shown to be stimulus-specific, as opposed to an “en masse” release of all granule contents, as evidenced by Lacy et al. [87]. While the exact mechanistic role of these cells is still under intense investigation, it is clear that they can elicit diverse effector functions.

Another key cell type within and interspersed among epithelial cells is the dendritic cell (DC). DCs share many properties of macrophages in that they are derived from the myeloid lineage. Unlike macrophages, however, they display different resident subpopulations prior to immune activation (for review, see [88, 89]). In general, DCs are positioned in proximity to all epithelial surfaces, and they are the primary APCs of the body. In the lung, the CD103+ conventional DC (cDC) use filopodia that migrate in between epithelial cells to reach into the airway lumen and take occasional samples of surrounding material (i.e. “periscoping”) to monitor the environment. DCs are armed with many PRRs with which to monitor possible presence of microbes. If microbes are sensed, DCs can become activated, which enhances secretion of cytokines and chemokines that promote DC migration to draining lymph nodes for activation of naïve T cells [90]. Like the epithelium, DCs are considered by many to be a part of both innate and adaptive immunity due to their “professional antigen presentation” function.

Antigen presentation to naïve T helper (T_H) cells is a vital starting point in transmitting adaptive immune responses. To initiate an adaptive immune response to T_H cells, DCs must first migrate to draining lymph nodes where they express major histocompatibility complex II (MHCII), which presents processed antigens to the T-cell receptor (TCR) and CD4 co-receptor. Presence of co-stimulatory molecules, classically CD28 on T cells and B7-1/B7-2 (CD80/CD86) on APCs are necessary to complete activation of T_H cells [65].

Adaptive immunity

While the innate immune mechanisms of the airway are essential and widespread, they do not recognize all threats, and they are poor at reacting to intracellular pathogens or extracellular pathogens that have developed evasion strategies. Thus, a more specific system of protection is needed to complement innate immunity. The adaptive immune system fills this functional gap, and is mediated by APCs, T and B cells, with signaling to other cellular effectors that include macrophages, neutrophils, eosinophils, basophils, and mast cells to orchestrate the effective immune responses.

Role of T cells in lung defense.

For the lung, T cells are positioned in the draining/hilar lymph nodes, where activation of T cells by activated dendritic cells occurs [91]. T cells are responsible for most cell-mediated immunity (direct action of cells), and mature T cells are classified by surface receptors CD4+ T helper (T_H) cells or CD8+ cytotoxic T lymphocytes (T_C). During an immune response, naïve T cells (T_0) are exposed to peptides on MHCII from APCs which must match the T_0 TCR in addition

to co-stimulatory binding of B7.1/B7.2 (CD80/CD86, on APCs) with CD28 (on T₀ cells). These two signals cause activation and survival of T cells, usually by IL-2 (T cell growth factor). Without co-stimulatory input, T cells undergo inactivation or clonal deletion (immune “tolerance”). In contrast, co-activation signals cause clonal expansion and differentiation of T cells (T cell “priming”), which causes expression of CD40 ligand (CD40L), a co-stimulator necessary for binding to B cells [92].

The process of naïve T cell (T₀) priming and activation into functional T_H cells is heavily dependent upon the cytokine milieu of the APC-T₀ interaction. Several pathways of differentiation can be followed (Figure 4) [93]. The resulting T_H cells can generally be defined by the cytokines they release, which further direct immune responses. The most commonly studied T_H cell populations in the lung to date are the T_H1 and T_H2 cells.

T-helper type 1 (T_H1) response

T_H1 responses are often seen with infections of intracellular pathogens such as viruses or Listeria. T_H1 cell priming requires the presence of IFN γ and IL-12. Production of these cytokines is generally performed by APCs, caused by activation of a combination of TLR3, 4, 7-9 or 11 or any one of these in the presence of a type I interferon (IFN α or IFN β) [94, 95]. IFN γ and IL-12 drive transcription factors Tbet and Stat4 which further upregulate IFN γ (positive feedback loop), IL-2 and lymphotoxin α (LT α). To combat intracellular pathogens, IFN γ stimulates macrophages to increase their microbicidal functions and stimulates many cells to

express MHC I and MHC II to aid in antigen presentation. Importantly, the presence of IFN γ inhibits the differentiation of both T_H2 and T_H17 cells. IL-2 promotes T cell and natural killer (NK) cell activation and proliferation. Lymphotoxin (TNF β) is similar to TNF α , and recruits and activates PMNs [93, 96]. A properly functioning T_H1 response is absolutely required for proper clearing of intracellular pathogens.

Figure 4

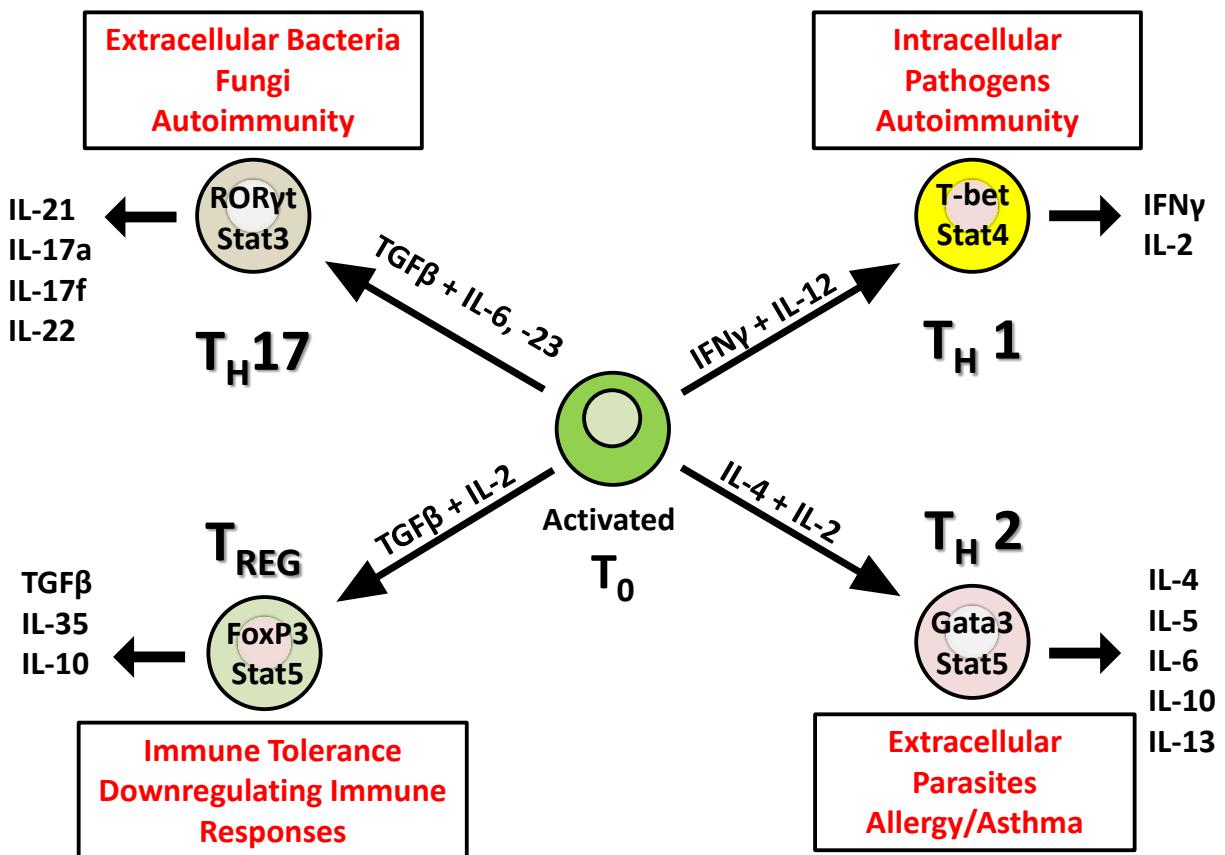


Figure 4. T-Helper (T_H) cell Subtypes. Naïve T cells (T₀, center) mature into effector T_H cells after a positive activation with an APC (not shown) based on presence of specific cytokines (shown above large arrows). Transcription factors responsible for the downstream maturation of each effector cell are labeled inside each cell. The small set of arrows indicates the secreted cytokines which further direct the various kinds of immune responses, and are most commonly used when attempting to identify T_H subtype. Boxes describe general immune functions of each subset. Modified from [93].

T-helper type 2 (T_H2) response

T_H2 responses are seen in extracellular parasitic infections (e.g. helminths), and are also the mechanisms behind allergic diseases such as asthma. T_H2 cell priming requires the presence of IL-4 and IL-2. IL-4 activates STAT6, which in turn upregulates GATA-binding protein 3 (GATA3), the master regulator of the T_H2 response. GATA3 acts as a master regulator by binding to the gene loci of several T_H2 cytokines to activate them while simultaneously represses T_H1 responses by repressing IL-12 receptor β2 and STAT4. The function of IL-2 in the T_H2 response is to activate STAT5, which in turn up-regulates IL-4, further driving the T_H2 population to differentiate. In recent years it has been determined that IL-2 can be bypassed by either IL-7 or thymic stromal lymphopoietin (TSLP) to activate STAT5. GATA3 and STAT5 cooperate to express T_H2 cytokines, including IL-4, -5, -9, -13 and -25. IL-4 stimulates B cell class-switching from IgM/IgG to IgE, which in turn activate basophils and mast cells to degranulate upon antigen recognition to cause vascular permeability, smooth muscle constriction and further recruitment of inflammatory cells. IL-5 acts to recruit and promote survival of eosinophils, whereas IL-9 has a similar function for mast cells. IL-13 works in concert with IL-4 on epithelial cells to induce mucous production and goblet cell metaplasia, and in smooth muscle cells to promote airway hyper-responsiveness. IL-25 promotes T_H2 responses by initiation and activation of IL-4, IL-5 and IL-13, though several experiments in RAG knockout (functional loss of B and T cells) mice have demonstrated that it can induce IL-5 and IL-13

expression from non-B, non-T cells, which have also been referred to as innate lymphoid cells or nuocytes [97]. IL-33 promotes alternatively activated macrophages and secretion of TSLP from epithelial cells in addition to production of other T_H2 cytokines, but like IL-25, more research is needed to elucidate its role more fully [98].

Other T-cell responses

While other T cell responses such as T_{REG} and T_H17 are important, induction of either T_H1 or T_H2 responses greatly inhibits the formation of the other populations by the dual action of their cytokines IFN γ and IL-4, respectively. In the absence of IFN γ or IL-4, high levels of TGF β activate the T_{REG} response, which serves to dampen the overall action of activate T cells, which induces tolerance and helps to resolve inflammation. Lower levels of TGF β can activate T_H17, which has been shown to be crucial for defense against some extracellular bacteria and fungi [93].

Mechanisms of lung neutrophilia and eosinophilia

Several factors are responsible for recruitment of different cell populations to the lung (Table 1). The most common cell types seen in airway inflammation are macrophages and PMNs, because of the general ability of these cells to kill pathogens and remove cellular debris. However, several molecular factors are responsible for recruiting specific cell types to the lung. The major groups of molecules that perform this function are the chemokines, several of which have been characterized to belong to the CC or CXC-family of chemokines (L designates ligand, R designates receptor). The CC and CXC receptors show ligand promiscuity, so there is often

Table 1. Partial summary of cytokine/chemokine-mediated recruitment of cellular effectors in the lung.

Cell Type Recruited/Activated	Chemokine	Cellular Source(s)	References
ALL – mixed leukocyte recruitment	MIP-1 α (CCL3)	Almost all induced immune and hematopoietic cells	[102]
Macrophages	MCP-1 (CCL2)	ATII cells	[103]
Neutrophils (PMNs)	TNF α	Macrophages (endothelial adhesion markers)	[65]
	IL-1	Macrophages (stim. PMN production)	[65]
	IL-8	Epithelial Cells, Macrophages	[101]
	MIP-2 α	Macrophages	[103]
	KC (CXCL1, GRO α)	Macs, Epithelial Cells, PMNs	[104]
Eosinophils, Basophils	Eotaxin (CCL11), Eotaxin2 (CCL24) Eotaxin3 (CCL26)	T cells, Epithelial cells	[105]
Eosinophils	IL-5	T _H 2 cells	[98]
Mast Cells	IL-9		
Eosinophils, T cells	RANTES (CCL5)	Macrophages	[106]
DCs (pro-T _H 2)	CCL20/ β -defensin	Epithelial Cells	[107]
	TSLP		[98, 108]
	IL-25		[98, 109]
	IL-33		[98, 110]
	GM-CSF		[111]
	IL-1 β		[108]
	Osteopontin		[112]
	MMP9		[113]
T _H 1	IP10 (CXCL10)	DCs, Epithelial cells, Macs	[114]
T _H 2	TARC (CCL17)	Epithelial Cells	[115]
	PARC (CCL18)		
	MDC (CCL22)		

redundancy of function. The CC family has several members that direct mixed leukocyte recruitment, including CCL2 (MCP-1), 3 (MIP-1 α), 5 (RANTES), 7 (MCP-3), 8 (MCP-2), 12, 13 (MCP-4) and 15 (MIP-1 δ). The CXC family usually directs neutrophils and effector T cells, though CXCL12 (SDF-1 α/β) has mixed leukocyte recruitment [65].

PMNs are more prevalent in the pulmonary capillaries than systemic blood, and while the reason is not fully understood, it is speculated to be from the nature of their cell shape in the narrow capillaries [99]. During an inflammatory stimulus from TNF α , IL-1 β or lymphotoxin (TNF β), activated neutrophils express a high-affinity integrin receptor and CD11/CD18, which causes them to bind more tightly to the endothelial cells [100].

In turn, the endothelial cells express adhesion molecules such as P-, E-, and L-selectins, vascular cell adhesion molecule 1 (VCAM-1), and intercellular adhesion molecule 1 (ICAM-1). The CXC receptors CXCR1 and CXCR2 on the surface of PMNs bind to GRO α (CXCL1), GRO β (CXCL2), GRO γ (CXCL3), IL-8 (CXCL8) to direct chemotaxis to the inflammation site [73, 101].

Eosinophilia is also seen in the lungs, usually in the context of allergic airway disease or parasitic worm infection (also known as helminths, a classic example in humans being several *Schistosoma* species). Recruitment of eosinophils is largely mediated by T_H2 cells through IL-5, though epithelial cells can secrete chemokines that target eosinophils directly (CCL11 (Eotaxin-1), CCL24 (Eotaxin-2), CCL26 (Eotaxin-3), CCL5 (RANTES), CCL7 (MCP-3), CCL13 (MCP-4) and CCL3 (MIP1 α)) or indirectly by recruiting T_H2 cells (CCL22 (MDC), CCL17 (TARC) and CCL18 (PARC)) [115, 116].

Epithelial-immune crosstalk in inflammatory responses

In the wake of all the recent advances made by immunologists in understanding adaptive immune mechanisms, the epithelium is finally getting some deserved attention as an active participant in the immune process. Epithelial and dendritic cells are now being viewed as key functional units of the innate/adaptive immunity transition, especially in the lungs [117]. Most studies to date have focused on communication between epithelial cells and dendritic cells.

Generally the direction of cytokines seems to be heavily one-way, that is from epithelial cells to DCs. Some of the documented cytokines (summarized in Table 1) released by epithelial cells to recruit and polarize DCs to induce a T_H2 response are CCL20, β -defensin, TSLP, IL-25, IL-33, GM-CSF, MMP9, IL-1 β and osteopontin [118, 119]. The T_H1/T_H17 response is less favored directly by epithelial cells, and seems to require both epithelial stimulation of the innate immune response, as well as, direct contact of DCs with the pathogen in question [120]. If the stimulation by local macrophages secreting IFN γ , (sometimes IL-1 β or TNF α) combined with the epithelial/DC innate response is enough to activate DCs, T_H1 responses can be induced. If IL-17A is secreted during this process, the response is skewed toward T_H17 . Other key players in the epithelial induction of T_H1 are the “inflammasome” proteins, Caspase-1 and NOD-like receptors (NLRs); for a review see Mariathasan and Monack, 2007 [121].

Alveolar epithelial type II (ATII) cells and immunity

In addition to their role in the production of surfactant and maintenance of the alveolar compartment, ATII cells have been recently shown to express MHCII and participate in the creation of FoxP3+CD4+ T cells (T_{REGS}) [122, 123]. The active role of epithelium in directing immunity has been increasingly important because the lung is no longer assumed to be a sterile environment. While lower in overall organism load, the lung microbiome is similar to upper respiratory tract microbiome in bacterial constituents [124, 125]. Other studies by Chuquimia et al. show the likely involvement of ATII cells in recognizing and amplifying response to infection [103]. One important consequence of the inflammatory response in the lung is a change in O₂ availability and its role in T cell and macrophage activation. Investigations into the contribution of ATII cells in immunity will be crucial in further developing this field, especially in regards to how the immune dynamics change based on presence of different cell types and the microenvironment (i.e. O₂ availability) of the alveolar space.

The Hygiene Hypothesis

The rise of allergic diseases in industrialized nations over many decades has prompted researchers to investigate the cause. In 1989, Strachan saw an inverse relationship between the number of siblings and the incidence of hay fever and atopy. He speculated that exposure to infections in childhood, either through decreased hygiene (caused by increases in family size or other causes), was required for proper development of the immune system and that the cleanliness of our modern lives was contributing to the rise of allergic disease [126]. This was dubbed the “hygiene hypothesis”. Years of study have helped develop this idea into a more

nuanced understanding that environmental exposures in early postnatal life having significant impact on later risk of allergic disease. While strides have been made in elucidating innate immune mechanisms, more understanding of the microbiome and epithelial signaling in regulating immune development is needed to clarify this hypothesis into a working molecular model of allergic disease risk [127].

Normoxia, hypoxia and oxygen sensing mechanisms

Air is composed of approximately 21% oxygen (O₂), 78% nitrogen (N₂), 0.9% argon (Ar) and 0.04% carbon dioxide (CO₂) with the remainder as very small amounts of several other gases. At sea level the pressure of air is 760 mmHg. When air is inspired into the respiratory tract, it is saturated by water vapor at a pressure of 47 mmHg, and thus the partial pressure of O₂ (pO₂) in inspired air is:

$$pO_2 = 0.21 \times (760 \text{ mmHg} - 47 \text{ mmHg}) = 150 \text{ mmHg}$$

As the inspired air is conducted deeper into the airway, it mixes with existing gases, and the alveolar pO₂ is approximately 105 mmHg. After diffusion across ATI cells and pulmonary endothelial capillaries, O₂ is bound to hemoglobin of the RBCs and the pO₂ of pulmonary venule blood (and arterial blood in the systemic circulation) is 100 mmHg. As blood carries O₂ to the peripheral tissues, the localized O₂ concentration decreases dramatically, and along with pH decreasing and allosteric regulation of hemoglobin drive the dissociation of O₂ and the association of CO₂ to hemoglobin (known as the Haldane effect), and O₂ diffuses through the local cells [128]. As venous blood returns to the right heart and pulmonary arteries, the pO₂ is 40 mmHg [20].

The exposure of each cell to oxygen depends greatly on many factors, including the distance of the cell to the nearest capillary, the specific tissue location of the cell (and extracellular milieu) and the metabolic demands of the tissue (rate of O₂ consumption) [129]. Levels of O₂ have been measured at 5 mmHg in the retina [130], 20-30 mmHg in skeletal muscle [131] and 45-65 mmHg in the brain [132]. Normal cells all develop and acclimate to a unique “normal” pO₂ (normoxia) through mechanisms that are not yet fully understood. When the supply of O₂ drops below this normal level, the cell is considered hypoxic [133, 134]. The lung epithelium, despite having proximity to the organism’s O₂ source, still can experience hypoxia in various disease states [135].

Hypoxia is the main cause of cell death in cardiovascular diseases, such as myocardial infarction and stroke, and is also seen at the sites of inflammation, cancer, and in varying degrees from normal physiological variation (physical exercise, altitude variation). Maintaining a steady supply of O₂ to cells is required for homeostasis, and organisms have evolved mechanisms to sense and physiologically regulate O₂ [136]. These include neuronal sensing of O₂ in the glomus cells of the carotid body [137], the neuroepithelial cells in bronchial airways [28], and smooth muscle cells in systemic and pulmonary vasculature [138]. Thought to operate through neuronal recognition of O₂ through K⁺-channels sensitive to hydrogen peroxide (H₂O₂) or ROS [139], these systems act in concert to optimize respiratory rate,

shunting of blood to well-ventilated regions, cardiac output and blood pressure to maintain O₂ homeostasis [136, 140]. While these systemic feedback systems are essential for homeostasis, they act in an acute setting and do not in and of themselves impart increased cellular tolerance directly. At the level of the cell, the ability to adapt to hypoxia is derived primarily by the hypoxia-inducible factors (HIFs).

Hypoxia Signaling

Hypoxia inducible factors

Hypoxia inducible factors (HIFs) are heterodimeric transcription factors composed of an α and β subunit. HIF1 α was first characterized by Wang and Semenza in 1993 as a protein binding DNA upstream of the erythropoietin (Epo) gene in hypoxic Hep3b cells [141]. The active transcription factor was found to be a dimer and the term HIF-1 beta (HIF1 β) was given to the new half of this protein. Subsequently, it was discovered HIF1 β was identical to the aryl hydrocarbon receptor nuclear translocator (ARNT), a member of the Per-Arnt-Sim (PAS) superfamily of environmental sensors [142]. In 1997, hypoxia inducible factor-2 alpha (HIF2 α) was discovered and originally named endothelial PAS-domain protein 1 (Epa1) [143]. In 1998 the first description of HIF3 α was reported [144]. Both HIF2 α and HIF3 α show sequence and functional similarities to HIF1 α .

In humans, there are three known HIF α subunits (HIF1 α , HIF2 α and HIF3 α) and two known HIF β subunits (Arnt and Arnt2). The alpha subunits reside in the cytoplasm, while the beta subunits remain in the nucleus. All contain a basic helix-loop-helix (bHLH) domain which is primarily responsible for DNA binding and dimerization (Figure 5). The characteristic PAS domain consists of an A and B domain, which assist in dimerization selectivity and binding of chaperones [145, 146]. The oxygen-dependent degradation domain (ODD) is a feature of the HIF α subunits and contains the structures necessary for O₂ sensitivity. Arnt and Arnt2 have a single transactivation domain (TAD), whereas all HIF α subunits have an N-terminal activation

Figure 5

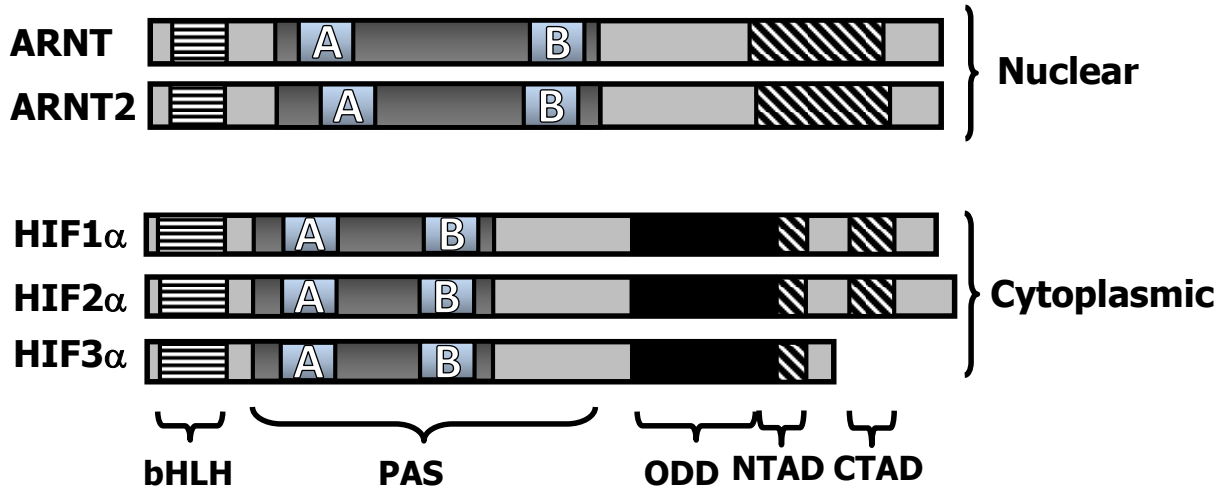


Figure 5. Cartoon of HIF α and HIF β subunit domains and functions. The hypoxia inducible factors consist of alpha subunits that reside in cytoplasm and beta subunits that reside in the nuclear compartment. Functional HIFs contain one alpha and one beta subunit. All contain an N-terminal basic Helix-Loop-Helix (bHLH) domain (horizontal lines) for DNA binding and dimerization as well as the PAS A and PAS B (PAS) domains for dimerization and binding other cofactors. Only the alpha subunits contain the oxygen-dependent degradation domain (ODD, black region) which contains conserved proline residues targeted for O₂-dependent hydroxylation and confers oxygen sensitivity to HIF α . All subunits contain transactivation domains (diagonal lines). The ODD overlaps with the N-terminal activation domain (NTAD) of alpha subunits, but not the C-terminal activation domain (CTAD) of HIF1 α and HIF2 α . Arnt and Arnt2 contain a single transactivation domain (TAD).

domain (NTAD, that overlaps with the ODD) and HIF1 α and HIF2 α have a second C-terminal activation domain (CTAD) [144].

HIFs are primarily regulated posttranslationally by a family of O₂-, 2-oxoglutarate- (2-OG), ascorbate- and Fe²⁺-dependent enzymes called prolyl hydroxylase-domain containing enzymes (PHDs). PHD1-3 have unique activities and tissue/cellular distribution [147, 148].

Under normoxic conditions, key proline residues (P402 and P564 in human HIF1 α [149]) in the

ODD are hydroxylated [150, 151]. Upon hydroxylation, the E3 ubiquitin ligase von-Hippel Lindau tumor suppressor protein (pVHL) targets HIF α for ubiquitination and subsequent degradation via the 26S proteasome [152-154] (Figure 6). Thus, under normoxic conditions, HIF α subunits are unstable and degraded. In contrast, under hypoxic conditions the PHD enzymes become limited by lack of O₂, and HIF α subunits stabilize, translocate to the nucleus and meet their heterodimeric partner Arnt [155, 156]. There has been much debate in the field about whether ROS are responsible for HIF activation or if it is due to loss of substrate. Recent experiments have begun to favor loss of substrate, although ROS-mediated inhibition of PHDs might play a role in certain cell types or conditions. The consensus opinion seems to be that the mitochondrial involvement of HIF signaling has more to do with their role as O₂ sinks than as producers of ROS, a debate which has been recently summarized expertly by Dr. Thilo Hagen [157].

As a functional dimer, HIFs seek out hypoxia response elements (HREs) in the genome, containing the core sequence of A/GCGTG. With the help of other co-activators, the HIFs drive expression of hypoxia-regulated genes. Well characterized HIF target genes include vascular endothelial growth factor (Vegf) which initiates angiogenesis, erythropoietin (Epo) which increases RBC production to increase O₂ carrying capacity, and many glycolytic enzymes which increase anaerobic metabolism to assist with cell adaptation to hypoxia [158, 159]. In addition to these adaptive enzymes, HIFs also upregulate pro-death genes such as Bnip3, Nix and Noxa which has led researchers to speculate that HIFs direct controlled cell death if adaptation is impossible, though how this distinction is made in the cell is still being investigated [160-162].

Figure 6

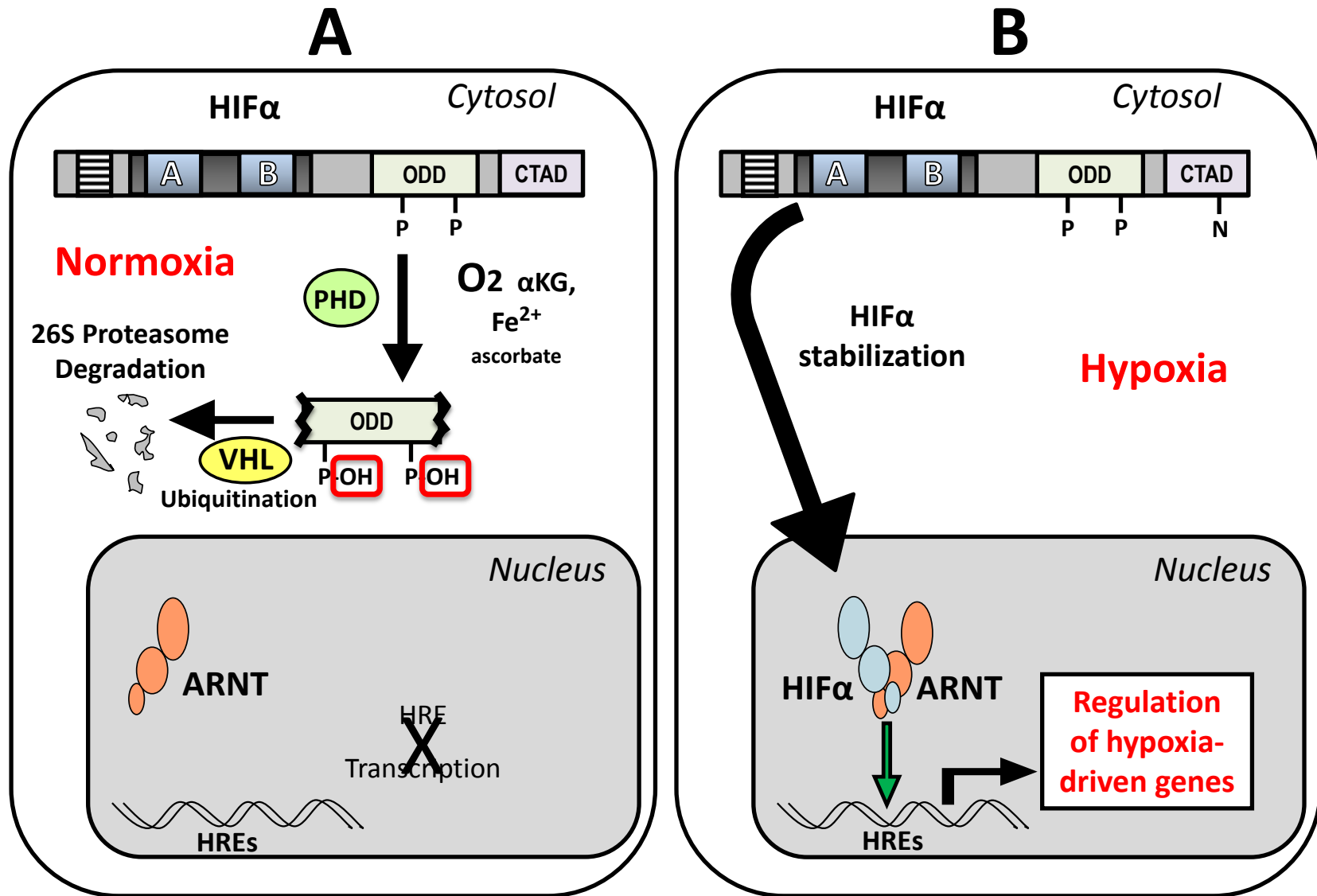


Figure 6. Review of HIF signaling. The alpha subunit resides in cytoplasm and beta subunit in the nuclear compartment. Under

Figure 6 (cont'd)

normoxic conditions **(A)**, conserved proline residues in the ODD and an asparagine residue in the CTAD are targeted for O₂-dependent hydroxylation by PHD. ODD hydroxylation targets HIF α for ubiquitination by pVHL and subsequent degradation in the 26S proteasome. Under hypoxic conditions **(B)** or in the presence of cobalt HIF α escapes degradation and translocates to the nucleus where it meets HIF β (Arnt) and locates HREs in DNA, regulating gene transcription.

There has been much interest in the different HIF α isoforms and their potentially unique roles. That first indication that HIF1 α and HIF2 α are not playing identical roles was illustrated in homozygous null mouse models of HIF1 α and HIF2 α . Both show embryonic lethality by approximately E10.5 [163-165] but have different phenotypic malformations. Mice lacking HIF1 α , the most ubiquitously expressed HIF, display disorganized yolk sac/neural fold/cephalad vascularization, lack of neural tube closure and an array of cardiovascular defects [166-168]. HIF-2 α knockout mice displayed a wider variety of phenotypes, thought to be strain-dependent, including bradycardia from reduced catecholamine synthesis, yolk sac vascular defects similar to HIF1 α knockouts, impaired lung maturation, and multiple organ malformations [169-172].

Further studies into gene target specificity between HIF1 and HIF2 have revealed that the NTAD confers some of this specificity, whereas the CTAD targets common genes between the two [173]. Studies to date seem to suggest that HIF1 α targets the glycolytic pathway [174, 175], where HIF2 α targets genes involved in cell cycle regulation, tumor growth factors such as cMyc [176] and pluripotency genes such as Oct4 [177]. In whole genome arrays, HIF1 α and HIF2 α targets showed some overlap (90 shared), though HIF2 α -specific targets were far fewer (40 genes compared to 304); additionally, when Z-scores for HIF1 α capture were relaxed, HIF1 α targets almost completely overlapped with HIF2 α (only 4 unique HIF2 α genes) [178]. These studies all suggest that while there are definitely overlapping gene targets, HIF2 α seems to be more selective in its unique gene targets, which is likely reflected in tissue distribution and function of these two HIFs. The role of HIF3 α is less studied, although it has been shown that splice variants of HIF3 α are capable of inhibiting hypoxia-induced gene expression [179-185].

Interestingly, HIF3 α is upregulated under hypoxia in a HIF-dependent fashion, suggesting HIF3 α as a potential feedback inhibition loop for the HIF system [186, 187].

Tissue expression of HIF isoforms seems to be in agreement with the overall ubiquitous nature of HIF1 α and more specific profile of HIF2 α . In tissues under hypoxic conditions, HIF1 α was inducible in nearly every tissue, and in some cases (muscle) was stable at normoxic conditions [188]. HIF2 α protein is far less detectable under normoxic conditions, but was inducible in brain, heart, lung, kidney, liver, pancreas, and intestine of mice, and also in several cell lines [189]. Interestingly, RNA analysis showed that lung contained the highest level of HIF2 α RNA [190].

Both HIF1 α and HIF2 α protein are expressed in the developing lung, although their distinct spatial and temporal expression patterns suggest differential roles in lung maturation. In first trimester human lungs, HIF1 α is found prominently in branching epithelium, while HIF2 α is found both in epithelial cells as well as mesenchymal tissues [191, 192]. In rodents, HIF2 α expression increases dramatically during lung maturation to become more highly expressed in adult lung than any other organ. In contrast, HIF1 α does not show this pattern of induction, though is more ubiquitously expressed [190, 192-195]. In our hands, the adult lungs of mice show HIF1 α being more detectable at normoxia in the bronchial epithelial cells and alveolar macrophages than HIF2 α . HIF1 α is also detectable in the arterial smooth muscle of the bronchial arteries adjacent to the axial airway (unpublished results).

HIFs in lung inflammation

Sites of inflammation tend to be hypoxic for many reasons. Edema, thrombosis and tissue injury increase the distance of parenchymal tissues to functional capillaries and disrupt the normal delivery of O₂ and nutrients to tissues. Infiltration of immune and inflammatory cells, with their high metabolic demand, also contributes to hypoxia [196]. HIFs have many functional roles in sites of inflammation, primarily for metabolic adaptation of all cells, and various cell-specific roles [197, 198]. For example, HIF1 α is essential for myeloid cell function [199]. Myeloid lineage-specific knockout models of HIF1 α prevents ovalbumin-induced allergic responses, likely from the decreased ability for these cells to become activated in the hypoxic microenvironment [200]. In phagocytes, HIF1 α plays an active role in bactericidal capacity [201] and nitric oxide (NO) homeostasis [202]. Additionally, HIF1 α can induce TLR2 and TLR6, which form a necessary protective role in allergic and fungal infections in the lung via IL-23 and IL-17 and T_H17 cells [203, 204].

HIF1 α regulates CD4⁺CD25⁺ T_{REGS}, which play important roles in resolution of acute lung injury (ALI) [205, 206]. HIF1 α is also essential for T cell survival [207]. It should be noted, however, that excessive thymocyte-specific HIF signaling induced T cell death [208]. Other studies have observed that hypoxia has a general negative regulatory role when it comes to T cells, and this is speculated to provide tissue-protection by preventing excessive T cell activation [209, 210].

Recent studies have attempted to target HIFs pharmacologically in the lung. In a study by Ahmad et al. (2012), mice in an ovalbumin model of asthma were treated with ethyl 3,4-dihydroxybenzoic acid (EDHB), an iron chelator and inhibitor of PHDs [211]. A low-dose was somewhat protective, but higher doses exacerbated allergic inflammation. These results led the authors to suggest that HIFs are mediators of allergy-induced inflammation. Another more detailed ovalbumin study by Huerta-Yepez et al. utilized an inducible system to knockout Arnt and showed that ARNT deficiency led to moderate protection following OVA sensitization and challenge. In addition, exposure of mice to EDHB (i.e. HIF activation) exacerbated the response [212]. Finally these authors also showed lavage fluid from asthmatic patients to have increased HIF1 α and VEGF. Although the data seems promising for causation, the authors did not have a convincing Arnt deletion, nor did they control for cell type, leaving the data in question because most of the results could be explained from HIF-signaling in myeloid and/or macrophage populations. If the mechanism cannot be isolated or better understood (e.g. why one dose is protective while another very harmful), the clinical utility of HIF-targeting pharmacologically is limited.

The studies for HIF-signaling specifically in the lung epithelium are usually limited to cell lines and *in vitro* models, most of which confirm that HIFs aid in hypoxic adaptation with some role for adhesion molecule expression (for review, see [213]). To date, ours is the only lab that has published the use of a lung-epithelial specific deletion of HIF1 α . Using this mouse model, we were able to show that loss of epithelial HIF1 α led to a switch from neutrophilic to eosinophilic inflammation following aspiration exposure to cobalt [214, 215]. When applied to the ovalbumin sensitization/challenge exposure, HIF1 α -deficient mice had an exacerbated

eosinophilic inflammation as well as increased total lung resistance. Both of these studies suggest that HIF1 α in the postnatal ATII and Club cells is important in airway immunity and immune regulation [51].

Other hypoxia-responsive signaling pathways in lung inflammation

Although HIFs play a central role in hypoxia adaptation, several other transcription factors also have responsiveness to hypoxia (Table 2) (reviewed in [216-218]). Two important hypoxia-responsive signaling pathways in lung inflammation are nuclear factor kappa B (NF- κ B) and purine signaling through adenosine receptors, specifically the A2B receptor (Adora2b).

Table 2. Non-HIF hypoxia-responsive transcription factors (modified from [216]).

Transcription Factor	Molecular Activation	Downstream Response	References
NFκB	↓ hydroxylation of IκB by PHDs and FIH; phosphorylation of IκB by Ras/Raf others unclear	↑ COX-2, IL-6, TNFα, MIP-2	[223]
AP-1 (Jun, Fos, ATF dimers)	Evidence for Jnk ↑ Ca ²⁺ cooperation with HIF/NF-κB	IL-8 upregulation	[216, 224-228]
p53	MDM2 and HIF interactions Phosphorylation of HIF and ROS implicated	Cell cycle arrest, apoptosis	[229]
cMyc	Competition with HIF for binding sites (p21) or partners (SP-1, Max)	Cell dependent +/- transformation potential	[217]
Notch	Hydroxylation, HIF-interaction	↓ Notch, ↑ HIF expression	[230]
CREBP (cyclic AMP response element binding protein)	Phosphorylation	Depending on stimulus duration: Pro-inflammatory/acute hypoxia Anti-inflammatory/chronic hypoxia	[231-233]
C/EBPβ (CCAAT/enhancer-binding protein, NF-IL6)	Phosphorylation	↑ IL-6, regulation	[234]
SP-1, SP-3	Unknown, localization and binding altered by hypoxia Cooperation with HIF/Smad3	↑ carbonic anhydrase IX, Epo (HIF/TGFβ-dependent)	[235, 236]
Egr-1	PKC, Ras/Raf and ERK HIF-independent	Tissue factor expression, thrombosis, vascular remodeling	[237, 238]

Nuclear factor kappa B (NF- κ B)

NF- κ Bs are a family of transcription factors that are considered the master regulators of the innate and adaptive immune response. NF- κ B signaling is one of the downstream targets of anti-inflammatory asthma medications, specifically through activation of the glucocorticoid receptor. The role in of NF- κ B signaling in the pathogenesis of asthma and other inflammatory diseases is well established [219]. In mammals, there are five members that function as homo- and/or hetero-dimers: NF- κ B1 (p105/p50), NF- κ B2 (p100/p52), RelA (p65), RelB and c-Rel. The NF- κ B response is complex, but in brief, all NF- κ B proteins contain a Rel-homology domain, which binds the inhibitor of kappa B (I κ B) protein that sequesters NF- κ B dimers in the cytosol until appropriately activated. Upon stimulation through many possible signals, the I κ B kinase (IKK) complex (also known as the “canonical NF- κ B pathway”) is activated and phosphorylates I κ B, which is subsequently polyubiquitinated and degraded by the 26S proteasome. The freed NF- κ B dimers translocate to the nucleus, bind DNA, and activate gene transcription, mostly of pro- inflammatory genes such as IL-6. They also are important regulators downstream of TNF α and IL-1 signaling [220-222].

Hypoxic activation of NF- κ B, while milder than for HIFs, has been reported for nearly 20 years, and its role in lung disease has been well documented [216, 239, 240]. Initial studies of mechanism indicated that phosphorylation via Ras/Raf was necessary [241], though more recently PHDs and FIH can also impact NF- κ B signaling [242, 243]. Other crosstalk with the HIF system is evident. For example, NF- κ B can affect basal levels of HIF1 α expression and HIF1 α can induce NF- κ B activation indirectly through the upregulation of cytokines IL-1 β and TNF α [244-247].

Purinergic (adenosine) receptors

Another family of sensory proteins which are susceptible to hypoxic regulation and important to lung immunity is the adenosine receptors, specifically Adora2b. Adenosine receptors are G-protein coupled receptors (GPCRs), and Adora2b is paired to a G_s and G_q subunit, so that it leads to both increased cAMP and activation of PKC. Compared to the A1 (G_i), A2A (G_s), and A3 (G_i) receptors, Adora2b is the least sensitive to adenosine, thought to be key in its ability to detect hypoxic environments where higher concentrations of adenosine metabolites would occur [248, 249].

Despite being the least sensitive receptor to adenosine, Adora2b has demonstrated key functions in the lung. WT mice live twice as long as Adora2b knockout mice in ventilator-induced lung injury [250]. Adora2b knockouts also demonstrated increased vascular leak to hypoxia, while knockouts of A1AR, A2AR and A3AR had no effect on these outcomes. Specificity to Adora2b was confirmed by inhibiting the Adora2b with PSB1115, resulting in a profound increase in hypoxia-induced vascular leakage, while stimulation of Adora2b with BAY60-6583 resulted in reversal of leakage [251]. Further studies showed that the A2B receptor is expressed highly in mouse ATII cells [252], and under hypoxia or ventilation-induced injury it is highly induced in the lung [250, 251]. HIF1 α regulates adenosine kinase, CD73 and Adora2b, all of which act to increase extracellular adenosine signaling during hypoxic conditions and amplify the protective Adora2b response [253-255]. The HIF1 α -Adora2b signaling pathway represents promising therapeutic potential in lung inflammation, especially acute lung injury (ALI) [256]. This signaling pathway also seems to apply to other organ systems, such as

protecting against intestinal epithelial inflammation. Mechanistically the hypoxic regulation of Adora2b in naïve T-cells is thought to promote T_{REGS} which dampens the resulting immune response [257, 258]. Taking the known interactions between HIF1 α , NF- κ B and adenosine signaling together, it is possible to see how loss of HIF1 α may disrupt this signaling to affect the resulting inflammatory profile in airway epithelial cells (Figure 7).

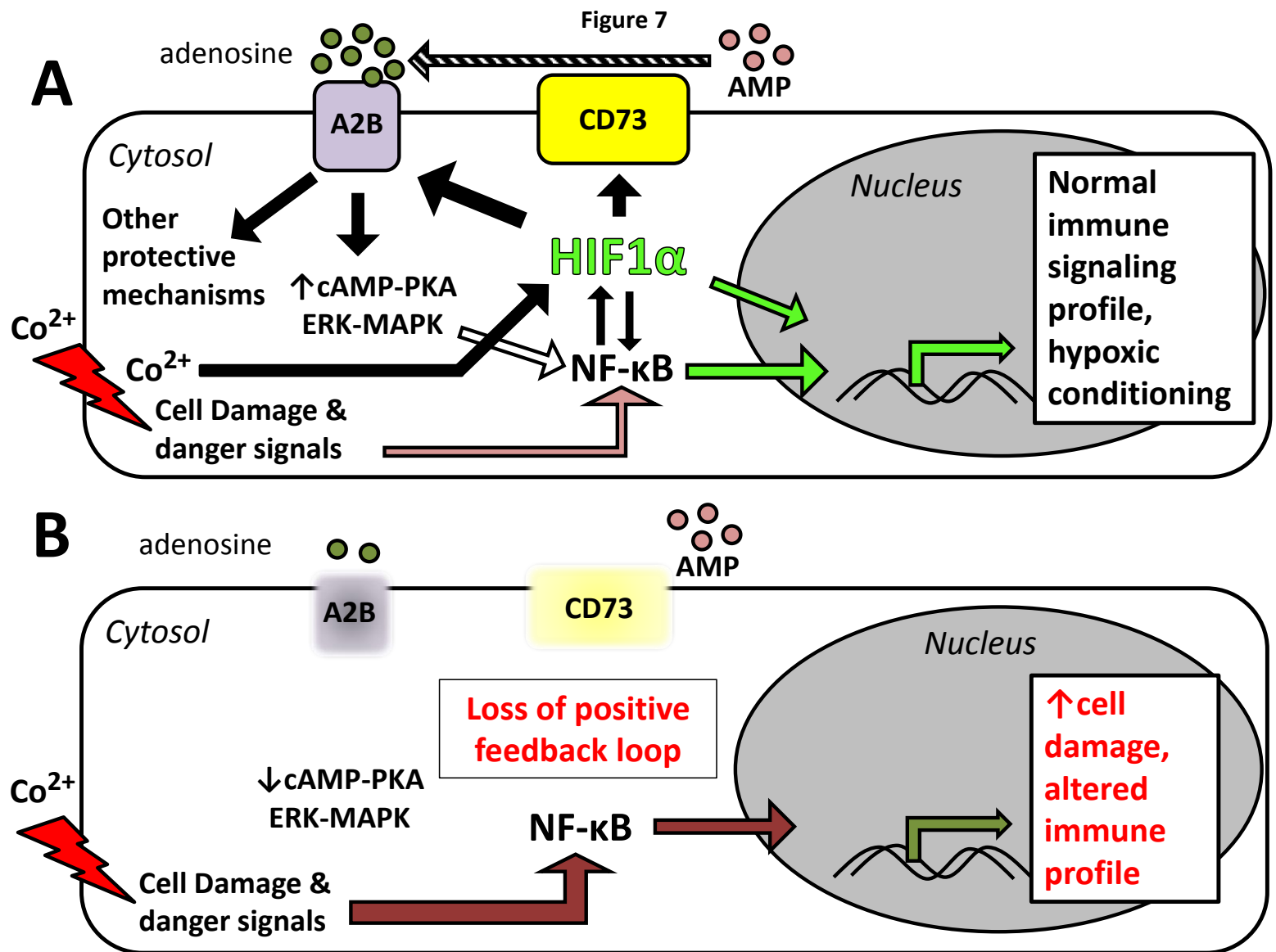


Figure 7. Possible crosstalk of HIF1 α with Adora2b and NF- κ B in CTL and HIF1 $\alpha^{\Delta/\Delta}$ cells. Representation of an ATII epithelial cell

Figure 7 (cont'd)

during an inflammatory insult such as cobalt. A cell from HIF-sufficient mice has a normal complement of HIF1 α which activates genes to assist in hypoxic adaptation, as well as a positive feedback loop with adenosine signaling to activate protective mechanisms during acute lung injury, and it also participates in crosstalk with NF- κ B to properly regulate expression of inflammatory cytokines (**A**). In contrast, cells from HIF1 $\alpha^{\Delta/\Delta}$ mice lack beneficial hypoxic adaptation from direct HIF1 α signaling, are prevented from making a HIF1 α -dependent positive feedback loop with adenosine receptor A2B and CD73, and lose crosstalk with NF- κ B such that cells experience increased cell damage and an altered response to inflammatory stimuli (**B**).

Cobalt

Occurrence and uses

Cobalt is a rare element in the Earth's crust, comprising anywhere from 20-23 ppm. There are many industrial uses for this ferromagnetic transition metal, most of which are in alloys. Recently, there has been an increased usage of cobalt in portable electronics and in the manufacture of rechargeable batteries [259, 260]. Prosthetic joints (e.g. Vitallium, CoCrMo) and sintered carbides (aka "hard metal") used for drilling and high-speed applications like jet engines also utilize cobalt in their alloys which imbues superior wear resistance and strength at high temperatures. In 2011, over 82,000 tons were produced (up 91% from 43,000 tons in 2003). Of all the cobalt used, approximately 44% goes into metals (19% of which are "superalloys" used for cutting tools, turbines and space vehicles), 30% to batteries, 14% to colors/paints, 9% to catalysts, 3% to biological applications [261]. Newer applications include using cobalt as a catalyst support used in the production of carbon nanotubes [262].

Biologically, cobalt is required in vitamin B₁₂ (cobalamin, created only by microbes), a cofactor of many methylation reactions, notably the creation of methionine from homocysteine and the conversion of methylmalonyl-CoA to succinyl-CoA in fatty acid metabolism. Clinically, due to its role in purine synthesis and myelin production, B₁₂ deficiencies present as anemia and neurologic deficits such as sensory impairment and ataxia. Supplementation success depends on whether an intact absorptive surface is present, mainly the parietal cells of the stomach producing acid and intrinsic factor and proper distal ileum absorption, the lack of

which produces “pernicious anemia” [14]. In the 1950’s, cobalt was used to treat certain anemias [263, 264]. Several cases of cobalt toxicity have occurred from this application prompting the removal of its use clinically.

Toxicity

Humans are generally exposed to low levels of cobalt through water and food sources. Toxicity only occurs as accidental ingestion, direct contact causing allergic dermatitis, iatrogenic use in medicine or with occupational exposures that are usually by inhalation of cobalt-containing dusts. Several exposure events in humans, in addition to its use for treatment of anemias [265], have aided greatly in our understanding of human toxicity. One notable route which caused multiple toxic exposures was the use of cobalt as a foam stabilizer in beer, where several high-volume consumers developed complications referred to as “beer-drinker’s cardiomyopathy” [266]. Inhalation of cobalt-dusts can cause a chronic disease called hard metal lung disease (HMLD) (discussed below) or “cobalt lung”. Additional exposures from groups of diamond polishers, again from inhalation of dusts, have been documented [267-269].

Hard metal lung disease

The most widely known cobalt-specific pathology is hard metal lung disease (HMLD) or “cobalt lung”. HMLD is a giant-cell interstitial pneumonitis caused from inhalation of cobalt-containing dusts, typically from hard metal grinding and drilling. It is characterized by chronic inflammation from repeated exposures, but also has a unique pathognomonic feature (with proper exposure history) of giant-cell pneumonitis. Giant cells are created by phagocytic cells, usually macrophages, thought to result from impaired clearance of foreign (dust in HMLD)

particles leading to chronic unresolved inflammation. HMLD symptoms include wheezing and cough, and on spirometry, patients are likely to show obstructive patterns but may also show a mixed obstructive/restrictive pattern [270, 271]. HMLD should be differentiated from hard metal asthma or cobalt asthma [272-274], which is likely to be a cobalt:albumin specific IgE-mediated type I hypersensitivity that is relieved when patients are removed from exposure conditions [275]. Some patients with cobalt asthma progress to HMLD, and it is thought this is due to multifactorial reasons causing some individuals to be more susceptible, though the mechanisms behind this susceptibility have not been identified to date. The mechanism of HMLD is also still largely unknown.

There are several mechanisms known by which cobalt can cause toxicity. Molecularly, it binds to thiol groups with high affinity, such as those in α -lipoic acid (used in the pyruvate dehydrogenase and α -keto glutarate dehydrogenase complexes) and glutathione (essential to the pool of antioxidants and regulation of oxidative stress) [276]. Cobalt can cause further oxidative stress by creation of ROS through Fenton chemistry [277]. More recently cobalt has received attention for its disruption of Ca^{2+} sequestration in cells [269, 278], though it is unknown if this is also related to metabolic disruption affecting ATPase-dependent ion transport. Finally, the displacement of Fe^{2+} from the active sites of enzymes by Co^{2+} has also been documented [279]. PHD enzymes which regulate HIF require Fe^{2+} in their active site, and disruption of this Fe^{2+} by Co^{2+} is possible based on ionic radius [280]. One group has shown that cobalt can cause ascorbate depletion and that this is the limiting factor for PHD activity

[281]. Regardless of the mechanism, cobalt causes PHD inhibition, which prevents HIF hydroxylation, leading to HIF stability and activation of HIF-signaling.

Role of HIFs in cobalt toxicity

Researchers and physicians have known for decades that cobalt is also a hypoxia mimic [282]. Subsequent research has shown that cobalt's mechanism for hypoxia mimicry involves activation of HIF-signaling. Cobalt has the ability to inhibit PHD activity, stabilize HIFs and induce transcription of HIF target genes [151, 280, 283, 284]. Considering these connections, our lab is interested in the role that HIFs may play in cobalt toxicity.

Previous work in our laboratory showed that HIF1 α ^{-/-} mouse embryonic fibroblasts (MEFs) were partially resistant to cobalt toxicity, suggesting HIF1 α contributes to the toxicity of cobalt *in vitro* [285]. The next logical step was to evaluate the *in vivo* role of HIFs in cobalt toxicity. Considering the most widespread exposures were respiratory in nature, this research focused on the lung. A series of transgenic mice were created that are capable of doxycycline-inducible, lung epithelial-specific deletion of HIF1 α , HIF2 α , or both HIF1 α and HIF2 α . Given the *in vitro* results, it was predicted that loss of HIF1 α might provide protection from cobalt-induced lung inflammation. Surprisingly, loss of HIF1 α increased the overall cellularity and significantly altered the inflammatory profile from neutrophilic to eosinophilic and increased markers of asthma, such as YM1/2 as well as other histopathologic changes consistent with allergic airway disease [214]. These results suggested that HIF1 α in lung epithelium has a more nuanced immune modulatory role in response to cobalt-induced inflammation, and may have implications for HIF signaling in allergic airway disease.

Hypotheses and Specific Aims

My hypothesis is that a proper balance of HIF1 α and HIF2 α in lung epithelium is necessary for the establishment of normal immunity in the lung through their influence on inflammation-regulating signaling pathways, including Adora2b and NF- κ B. To test this hypothesis, I have three specific aims:

1. Characterize the relationship between loss of HIF1 α and the changes in lung immunity following cobalt exposure by altering the timing of HIF1 α deletion, performing flow cytometry of lung immune cells, and testing the clinical relevance of this inflammatory switch by determining the impact of neonatal hyperoxia exposure on cobalt-induced inflammation.
2. Determine the role of Adora2b and NF κ B in an oropharyngeal aspiration model of cobalt-induced lung inflammation in HIF1 α -deficient mice using pharmacological inhibitors.
3. Determine the role of epithelial-derived HIF2 α signaling on cobalt-induced inflammation and phenotypically compare these results to HIF1 α -deficient and HIF1 α /2 α -deficient mice.

This dissertation is a summary of experiments performed to fulfill these specific aims.

CHAPTER 2 – MATERIALS AND METHODS

Description of mice

Three strains of mice were used in these studies, all of which utilize the SP-C-rtTA^{+ /tg} / (TetO)₇-CMV-Cre^{tg /tg} system, a doxycycline-inducible, lung epithelial-specific Cre-recombinase system were a gift Jeffrey Whitsett (Cincinnati Children's Hospital Medical Center). Mating between these mice and HIF1 α ^{flox/flox} (a gift from Randall Johnson, University of Cambridge) and/or HIF2 α ^{flox/flox} (a gift from M. Celeste Simon, University of Pennsylvania) resulted in three strains:

1. SP-C-rtTA^{+ /tg} / (TetO)₇-CMV-Cre^{tg /tg} / HIF1 α ^{flox/flox} (HIF1 α ^{fl/fl}) [51, 214, 215, 286],
2. SP-C-rtTA^{+ /tg} / (TetO)₇-CMV-Cre^{tg /tg} / HIF2 α ^{flox/flox} (HIF2 α ^{fl/fl}), and
3. SP-C-rtTA^{+ /tg} / (TetO)₇-CMV-Cre^{tg /tg} / HIF1 α ^{flox/flox} / HIF2 α ^{flox/flox} (HIF1/2 α ^{fl/fl}).

Recombination in the floxed HIF1 α and/or HIF2 α gene, specifically in the respiratory epithelium, occurs when mice are exposed to doxycycline (DOX) (Figure 8) [287]. Throughout this paper these DOX-treated strains will be referred to as HIF1 α ^{Δ/Δ} , HIF2 α ^{Δ/Δ} , or HIF1/2 α ^{Δ/Δ} . Also, the term “-deficient” will also be used interchangeably with the “ Δ/Δ ” to describe the recombined/DOX-treated mice. The bias toward eosinophilic inflammatory response to cobalt in the HIF1 α ^{Δ/Δ} mice does not occur in any other strain or treatment combination except for mice containing all three transgenes that were treated with doxycycline, thus eliminating the possibility that these observed inflammatory changes are due to doxycycline alone or Cre toxicity (Figure 9) [215]. Genotyping of the mice was performed by PCR for the four loci as

Figure 8

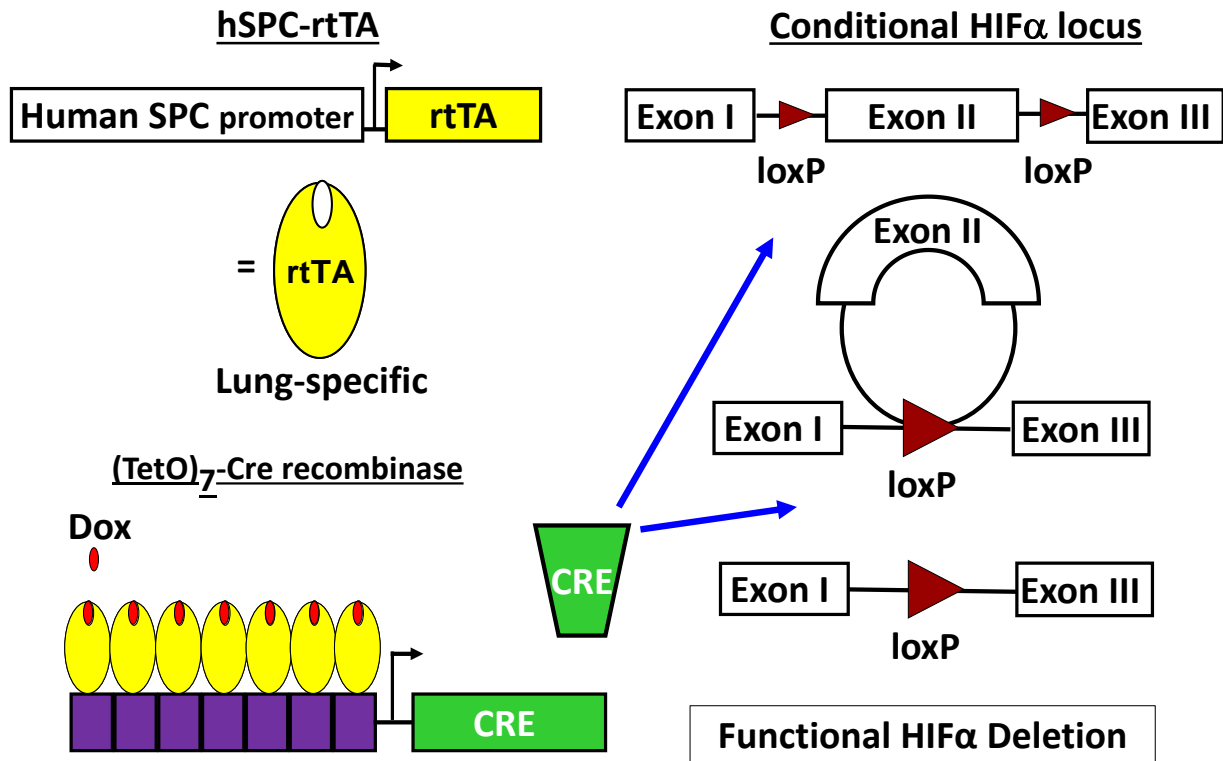


Figure 8. Inducible, lung epithelium-specific transgenic knockout mouse model. The SP-C-rtTA^{tg/-}/(TetO)₇-CMV-Cre^{tg/tg} model system in combination with HIF1 α ^{fl/fl} and/or HIF2 α ^{fl/fl} alleles generates mice functionally deficient in either HIF1 α (HIF1 α ^{Δ/Δ}), HIF2 α (HIF2 α ^{Δ/Δ}) or HIF1 and HIF2 both (HIF1/2 α ^{Δ/Δ}). The first transgene of the system, hSPC-rtTA, features the reverse tetracycline trans-activator (rtTA) protein driven by the human surfactant protein-C (SP-C) promoter, making rtTA expression lung-specific to Club and alveolar epithelial type II (ATII) cells. The second gene in the system, (TetO)₇-CMV-Cre recombinase, allows for Cre-recombinase expression only in the presence of rtTA and doxycycline (DOX) given in food and water. Finally, Exon II of HIF1 α or HIF2 α , required for DNA binding and dimerization of the HIF:ARNT complex, is flanked by loxP sites. These triple transgenic mice are capable of functional deletion of the respective HIF α in the presence of doxycycline.

Figure 9

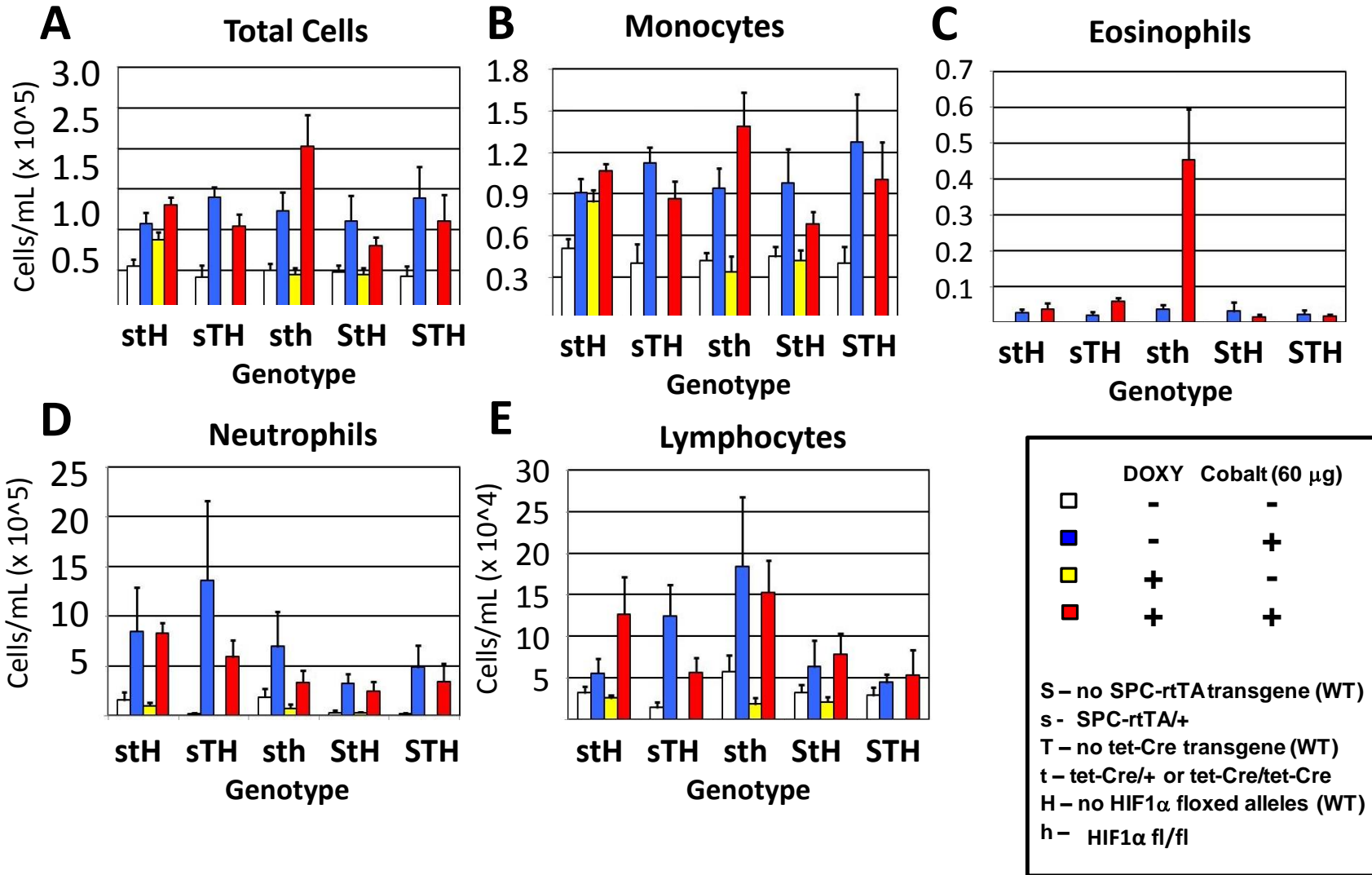


Figure 9. Eosinophilia in HIF1 α ^{fl/fl} mice by genotype and DOX treatment. Mice from every possible genotype in the SP-C- rtTA/

Figure 9 (cont'd)

(TetO)₇-CMV-Cre/HIF1 α ^{fl/fl} were treated with cobalt or saline and BAL was assessed for total cells (**A**) and differentials: macrophages/monocytes (**B**), eosinophils (**C**), neutrophils/PMNs (**D**) and lymphocytes (**E**). *white box = No Dox, Saline; blue box = No Dox, Cobalt; yellow box = DOX, Saline; red box = DOX, Cobalt.* *S = no SPC-rtTA transgene; s = SPC-rtTA^{+/+}; T = no tet-Cre transgene; t = tet-Cre^{/+} or tet-Cre^{+/+}; H = homozygous WT HIF1 α locus; h = HIF1 α ^{fl/fl}*

described previously [286]. Genotyping primers for HIF2 α locus are as follows: 5'-CAG GCA GTA TGC CTG GCT AAT TCC AGT T-3' (Forward) and 5'-CTT CTT CCA TCA TCT GGG ATC TGG GAC T-3' (Reverse) creating fragments of 410bp in the wild-type HIF2 α locus and 444bp in the floxed HIF2 α locus.

All of the mice used in this study were males, and were maintained in a mixed C57BL/6 and FVB/N background. All the procedures regarding the handling, maintenance, exposure and necropsy protocols of the mice used in this study were approved by the university laboratory animal resources (ULAR) regulatory unit at Michigan State University.

Doxycycline treatment and animal husbandry

The SP-C-rtTA^{+/*tg*}/(tetO)₇-CMV-Cre^{*tg*/*tg*} model system, HIF1 α ^{*fl/fl*} mice exposed *in utero* to DOX show lethality upon parturition [286]. Postnatal exposure leads to almost complete loss of HIF1 α from Club and ATII cells without lethality or signs of gross morphologic differences [215]. These studies utilize three different DOX timing protocols, designated as P4-14 (early recombination group), P4-30 (standard recombination group) or P32-42 (adult recombination group). To achieve these different groups, pups were first exposed to DOX through mother's milk, then directly after weaning. Specifically, lactating dams were given DOX-containing feed (625 mg doxycycline/kg; Harlan Teklad, Madison, WI) and drinking water (0.8 mg/ml; MP Biochemicals, Solon, OH) ad libitum beginning on postnatal day 4 (P4) until either cessation at P14 (for P4-14 group) or weaning (occurring around P21) for the P4-30 group). After weaning, mice from the P4-30 groups were maintained on the same DOX-containing food and water directly (ad libitum) for no less than P30. The P32-42 group was given DOX food and water only

from P32-42, and then allowed no less than 10 days to clear the doxycycline from their systems before the start of cobalt dosing (Figure 10). The dose of doxycycline used was slightly lower than the concentration that has been used to induce recombination without any observable toxicity or impact on alveolarization [288]. Control animals in this study were mice containing all the same transgenes ($\text{HIF1}\alpha^{\text{fl/fl}}$, $\text{HIF2}\alpha^{\text{fl/fl}}$ or both in addition to $\text{SP-C-rtTA}^{+/tg}/(\text{tetO})_7\text{-CMV-Cre}^{tg/tg}$) but were given normal (without DOX) food and water ad libitum.

Figure 10

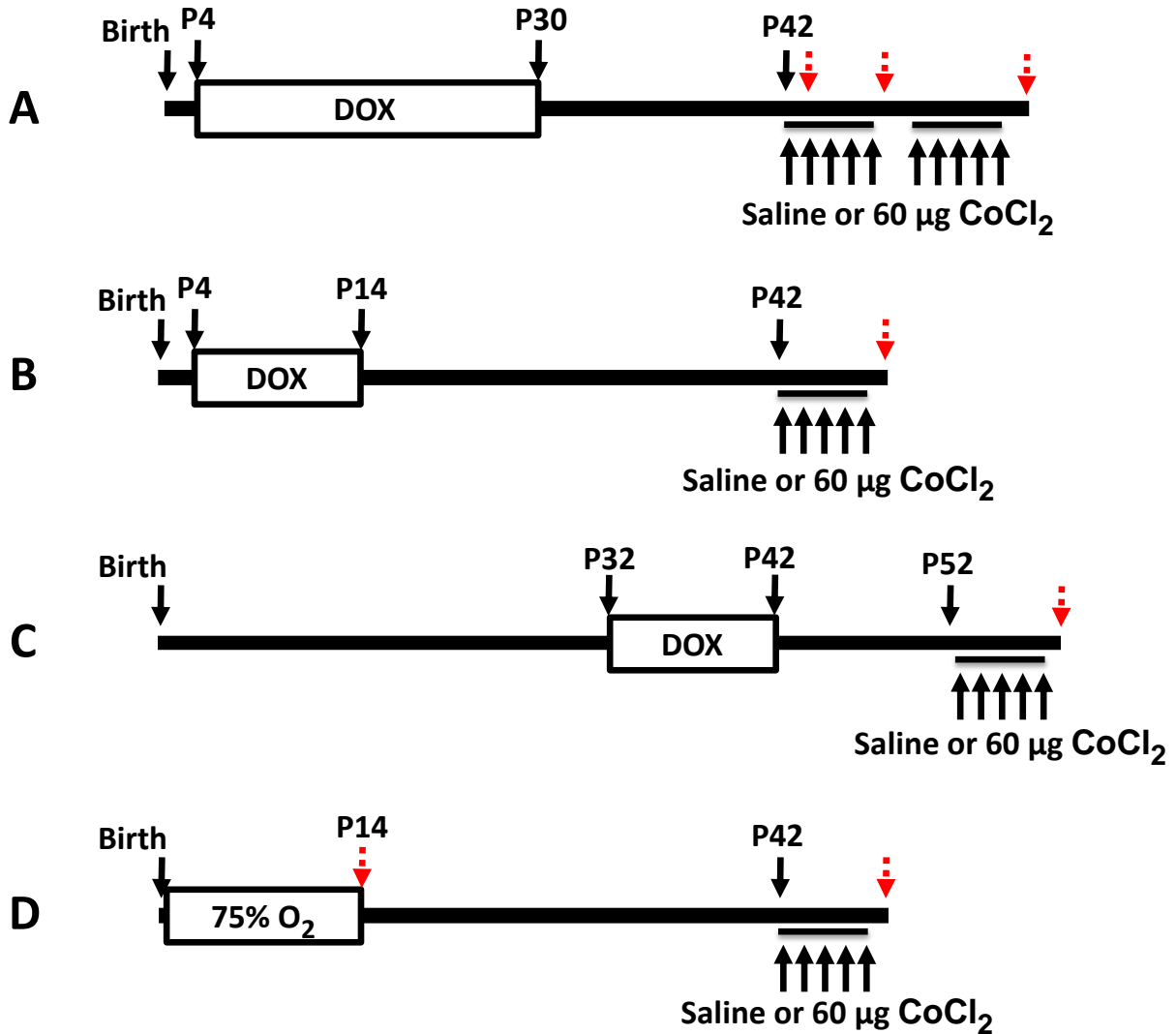


Figure 10. Mouse experiment treatment and dosing schemes. The experimental timeline schemes that were used in these studies. At least one of the schemes in A-D was used in every study. P = postnatal day of mouse age. Sacrifice of mice was made 24 hours after the final dose (red dashed arrows), corresponding to Day 2 (1 dose), Day 6 (5 doses) and Day 14 (10 doses given as 5 once daily doses, 2 day break, 5 once daily doses, 2 day break) (A). The P4-14 DOX protocol (B) and P32-42 DOX protocol (C) were for HIF1 α mice only, and sacrifice was all after 5 doses. Finally, hyperoxia (75% O_2) was given to mouse pups from P0-P14, and samples were taken both at P14 and also after 5 doses (D).

Cobalt exposure

HIF1 $\alpha^{\Delta/\Delta}$, HIF2 $\alpha^{\Delta/\Delta}$, HIF1/2 $\alpha^{\Delta/\Delta}$ mice and their respective floxed controls were randomly assigned to receive either cobalt or saline vehicle. Prior to each daily aspiration, mice were anesthetized with isoflurane using the drop jar method. Oropharyngeal aspirations of 25 μ L of either 10 mM cobalt chloride or sterile saline vehicle were given once daily. This dose of cobalt corresponds to a daily dose of 60 μ g CoCl₂ per mouse, doses known to reliably reproduce substantial inflammation [214, 215]. Most commonly, five consecutive daily doses of cobalt were given after DOX has cleared from the system of mice (no less than 10 days). However, for HIF2 α mice, a single cobalt dose group (called “1 day” group) or 2 weeks of dosing (5 days dosed, 2 days off, 5 days dosed, 2 days off, called “14 day” group) were also performed to better understand the time-course of cobalt exposure in this strain. All mice were sacrificed 24 hours after their final dose (Fig. 10).

PSB1115 exposure

PSB1115 is a specific inhibitor of the adenosine A2B receptor. It was utilized in a pilot study of acute (5 day) cobalt-induced lung inflammation in HIF1 α -deficient mice. PSB1115 (Tocris Bioscience) was dissolved in saline and sterilized via a 0.22 μ m filter each day before injection. Fifteen (15) minutes prior to each cobalt exposure, mice were injected i.p. at 30 mg/kg. Previous studies by Eckle et al. using this compound at 10 mg/kg in mice have shown that Adora2b antagonism increases vascular leak and prevents the usual fluid clearance from the lung [251]. The 30 mg/kg dose was chosen to minimize the number of injections to the mice and also ensure that adequate PSB1115 reached the lung.

TCH013 exposure

TCH013 is a compound comprised of an imidazoline scaffold with four benzene rings created at Michigan State University by Dr. Jetze Tepe and colleagues. This compound decreased TNF α concentrations and histopathologic severity of a collagen-induced rheumatoid arthritis mouse model [289]. This compound was tested for its ability to alter the response to cobalt-induced lung injury in CTL and HIF1 α -deficient mice. Fresh TCH013 was prepared immediately prior to each daily dosing by combining 97.5 mg of TCH013 (white powder) and 2 mL of 30% propylene glycol (vortexing vigorously until dissolved), and then adding a total of 4.5 mL of 5% dextrose (warmed to 37°C) in 1 mL aliquots (vortexing with each addition so each aliquot was well incorporated into homogeneous solution). Concentration of final solution was 15 mg/mL, and each mouse received 150 mg/kg (or vehicle control). Mice were injected intraperitoneal (i.p.) with TCH013 one hour prior to receiving their daily doses of cobalt.

LPS exposure

HIF1 α ^{fl/fl} mice treated with regular food and water or DOX from P4-30 or P4-32 were dosed once intranasally (under regulated isoflurane anesthesia) with 15 μ L in each nostril of LPS (1.67 μ g/ μ L) for a total of 50 μ g LPS (Sigma, St. Louis, MO) per mouse. Mice were sacrificed 24 hours later and standard tissues taken (described below).

Hyperoxia exposure

Mice were exposed to hyperoxia using a custom airtight regulated plexiglass glove box from Coy Laboratories (Grass Lake, MI). Temperature was controlled via the main control unit

that can be manually controlled to within 0.1°F or C. Humidity was automatically set to prevent condensation based on temperature by the main control unit and is impossible to change manually. O₂ and CO₂ concentrations were regulated by sensors opening to the inside of the glove box and a control unit for each above the glove box, and N₂ was used as a background gas. O₂ could be set from 0-100% in 0.1% increments. CO₂ could be set from 0-20% in 0.1% increments. Additionally, the glove box was fitted with a filtration system to avoid accumulation of ammonia and carbon dioxide by animals. The filtration system was activated by CO₂ concentrations that reach 0.1% or greater, and when activated a pump pushed air from chamber through the filtration system and back into the chamber, until CO₂ again reached 0-0.1%.

Mice from litters born on the same day were randomized into litters of 10 before the exposure began. Hyperoxia exposed mice were placed in the chamber (75% O₂, 0% CO₂ and 25°C). Lactating dams were removed from the hyperoxia and replaced every 12 hours to avoid causing their hyperoxic stress, and animals were kept on a 12 hour light/dark cycle. Additionally, pups were checked every 12 hours for signs of hyperoxic stress or death, and removed if death occurred. Conditions were maintained throughout the experiment by using the purge box for anything entering or leaving the glove box, replacing animal food, gases and filtration material as needed. Exposures began on P0 (first post-natal day) and continued until P14, at which point mice were returned to normoxia. No doxycycline was given at any point

during these experiments. Mice were dosed with a 5d cobalt oropharyngeal aspiration protocol (described above), and sacrificed for necropsy 24 hours after the last dose of cobalt.

Necropsy, tissue harvesting and processing

Mice to be sacrificed were anesthetized by an i.p. injection of 1000-1300 mg/kg Avertin (2,2,2-tribromoethanol, Sigma-Aldrich, St. Louis, MO). Upon successful blockade of afferent pain sensation, a midline laparotomy was performed and mice were exsanguinated by transecting the renal artery. The lungs were exposed, and trachea cannulated. Heart and lungs were removed en bloc and sterile saline was used in two successive 1 mL lavages to make bronchoalveolar lavage (BAL). Total cells were counted using a hemacytometer and differential cell counts were made from CytoSpin samples of BAL stained with DiffQuick reagent (Baxter, FL). Right lung lobes were snap-frozen in liquid nitrogen for later RNA and protein analysis. Left lung lobes were gravity-inflation fixed at 30 cm pressure with 10% phosphate buffered formalin for histopathological and immunohistochemistry (IHC) analyses.

Histopathology and immunohistochemistry

Changes in histopathological properties were assessed by using formalin-fixed left lung lobes cut at the 5th and 11th generation (G5/11, to differentiate shallow from deeper lung). Dissected lungs were paraffin embedded, cut to 5 µm sections, mounted on glass slides, and stained with hematoxylin and eosin (H&E) for general histopathology. Alcian blue (pH 2.5) periodic acid Schiff (AB-PAS) stain was used to detect mucosubstances. Immunostaining was performed for major basic protein (MBP; polyclonal rabbit anti-mouse MBP, 1:500, Mayo Clinic, Scottsdale, AZ) as described previously [214]. Immunostaining for HIF1α (polyclonal rabbit anti-

HIF1 α , 1:100, Novus Biologicals NB100-479, Littleton, CO) or HIF2 α (polyclonal rabbit anti-HIF2 α , 1:100, Novus Biologicals NB100-122, Littleton, CO) was performed using the Vectastain Elite ABC Kit (Rabbit IgG) as described previously [286].

Gene expression analysis by qRT-PCR

Snap frozen lung tissue was homogenized in TRIzol reagent (Life Technologies, Carlsbad, CA) using a Retsch MM200 bead beater system (Retsch, Haan, Germany). Total RNA was quantitated spectrophotometrically (Nano-Drop ND-1000 UV-Vis Spectrophotometer). Total RNA (1 μ g) was reverse transcribed using Superscript III (Life Technologies, Carlsbad, CA), and quantitative real-time PCR reactions were performed using gene-specific primers (listed in Table 3) and Power SYBR Green PCR Master Mix on an ABI PRISM 7000 (Life Technologies, Carlsbad, CA). Gene expression was measured using the standard curve method with hypoxanthine guanine phosphoribosyl transferase (Hprt) as the housekeeping gene. Expression was normalized to Hprt for all samples, and the fold change of the control saline treated group was set to 1.

Table 3. List of primers for mouse genotyping and qRT-PCR.

Gene	For (5'-3')	Rev (5'-3')	Amplicon Size (bp)
SP-C-rtTA	GACACATATAAGACCCTGGTCA	AAAATCTTGCCAGCTTTCCCC	350
Cre	TGCCACGACCAAGTGACAGCAATG	AGAGACGGAAATCCATCGCTCG	374
HIF1 α	GCAGTTAAGAGCACTAGTTG	GGAGCTATCTCTCTAGACC	274(fl) 240 (wt)
HIF2 α	CAGGCAGTATGCCTGGCTAATTCCAGTT	CTTCTTCCATCATCTGGGATCTGGGACT	444 (fl) 410 (wt)
Hprt	TTCCGGAGCGGTAGCACCTCC	ATCATCGCTAATCACGACGCTGGG	113
Bnip3	GGCGTCTGACAACCTTCCACT	AACACCCAAGGACCATGCTA	123
Csf2	ATTCGAGCAGGGTCTACGGGGC	TTTCACAGTCCGTTTCCGGAGTTGG	110
Adora2b	CGGACTTCCACGGCTGCCTC	TTTATACCTGAGCGGGACGCGA	125
p65/relA	TGCCTACCCGAAACTCAACT	TTGAGATCTGCCCTGATGGT	126
Hmox1	GGCCTGAACTTTGAAACCAG	GTCGTGGTCAGTCAACATGG	122
TNF α	CCACGTCGTAGCAAACCACC	ACAAGGTACAACCCATCGGC	132
IFN γ	CACGGCACAGTCATTGAAAGC	TTCATGTCACCATCCTTTTGCC	125
IL-1 β	GCAGCTGGAGAGTGTGGATCCCA	GGTGTGATGTACCAGTTGGGGA	133
Ccl17	CATGCCAGAGCTGCTCGAGCC	ACACGATGGCATCCCTGGAACA	133
Ccl20	CCAGGCAGAAGCAGCAAGCAAC	TCACAAGCTTCATCGGCCATCTGTC	111
Arg1	AAAGGACAGCCTCGAGGAGGGG	AGGTCCCCGTGGTCTCTCACG	110
iNOS	GCAACTACTGCTGGTGGTGA	AAGGCCAAACACAGCATACC	129
IL-2	AGATGAACTTGGACCTCTGCG	TGTGTTGTCAGAGCCCTTAG	130
IL-4	AGGTCACAGGAGAAGGGACGCC	TGCGAAGCACCTTGAAGCCC	114
IL-5	CCGCCAAAAAGAGAAGTGTGGCGA	GCCTCAGCCTTCCATTGCCCA	112

Table 3 (cont'd)

IL-6	TCCTCTCTGCAAGAGACTTCCATCC	ACAGGTCTGTTGGGAGTGGTATCC	127
IL-10	CCAGTTTTACCTGGTAGAAGTGATG	TGTCTAGGTCCTGGAGTCCAGCAG ACTC	324
IL-13	GCTGGCGGGTTCTGTGTAGCC	ATCGGGGAGGCTGGAGACCG	132
IL-17A	GGACTCTCCACCGCAATGAAGACC	TCATGTGGTGGTCCAGCTTTCCC	111
IL-25	TGTACCAGGCTGTTGCATTCTTGGC	CACTCCTCCGGGGTTCTTGC	127
IL-33	CAGGCGACGGTGTGGATGGG	CGTCACCCCTTTGAAGCTCCACG	117
TSLP	GGACTGTGAGAGCAAGCCAGC	CTGGGCAGTGGTCATTGAGGGC	134
Ym1	AGCTTTTGAGGAAGAATCTGTGG	AAGAGACTGAGACAGTTCAGGG	121
Ym2	TGAGGAAGAATCCACTTTGAACC	GAGAGACTGAGACAGTTCAGGG	115
Eotaxin	GCGCTTCTATTCTGCTGCTCACGG	GTGGCATCCTGGACCCACTTCTTC	239
Eotaxin2	CTTGCTGCACGTCCTTTATTTCCA	GGTCAGTACAGATCTTATGGCCCT	135

Cytokine bead array

Cytokines were measured from BAL or whole lung lysates (WLL). WLL is generated from snap-frozen tissues in RIPA buffer using the bead beater system described above. RIPA buffer contained protease inhibitors aprotinin, leupeptin and pepstatin (1 µg/mL each, Sigma-Aldrich, St. Louis, MO), complete Mini Protease Inhibitor Cocktail (1 pellet / 10 mL RIPA Buffer, Roche) and phenylmethylsulfonyl fluoride (PMSF, 1 mM), phosphatase inhibitors sodium orthovanadate (Na_3VO_4 , 1 mM) and sodium fluoride (NaF, 1 mM), and EDTA (1 mM).

Homogenates were centrifuged at 16,000 g for 15 min at 4°C and the supernatant was quantified for protein content using the Bradford Assay (BioRad, Hercules, CA) [290]. 50 µL of each sample supernatant was used for maximum detection of cytokines IL-2, IL-4, IL-5, IL-6, IL-10, IL-13, IL-17A, IFN γ and TNF α using the Th1/Th2/Th17 Cytometric Bead Array Kit, IL-5/IL-13 Flex Sets and analyzed on a FACSCalibur flow cytometer according to manufacturer's protocols (BD Biosciences, San Jose, CA). For WLL, cytokine content was then normalized to total protein in each sample, whereas BAL was analyzed without normalization.

Flow cytometry of lung immune cells

Right lung lobes from each treatment group were disrupted using a cell dissociation sieve kit (CD-1, Sigma) to obtain a single cell suspension and stored in ice-cold RPMI. After suspensions were obtained, cells were restimulated with phorbol myristate acetate (PMA; 40 nM) and ionomycin (Io; 0.5 µM) (both from Sigma) for 6h in 2% fetal bovine serum (FBS) RPMI and 1× Brefeldin A (Biolegend, San Diego, CA). All staining was performed in 96-well round bottom plates (BD Falcon, Franklin Lakes, NJ). Cells isolated from the lungs were washed with

FACS buffer (1× HBSS, 1% bovine serum albumin, 0.1% sodium azide, pH 7.6), and surface Fc receptors were blocked with anti-mouse CD16/CD32 (BD Biosciences, Franklin Lakes, NJ) for 15 min at 4°C. Cells were labeled for 30 min at 4°C with CD4 (clone RM4-5) and CD8 (53–6.7) (Biolegend). Subsequently cells were washed thrice with FACS buffer, fixed with Cytofix (BD Biosciences) for 15 min, and resuspended in FACS buffer. After surface staining, cells were washed twice with 1× Perm/Wash (BD) and incubated with 1× Perm/Wash for 30 min at room temperature in 96-well round bottom plates. Fluorescently labeled antibodies were added at 0.25–0.5 µg/mL in 200 µL for 30 min. The following fluorescently labeled antibody clones were used: IFN γ (XMG1.2, Biolegend) and GATA-3 (TWAJ, eBioscience). Cells were washed twice with 1× Perm/Wash and subsequently resuspended in FACS buffer. After intracellular staining, cells were analyzed the same day. Compensation and voltage settings of fluorescent parameters were performed using single color staining controls. Cells were identified as positive for cytokine secretion after gating on the negative population in unstimulated samples (without PMA/Io or Brefeldin A). Fluorescent staining was analyzed using a BD Accuri C6 flow cytometer (Franklin Lakes, NJ). Fluorescence was quantified using CFlow software (BD Accuri, San Jose, CA).

Statistical analytical methods

All quantitative analyses were performed using the OriginPro 8 suite of statistical software (OriginLab, Northampton, MA). Unless otherwise stated, analyses were by One-way ANOVA using Fisher's LSD method ($\alpha=0.05$). All error bars are presented as standard error of the mean (SEM). Any data with P value < 0.05 were considered significant.

**CHAPTER 3 – MECHANISTIC INVESTIGATIONS OF THE EOSINOPHILIC PHENOTYPE
OF MICE DEFICIENT IN HIF1 α IN LUNG EPITHELIUM TREATED WITH COBALT**

Results

Timing of HIF1 α Deletion and Eosinophilia

HIF1 α ^{fl/fl} mice were randomly assigned to receive either regular food and water or DOX food and water in 3 time points: P4-14, P4-30, or P32-42. After no less than 10 days to clear DOX, mice received 5 consecutive once daily doses of 25 μ L saline or 10 μ M CoCl₂ via oropharyngeal aspiration, and were sacrificed 24 hours after final dose (~P58). Total cells and differentials were counted from BAL. Total cells from BAL of saline-treated mice were negligible and did not change with DOX treatment. Total cells from BAL of cobalt-treated mice were higher than in their saline counterparts, except for the P32-42 group, suggestive that this latter group of mice was protected. The number of total cells was highest in the P4-14 group, which was statistically different than all other cobalt treated groups. Numbers of total cells from the control and P4-30 groups treated with cobalt were both statistically lower than the P4-14 group, though they did have higher number of total cells than their saline controls (Figure 11A). When looking at the differentials of these total cells, the P32-42 group had fewer numbers of all types of cells (macrophages, eosinophils, PMNs and lymphocytes) (Figure 11B, 12 and 13). The macrophages in the P4-30 group were higher than the P4-14 and P32-42 cobalt treated groups (Figure 11B). Numbers of eosinophils increased in both the P4-14 and P4-30 groups compared to the control (Figure 12A). The eosinophilic response from the P4-14 group was higher than we generally see in our P4-30 model, and are likely the major contributing factor to the P4-14 group having the highest number of total cells. Numbers of neutrophils did

Figure 11

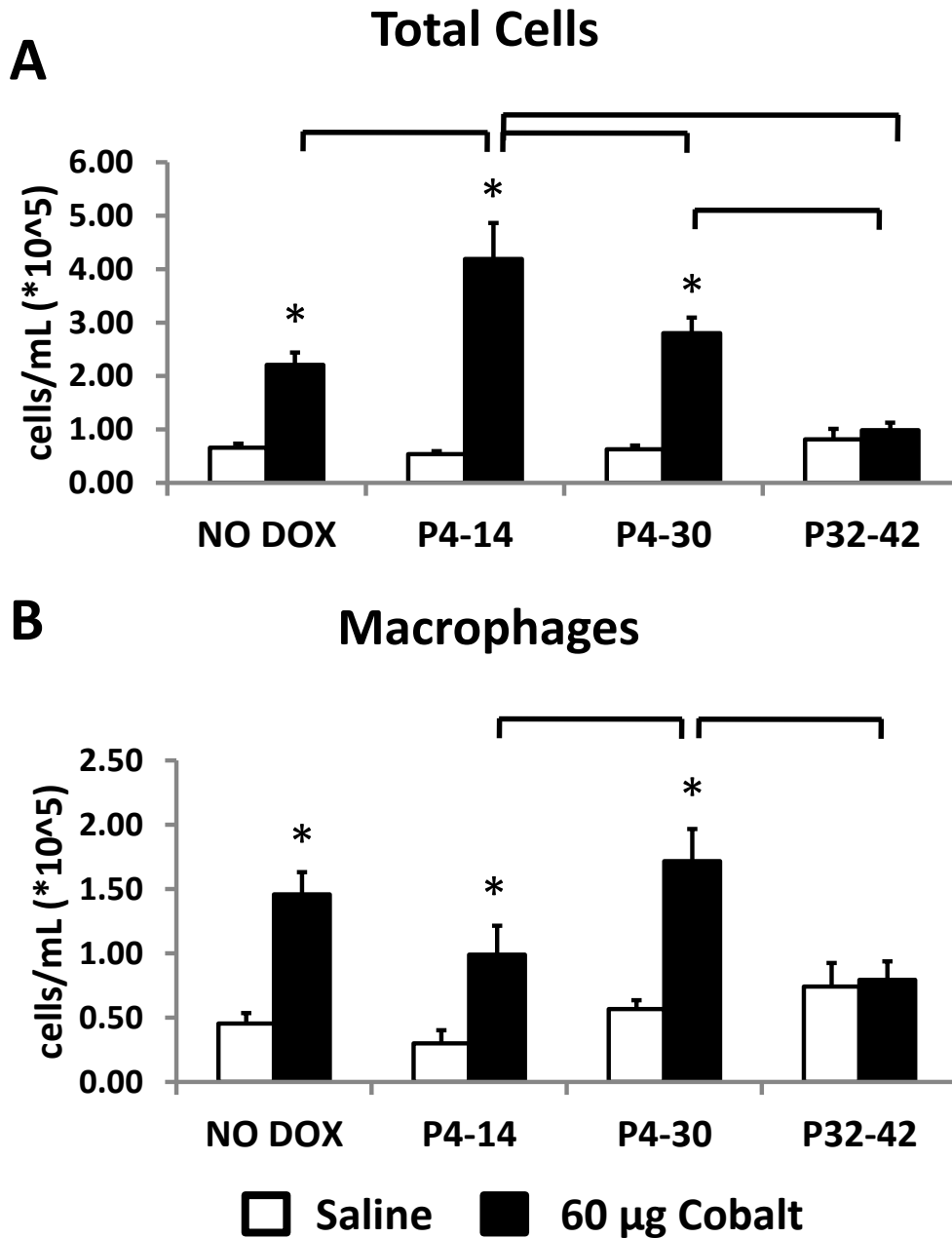


Figure 11. BAL total cells and macrophages from various DOX regimens in HIF1 α mice treated with 5d cobalt. Mice treated once daily for 5 days with 60 μ g Co/mouse/day. **A.** Total Cells; **B.** Macrophages; white bars = SAL, black bars = COB; * = significant compared to SAL control, black brackets = significant across groups of cobalt exposed mice ($\alpha=0.05$ for One-way ANOVA with Fisher's LSD).

Figure 12

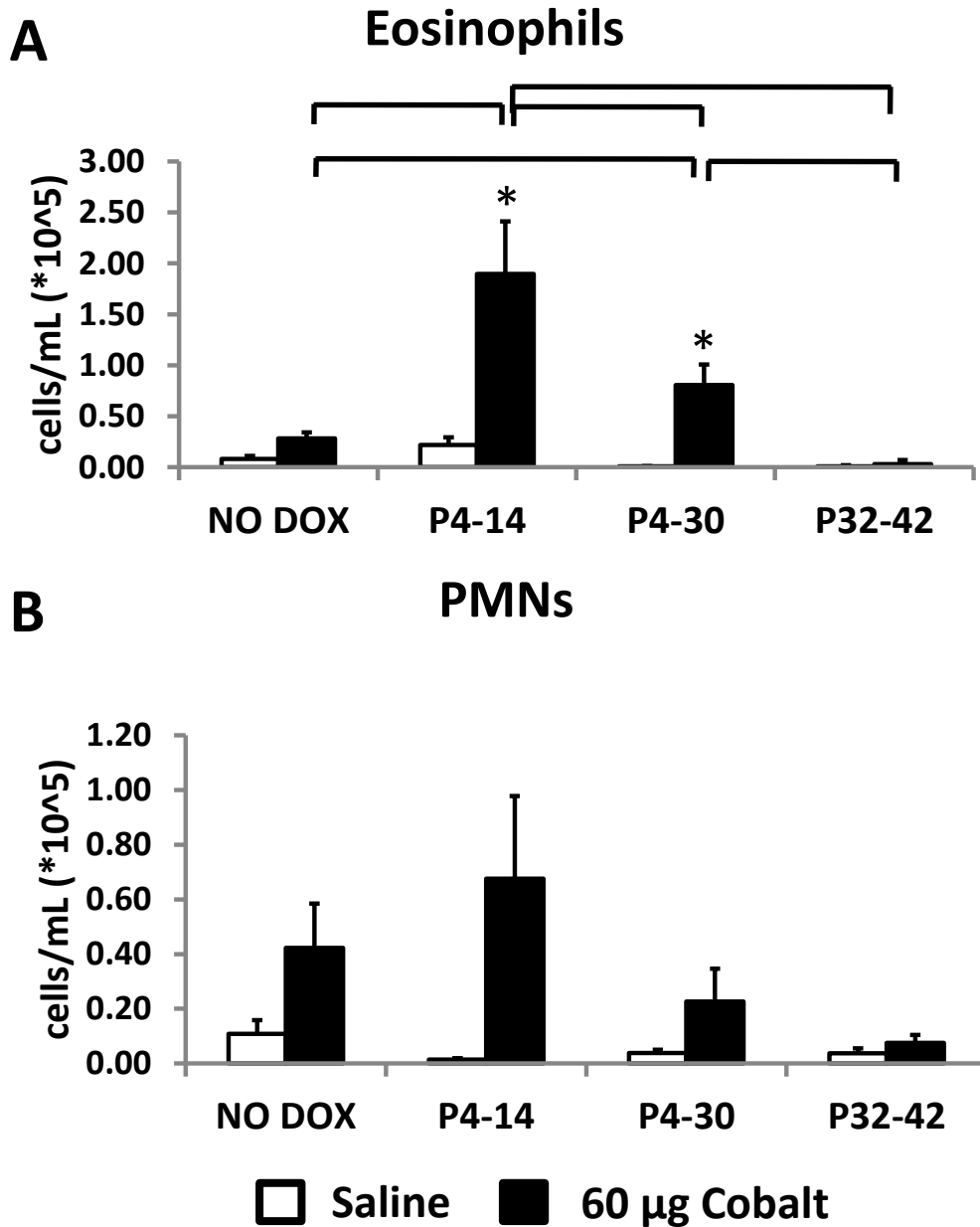


Figure 12. BAL eosinophils and neutrophils (PMNs) from various DOX regimens in HIF1 α mice treated with 5d cobalt. Mice treated once daily for 5 days with 60 μ g Co/mouse/day. **A.** Eosinophils; **B.** PMNs; white bars = SAL, black bars = COB; * = significant compared to SAL control, black brackets = significant across groups of cobalt exposed mice ($\alpha=0.05$ for One-way ANOVA with Fisher's LSD).

not change across the control, P4-14 or P4-30 groups treated with cobalt, but P32-42 had a statistically lower amount than all the others (Figure 12B). Interestingly, lymphocytes in the P4-

14 and P4-30 groups increased when treated with cobalt, and in the P4-14 group were higher than all other cobalt-treated groups (Figure 13).

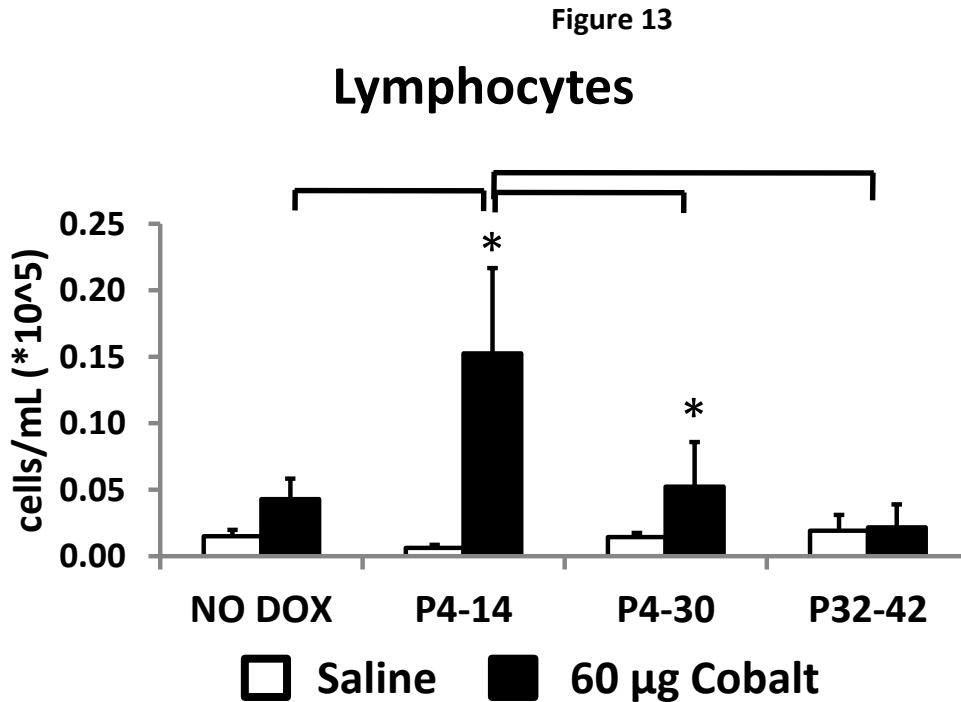


Figure 13. BAL lymphocytes from various DOX regimens in HIF1 α mice treated with 5d cobalt. Lymphocytes from BAL of mice treated once daily for 5 days with 60 μ g Co/mouse/day; *white bars = SAL, black bars = COB; * = significant compared to SAL control, black brackets = significant across groups of cobalt exposed mice ($\alpha=0.05$ for One-way ANOVA with Fisher's LSD).*

Determination of T_H2 Inflammation by Flow Cytometry

Mice that followed a standard 5 day cobalt exposure protocol had BAL taken and single cell suspensions were made from the right lung lobes. BAL cells in addition to lung suspensions were stained with different fluorescent markers. Extracellular staining for CD4 (T_H) and CD8 (T_C) was performed, followed by intracellular staining for IFN γ (T_H1 marker) and GATA3 (T_H2 marker) and analyzed by flow cytometry. Mice lacking one of the transgenes of our model, the

SP-C-rtTA (rtTA), were included to determine if there was an effect of DOX treatment alone. Strikingly, the T_H2 cells (CD4+GATA3+) were highest among the cobalt treated mice that received DOX and were also rtTA+, showing direct evidence of an exacerbated T_H2 response (Figure 14). There were no statistically significant differences in the T_H1 population across the groups, though the absolute mean for cobalt treated HIF1 α -sufficient mice (with all 3 transgenes, but no DOX) was highest. The overall percentage of the T-helper population that was T_H1 was much lower than the other two populations (Figure 15). The cytotoxic T cell population (T_C) was highest in the DOX/Cobalt/rtTA+ group (Figure 16).

Figure 14

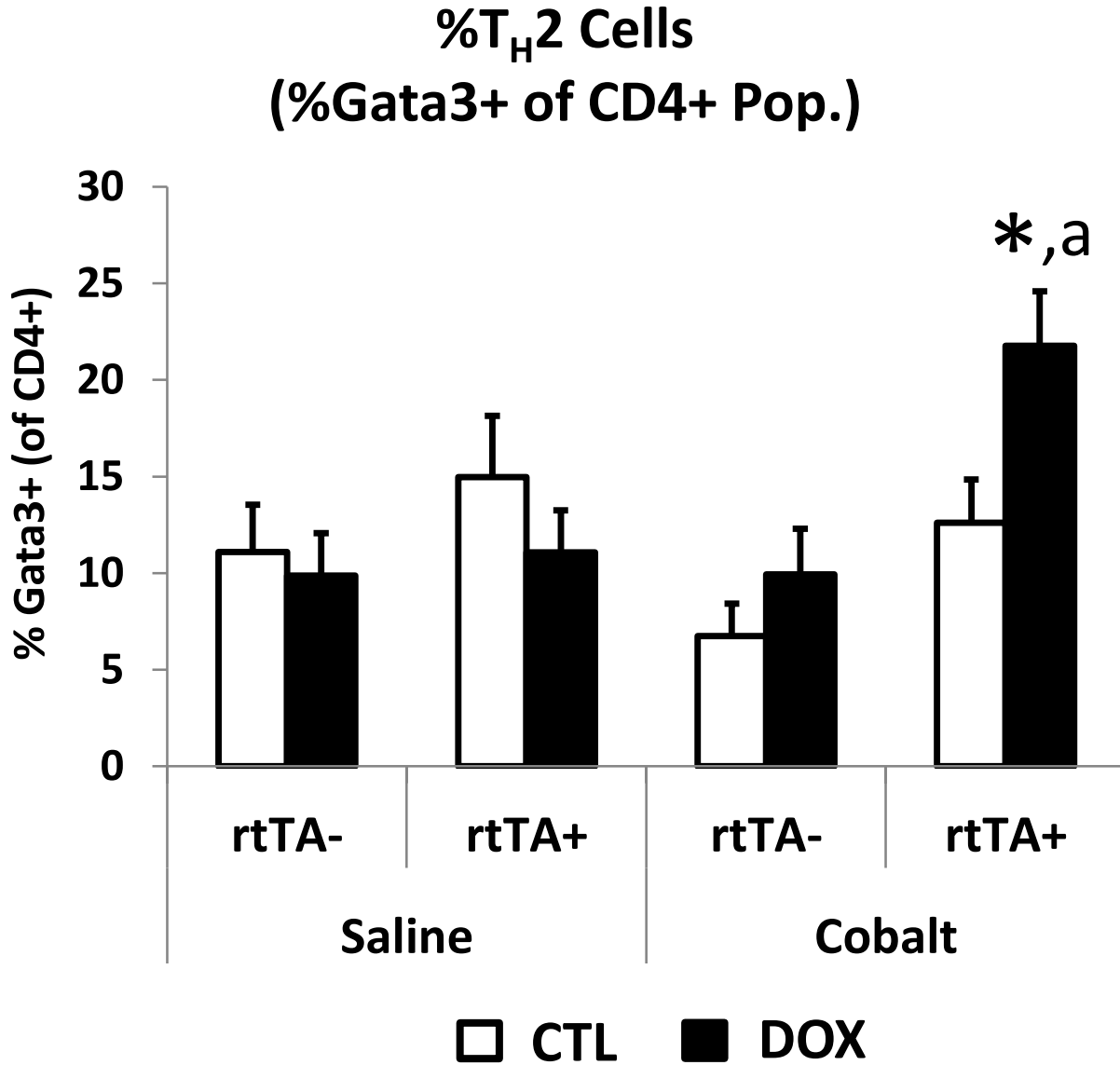


Figure 14. T_H2 immune cell populations in HIF1 α mice with 5d cobalt. T_H2 cells are quantified as a percentage of CD4+ cells that show GATA3+ staining. Data above represents a combination of both cells from BAL and whole lung suspensions. * = significant from CTL within treatment and genotype, a = significant from all other cobalt treated groups, brackets = significant across genotype or treatment, One-way ANOVA with Fisher's LSD, $\alpha = 0.05$.

Figure 15

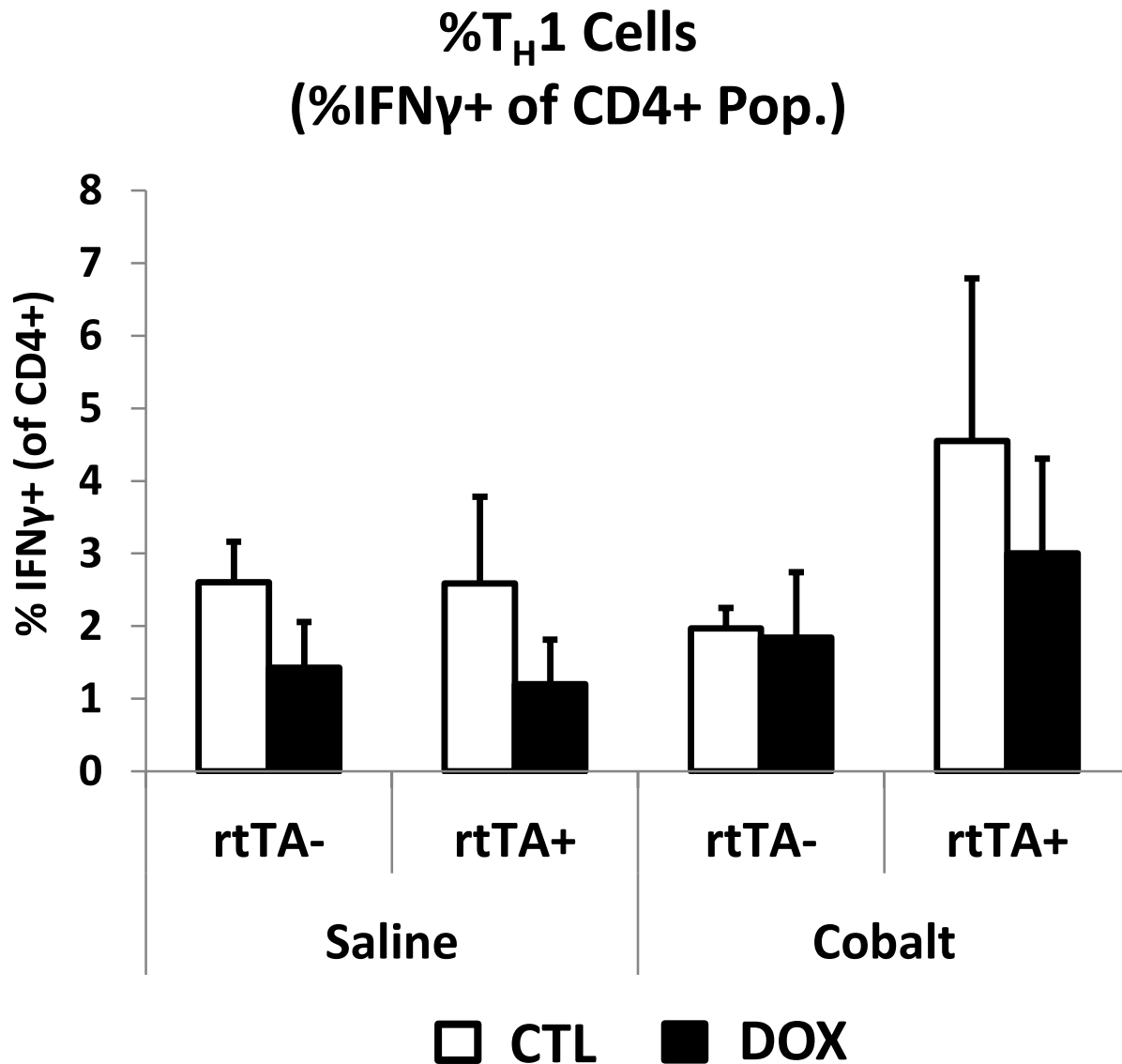


Figure 15. T_H1 immune cell populations in HIF1 α mice with 5d cobalt. T_H1 cells are identified as a percentage of CD4+ cells also staining positive for IFN γ . Data above represents a combination of both cells from BAL and whole lung suspensions. * = significant from CTL within treatment and genotype, a = significant from all other cobalt treated groups, brackets = significant across genotype or treatment, One-way ANOVA with Fisher's LSD, $\alpha = 0.05$.

Figure 16

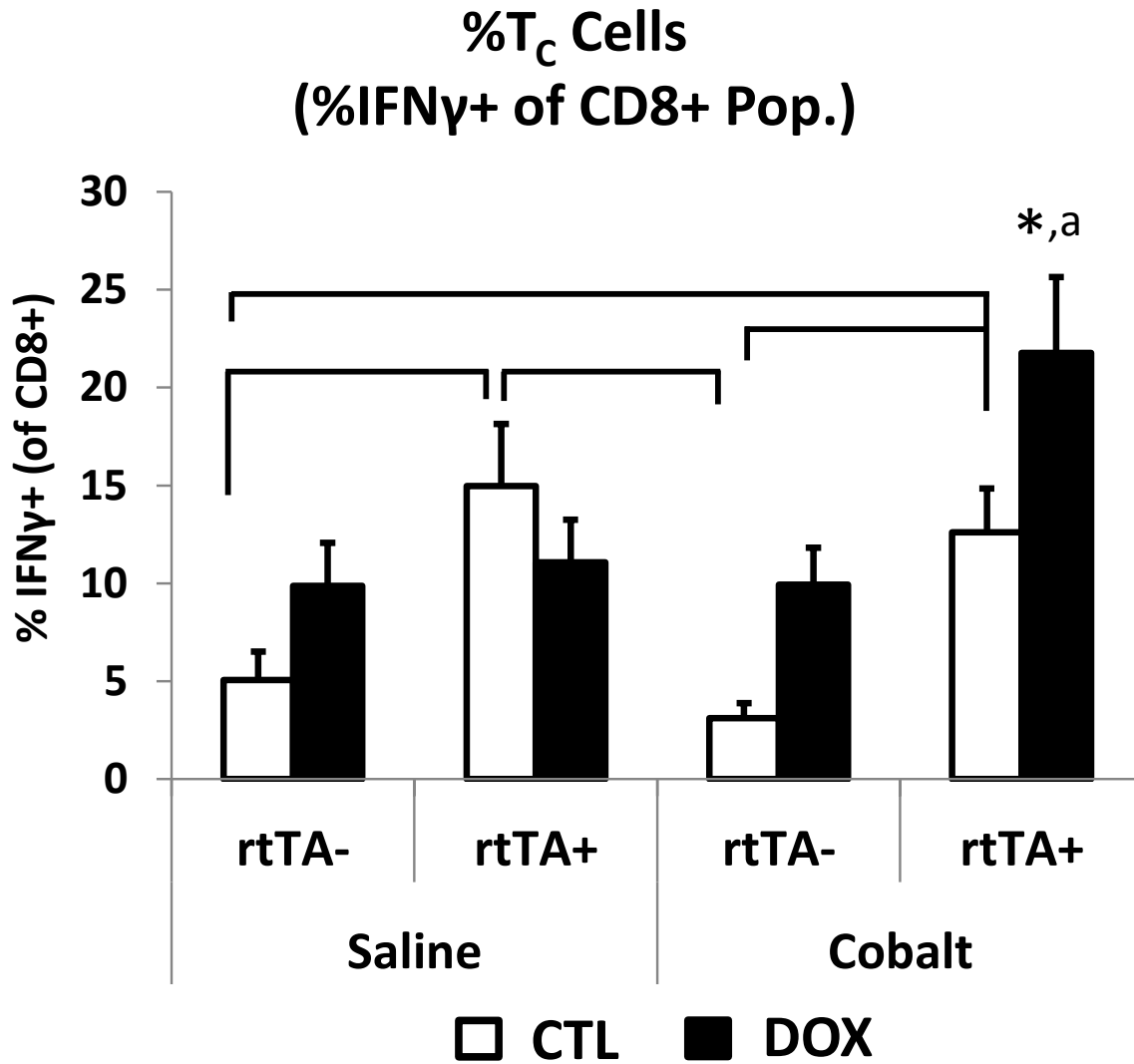


Figure 16. T_C immune cell populations in HIF1 α mice with 5d cobalt. Cytotoxic T lymphocytes (T_C) are quantified as a percentage of CD8+ cells also showing IFN γ staining. Data above represents a combination of both cells from BAL and whole lung suspensions. * = *significant from CTL within treatment and genotype*, a = *significant from all other cobalt treated groups*, brackets = *significant across genotype or treatment*, One-way ANOVA with Fisher's LSD, $\alpha = 0.05$.

PSB1115 and Adora2b in Cobalt-Induced lung injury

Previous investigation revealed that the HIF1 $\alpha^{\Delta/\Delta}$ mice lost staining for Adora2b in the lung epithelium, though it was still visible in the alveolar macrophages (Figure 17). Both the bronchial airway (BA) (Figure 17A and C) and parenchymal (Figure 17B and D) regions show the same pattern of stain loss.

Figure 17

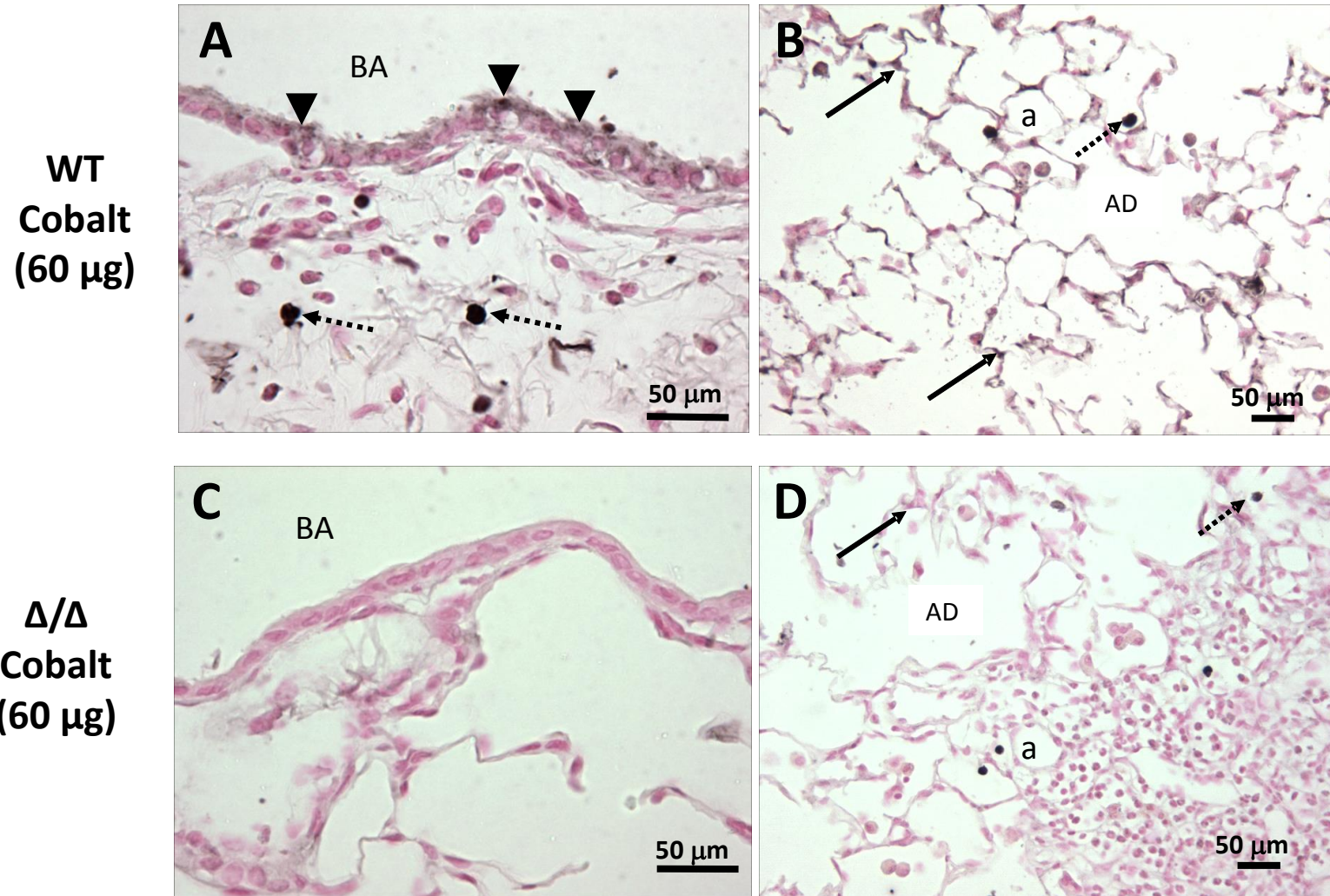


Figure 17. IHC for Adora2b in lungs of cobalt treated CTL and HIF1 $\alpha^{\Delta/\Delta}$ mice. All mice were treated with cobalt. Control mice (containing all transgenes necessary for HIF1 α deletion but kept on regular food and water) are on top (**A and B**), while DOX-treated

Figure 17 (cont'd)

mice ($\text{HIF1}\alpha^{\Delta/\Delta}$) are below (**C and D**). Panels A and C taken from bronchial airway, B and D from the parenchymal regions. *Arrowhead = bronchial epithelial cell, solid arrow = ATII cell, dashed arrow = alveolar macrophage; BA=bronchial airway, AD=alveolar duct, a=alveolus. Black line indicates 50 μm .*

Given the loss of Adora2b staining in HIF1 $\alpha^{\Delta/\Delta}$ mice, it was hypothesized that Adora2b inhibition would exacerbate cobalt-induced lung inflammation in controls, with little to no effect on the HIF1 $\alpha^{\Delta/\Delta}$ mice. To test this, mice were exposed to the Adora2b-specific inhibitor, PSB1115 (30 mg/kg injected i.p.) prior to a once daily dosing of 60 μ g cobalt for 5 days. Upon sacrifice, BAL fluid was taken from the mice to assess total cells and differentials as a measure of inflammation. PSB1115, which has been shown to exacerbate models of inflammation in the lung, had little to no exacerbating effect on cobalt-induced lung inflammation (Figures 18-20). Total cells did increase in HIF1 $\alpha^{\Delta/\Delta}$ mice treated with cobalt, though PSB1115 treatment did not worsen this effect (Figure 18A). There were no observable changes in macrophage populations (Figure 18B). Unexpectedly, the number of eosinophils decreased with PSB1115 treatment in cobalt-treated HIF1 $\alpha^{\Delta/\Delta}$ mice (Figure 19A), and numbers of neutrophils seemed to increase with PSB1115 treatment, but only in HIF1 $\alpha^{\Delta/\Delta}$ mice (Figure 19B). There were no observable changes in lymphocyte populations (Figure 20).

Figure 18

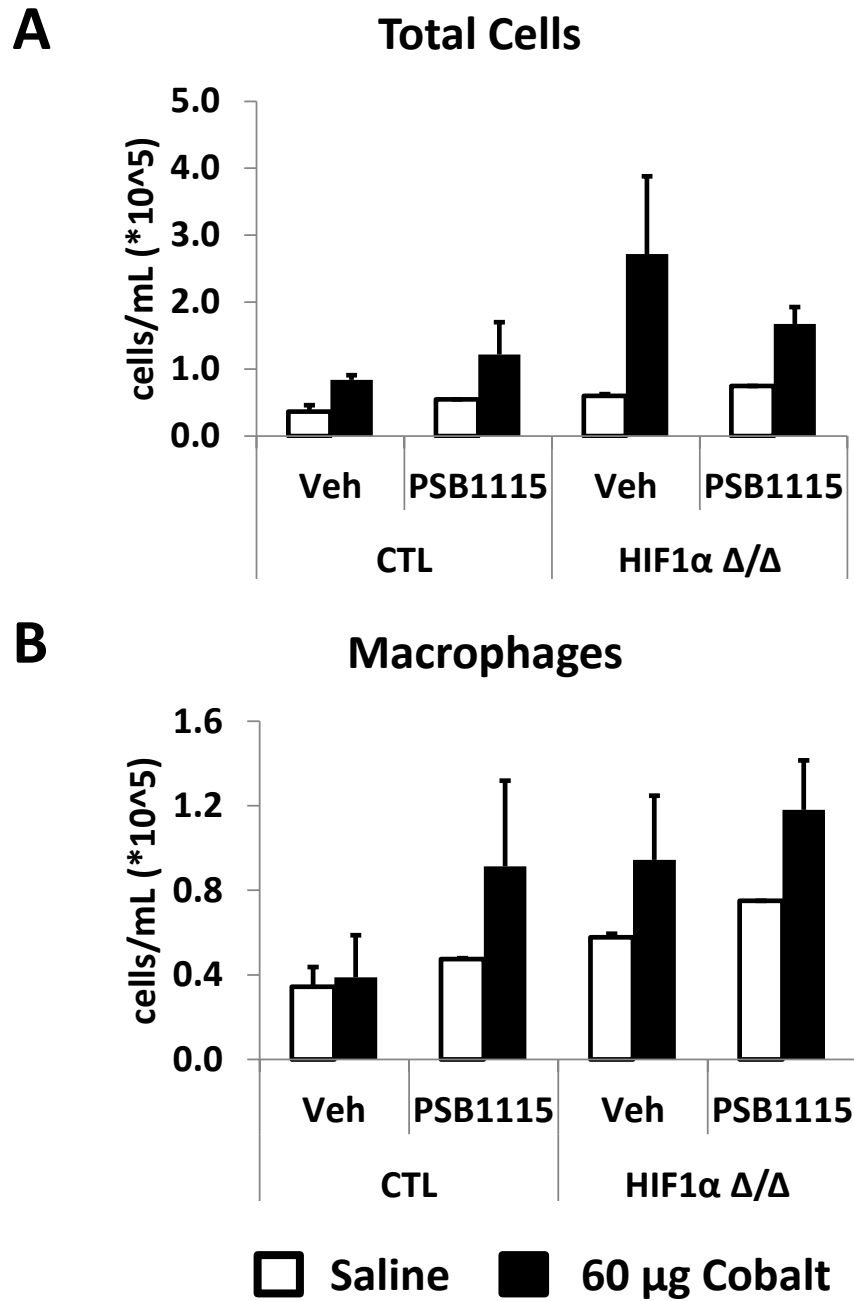


Figure 18. BAL total cells and macrophages from HIF1 α mice treated with cobalt for 5 days +/- PSB1115. Bronchoalveolar lavage (BAL) was counted for total cells (A) and macrophages (B). Some groups contained 2 mice due to deaths which rendered the data insufficient for statistical analyses.

Figure 19

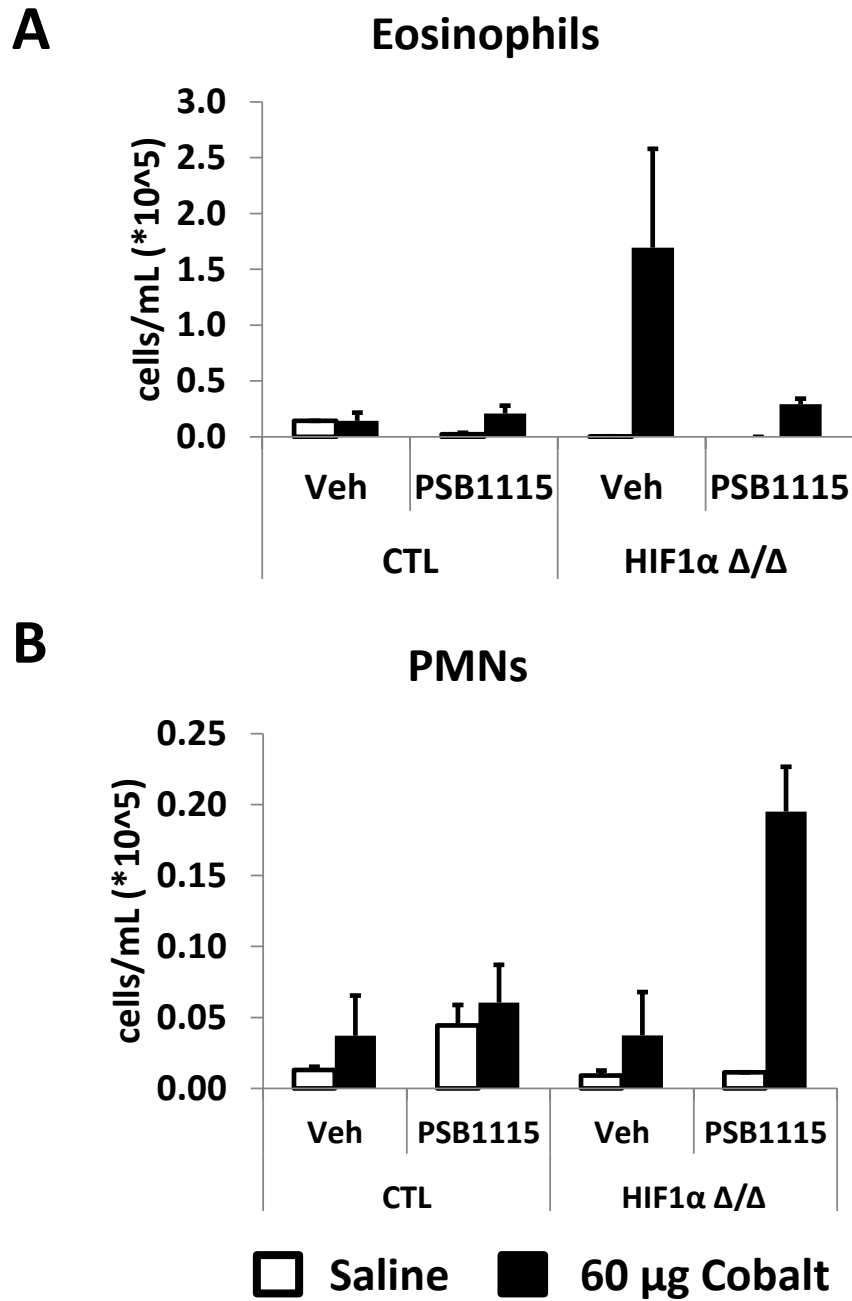


Figure 19. BAL eosinophils and PMNs from HIF1 α mice treated with cobalt for 5 days +/- PSB1115. Bronchoalveolar lavage (BAL) was counted for eosinophils (A) and neutrophils (PMNs) (B). Some groups contained 2 mice due to deaths which rendered the data insufficient for statistical analyses.

Figure 20

Lymphs

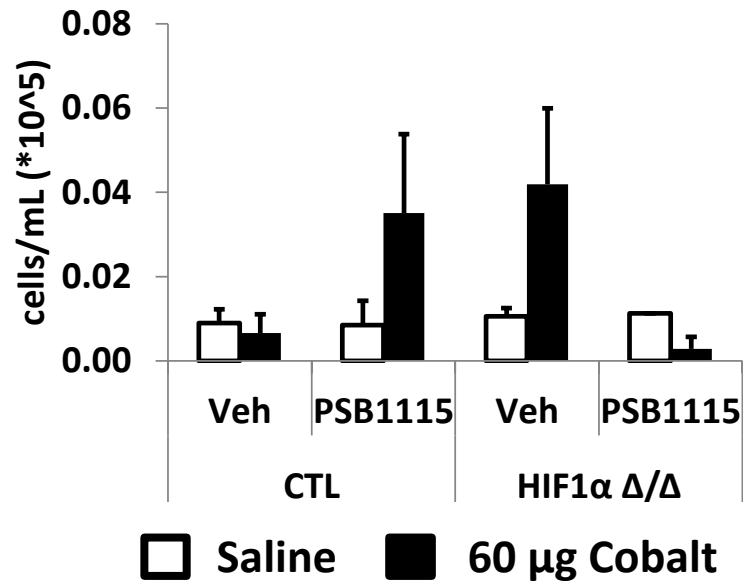


Figure 20. BAL lymphocytes from HIF1 α mice treated with cobalt for 5 days +/- PSB1115. Bronchoalveolar lavage (BAL) was counted for lymphocytes. Some groups contained 2 mice due to deaths which rendered the data insufficient for statistical analyses.

NF- κ B in Cobalt-induced lung injury

TCH013

TCH013 is a compound composed of an imidazoline scaffold with four benzene rings created at Michigan State University by Dr. Jetze Tepe and colleagues (Figure 21). According to preliminary testing of this compound, it has proteasome inhibitory capabilities that appear specific for inhibiting activation of NF- κ B. When TCH013 was given with IL-1 β , it prevented the induction of TNF α and IL-6 production *in vitro* [291]. In a mouse model of rheumatoid arthritis, this compound decreased TNF α concentrations and histopathologic severity of arthritic disease [289].

Figure 21

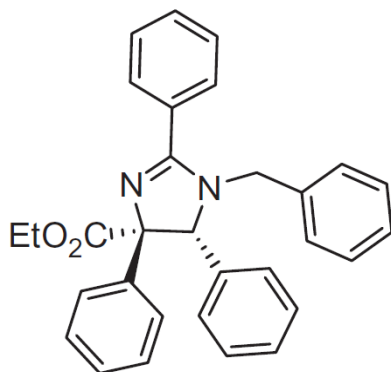


Figure 21. Structural schematic of TCH013. Modified from [289].

HIF1 α mice were exposed to TCH013 (150 mg/kg, i.p.) one hour prior to each daily dosing of 60 μ g cobalt. Mice were sacrificed one day after the last cobalt dose and standard samples were taken. Treatment with TCH013 did not protect the mice from cobalt-induced lung injury as noted by no change to total cells (Figure 22A). Macrophages increased with cobalt treatment and the HIF1 $\alpha^{\Delta/\Delta}$ mice treated with TCH013 had higher macrophage numbers than the CTL mice treated with TCH013 (Figure 22B). A similar pattern is seen with eosinophils (Figure 23A). Neutrophils were lower in HIF1 $\alpha^{\Delta/\Delta}$ mice treated with cobalt, and treatment with TCH013 seemed to have no effect (Figure 23B). Lymphocytes showed only an increase in CTL mice treated with vehicle (Figure 24). Even though TCH013 caused statistically significant increases in macrophages and eosinophils, this change was not significant when taken to total cells. Overall, these data suggest that TCH013 had little effect on overall inflammatory profile in cobalt induced lung inflammation.

Figure 22

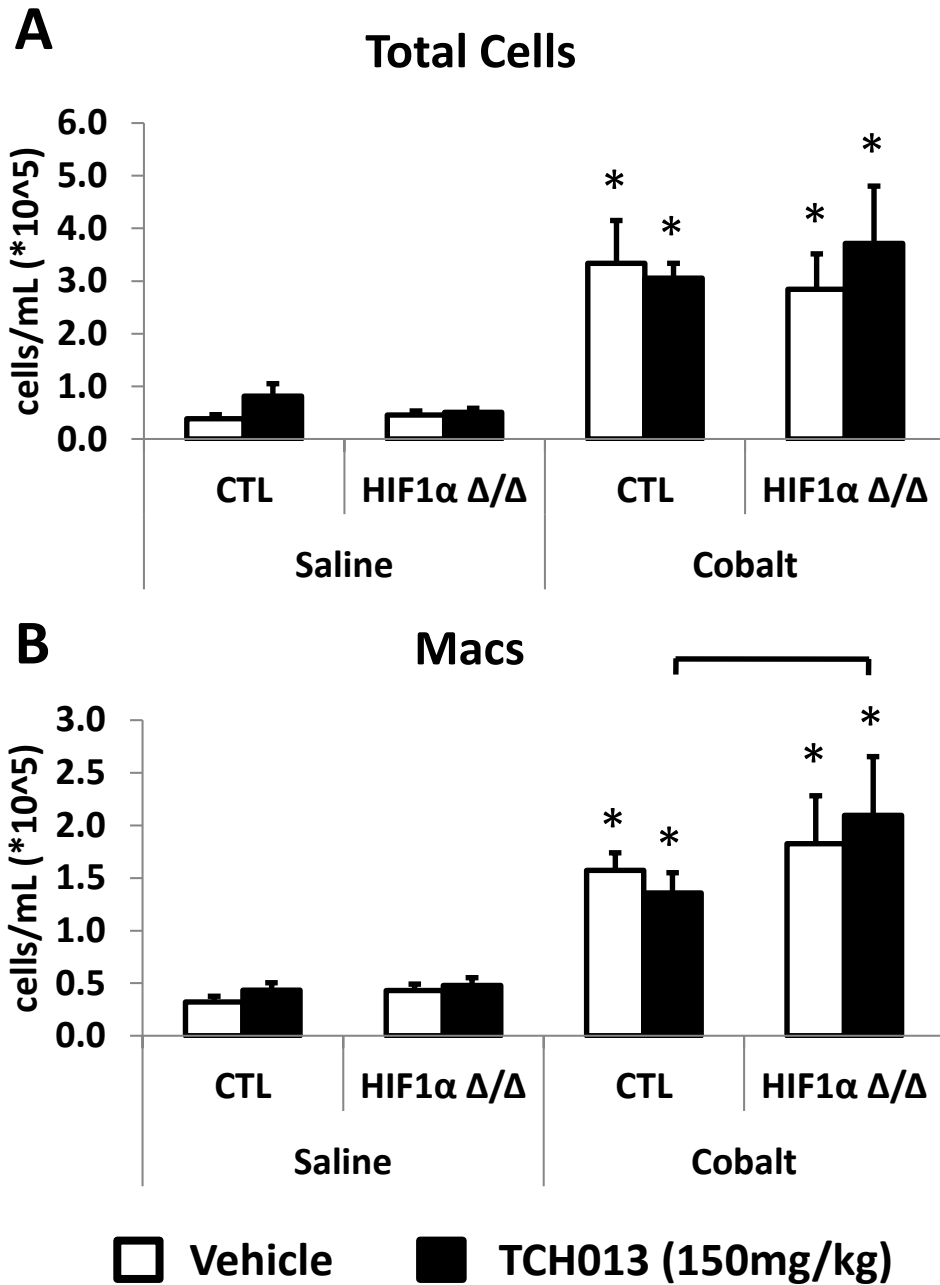


Figure 22. BAL total cells and macrophages from HIF1 α mice treated with cobalt for 5 days +/- TCH013. Bronchoalveolar lavage (BAL) was counted for total cells (A) and macrophages (B). * = significant from saline-treated control, brackets = significant across DOX or VEH/TCH groups, One-way ANOVA with Fisher's LSD, $\alpha = 0.05$. N=4-7 mice/group.

Figure 23

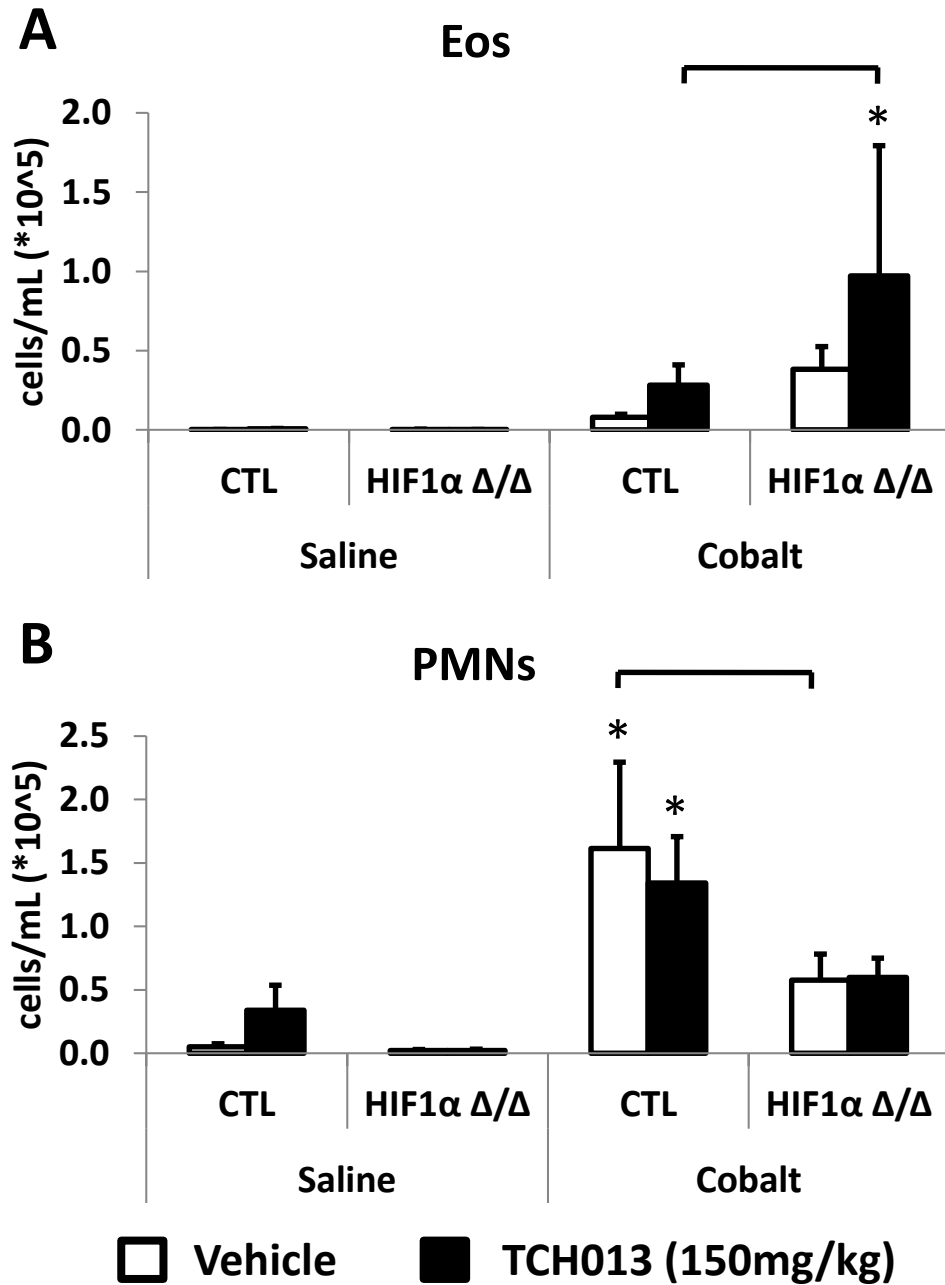


Figure 23. BAL eosinophils and PMNs from HIF1 α mice treated with cobalt for 5 days +/- TCH013. Bronchoalveolar lavage (BAL) was counted for eosinophils (Eos) (A) and neutrophils (PMNs) (B). * = significant from saline-treated control, brackets = significant across DOX or VEH/TCH groups, One-way ANOVA with Fisher's LSD, $\alpha = 0.05$. N=4-7 mice/group.

Figure 24

Lymphs

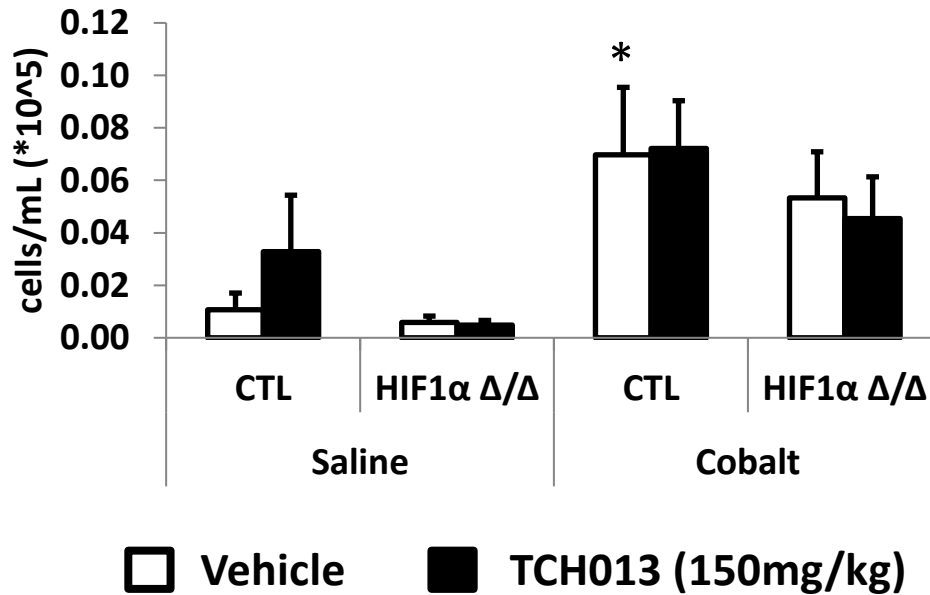


Figure 24. BAL lymphocytes from HIF1 α mice treated with cobalt for 5 days +/- TCH013. Bronchoalveolar lavage (BAL) was counted for lymphocytes. * = significant from saline-treated control, brackets = significant across DOX or VEH/TCH groups, One-way ANOVA with Fisher's LSD, $\alpha = 0.05$. N=4-7 mice/group.

LPS

Previous experiments have shown a T_H2 bias in the HIF1 α ^{Δ/Δ} mice treated with cobalt, and suggested that some element of the inflammatory response in these mice was disrupted. Lipopolysaccharide (LPS) is a constituent of gram negative bacterial cell walls, and it is used frequently in animal experiments as a challenge to the innate immune response or as a general inflammatory stimulus. To investigate whether this vital system of innate immunity was functioning in the HIF1 α ^{Δ/Δ} mice, animals were given 50 μ g of LPS total (25 μ g LPS in 15 μ L given twice, once in each nostril, under isoflurane anesthesia) and sacrificed 24 hours later.

BAL was assessed for cellularity, and total cells increased in all LPS-treated mice (Figure 25A).

Macrophages, eosinophils and lymphocytes showed no statistically significant changes across groups (Figure 25B, 26A and 27, respectively). Neutrophils dominated the cellular response to LPS for all groups (Figure 26B).

Figure 25

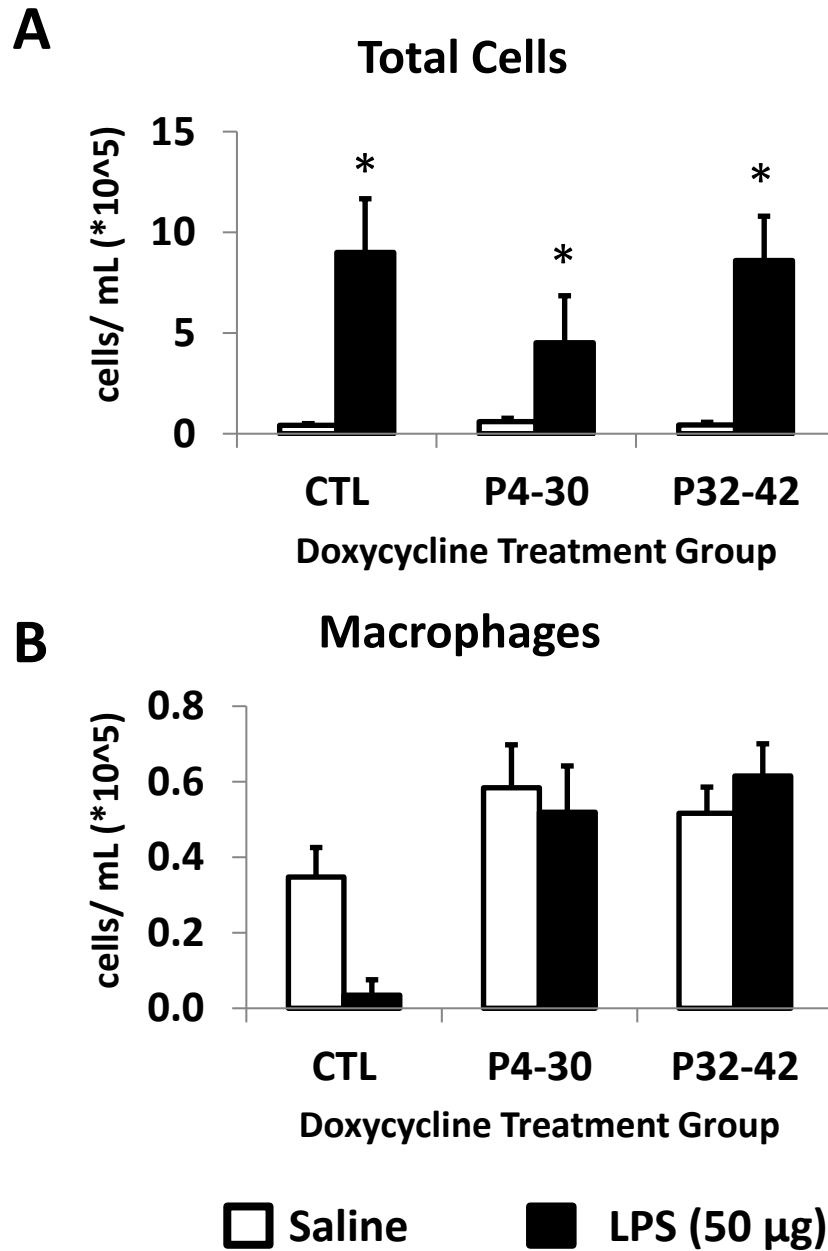


Figure 25. BAL total cells and macrophages from HIF1 α mice in P4-30 and P32-42 DOX groups treated +/- LPS. Mice were treated once with 50 μ g total LPS (25 μ g LPS in 15 μ L, given once in each nostril) under anesthesia and sacrificed 24 hours later. Total cells (A) and macrophages (B) were counted. * = significant from saline-treated control; One-way ANOVA with Fisher's LSD, $\alpha = 0.05$. N=5-9 mice/group.

Figure 26

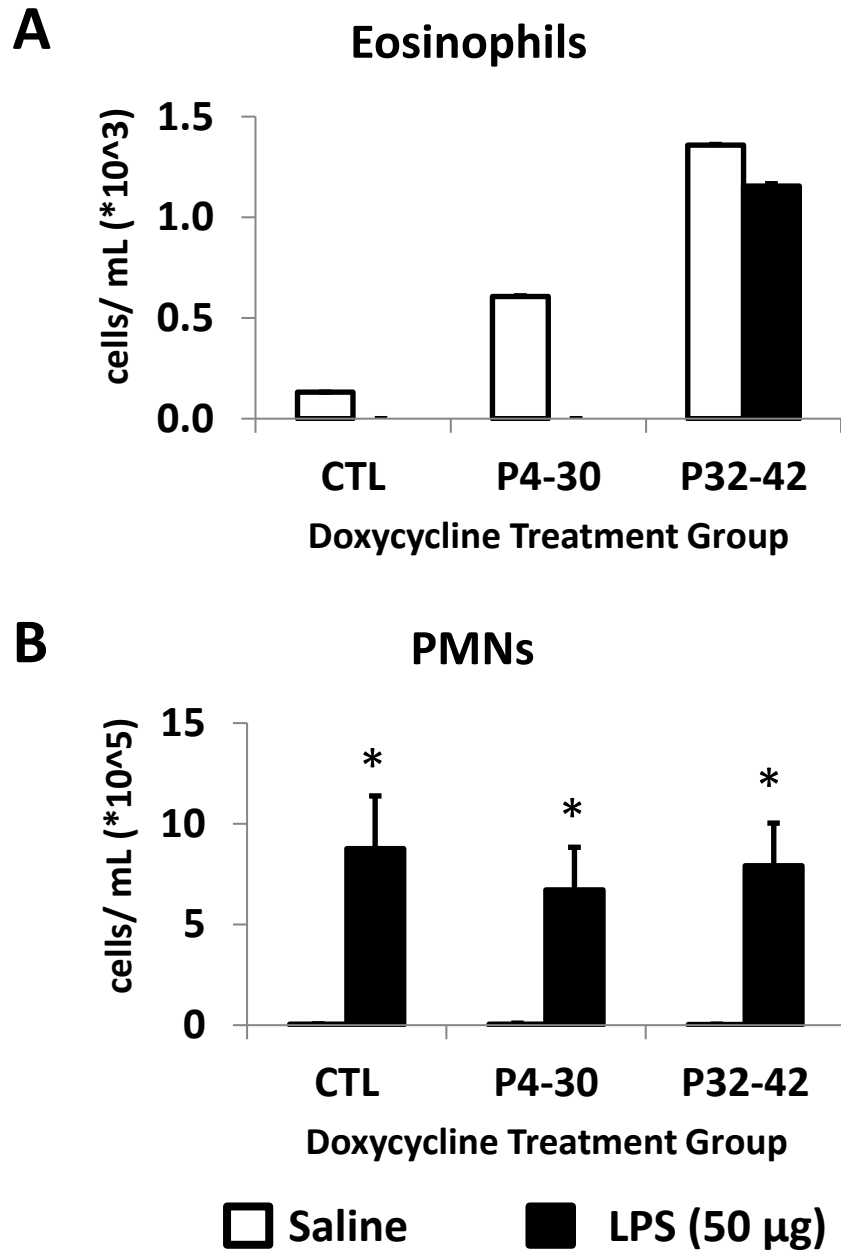


Figure 26. BAL eosinophils and PMNs from HIF1 α mice in P4-30 and P32-42 DOX groups treated +/- LPS. Mice were treated once with 50 μ g total LPS (25 μ g LPS in 15 μ L, given once in each nostril) under anesthesia and sacrificed 24 hours later. BAL eosinophils (A) and neutrophils (PMNs) (B) were counted. * = significant from saline-treated control; One-way ANOVA with Fisher's LSD, $\alpha = 0.05$. N=5-9 mice/group.

Figure 27

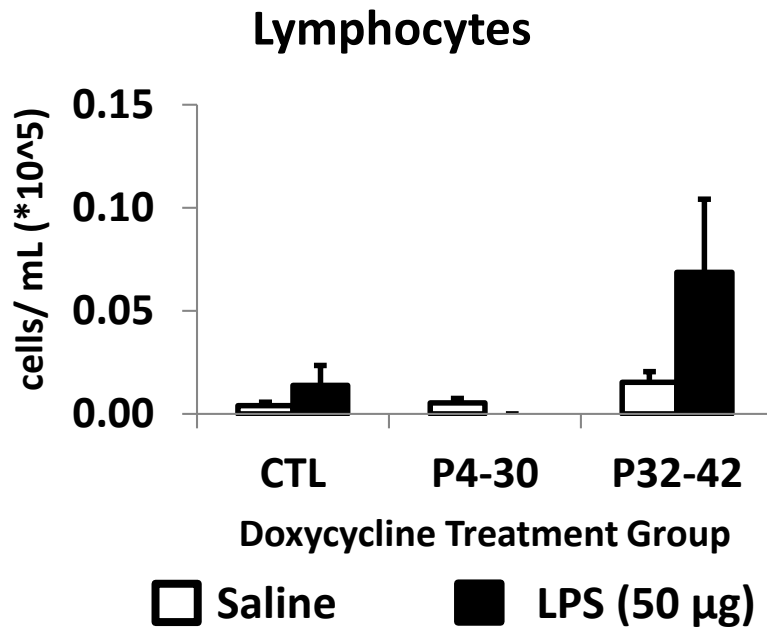


Figure 27. BAL lymphocytes from HIF1 α mice in P4-30 and P32-42 DOX groups treated +/- LPS. Mice were treated once with 50 μ g total LPS (25 μ g LPS in 15 μ L, given once in each nostril) under anesthesia and sacrificed 24 hours later. BAL lymphocytes were counted. * = significant from saline-treated control; One-way ANOVA with Fisher's LSD, $\alpha = 0.05$. N=5-9 mice/group.

Hyperoxia during early postnatal phase

Several studies have illustrated that premature infants are more likely to be diagnosed with asthma through childhood, and infants in the “extremely premature” group, typically GA 24-28 weeks, are more likely to have asthma that continues into adulthood [47-49]. The lungs of premature infants are exposed to higher levels of O₂ than they would normally experience *in utero*; additionally, one supportive therapy present in nearly all premature infants with underdeveloped lungs is supplemental O₂. Given that HIF1 α loss in lung epithelium has shown a predisposition for a T_H2 response, and the high levels of O₂ that premature infants

experience has the potential to negatively regulate HIF-signaling in the lungs, we wanted to know whether high O₂ levels for mice in the early postnatal phase would mimic the HIF1 $\alpha^{\Delta/\Delta}$ phenotype.

Early postnatal hyperoxia is known to produce pathologic effects, including alveolar simplification, and is sometimes used in models of bronchopulmonary dysplasia. Mice exposed to hyperoxia (75% O₂, for 14 days as described in materials and methods section) displayed alveolar simplification (Figure 28B). In contrast, mice exposed to room air, or dosed with DOX from P0-14 displayed normal lung architecture (Figure 28A and C). Additionally, the impact of 75% O₂ on HIF1 α levels was assessed by immunohistochemistry. Hyperoxic exposure had little impact on HIF1 α levels in the lung (Figure 29). Both normoxia and hyperoxia mice were carried out to adulthood and dosed with a 5d cobalt protocol. Results show that mice responded similarly between groups. BAL total cells were increased in both groups (Figure 30A) and most cells induced by cobalt challenge were macrophages (Figure 30B). Eosinophils, neutrophils and lymphocytes were not increased with 75% O₂ treatment (Figure 31A & B and Figure 32), suggesting that early postnatal exposure to hyperoxia does not phenotypically match that of HIF1 α loss due to recombination.

Figure 28

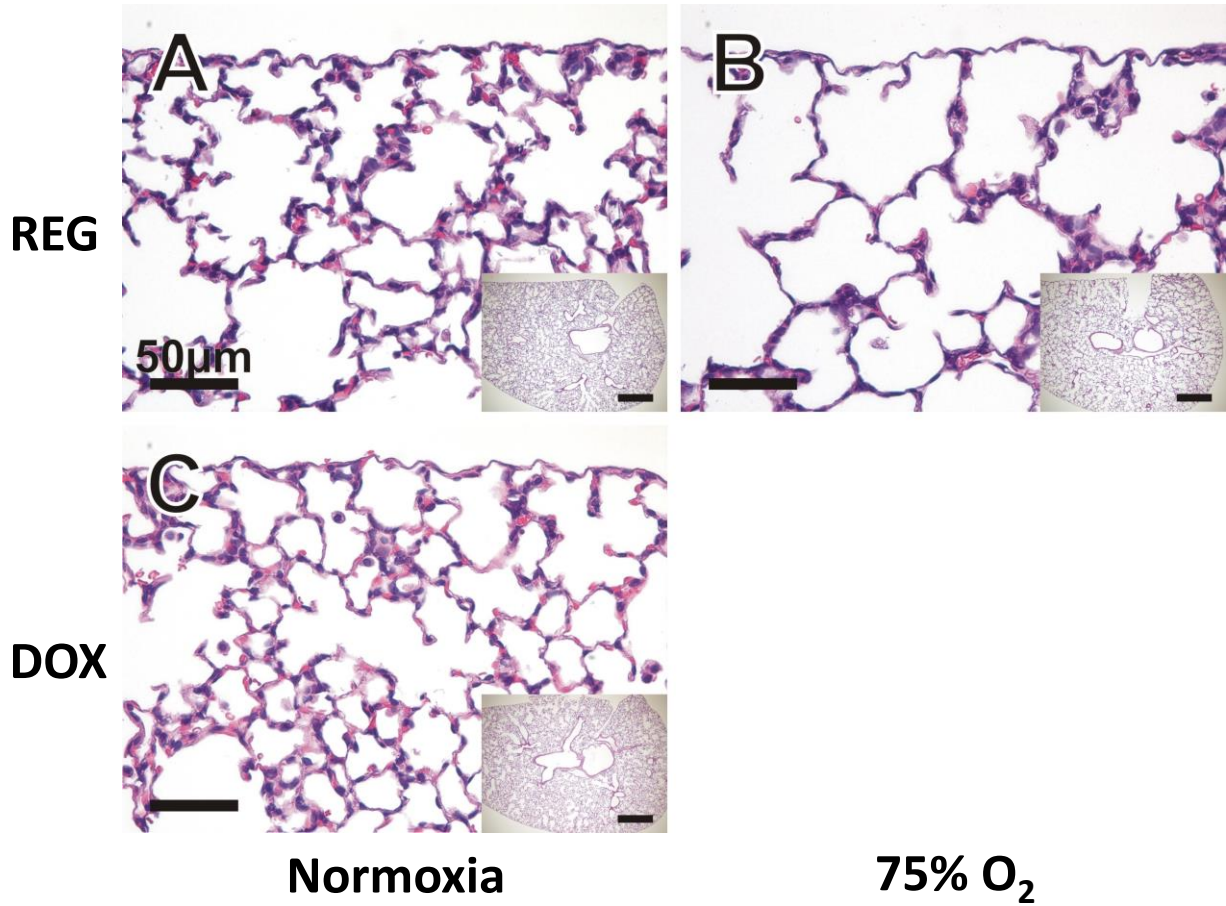


Figure 28. H&E Staining for P0-14 mice exposed to 75% O₂. Mice were either exposed to normoxia (A) or 75% O₂ (B) from birth for 14 days and sacrificed. A group of normoxia mice were also given DOX to compare any effects of DOX on development of normal lung architecture (C). Size bars are 50 μm for large images and 200 μm for insets.

Figure 29

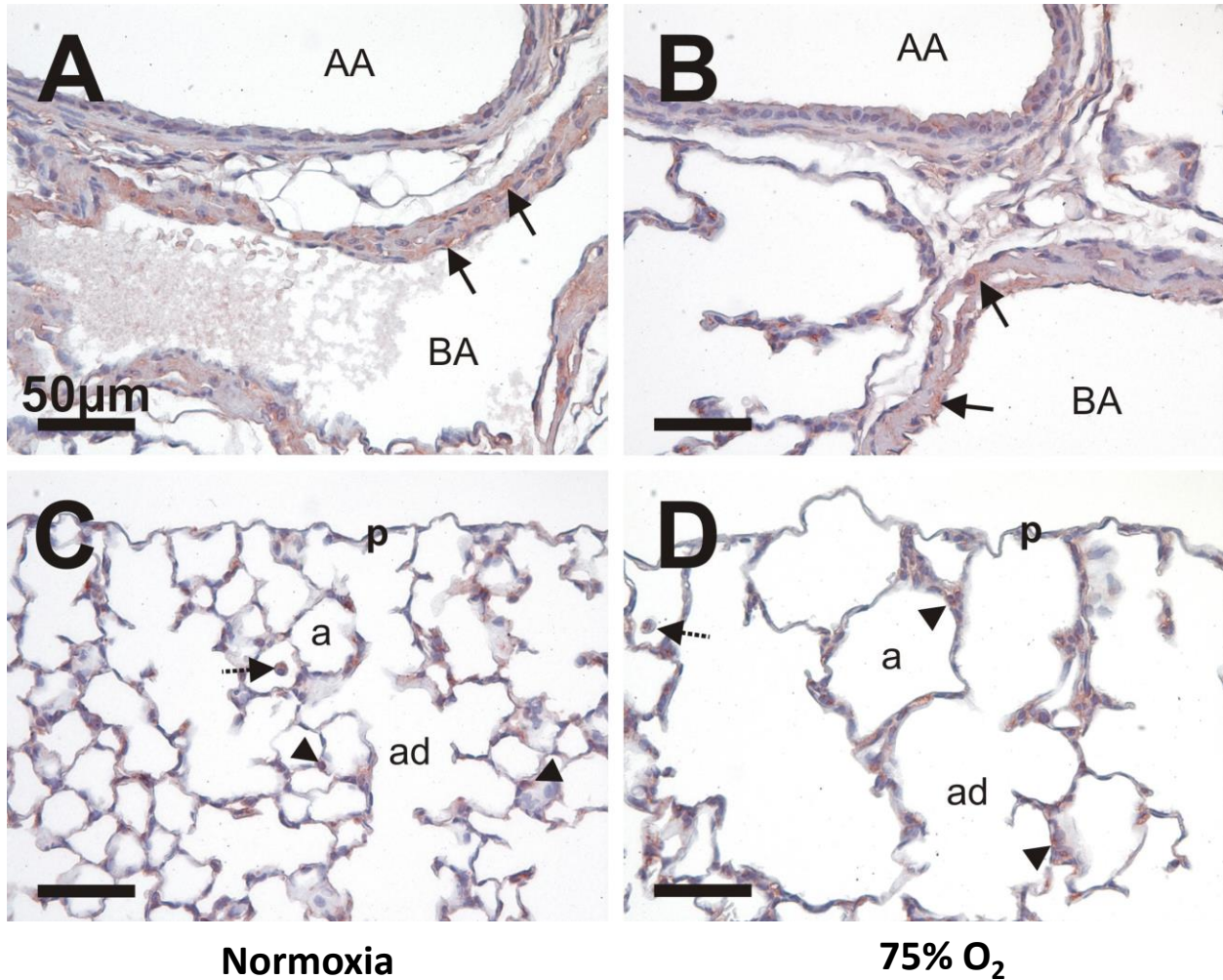


Figure 29. HIF1 α IHC for mice exposed to 75% O₂ from P0-14. HIF1 α (NB100-479 Rabbit plgG, 1:100) with Vectastain ABC Rabbit Kit, NovaRed coloring agent, and light hematoxylin counterstain was performed on mice exposed to 75% O₂ from P0-14 and sacrificed under hyperoxic conditions at P14. Normoxia (A, C) and 75% O₂ (B, D) were compared. (A) and (B) show axial airways and adjacent bronchial arteries, with heaviest staining for HIF1 α in the bronchial artery smooth muscle cells (solid arrows). (C) and (D) show pleural sections, with staining in macrophages (dashed arrows) and alveolar type II cells (arrowheads). Black line indicates 50 μ m.

Figure 30

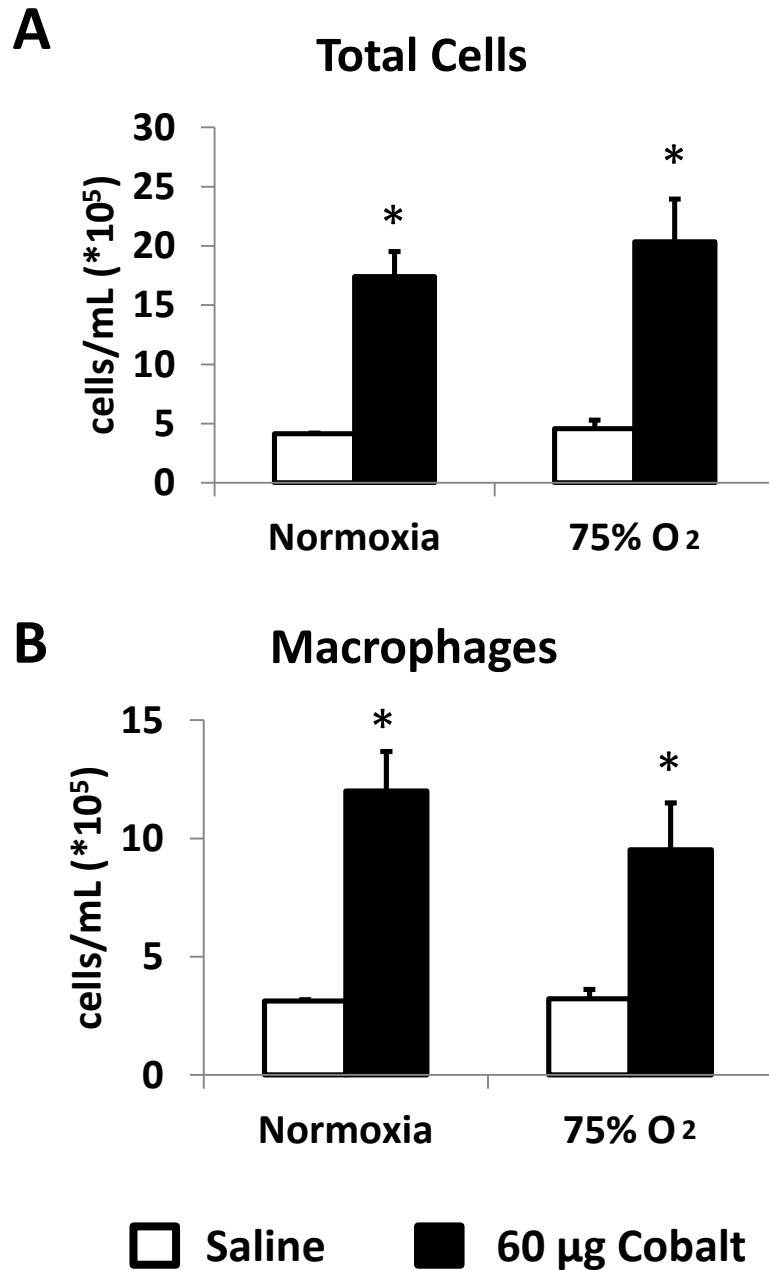


Figure 30. BAL total cells and macrophages from CTL mice exposed to 75% O₂ from P0-14 and 5d cobalt as adults. Mice were allowed to age until P42 when first cobalt dose occurred. Total cells (**A**) and macrophages (**B**) are shown. Most cells observed were in cobalt treated mice and were macrophages. * = significant from saline-treated control. One-way ANOVA with Fisher's LSD, $\alpha = 0.05$. $N = 3-5$ mice.

Figure 31

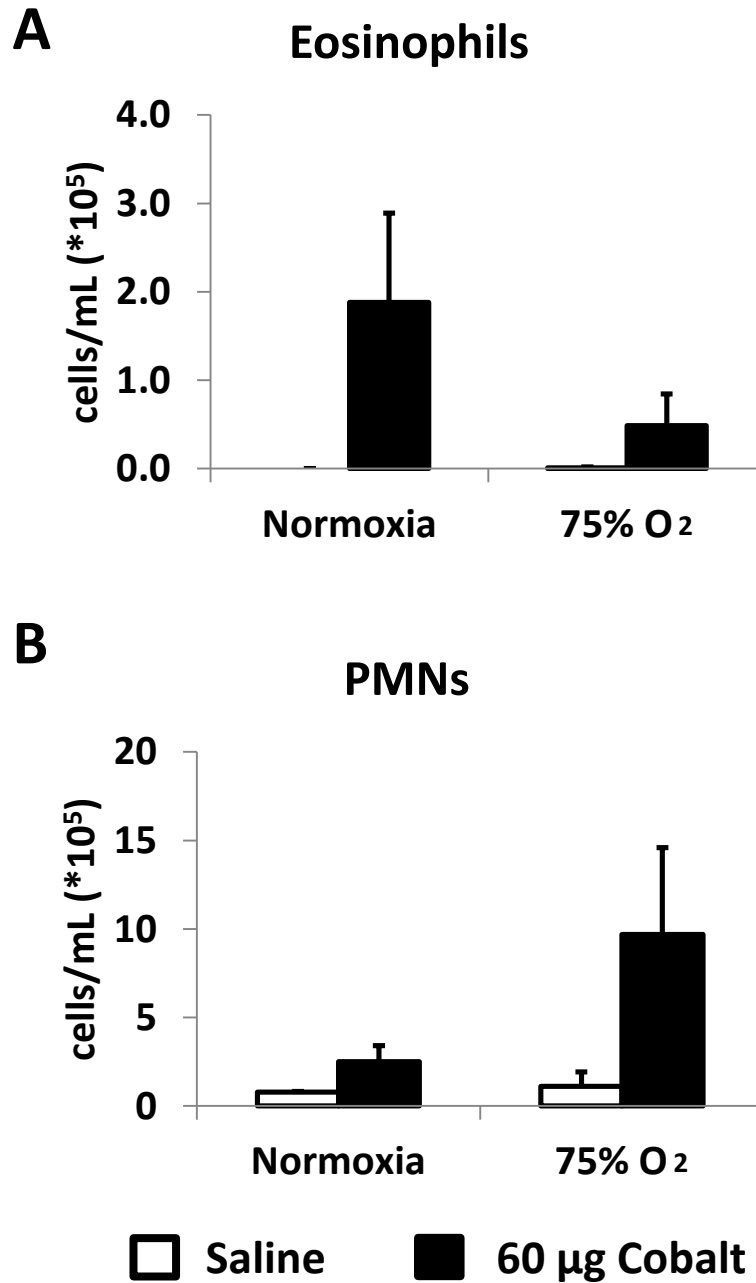


Figure 31. BAL eosinophils and PMNs from CTL mice exposed to 75% O₂ from P0-14 and 5d cobalt as adults. Mice were allowed to age until P42 when first cobalt dose occurred. Eosinophils (A) and neutrophils (PMNs) (B) are shown. * = significant from saline-treated control. One-way ANOVA with Fisher's LSD, $\alpha = 0.05$. N = 3-5 mice.

Figure 32

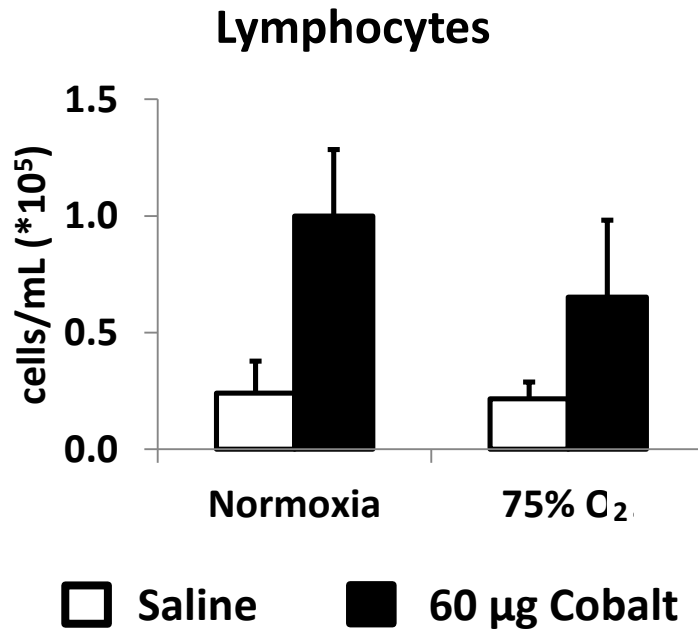


Figure 32. BAL lymphocytes from CTL mice exposed to 75% O₂ from P0-14 and 5d cobalt as adults. Mice were allowed to age until P42 when first cobalt dose occurred. Lymphocytes are shown. * = significant from saline-treated control. One-way ANOVA with Fisher's LSD, $\alpha = 0.05$. $N = 3-5$ mice.

Discussion

The final stages of lung development occur after birth in both mice and humans. The early postnatal time period has also been shown to be crucial for development of the immune system, especially in the context of risk of humans developing allergic airway disease (i.e. the hygiene hypothesis). Therefore, when initial experiments in our laboratory indicated that loss of HIF1 α in the lung (over a 26 day period of doxycycline exposure from P4-30) caused an eosinophilic inflammation in adult mice, it was important to know whether or not lung development may have played a role. We attempted to isolate this developmental window by

performing DOX exposures prior to (P4-14) or after (P32-42) the consensus age of P30 for the completion of postnatal mouse lung development.

Results from the DOX timing experiments here revealed that DOX given to mice from P4-14 was adequate in reproducing the eosinophilic phenotype in response to cobalt-induced lung inflammation. In addition, the P32-42 DOX treatment did not cause eosinophilia in cobalt treatment, suggesting that loss of HIF1 α by itself is not sufficient to drive eosinophilic inflammation, but that the timing of the exposures was important in establishing this phenotype. Further studies using a model of ovalbumin sensitivity and challenge with HIF1 $\alpha^{\Delta/\Delta}$ mice revealed that HIF1 α loss caused an exacerbation of eosinophilic inflammation [51]. This suggests that mice lacking HIF1 α in their ATII and Club cells in the early postnatal phase are predisposed to eosinophilic inflammation. This is highly relevant for the idea of the hygiene hypothesis of asthma, where exposures to microbes during early development drives later allergic disease, and implicates HIF1 α as a potential target gene for developing allergic inflammation.

Perhaps the most interesting finding of these timing studies is that the P32-42 DOX treated mice seemed not only unresponsive, but almost protected from cobalt-induced lung injury, in agreement with the very first hypothesis we made regarding HIF1 α contributing to cobalt toxicity. This may indicate that HIF-signaling is contributory to the pathogenesis of HMLD. While several aspects of our cobalt exposure model are not ideal for mimicking HMLD (lack of tungsten carbide or other particulates, aspiration instead of inhalation and a subchronic exposure period), the idea that loss of HIF1 α in epithelial cells is protective in cobalt-induced

inflammation must be confirmed and pursued with further studies. The presence of two distinct epithelial-HIF1 α -deficiency phenotypes, either a pro-eosinophilic phenotype in the early postnatal phase or an unresponsive/protective phenotype in the adult phase warrants further study, but is highly suggestive that another (non-HIF) signal is responsible for these distinct phenotypes. Several possibilities exist for this other signal, including a neighboring cell type (immune or otherwise) or some developmentally controlled signaling within the epithelial cell that interacts with HIF1 α or its targets. Along these lines, our first experiment was to characterize the most likely cell type involved in eosinophilia of the lung, the T_H2 population.

Flow cytometry studies revealed that the T_H2 cell population was higher only in HIF1 α ^{fl/fl} mice that contained all necessary transgenes for our inducible knockout system and that received doxycycline. Not only does this confirm our previous assumptions about T_H2 inflammation, it also illustrates the robustness of the SP-C/Cre model system. Whether the T_H2 bias experienced in HIF1 α ^{Δ/Δ} mice extends beyond the pulmonary system has yet to be determined, but these data are highly suggestive that whatever is happening in the lung epithelium, there are far more T_H2 cells migrating to the lung in cobalt-treated HIF1 α ^{Δ/Δ} mice.

Additionally, this data provides the first direct evidence that cobalt-induced lung injury does not, in fact, activate T_H1 cells, as has been proposed in our previous studies. In previously published work with HIF1 α mice, IFN γ , the primary T_H1 cytokine, is minimally increased in both

control and HIF1 $\alpha^{\Delta/\Delta}$ mice treated with cobalt. Further, the only reported IL-12 measurements were non-detectable [215]. Data in Figure 15 shows that CTL mice do not have a higher number of T_H1 cells, and further data regarding the cytotoxic T cell (T_C) population (CD8+) in Figure 16 suggests that any IFN γ detected is more likely to come from these cells (or other cells such as innate lymphoid cells) than T_H1 cells. Our previous studies of cobalt-induced lung inflammation have never directly measured T helper bias, and the idea that lack of T_H2 cytokines IL-4 and IL-5 (together with presence of some detectable T_H1 cytokines) was equivalent to activation of T_H1 cells relied too heavily on the idea of a T_H1 vs T_H2 axis where one or the other must be activated. This mentality failed to take into consideration the important fact that one can have either T_H1 or T_H2 cell activation without the other, and the current prevailing understanding of lymphocyte activation which includes other T helper subtypes such as T_H17 and T_{REG}, or the innate lymphoid populations (which lack CD4 entirely but still contribute to the “classic T_H1/T_H2 cytokine” pool). The studies of T helper bias described here provide some clarity to our previous lung cytokine measurements, and imply that cobalt treatment alone does not induce any specific T helper response, but that loss of HIF1 α in lung epithelium leads to activation of T_H2 cells.

The current literature is highly suggestive that HIF1 α has important levels of crosstalk in several signaling pathways during inflammation, including NF- κ B and Adora2b signaling [242-

247, 253-255]. To determine if either of these play a role in the change in inflammation observed in the HIF1 $\alpha^{\Delta/\Delta}$ mice, pharmacological inhibitors were used. Previous IHC for Adora2b suggests that loss of HIF1 α also causes loss of Adora2b, which could impact the ability for the HIF1 $\alpha^{\Delta/\Delta}$ lungs to respond with the appropriate protective downstream signaling. The Adora2b inhibitor, PSB1115, did not worsen the response of control mice to cobalt, as was hypothesized; however, PSB1115 treatment did decrease the eosinophilia seen in HIF1 $\alpha^{\Delta/\Delta}$ mice. These results are difficult to explain, given the role that Adora2b has been shown to play in epithelial fluid clearance in the lung and upregulation of FoxP3+ T_{REG} cells to limit inflammation; however, several confounding variables exist when incorporating pharmacologic agents (affecting all cells) in a cell-type-specific system. Additionally, further studies with an Adora2b agonist would likely be helpful in clarifying the role of Adora2b in this context.

Several limitations of the study of Adora2b may explain the unexpected nature of the results. Firstly, sample sizes were small in the experiment utilizing PSB1115 (N=1-3). At the very least, repeating the experiment is required before any conclusions can be drawn. Secondly, pharmacologic treatment has effects on cells other than ATII cells (where HIF1 α was recombined). These confounding effects on other cell types, especially the alveolar macrophage, are potentially substantial, considering that the alveolar macrophage had the highest staining for Adora2b of all the lung cell types identified (Figure 17A, B and D). In the context of these limiting factors, few conclusions can be drawn on the link between HIF1 α and

Adora2b from these studies, but further experimentation, especially from isolated ATII cells or alveolar macrophages from the HIF1 α mice would be helpful.

Given its role in regulating the expression of many cytokines, blockade of NF- κ B was also attempted in combination with cobalt exposure in the HIF1 $\alpha^{\Delta/\Delta}$ mice. TCH013, a recently designed proteasome inhibitor, is known to limit the inflammatory response in certain contexts and was used in coexposure studies with cobalt in the HIF1 α mouse model. The results show that TCH013 did not protect mice from cobalt-induced lung inflammation, as evidenced by unchanged numbers of total cells. Numbers of macrophages and eosinophils increased in the TCH013 treated HIF1 $\alpha^{\Delta/\Delta}$ mice compared to their HIF1 α -sufficient controls; however, these combined increases were not enough to increase the number of total cells. It is possible that TCH013 affected alveolar macrophages and eosinophils to increase their numbers in mice lacking epithelial HIF1 α , but the biological significance of these changes is inconclusive.

Several limitations on the studies of TCH013 and NF- κ B warrant scrutiny of results. Firstly, the specific mechanism of TCH013 is unknown. Additionally, only one time point was used for cobalt exposure, and while the 5 day response was common for many of our cobalt studies, the pharmacodynamics of TCH013 are not characterized, so timing, dose, and route of administration were not optimized before the study was performed. More experiments would be required to characterize the response to cobalt with TCH013, including more time points, an assessment of cytokine production and direct probing for NF- κ B in different cell constituents. Further experiments with TCH013 were performed with BALB/c mice and the ovalbumin sensitivity/challenge model, where TCH013 administration was identical to this experiment.

TCH013 prevented inflammation in BAL cellularity. However, further histopathologic investigation of the lung revealed little effect on eosinophilic inflammation (unpublished results). Thus, use of the TCH013 compound has produced mixed results, likely from an incomplete understanding of its mechanism. Additionally, these studies were limited by lack of measurement of NF- κ B activity. Also, pharmacologic investigations suffer from lack of cell type specificity, since TCH013 undoubtedly has effects on all cell types, not just the ATII cells. If HIF1 α and NF- κ B had meaningful crosstalk within the ATII cell, the effects of TCH013 on other cell types may have confounded the results. Use of a fully characterized NF- κ B inhibitor, along with its use in isolated ATII cells, may produce more consistent results in future studies.

Another way of probing the NF- κ B system and innate immunity is through the use of LPS, which stimulates the Toll-like receptor pathway, specifically TLR4, which acts through NF- κ B to initiate the innate immune response. It has been reported that small amounts of LPS can produce T_H2 inflammation, but before we were able to address this question we first had to know if the detection and response to LPS was still intact. Mice in which HIF1 α was recombined during early postnatal development (P4-30) and during early adulthood (P32-42) were phenotypically identical to control mice in their response to LPS. All three groups displayed a robust neutrophil-dominant infiltrate to the lungs. These results showed that despite HIF1 α deletion, the LPS response was robust and similar.

Taking all of the pharmacologic, DOX timing and T-cell population data into account, it seems the timing of HIF1 α deletion is the most important determinant we have been able to change and observe. Acute signaling (during the inflammatory response) is very important, but

the mixed results of the studies targeting Adora2b and NF- κ B leave many questions. The data thus far seem to suggest that there is something occurring in lung epithelial cells that lose HIF1 α during the early postnatal phase of development to prime the T_H2 immune response. Isolating the ATII cells will allow probing to one of the primary cell types affected by loss of HIF1 α .

Focusing our attention on the early postnatal developmental period, we wondered if high O₂ levels during the early postnatal phase could decrease the amounts of HIF1 α present, and potentially mimic our lung-specific HIF1 α deletion phenotype. Considering the importance of supplemental O₂ use in extremely premature infants and their increased likelihood of developing asthma as children and adults make this idea intriguing as a potential molecular mechanism by which this predisposition occurs. Looking at lungs from mice receiving high O₂ revealed their alveoli to be much larger and overall more simplified with less septations, consistent with other models of high O₂ during this time period. However, analysis of HIF1 α via IHC was unconvincing for a decrease in HIF1 α from high O₂ levels, even when tissues were taken and fixed in the hyperoxic environment. Further, dosing these mice in adulthood with cobalt reveals that high O₂ from P4-14 did not exacerbate eosinophilia, reducing the likelihood that high O₂ can mimic this phenotype.

There are several potential reasons why the hyperoxia treatments did not mimic the HIF1 $\alpha^{\Delta/\Delta}$ phenotype. With high concentrations of O₂ there are several important changes occurring in the lung other than just potentially lower HIF α levels in epithelial cells, such as production of ROS, activation of nuclear factor-erythroid 2 related factor (Nrf2) pathway and proinflammatory cytokines such as IL-1 β , IL-6 and TNF α [292-295]. Much like with pharmacologic interventions, off-target effects of high concentrations of O₂ could affect any number of cell types involved in the pathogenesis of hyperoxia-induced lung injury, which could have altered the lung in different ways than our model of loss of HIF1 α in ATII and Club cells.

In summary, early postnatal HIF1 α deletion seems to be very important in producing the eosinophilic phenotype, which has been shown to include induction of T_H2 responses in cobalt-induced lung injury. It also shows that T_H1 responses are not a part of normal response to injury from 10 mM CoCl₂, which has implications for the pathogenesis of HMLD. Pharmacologic inhibition of the Adora2b and NF- κ B had some effect on cobalt induced lung injury, though the role of HIF1 α in these processes remains unclear. What is evident is that HIF1 α in lung epithelial cells seems to function more in a protective role in cobalt injury, which is contrary to our initial suspicions about HIF1 α contributing to cobalt toxicity. Finally, hyperoxia exposure during the early postnatal time period does not mimic the loss of HIF1 α in cobalt-induced lung injury, though cell-type specificity is likely a factor. Further studies, especially of epithelial cell crosstalk to other populations are required to elucidate more carefully the crosstalk of these signaling pathways and other possible cell populations in cobalt-induced lung injury.

**CHAPTER 4 – COMPARATIVE PHENOTYPES OF COBALT-INDUCED RESPIRATORY
INFLAMMATION IN MICE DEFICIENT FOR HIF1 α , HIF2 α or HIF1 α /2 α IN LUNG
EPITHELIUM**

Results

HIF2 $\alpha^{\Delta/\Delta}$ mice 60 μg CoCl $_2$ time course

Mice containing all three transgenes necessary for lung epithelial HIF2 α -specific deletion were exposed to DOX from P4 to P30. DOX was allowed to leave system for 10 days afterward at which point mice were exposed to either sterile saline vehicle or 60 μg CoCl $_2$ via oropharyngeal aspiration once daily for 1, 5 or 14 (5 days on, 2 days off, 5 days on, 2 days off) days, and sacrificed 24 hours after last dose. Normal necropsy tissues were taken.

HIF2 α IHC

Immunohistochemistry for HIF2 α was performed to show specific deletion in the lung tissue (Figure 33). Dark staining indicates the presence of HIF2 α protein in the Club cells of the bronchial airway in control mice (arrow, Figure 33A) which is vastly decreased in the Club cells of DOX treated mice (arrow, Figure 33C). Similar positive staining was observed in the parenchymal portions of the airway, predominantly in the ATII cells in control mice (arrows, Figure 33B) which is lost in DOX treated mice (arrow, Figure 33D). This staining confirms the epithelial-specific nature of our DOX-inducible recombination system.

BAL Cellularity

BAL fluid was taken and total cells counted and differentials obtained from control and HIF2 $\alpha^{\Delta/\Delta}$ mice at 1 day, 5 day and 14 day time points (Figures 34-36). The number of total cells increases following 5 days of cobalt treatment with no difference between CTL and HIF2 $\alpha^{\Delta/\Delta}$

Figure 33

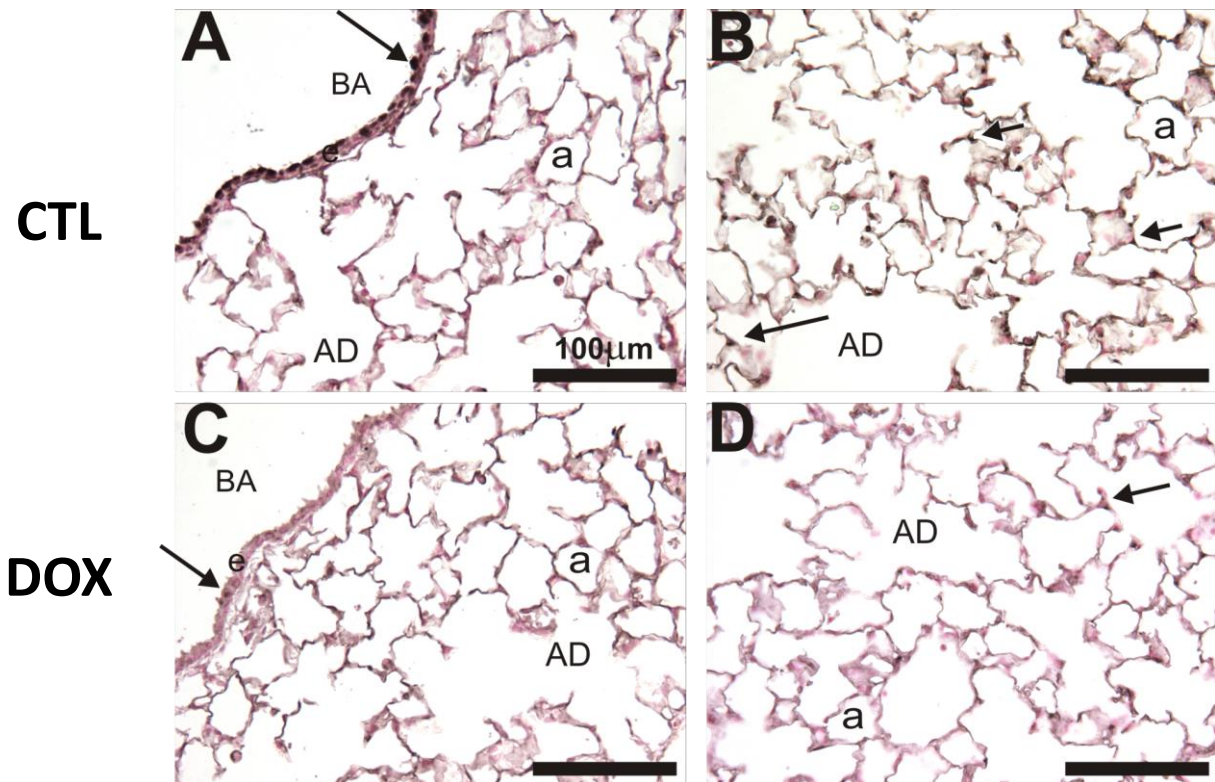


Figure 33. HIF2 α IHC for CTL and P4-30 DOX treated mice. HIF2 α (NB100-122 Rabbit pIgG, 1:100) with Vectastain ABC Rabbit Kit, DAB coloring agent, and light hematoxylin counterstain was performed on control (A and B) and DOX treated (C and D) mice. A and C show the bronchial airway, and Club cells are indicated with solid arrows. B and D show the parenchymal compartment. Black line indicates 100 μ m.

mice. At 14 days the total cells of CTL mice go down but remain high in HIF2 $\alpha^{\Delta/\Delta}$ mice (Figure 34A). Macrophages show a similar increase at 5 days in the cobalt treated groups that decreases by 14 days (Figure 34B). Interestingly, at 14 days eosinophils went up significantly in the HIF2 $\alpha^{\Delta/\Delta}$ mice only, similar to what has been observed with HIF1 $\alpha^{\Delta/\Delta}$ mice at 5 days (Figure 35A). Neutrophils did not make up a significant portion of the cellularity, but at 5 days the cobalt treated CTL mice had higher levels than HIF2 $\alpha^{\Delta/\Delta}$ mice that dropped down at 14 days

(Figure 35B). Lymphocytes in cobalt-treated control mice were higher at 5 days than 1 and 14 days, and in HIF1 $\alpha^{\Delta/\Delta}$ mice were higher at 5 days than 14 days (Figure 36).

Figure 34

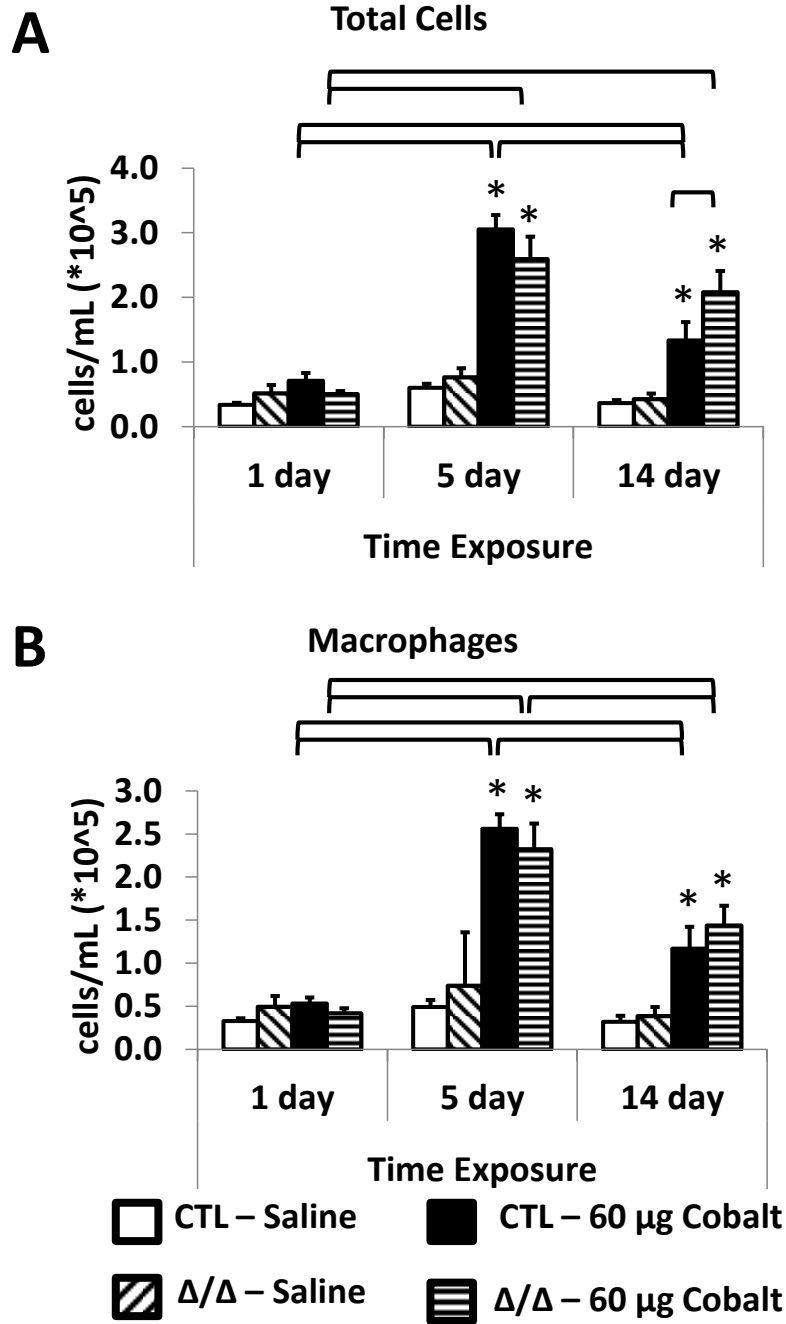


Figure 34. BAL total cells and macrophages from HIF2 α mice treated with cobalt for 1, 5 and 14 days. Mice were treated for 1, 5, and 14 days with 60 μ g CoCl₂ or sterile saline vehicle. BAL was taken and total cells (A) and macrophages (B) are presented. * = significant from saline-treated control, brackets = significant across CTL/ Δ/Δ groups or same group on different time point, One-way ANOVA with Fisher's LSD, $\alpha = 0.05$.

Figure 35

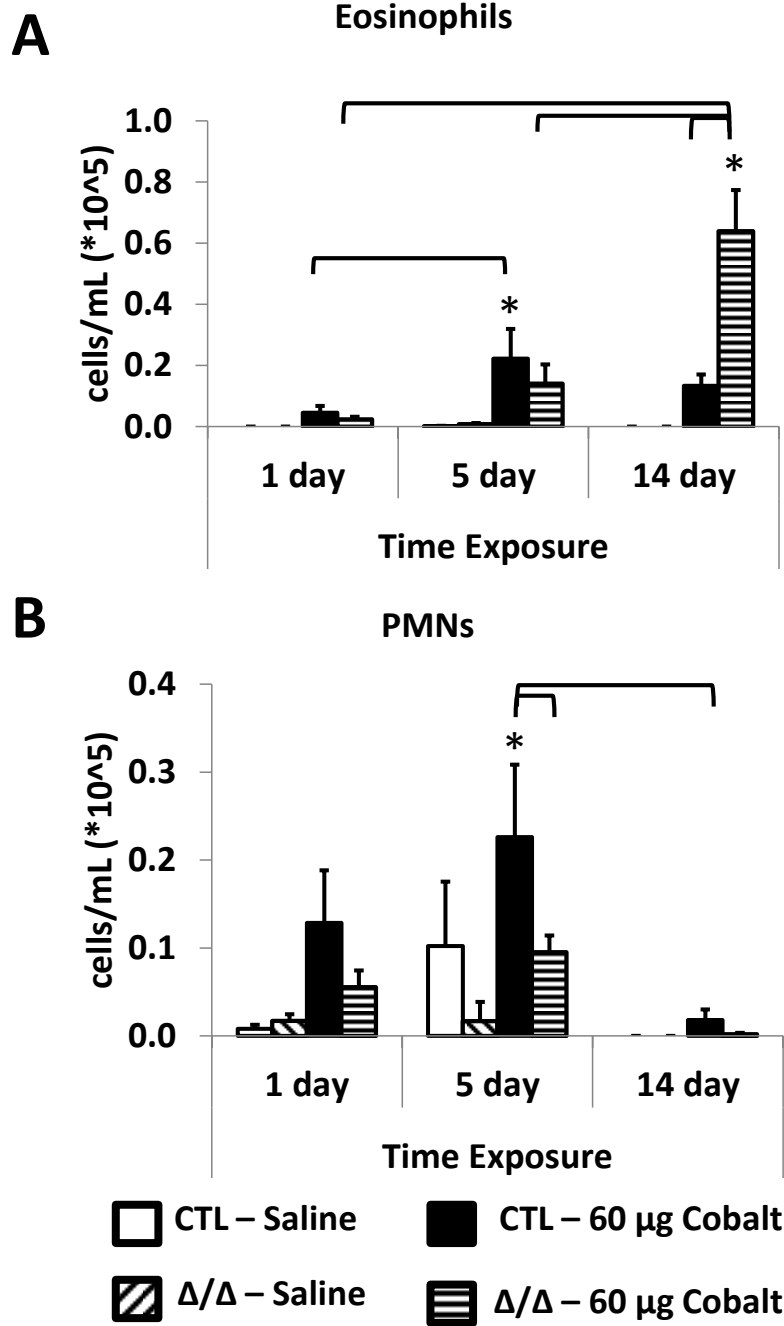


Figure 35. BAL eosinophils and PMNs from HIF2 α mice treated with cobalt for 1, 5 and 14 days. Mice were treated for 1, 5, and 14 days with 60 μg CoCl_2 or sterile saline vehicle. BAL was taken and eosinophils (A) and neutrophils (PMNs) (B) are presented. * = significant from saline-treated control, brackets = significant across CTL/ Δ/Δ groups or same group on different time point, One-way ANOVA with Fisher's LSD, $\alpha = 0.05$.

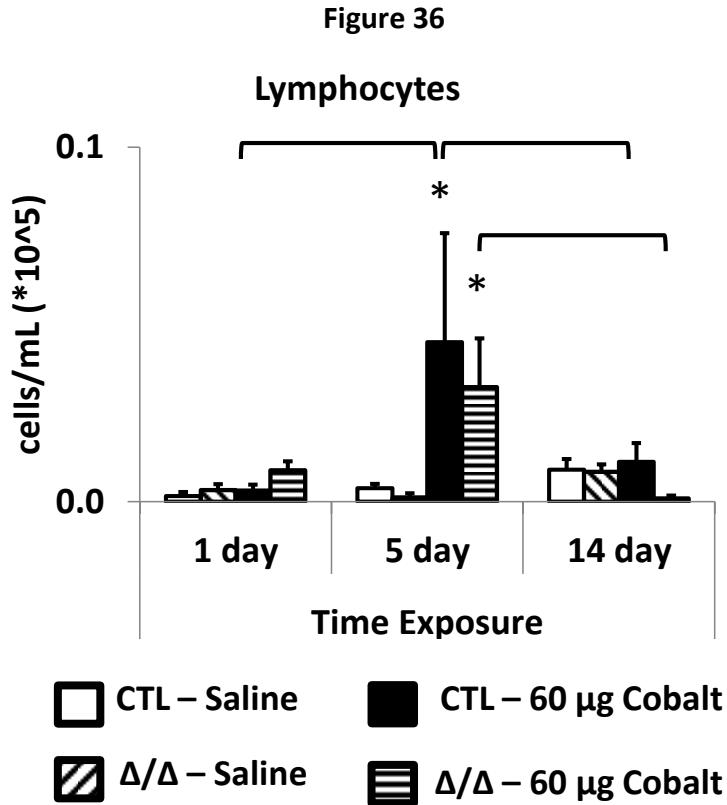


Figure 36. BAL lymphocytes from HIF2 α mice treated with cobalt for 1, 5 and 14 days. Mice were treated for 1, 5, and 14 days with 60 μ g CoCl₂ or sterile saline vehicle. BAL was taken and lymphocytes are presented. * = significant from saline-treated control, brackets = significant across CTL/ Δ/Δ groups or same group on different time point, One-way ANOVA with Fisher's LSD, $\alpha = 0.05$.

Histopathology and Immunohistochemistry

Saline mice exhibited no visible pathology or notable difference between CTL and DOX treated mice (Figure 37A and E). At 1 day cobalt exposure (Figure 37B and F), lungs from both CTL and DOX treated mice showed evidence of perivascular infiltrates to the bronchial regions. At 5 days (Figure 37C and G) the infiltrates had expanded to the parenchymal regions, and thickening of bronchial lamina propria was evident in cobalt treated lungs. Additionally, thickening of the bronchial epithelium was noted at 5 days in both CTL and HIF2 $\alpha^{\Delta/\Delta}$ mice,

which resolved in the CTL mice at 14 days, but worsened in the HIF2 $\alpha^{\Delta/\Delta}$ mice at 14 days. The overall peak for pathology of the control lungs treated with cobalt appeared to be 5 days, with a slight reduction in the amounts of affected lung at 14 days (Figure 37D), in agreement with the BAL cellularity data. DOX treated mice receiving cobalt looked similar in severity at 5 and 14 day time points (Figure 37F and G), suggesting that resolution of infiltrates and bronchial epithelial thickening was somewhat dependent on presence of HIF2 α .

Figure 37

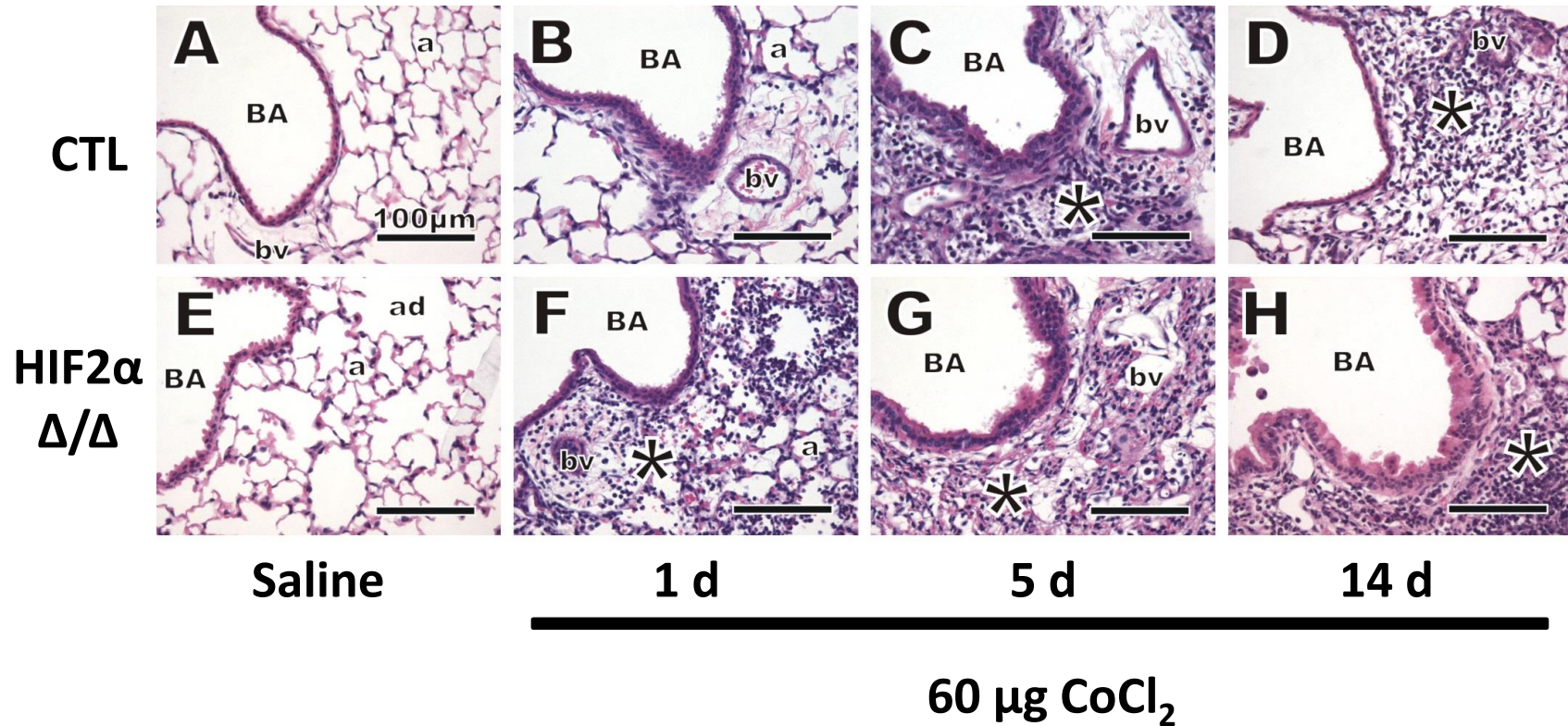


Figure 37. HIF2 α strain H&E stain for mice with 1, 5 and 14 days cobalt. Control mice (A-D) and HIF2 $\alpha^{\Delta/\Delta}$ (E-H) are treated with sterile saline vehicle (A and E) or 60 $\mu\text{g CoCl}_2$ after 1 day (B and F), 5 days (C and G) and 14 days (D and H). All images were taken from the G5 section. BA=bronchial airway, bv=blood vessel, ad=alveolar duct, a=alveolus, *=site of mixed inflammatory cell infiltrates. Black line indicates 100 μm .

MBP, a key constituent in eosinophil secretory granules, was probed using IHC to assess eosinophilia. As expected, saline treated mice did not show visible signs of eosinophil infiltration (Figure 38A and E). This was similar for 1 day cobalt exposure (Figure 38B and F), where some positive cells existed, but did not make up an appreciable amount of the inflammatory cells. At day 5, many more eosinophils are seen in the tissues of both CTL and HIF2 $\alpha^{\Delta/\Delta}$ mice (Figure 38C and G, respectively), though these resolve somewhat in control mice for day 14 (Figure 38D). Interestingly, the number of eosinophils greatly increases at 14 days in the HIF2 $\alpha^{\Delta/\Delta}$ mice (Figure 38H), in agreement with the BAL data. These data mimic the results of HIF1 $\alpha^{\Delta/\Delta}$ mice, except that the HIF1 $\alpha^{\Delta/\Delta}$ mice develop eosinophilia earlier, around day 5. Another aspect of the HIF1 $\alpha^{\Delta/\Delta}$ phenotype that is also seen in these HIF2 $\alpha^{\Delta/\Delta}$ mice is eosinophilia of parenchymal tissues. In allergic airway disease, eosinophils are somewhat restricted to the bronchi and bronchioles, so this finding may be significant.

Figure 38

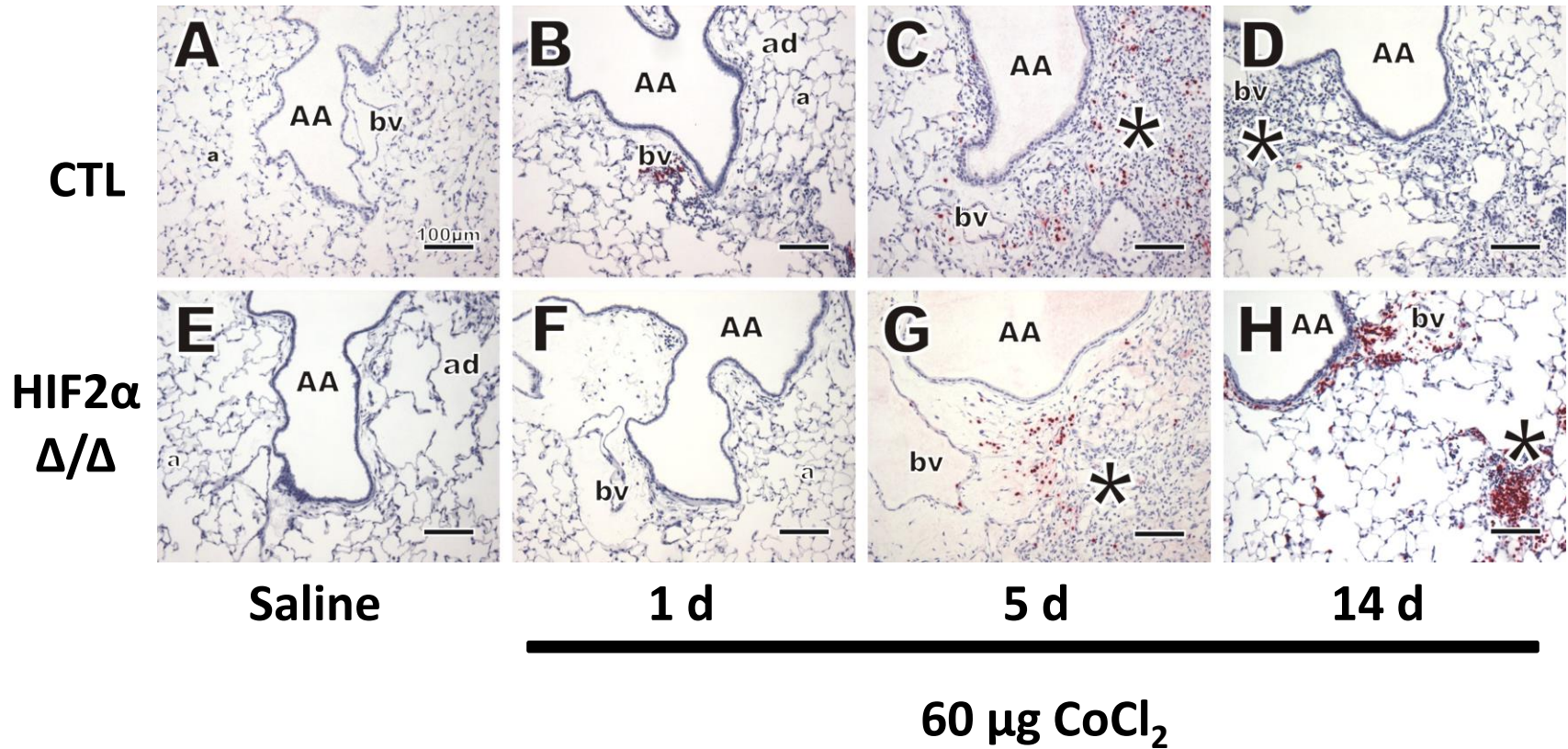


Figure 38. HIF2 α strain major basic protein IHC for mice with 1, 5 and 14 days cobalt. Immunostaining was performed for major basic protein (MBP; polyclonal rabbit anti-mouse MBP, 1:500, Mayo Clinic, Scottsdale, AZ). Control mice (**A-D**) and HIF2 $\alpha^{\Delta/\Delta}$ (**E-H**) are treated with sterile saline vehicle (**A and E**) or 60 μ g CoCl $_2$ after 1 day (**B and F**), 5 days (**C and G**) and 14 days (**D and H**). AA=axial airway, bv=blood vessel, a=alveolus, *=site of mixed inflammatory cell infiltrates, eosinophils in red stain. Black line indicates 100 μ m.

Alcian blue periodic acid Schiff (AB-PAS) stain was performed to visualize acidic and neutral polysaccharides and mucosubstances in goblet cells. No mucosubstances were observed in the saline treated mice (Figure 39A and E), and very few were seen in 1 day exposures to cobalt (Figure 39B and F). The 5 day exposures began to reveal increases in mucous material, though no real differences between the groups were apparent (Figure 39C and G). At 14 days, a much clearer difference in mucous material could be visualized (solid arrows), with CTL mice showing sporadic mucous material (Figure 39D), while HIF2 $\alpha^{\Delta/\Delta}$ mice had substantial increases in visualized mucous substances of goblet cells of the epithelium (Figure 39H).

Figure 39

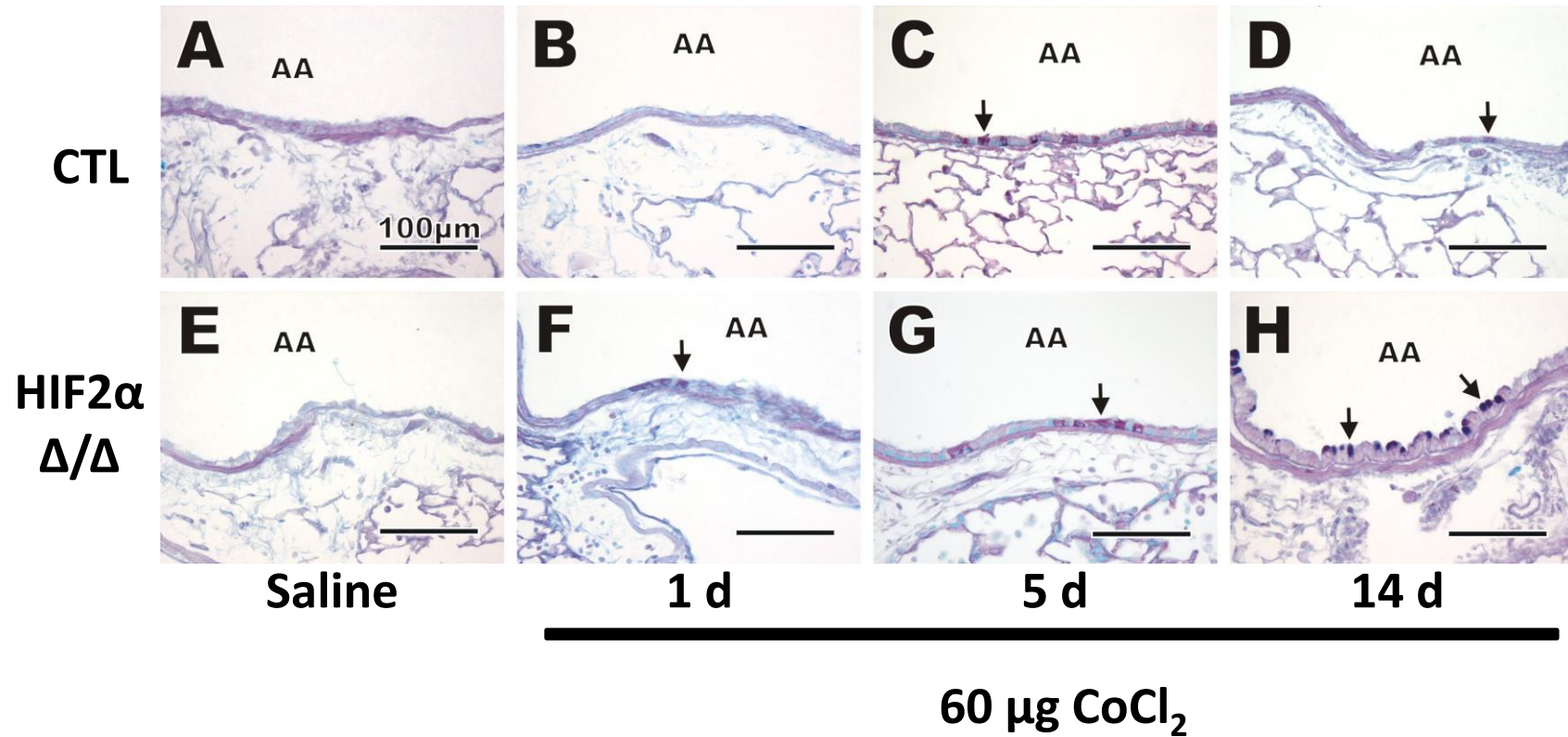


Figure 39. AB-PAS stain for HIF2 α mice with 1, 5 and 14 days cobalt. Control mice (A-D) and HIF2 α Δ/Δ (E-H) are treated with sterile saline vehicle (A and E) or 60 $\mu\text{g CoCl}_2$ for 1 day (B and F), 5 days (C and G) and 14 days (D and H). AA=axial airway, black arrows=mucous material visualized in goblet cells. Black line indicates 100 μm .

Cytokine analysis

Cytokines were analyzed from the BAL of the 1 day and 14 day time points using a cytokine bead array system. T_H2 cytokine IL-4 (Figure 40A) did not show substantial changes across groups, whereas T_H2 cytokine IL-5 (Figure 40B), pro-inflammatory cytokine IL-6 (Figure 41A) and leukocyte chemokine KC (Figure 41B) all showed increases at 1 day more in the HIF2 $\alpha^{\Delta/\Delta}$ mice than controls. At 14 days, these cytokines returned to decreased levels. T_H1 cytokine IFN γ (Figure 42A) was not measurable in cobalt-treated HIF2 $\alpha^{\Delta/\Delta}$ mice at both time points, suggesting that HIF2 $\alpha^{\Delta/\Delta}$ mice treated with cobalt were less likely to activate T_H1 cells. Similarly, T_{REG} cytokine IL-10 (Figure 42B) was not measurable in the cobalt treated HIF2 $\alpha^{\Delta/\Delta}$ mice, potentially signifying a lack of T_{REG} promotion in HIF2 $\alpha^{\Delta/\Delta}$ mice, which would prolong the resolution of any inflammatory immune response.

Figure 40

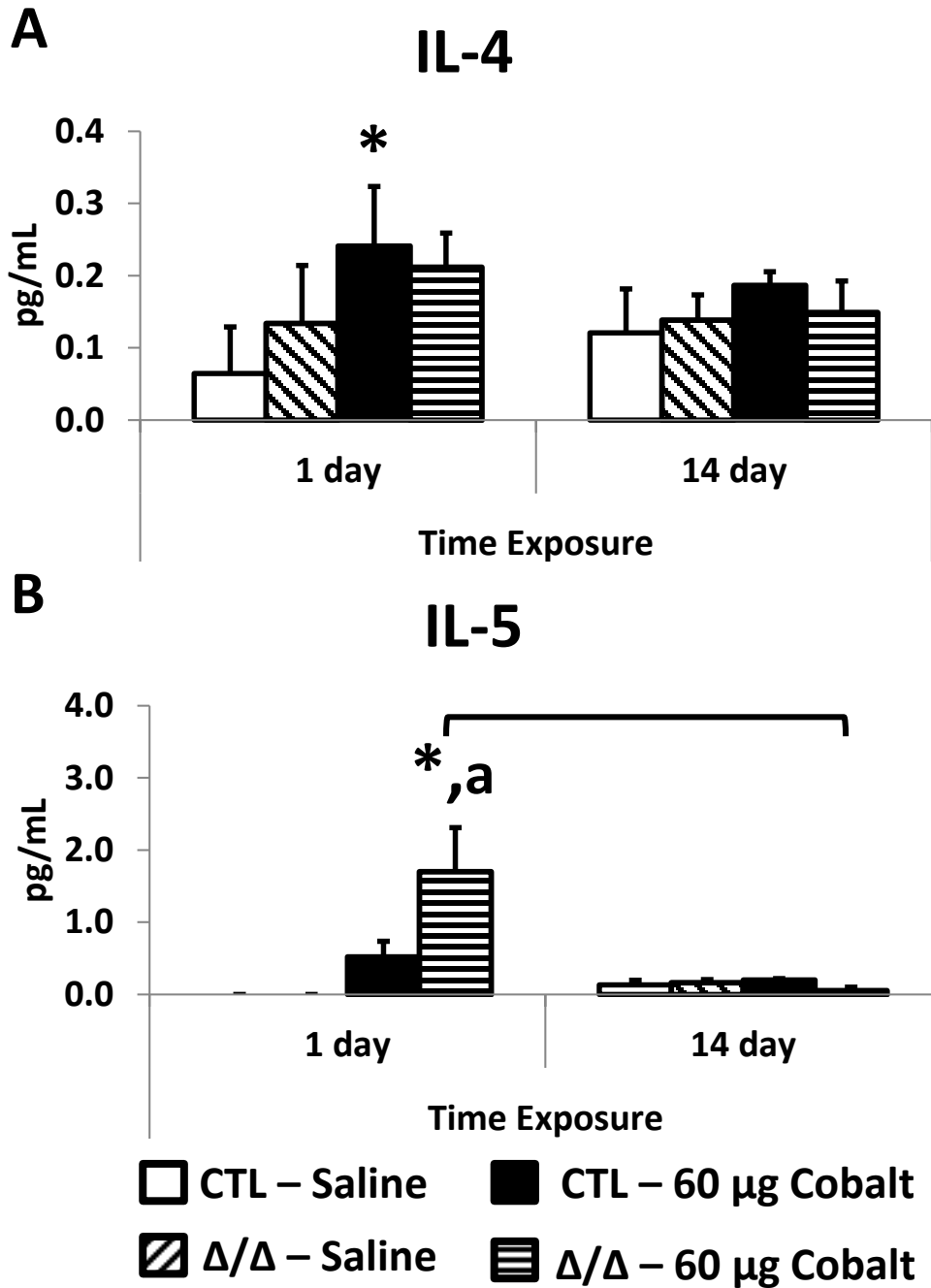


Figure 40. IL-4 and IL-5 cytokine levels from bead array in HIF2 α mice. BAL was tested for cytokine levels using a cytokine bead array (CBA) and run on a FACSCalibur flow cytometer (BD Biosciences). Shown are IL-4 (A) and IL-5 (B). N=4-5 mice/group. One-way ANOVA was performed and significance using Fisher's LSD of $\alpha=0.05$ is indicated by: * (from saline treated control), a (from CTL or Δ/Δ counterpart within time point) or bracket (from same treatment in different time point).

Figure 41

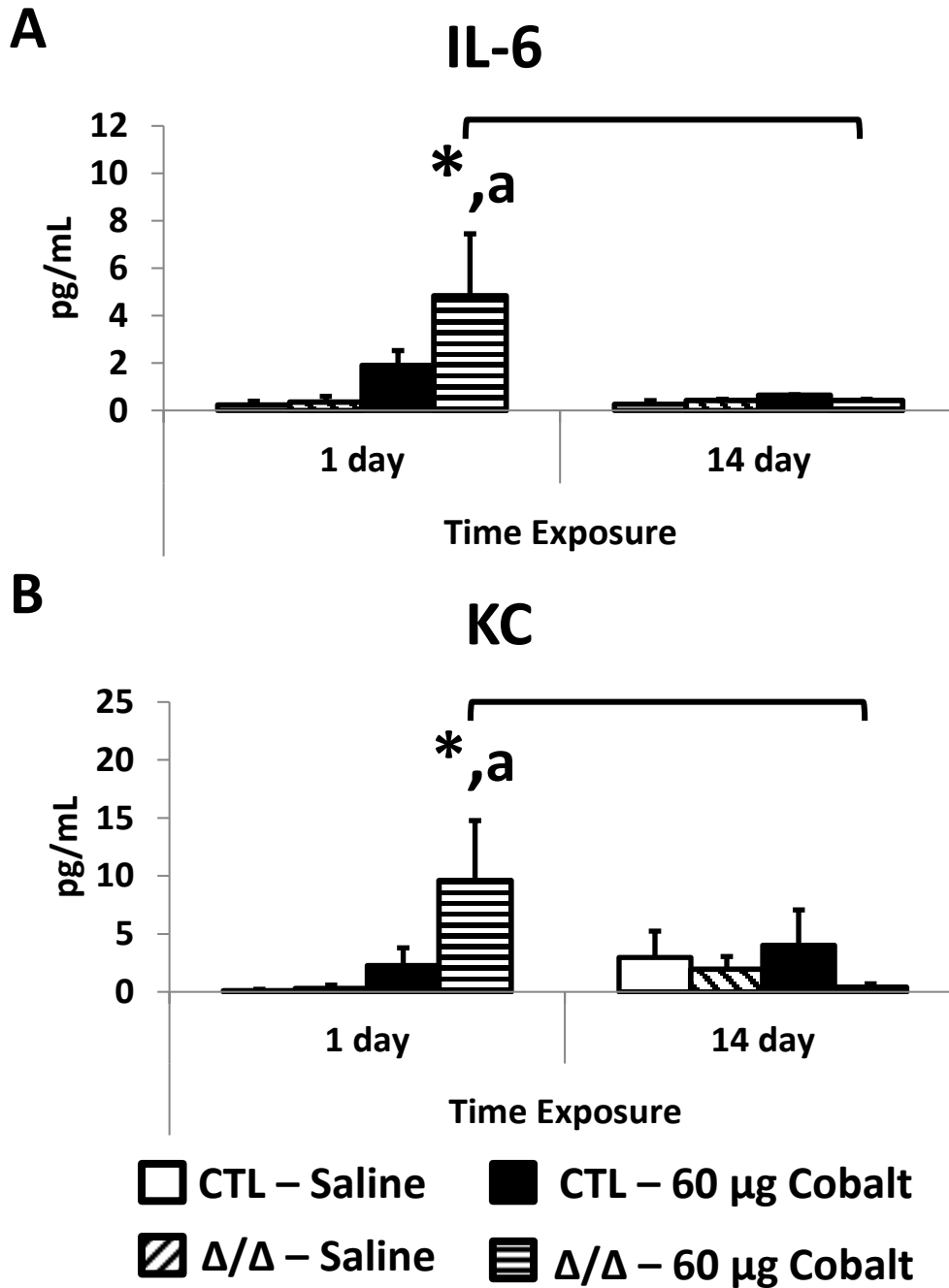


Figure 41. IL-6 and KC cytokine levels from bead array in HIF2 α mice. BAL was tested for cytokine levels using a cytokine bead array (CBA) and run on a FACSCalibur flow cytometer (BD Biosciences). Shown are IL-6 (A) and KC (B). N=4-5 mice/group. One-way ANOVA was performed and significance using Fisher's LSD of $\alpha=0.05$ is indicated by: * (from saline treated control), a (from CTL or Δ/Δ counterpart within time point) or bracket (from same treatment in different time point).

Figure 42

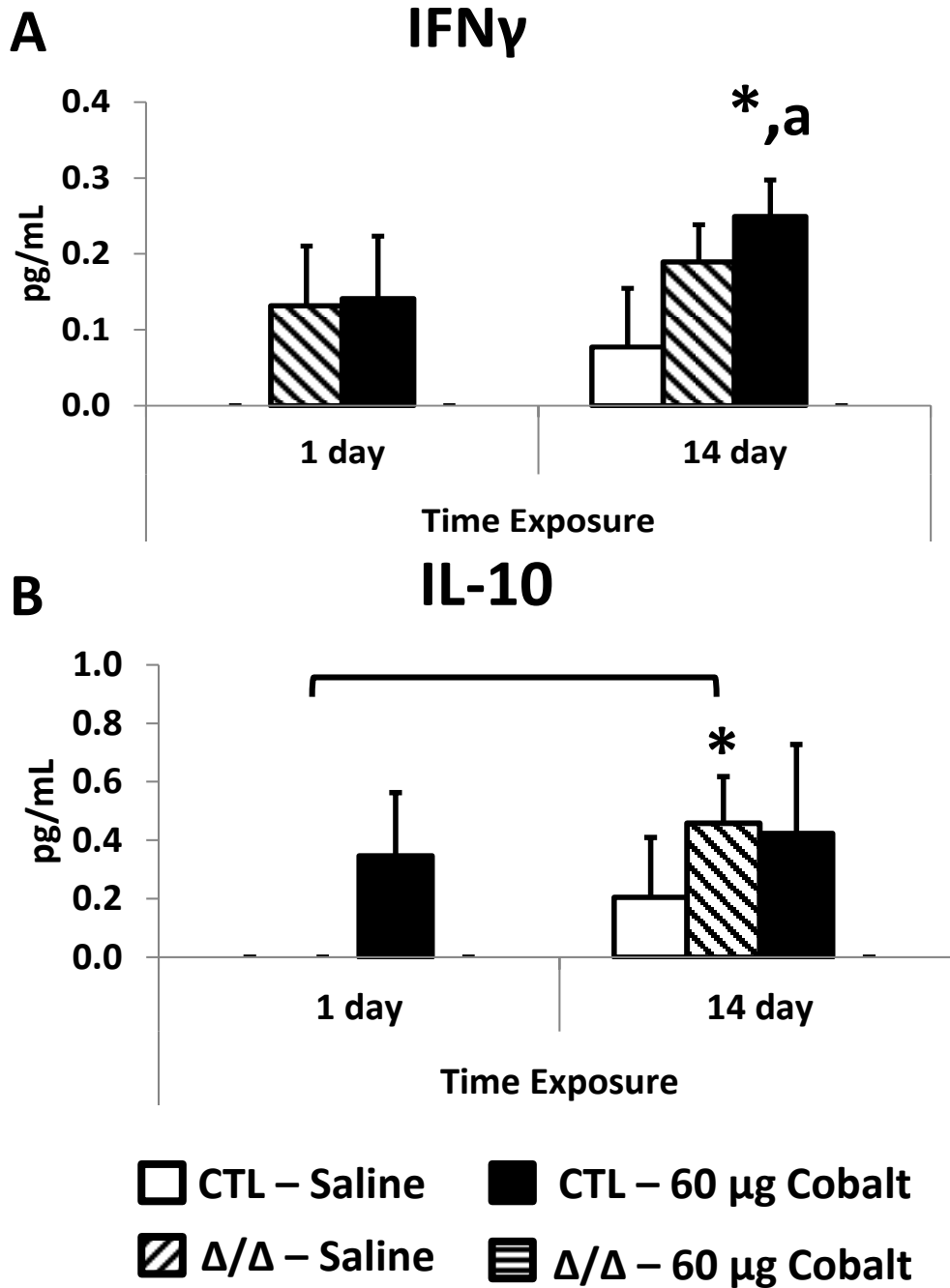


Figure 42. IFN γ and IL-10 cytokine levels from bead array in HIF2 α mice. BAL was tested for cytokine levels using a cytokine bead array (CBA) and run on a FACSCalibur flow cytometer (BD Biosciences). Shown are IFN γ (A) and IL-10 (B). N=4-5 mice/group. One-way ANOVA was performed and significance using Fisher's LSD of $\alpha=0.05$ is indicated by: * (from saline treated control), a (from CTL or Δ/Δ counterpart within time point) or bracket (from same treatment in different time point).

HIF1 α /2 α mice treated at 5 days

Given the change in inflammation observed in the HIF1 α and HIF2 α deficient mice, it was of interest to determine if the phenotype could be exacerbated upon loss of both HIF α isoforms in the same mouse. Therefore, HIF1 α /2 α mice were treated with regular food and water or DOX food and water for the P4-30 time period, and after 10 days of DOX clearing, were treated with the usual 5 days of 60 μ g CoCl₂ per mouse per day oropharyngeal aspiration dosing scheme discussed previously, with sacrifice and samples taken 24 hours after final dose.

HIF1 α and HIF2 α IHC

To illustrate the HIF1 α and HIF2 α knockout, IHC was performed for both HIF1 α and HIF2 α using lungs from control and DOX mice. In both cases, a clear loss of staining in the lung is seen in Club cells (dashed arrows) and the parenchymal region in general, though staining in macrophages and other inflammatory cells remains (solid arrows)(Figure 43).

BAL Cellularity

BAL fluid collected from the 5 day time point was compared to previous data from the HIF1 α and HIF2 α mice. Total cells increased with cobalt treatment across all strains when compared to saline treated mice. HIF1 α /2 α CTL mice treated with cobalt had less total cells than their HIF1 α and HIF2 α counterparts, which was not expected, and may be due to slight variation in the mixed C57/FVB strains (black bars, Figure 44A). Macrophages make up most cells in BAL regardless of treatment (Figure 44B). Eosinophils from HIF1 α /2 α ^{Δ/Δ} mice are much like the HIF1 α ^{Δ/Δ} mice, increasing with cobalt treatment compared to the cobalt-treated HIF-

sufficient controls (black bars, Figure 45A). Numbers of neutrophils and lymphocytes were highest in the HIF1 α cobalt-treated mice than the other 2 strains (Figure 45B and Figure 46). The BAL cellularity suggests the HIF1 $\alpha/2\alpha^{\Delta/\Delta}$ mice behave much like the HIF1 $\alpha^{\Delta/\Delta}$ mice only at 5 days.

Figure 43

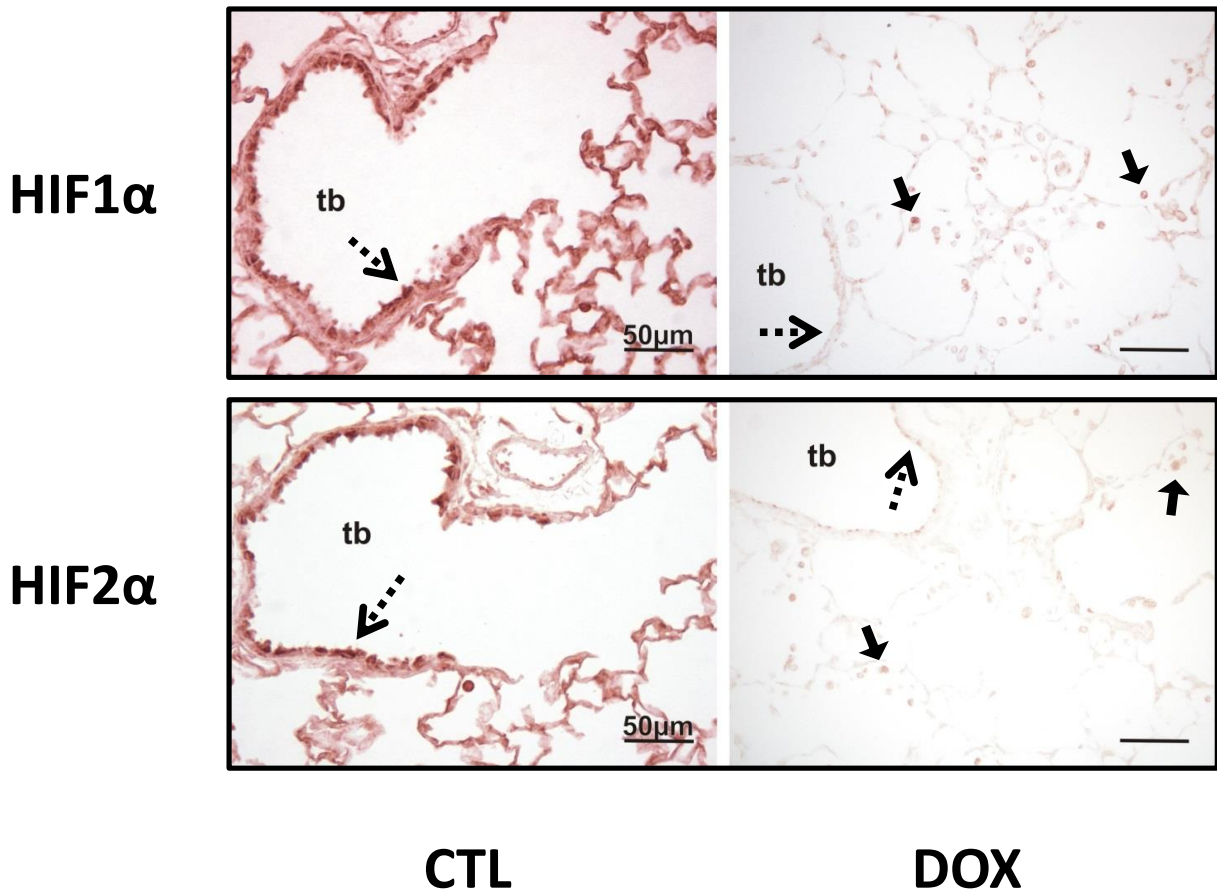


Figure 43. HIF1 α and HIF2 α IHC for HIF1 $\alpha/2\alpha$ mice. Mice received regular food and water (CTL) or DOX food and water (DOX) from P4-30. Sections were stained for HIF1 α (NB100-479, 1:100, Novus Biologicals) and HIF2 α (NB100-122, 1:100, Novus Biologicals). No counterstain was used in order to highlight the loss of HIF-staining.

Figure 44

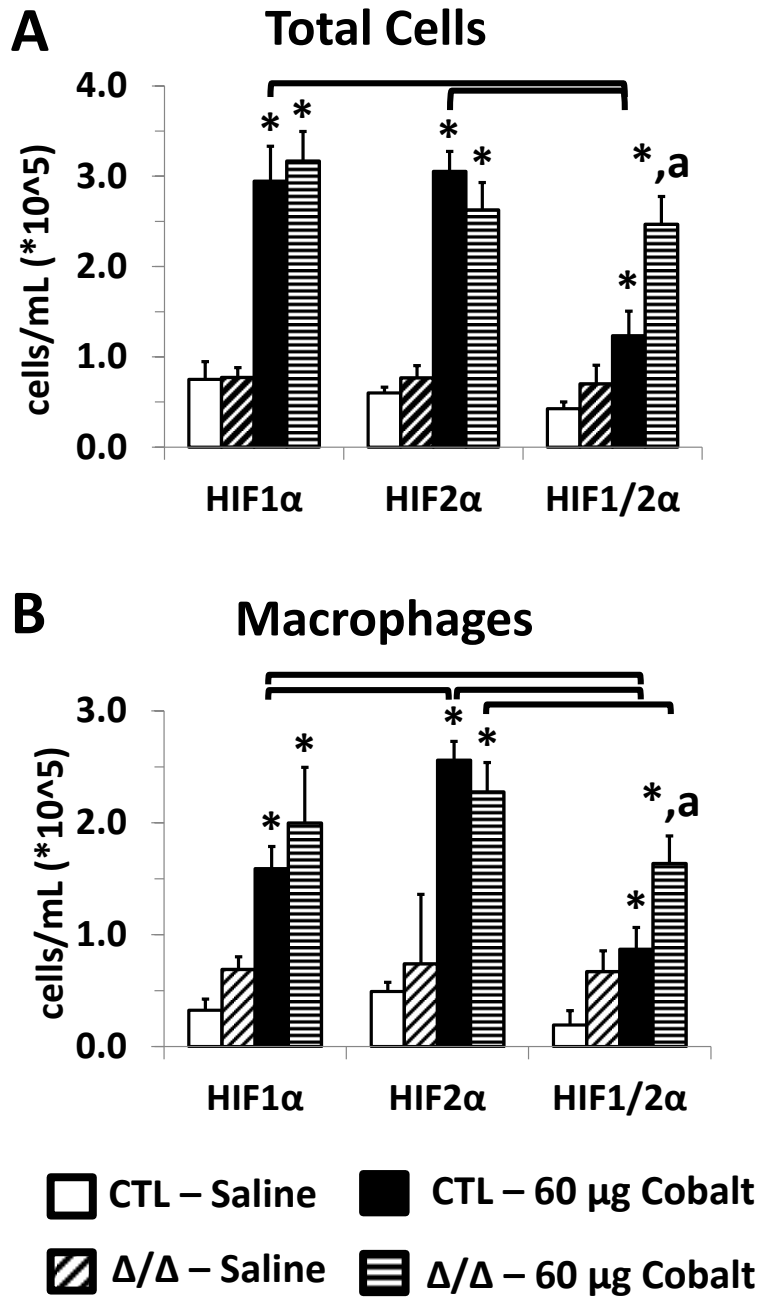


Figure 44. BAL total cells and macrophages from HIF1 α , HIF2 α and HIF1 α /2 α mice at 5 days cobalt exposure. BAL total cells (A) and macrophages (B) are shown. One-way ANOVA was performed and significance using Fisher's LSD of $\alpha=0.05$ is indicated by: * (from saline treated control), a (from CTL or Δ/Δ counterpart within strain), brackets (from same treatment across HIF strain). N=5-8 mice/group.

Figure 45

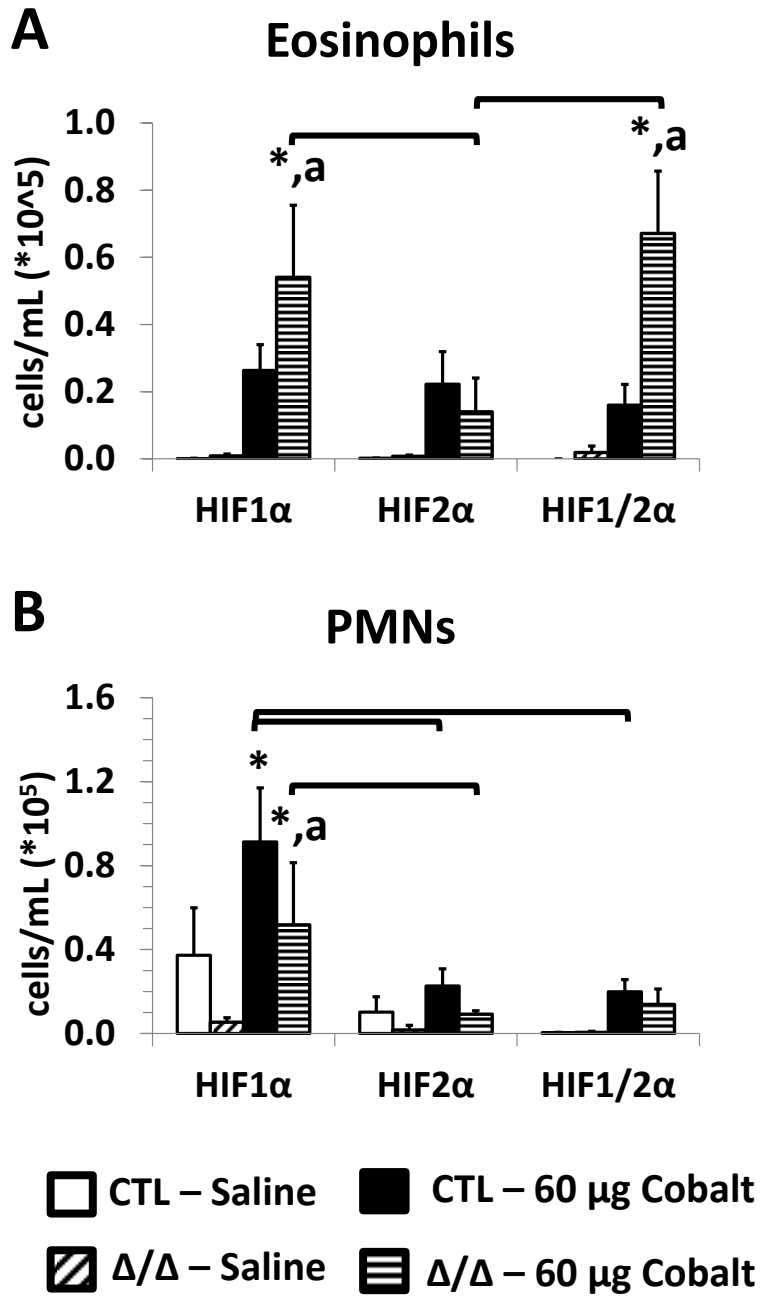


Figure 45. BAL eosinophils and PMNs from HIF1 α , HIF2 α and HIF1 α /2 α mice at 5 days cobalt exposure. BAL eosinophils (A) and neutrophils (PMNs) (B) are shown. One-way ANOVA was performed and significance using Fisher's LSD of $\alpha=0.05$ is indicated by: * (from saline treated control), a (from CTL or Δ/Δ counterpart within strain), brackets (from same treatment across HIF strain). N=5-8 mice/group.

Figure 46

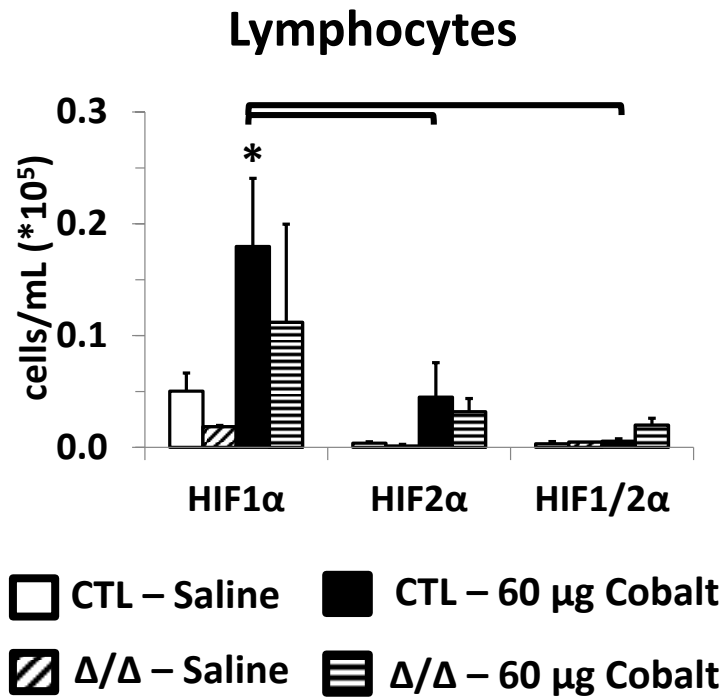


Figure 46. BAL lymphocytes from HIF1 α , HIF2 α and HIF1 α /2 α mice at 5 days cobalt exposure. BAL lymphocytes are shown. *One-way ANOVA was performed and significance using Fisher's LSD of $\alpha=0.05$ is indicated by: * (from saline treated control), a (from CTL or Δ/Δ counterpart within strain), brackets (from same treatment across HIF strain). N=5-8 mice/group.*

Histopathology and Immunohistochemistry

With hematoxylin and eosin staining, saline mice showed no visible pathology or notable difference between CTL and DOX treated mice (Figure 47A and B). HIF2 α and HIF1 α /2 α mice treated with cobalt were similar in severity of inflammation, in agreement with the BAL cellularity (Figure 47C-E). Lesions were sporadic and mostly seen in G5 (upper airway) sections. Major basic protein IHC revealed that both strains of HIF2 α and HIF1 α /2 α mice displayed mild

Figure 47

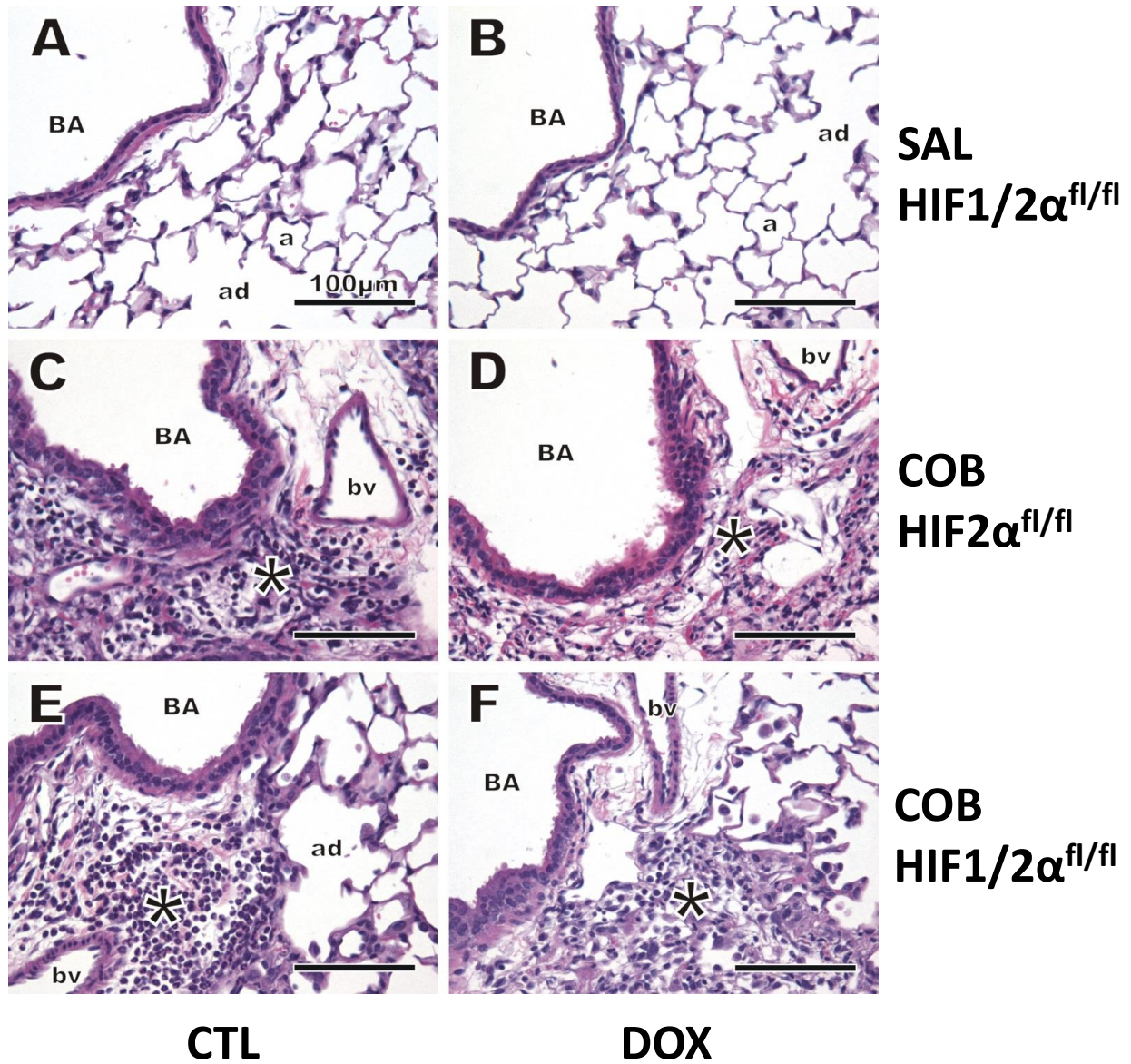


Figure 47. H&E stain from HIF2 α and HIF1 α /2 α mice at 5 days cobalt exposure. Lungs at G5 were stained with hematoxylin and eosin (H&E). Saline treated lungs (SAL, from HIF1 α /2 α strain) were similar. Black line indicates 50 μ m. * = mixed inflammatory cell infiltrate; BA=bronchial airway; bv=blood vessel; ad=alveolar duct; a=alveolus

eosinophilia with cobalt exposure (Figure 48C and D), though HIF1 α /2 α ^{Δ/Δ} mice showed the highest concentration of eosinophils in focal lesions both near bronchial blood vessels/lamina

propria and in the parenchymal regions (dashed arrows, Figure 48F). Alcian blue periodic acid Schiff (AP-PAS) staining was performed (Figure 49), and while mucosubstances were increased in cobalt-treated strains, all seemed similar to one another.

Cytokine analysis of whole lung lysate by bead array

Cytokines were analyzed from whole lung lysate (WLL) generated from right lung lobes flash-frozen in liquid nitrogen at necropsy (Figures 50, 51 and 52). There was a general agreement between the HIF1 α and HIF1 α /2 α mice in that IL-4 and IL-5 were both increased in these strains treated with cobalt (Figure 50A and B). Additionally, the presence of high levels of IL-6 in cobalt-treated HIF2 α mice and low levels of IL-6 in the HIF1 α and HIF1 α /2 α strains (Figure 51A) demonstrate these strains could be following disparate cytokine profiles which could be contributing to eosinophilia seen at 5 days in the mice lacking HIF1 α or HIF1 α /2 α but not HIF2 α alone. Along these lines, the presence of IL-17 in HIF1 α /2 α -deficient mice treated with notable (Figure 51B). Levels of IFN γ (Figure 52A) had some significant changes but did not follow any observable pattern across groups. TNF α levels (Figure 52B) did not show any changes across groups.

Gene expression analyses

Total lung mRNA was extracted from frozen right lung lobes and cDNA was generated from 1 μ g mRNA. Quantitative real time PCR was performed for several genes known to have roles in lung inflammation and/or HIF-signaling using SYBR green as a detector (Figure 53).

Figure 48

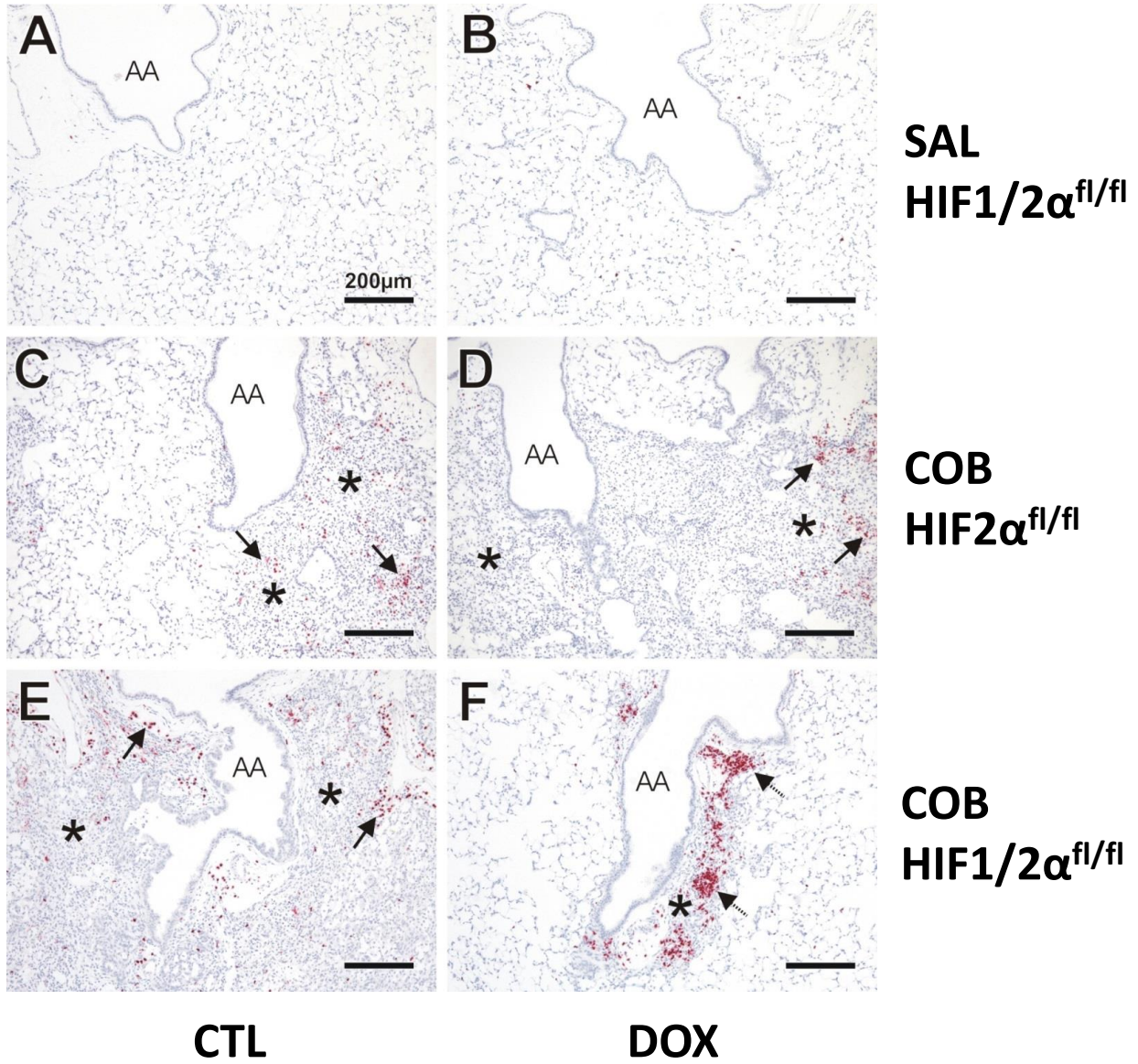


Figure 48. MBP IHC from HIF2 α and HIF1 α /2 α mice at 5 days cobalt exposure. Lungs were immunohistochemically stained for MBP (red) and counterstained with light hematoxylin. Eosinophils (Eos) were present in all infiltrates of cobalt-treated mice (stars, C-F). Higher concentrations of Eos were within some infiltrates (dashed arrows) compared to more mixed inflammatory infiltrates (solid arrows). Black line indicates 200 μ m.

Figure 49

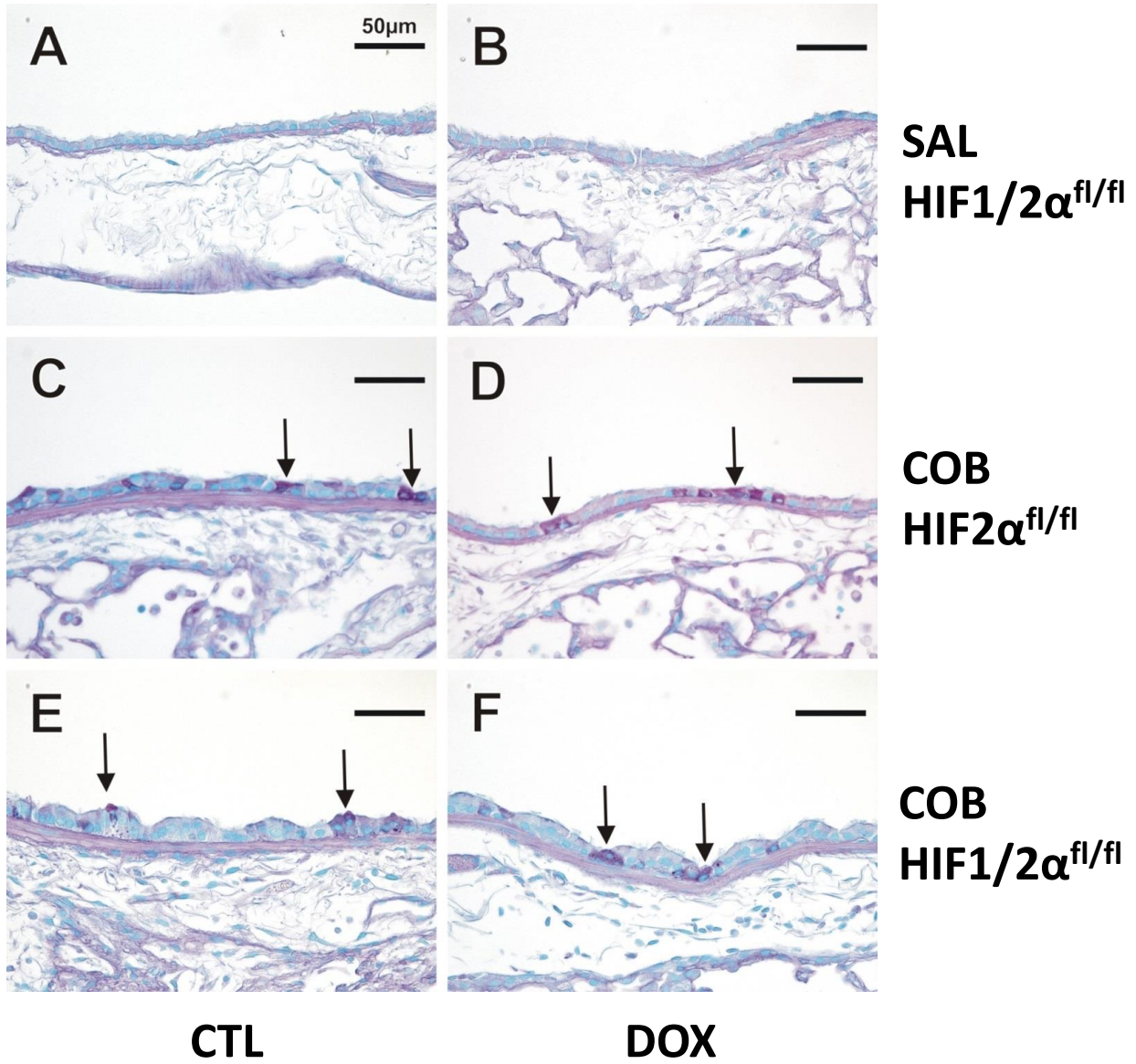


Figure 49. AB-PAS stain from HIF2 α and HIF1 α /2 α mice at 5 days cobalt exposure. Lungs were stained with Alcian Blue – Periodic Acid Schiff to visualize production of mucosubstances, and counterstained with light hematoxylin. Black line indicates 50 μ m. Solid arrows indicate location of mucosubstances in the axial airway.

Figure 50

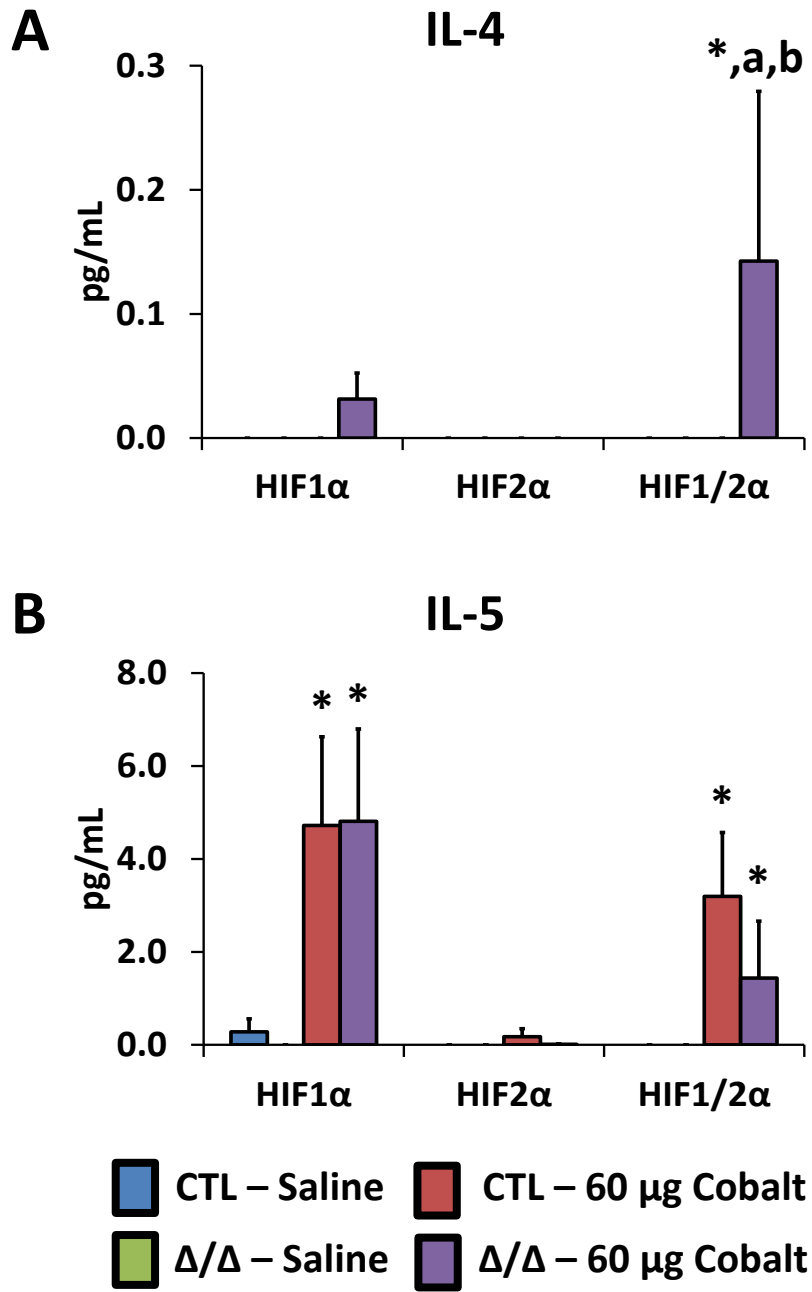


Figure 50. IL-4 and IL-5 cytokines from WLL of HIF1 α , HIF2 α and HIF1 α /2 α mice after 5 days cobalt exposure. Right lung lobe homogenate was analyzed via cytokine bead array for IL-4 (A) and IL-5 (B). One-way ANOVA was performed and significance using Fisher's LSD of $\alpha=0.05$ is indicated by: * (from saline treated control), a (from CTL or Δ/Δ counterpart within strain), b (from same treatment across HIF strains). N=5-8 mice/group.

Figure 51

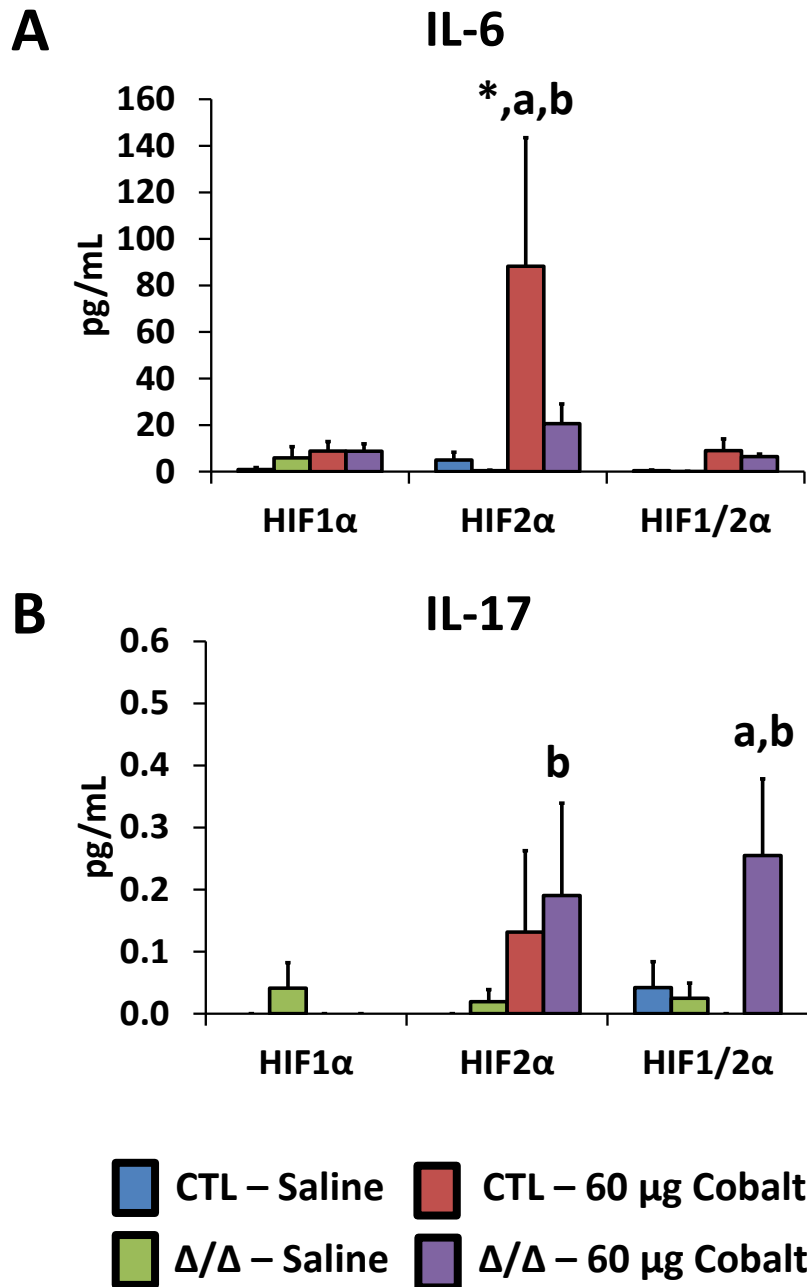


Figure 51. IL-6 and IL-17 cytokines from WLL of HIF1 α , HIF2 α and HIF1 α /2 α mice after 5 days cobalt exposure. Right lung lobe homogenate was analyzed via cytokine bead array for IL-6 (A) and IL-17 (B). One-way ANOVA was performed and significance using Fisher's LSD of $\alpha=0.05$ is indicated by: * (from saline treated control), a (from CTL or Δ/Δ counterpart within strain), b (from same treatment across HIF strains). N=5-8 mice/group.

Figure 52

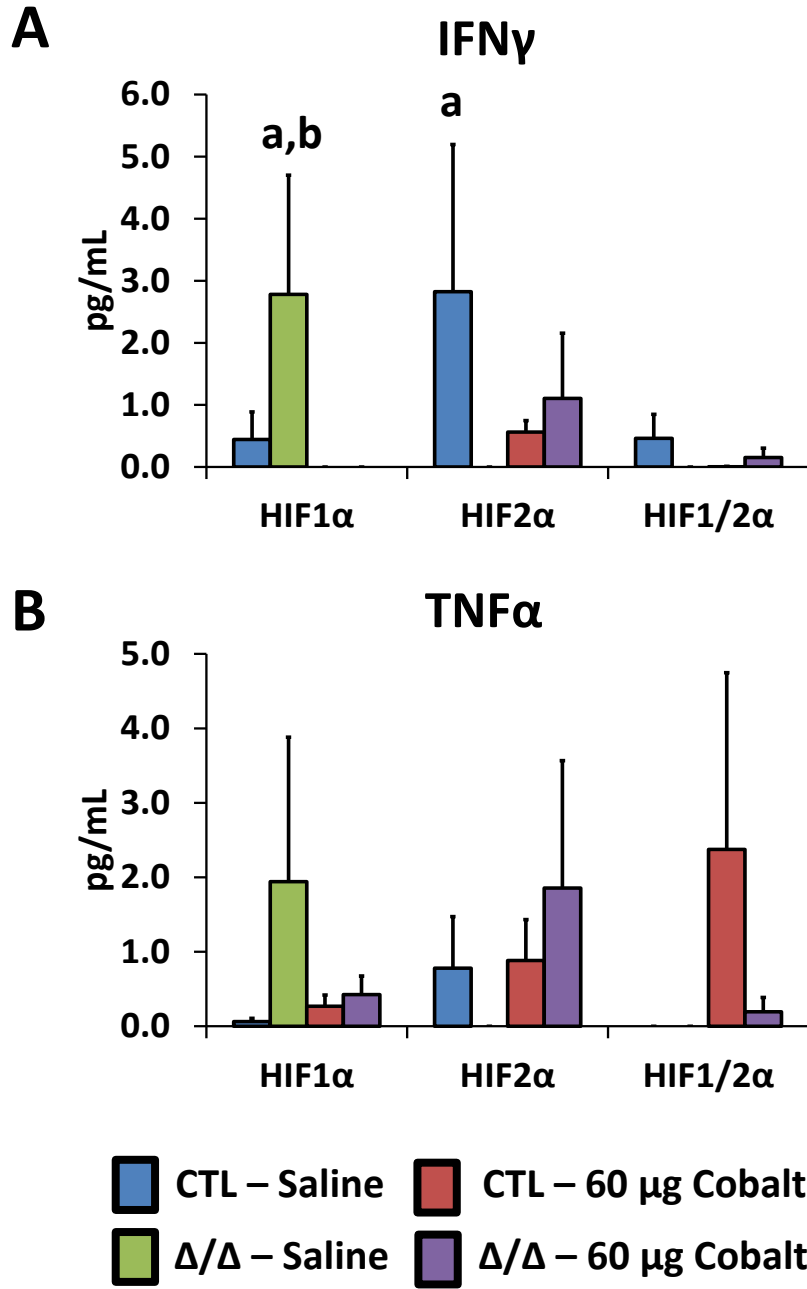


Figure 52. IFN γ and TNF α cytokines from WLL of HIF1 α , HIF2 α and HIF1 α /2 α mice after 5 days cobalt exposure. Right lung lobe homogenate was analyzed via cytokine bead array for IFN γ (A) and TNF α (B). One-way ANOVA was performed and significance using Fisher's LSD of $\alpha=0.05$ is indicated by: * (from saline treated control), a (from CTL or Δ/Δ counterpart within strain), b (from same treatment across HIF strains). N=5-8 mice/group.

Figure 53

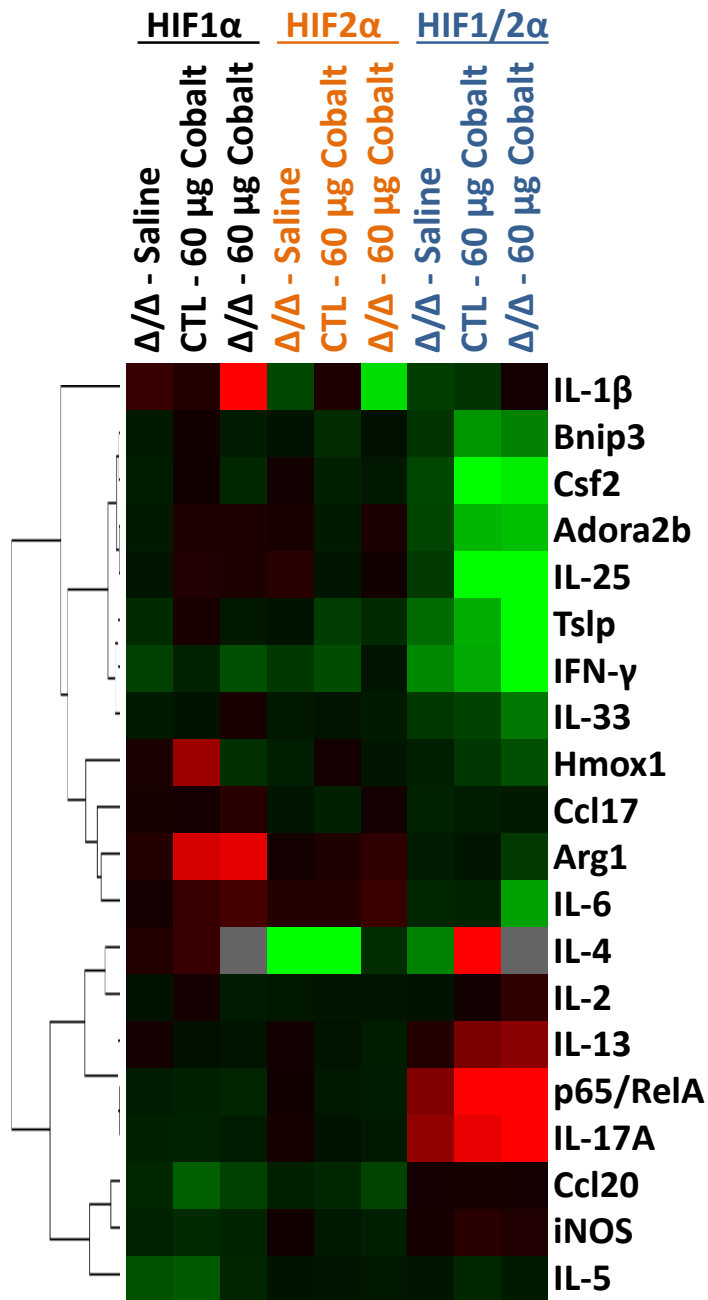


Figure 53. WLL gene expression profiles of HIF1α, HIF2α and HIF1α/2α mice with 5 days cobalt exposure. Heat map and cluster analysis of the gene expression data are shown. Within genotype, each group was normalized to the CTL-Saline group. Red indicates relative up-regulation compared to CTL-Saline group, whereas green indicates relative down-regulation.

According to the phenotype of eosinophilia, we anticipated the HIF1 $\alpha^{\Delta/\Delta}$ mice to behave similarly to HIF1 $\alpha/2\alpha^{\Delta/\Delta}$ mice, but the HIF1 $\alpha/2\alpha^{\Delta/\Delta}$ mice seemed to have their own unique gene expression profile. IL-4, IL-5 and IL-13, classic T_H2 cytokines, clustered together, though not in a way that agrees with the phenotype.

Discussion

These studies are the first to investigate the role of lung epithelial HIF2 α in cobalt-induced lung inflammation. Though HIF2 α shares sequence homology with HIF1 α , the differential expression of HIF2 α , notably the lung-specific presence of large amounts of HIF2 α mRNA transcript, suggests that they play unique roles [189, 190]. This idea is further supported by unpublished results in our lab from *in utero* knockouts of HIF1 α and HIF2 α , and though these roles are almost certainly a result of transcription factor networks engaged in lung development, the differences are notable. The data presented here supports the idea that HIF1 α and HIF2 α play similar, but not completely overlapping roles in cobalt-induced lung inflammation.

Interestingly, eosinophilia was induced in cobalt treated HIF2 $\alpha^{\Delta/\Delta}$ mice at 14 days, which is a similar response to that seen at 5 days in HIF1 $\alpha^{\Delta/\Delta}$ mice. Explanations for this eosinophilia might lie in cytokine secretion such as IL-5. In studies of HIF1 α by Saini et al., IL-5 increases very early (after 1 day of exposure to cobalt) in the HIF1 $\alpha^{\Delta/\Delta}$ mice compared to

controls, which is soon followed at the day 5 time point by large eosinophil populations in these lungs [214]. In HIF2 $\alpha^{\Delta/\Delta}$ mice, IL-5 is also induced early at 1 day (Figure 40B), though the higher eosinophil BAL counts do not occur until later at 14 days (Figure 35A) and IHC results (Figure 38H). Whether IL-5 represents a functional link between HIF1 $\alpha^{\Delta/\Delta}$ and HIF2 $\alpha^{\Delta/\Delta}$ phenotypes remains to be determined by future studies, though it is tempting to believe that a common target of HIF1 α and HIF2 α (that is not induced or repressed normally in recombined mice) is responsible for the induction of IL-5 in both HIF1 $\alpha^{\Delta/\Delta}$ and HIF2 $\alpha^{\Delta/\Delta}$ mice. Other cytokines were increased early in HIF2 $\alpha^{\Delta/\Delta}$ mice treated with cobalt, including IL-6 and KC, though these cytokines do not necessarily have a direct role in eosinophilia. IL-6 induces T_H2 maturation through the production of IL-4 and suppress T_H1 maturation [296]. In the HIF1 α mice treated with cobalt, however, IL-6 was only induced strongly in control mice treated with cobalt [214].

Histopathologically it appears that at 14 days of cobalt treatment, control mice have mild recovery of overall injury compared to HIF2 $\alpha^{\Delta/\Delta}$ mice (Figure 37D and H, respectively). This observation is supported by total cell counts (Figure 34A). Mucous substances also seem to decrease for control mice from 5 days to 14 days (Figure 39C and D, respectively) compared to HIF2 $\alpha^{\Delta/\Delta}$ mice which show increased mucous substances from 5 to 14 days (Figure 39G and H, respectively). When comparing these results to our previous studies of HIF1 $\alpha^{\Delta/\Delta}$ mice, we see very similar amounts of total cells at 14 days for both controls and HIF-deficient mice, indicating that a slight recovery or normalization is achieved at the 14 day time point which is

prevented in both HIF1 $\alpha^{\Delta/\Delta}$ and HIF2 $\alpha^{\Delta/\Delta}$ mice. It will be interesting to see whether these histopathologic observations of recovery in the controls become important in future investigations of the mechanisms of these injury dynamics are elucidated.

Comparing the combination HIF1 $\alpha/2\alpha^{\Delta/\Delta}$ mice to HIF2 $\alpha^{\Delta/\Delta}$ mice (and published results from HIF1 $\alpha^{\Delta/\Delta}$ mice) we see an eosinophilia similar to that observed by HIF1 $\alpha^{\Delta/\Delta}$ mice apparent at the 5 day time point, whereas the HIF2 $\alpha^{\Delta/\Delta}$ mice are not yet displaying eosinophilia at 5 days (Figure 45A and 48D). The timing of this phenotype suggests that HIF1 α -deficiency is dominant in inducing an earlier eosinophilia compared to HIF2 α -deficiency, which could have implications for specificity of HIF1 α and HIF2 α target genes. Gene expression profiles to date do not share this phenotypic similarity, however, and HIF1 $\alpha/2\alpha^{\Delta/\Delta}$ mice show a unique expression signature at 5 days (Figure 53). Upregulation of IL-17 expression (Figure 53) correlates with increased levels of this cytokine in WLL (Figure 51B) in HIF1 $\alpha/2\alpha^{\Delta/\Delta}$ mice, suggesting T_H17 cells may be contributing to this strain's phenotype. Despite the differences between HIF1 $\alpha/2\alpha$ mice and the others, the T_H2 cytokines IL-4, IL-5 and IL-13 clustered together, away from IFN γ . Further verification of these data, possibly through whole genome arrays of the postnatal HIF1 α , HIF2 α and combo HIF1 $\alpha/2\alpha$ alveolar type II cells will potentially yield insight into the time-dependent changes in gene expression and may identify targets or target networks responsible for influencing the phenotype.

These studies of HIF1 α and HIF2 α improve our understanding of the roles that these transcription factors play in cobalt-induced lung injury. Primarily, we have learned that lack of these transcription factors can alter the inflammatory and immune response, predisposing tissues to an eosinophilic inflammation (and T_H2 in HIF1 α ^{Δ/Δ} mice) correlating with IL-5 expression. At the very least this prompts further investigation into the effect that loss of HIF1 α and HIF2 α in epithelial cells may have in other allergic and inflammatory diseases involving the epithelium such as inflammatory bowel disease and eczema. The alteration of the immune response based on presence or absence of HIF α s, as well as their dual roles in targeting pro-survival and pro-death genes suggests that overexpression of HIFs may also be detrimental, as targeting the HIFs pharmacologically has shown mixed results [211]. Additionally, different knockout systems have shown contradictory roles for HIFs in epithelial cells (our data), myeloid cells [200], and more widespread knockouts [212]. We have learned that HIF1 α and HIF2 α deletion in the lung epithelium using our inducible knockout system is not protective to cobalt injury per se as previously thought to be the case from *in vitro* data [285, 297]. In retrospect it is not surprising that the HIF α -deficiency in a specific group of cells would be complicated, yet the results clearly warrant further investigation and clarification.

There are several limitations to the current studies. First and foremost, our investigations to date on all HIF α -deficient mice have focused on whole lung analyses (either protein or RNA), which, while useful, may not reveal meaningful insights into the mechanism of the eosinophilic phenotypes observed. More targeted analysis of ATII cells, such as through primary isolation, both early in postnatal development and later during cobalt injury will be

helpful in determining the sequence of events leading to eosinophilia. Further clarification of which cytokines are involved and their source is warranted now more than ever, as the repertoire of cytokines and chemokines that the epithelium is capable of secreting that increases the likelihood of eosinophilia has grown substantially in recent years. These include but are not limited to: IL-25, IL-33, TSLP, Eotaxin1-3, GM-CSF, Ccl20, β -defensin, IL-1 β , osteopontin, TARC (Ccl17), PARC (Ccl18) and MDC (Ccl22), which are the target of active investigation by our lab.

The second limitation to these studies, especially in regards to the combination HIF1 α /2 α mice, was lack of similar time-course data than that for the HIF2 α mice. Focusing on 5 days was considered the best starting point, but many more gaps exist. Since HIF2 $\alpha^{\Delta/\Delta}$ mice follow a delayed eosinophilia, mechanistic questions may be better answered by comparing all strains at their peak eosinophilic time point, such as 14 day exposures from HIF2 α mice to 5 day exposures of HIF1 α and HIF1 α /2 α mice. Additionally, in either strain, a 2 day time point and/or 10 day time point may provide more detailed information about the leukocyte dynamics in these lungs.

The impact of these studies on our understanding of HMLD is difficult primarily because the animal model we have chosen to incorporate has several important differences to that of HMLD. Firstly, our model system utilizes cobalt that is highly water soluble (and thus distribution throughout the body and away from the lung occurs much faster than cobalt seen in tungsten carbide) and does not incorporate particulates, which have been theorized to contribute to ROS production in the prolonged presence of cobalt [270]. Secondly, mimicry of

HMLD probably requires more chronic exposures than 14 days, since exposed people have a history of chronic occupational exposures followed by many years of being asymptomatic before presenting with pulmonary symptoms. Finally, while the allergic sensitivity of cobalt has been defined as a separate entity than HMLD, this allergic component to cobalt exposure is more prevalent than HMLD, and it is difficult to determine with confidence whether (and to what extent) these two processes are distinct.

Thus, with the several differences between HMLD and the chosen model, and with a majority of the investigations focusing on the altered inflammatory response to cobalt with and without HIF1 α and/or HIF2 α , the clinical impact of these findings to patients with HMLD is difficult to predict. It is safe to say that while HMLD was the primary driver of developing this model system, incorporating particulates into this model was impractical for several reasons, and cobalt was used more as an inducer of an inflammatory response than for mimicry of HMLD. Impact of this research model on our understanding of HMLD will be higher if particulates and more chronic exposures are incorporated in future studies. The most important aspect of the investigations here was the altered eosinophilic infiltration, which highlights the importance of epithelial signaling in recruitment of inflammatory and immune cells into the lung. These dynamics must be considered in any future study of HMLD and cobalt-induced lung injury.

CHAPTER 5 – SUMMARY AND CONCLUSIONS

Summary of Research

The work I have presented here clarifies the role of lung-epithelial specific HIF1 α -deficiency in cobalt-induced lung injury. First, I have investigated the timing of HIF1 α deletion necessary for eosinophilic predisposition, and also characterized the T cell populations in cobalt-treated control and HIF1 $\alpha^{\Delta/\Delta}$ mice. I have further performed preliminary investigations into the roles of adenosine receptor A2B and NF- κ B signaling in the creation of the eosinophilic phenotype of HIF1 $\alpha^{\Delta/\Delta}$ mice. Investigations into the time course of HIF2 α -deficiency as well as the combination HIF1 $\alpha/2\alpha^{\Delta/\Delta}$ mice at 5 days in cobalt-induced lung injury illustrate the active role that these proteins play in directing the immune response in the lung. Finally, these results have strong implications for overlap of cobalt asthma and hard metal lung disease, namely that alteration of HIF α signaling can alter the nature and timing of the immune response to cobalt. In this way, epithelial HIF α s represent a potential key bridge and control point for pathogenesis of both cobalt asthma and HMLD.

Major findings and implications

1. Deletion of HIF1 α in the early postnatal development period (P4-14 and P4-30) is required for the eosinophilic phenotype of cobalt-induced lung inflammation. This finding is supported by other work in our lab utilizing an allergic airway disease model, and may implicate HIF1 α as an important target gene for the hygiene hypothesis.
2. Eosinophilic inflammation seen in HIF1 $\alpha^{\Delta/\Delta}$ mice is driven in part by an increase in T_H2 cells. In contrast, control mice treated with cobalt do not display T_H1 responses.

3. Influence of NF- κ B and Adora2b signaling on the HIF1 $\alpha^{\Delta/\Delta}$ phenotype are inconclusive, and require further clarification and characterization.
4. Loss of HIF2 α in lung epithelium also produces an eosinophilic phenotype following a 14 day occupational exposure. This is different from the HIF1 $\alpha^{\Delta/\Delta}$ mice, which display eosinophilia after 5 days. Both HIF1 $\alpha^{\Delta/\Delta}$ mice and HIF2 $\alpha^{\Delta/\Delta}$ mice showed increased IL-5 cytokine levels in BAL and thus IL-5 may be a key molecular effector of these responses.
5. Loss of both HIF1 α and HIF2 α in lung epithelium has a phenotype similar to HIF1 $\alpha^{\Delta/\Delta}$ mice, with eosinophilia after 5 days of cobalt exposure, indicating that HIF1 α -deficiency drives an earlier eosinophilic infiltration.

Proposed Working Model

Given the findings and implications mentioned previously, a working model is given in Figure 54. HIF2 α -deficiency in lung epithelium behaves in a similar fashion as HIF1 α -deficiency during cobalt induced lung inflammation, confirming that both isoforms play a role in altering inflammatory responses. Upon inflammatory stimulation from cobalt, crosstalk with other inflammatory signaling proteins or transcription factors directs transcription of normal cytokines such as TNF α , IL-1, and IL-8 to produce a primarily neutrophilic and macrophage-driven response (Figure 54A). In contrast, lung epithelium lacking HIF α s does not participate in crosstalk, which generates a unique set of cytokines such as IL-5, TSLP, IL-25 and IL-33, which recruit eosinophils and probably involves innate lymphoid type 2 cells (ILC2s) (Figure 54B).

Figure 54

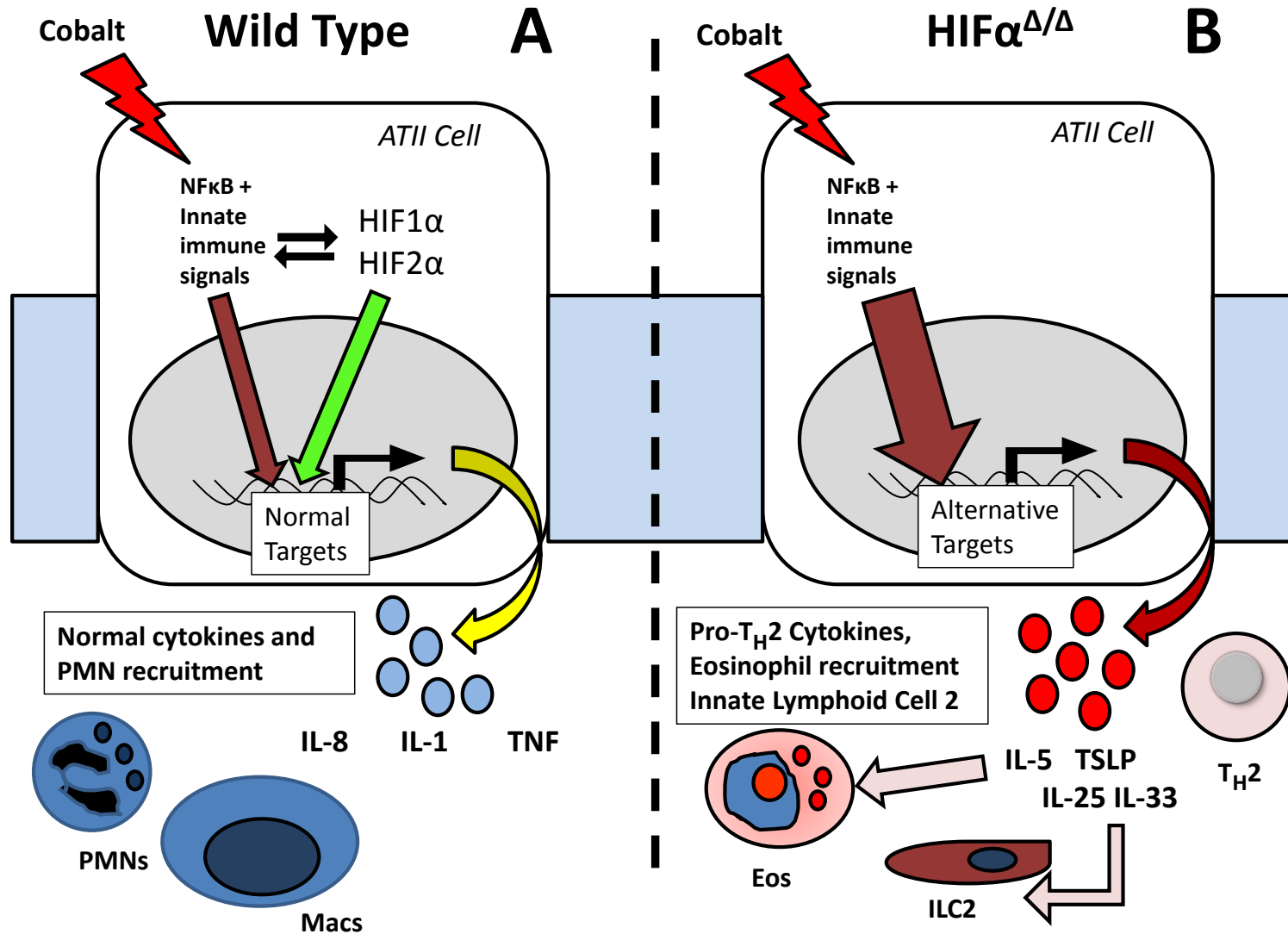


Figure 54. Working model of WT and HIF $\alpha^{\Delta/\Delta}$ lung epithelial cells exposed to cobalt. In normal cells exposed to an inflammatory

Figure 54 (cont'd)

stimulus, HIF1 α and HIF2 α have crosstalk with inflammatory signaling molecules, their transcriptional partners, or the products of the combined signaling to produce a neutrophilic and macrophage-dominant response **(A)**. In contrast, lung epithelium lacking HIF1 α or HIF2 α creates an unbalanced transcriptional profile which leads to secretion of IL-5 and other pro-TH2 cytokines which may involve innate lymphoid type 2 cells (ILC2s) to promote a primarily eosinophilic response **(B)**.

Knowledge gaps and future studies

The most difficult obstacle in attempting to determine any mechanism caused by a cell-type specific deletion is that initial analyses typically include whole tissues, which could potentially confound data. We are actively performing isolations of alveolar type II cells from our mice to obtain a more direct assessment of HIF1 α - and HIF2 α -dependent gene expression changes in these cells. These studies have the greatest potential to yield mechanistic information about the start of the eosinophilic phenotype, assuming pure populations can be isolated. They will also help determine the recombination efficiency of the SP-C/Cre model.

Another useful approach to characterizing the eosinophilic inflammation in these mice is to measure the immune cell populations in the lung. Recent studies have indicated the existence and functional relevance of several new classes of immune cells in lung inflammation and allergic disease. One of the cell types, called nuocytes or innate lymphoid cells (ILCs) have been shown to respond to epithelial inflammatory signals. In the case of ILC2s (the T_H2 version of this population), high levels of IL-4, IL-5 and IL-13 are secreted despite lacking recombined surface receptors (TCR) and are important for early responses to helminth infection [97]. Considering that initial studies of dendritic cells did not show many changes in populations (Greenwood, unpublished results), and that these ILC2 cells are capable of inducing eosinophilic inflammation, they are likely important players to consider in our model.

In addition to further exploration into ILC2s/nuocytes, ATII cells have recently been shown to express MHCII and participate in immune tolerance by inducing FoxP3+T_{REG} cells

[122]. Immune tolerance (forming active T_{REG} cells) depends on presentation of antigens to APCs without additional inflammatory stimuli. If the pool of these APCs decreases considerably, it can in theory decrease T_{REG}s and thus increase the likelihood that tolerance is broken (active T-cell responses are initiated from innocuous stimuli). It is possible that loss of HIF α subunits in ATII cells may be directly impacting their survival and function from a metabolic standpoint, which secondarily prevents their ability to induce tolerance in the lung in the early postnatal time period. ATII cells require large amounts of energy to synthesize surfactant and participate in fluid transport during pulmonary edema, so disruption of metabolic adaptations to hypoxia by loss of HIF α s could certainly occur. Probing the lungs of HIF α -deficient mice for overall populations of ATII cells and any notable morphologic differences will be important for future studies.

There are several knowledge gaps in the crosstalk of NF- κ B and Adora2b in our model, and further characterization of these pathways, especially in isolated ATII cells, will clarify their relevance to the eosinophilic phenotype of HIF α loss. Dedicated studies with the use of several pharmacologic inhibitors and stimulators for either pathway, as well as isolating cell types (such as through lavage vs. lung mash, specific isolation of ATII cells or the use of *in vitro* systems to supplement *in vivo* studies) will likely be required to probe further into their relevance in our model of cobalt-induced lung inflammation.

The other noteworthy aspect of our studies is the use of a broad spectrum antibiotic, doxycycline, to induce recombination of HIF α s. While we have performed controls with DOX-

only animals to establish eosinophilia dependence in HIF1 α ^{fl/fl} mice on all 3 transgenes and DOX, clinical and experimental evidence is mounting regarding the impact of the microbiome and the use of antibiotics in early life having substantial impact on severity of allergic diseases. While the mechanism of antibiotic interference in allergic diseases is still unknown and under investigation, use of antibiotics besides doxycycline (non-tetracycline antibiotics) as well as differing housing environments (specific pathogen free conditions or cleaner) may help to put the effects of HIF1 α loss in early postnatal development into context with these other variables receiving attention in clinical studies.

REFERENCES

REFERENCES

1. Proctor, D. F., *A history of breathing physiology*. Lung biology in health and disease. 1995, New York: M. Dekker. xxii, 391 p.
2. *John Mayow (1641-1679)*. JAMA, 1966. **197**(5): p. 364-5.
3. Priestley, J., *An Account of Further Discoveries in Air*. By the Rev. Joseph Priestley, LL.D. F. R. S. in *Letters to Sir John Pringle, Bart. P. R. S. and the Rev. Dr. Price, F. R. S.* Philosophical Transactions, 1775. **65**: p. 384-394.
4. Cook, G. A. L., Carol M., *Oxygen*, in *The encyclopedia of the chemical elements*, Hampel, C. A., Editor. 1968, Reinhold Book Corp.: New York,. p. 499-512.
5. Severinghaus, J. W., *Fire-Air and Dephlogistication - Revisionisms of oxygen's discovery*, in *Hypoxia : through the lifecycle - Advances in experimental medicine and biology*, Roach, R. C., P. D. Wagner, and P. H. Hackett, Editors. 2003, Kluwer Academic/Plenum Publishers: New York. p. 7-19.
6. Anders, E. and M. Ebihara, *Solar-system abundances of the elements*. Geochimica et Cosmochimica Acta, 1982. **46**(11): p. 2363-2380.
7. Lyons, T. W., *Palaeoclimate: oxygen's rise reduced*. Nature, 2007. **448**(7157): p. 1005-6.
8. Farquhar, J., A. L. Zerkle, and A. Bekker, *Geological constraints on the origin of oxygenic photosynthesis*. Photosynth Res, 2011. **107**(1): p. 11-36.
9. Lyons, T. W. and C. T. Reinhard, *Early Earth: Oxygen for heavy-metal fans*. Nature, 2009. **461**(7261): p. 179-81.
10. Powell, F. L., *Studying biological responses to global change in atmospheric oxygen*. Respir Physiol Neurobiol, 2010. **173 Suppl**: p. S6-12.
11. Berner, R. A., J. M. Vandenbrooks, and P. D. Ward, *Evolution. Oxygen and evolution*. Science, 2007. **316**(5824): p. 557-8.
12. Thannickal, V. J., *Oxygen in the evolution of complex life and the price we pay*. Am J Respir Cell Mol Biol, 2009. **40**(5): p. 507-10.
13. Ward, P. D., *Out of thin air : dinosaurs, birds, and Earth's ancient atmosphere*. 2006, Washington, D.C.: J. Henry Press. xiii, 282 p.
14. Champe, P. C., R. A. Harvey, and D. R. Ferrier, *Biochemistry*. 3rd ed. Lippincott's illustrated reviews. 2005, Philadelphia: Lippincott/Williams & Wilkins. x, 534 p.

15. Maina, J. N., *Structure, function and evolution of the gas exchangers: comparative perspectives*. J Anat, 2002. **201**(4): p. 281-304.
16. Forster, T. D. and H. A. Woods, *Mechanisms of tracheal filling in insects*. Biol Rev Camb Philos Soc, 2013. **88**(1): p. 1-14.
17. Powell, F. L. and S. R. Hopkins, *Comparative physiology of lung complexity: implications for gas exchange*. News Physiol Sci, 2004. **19**: p. 55-60.
18. West, J. B., *Respiratory physiology : the essentials*. 9th ed. 2012, Philadelphia: Wolters Kluwer Health/Lippincott Williams & Wilkins. viii, 200 p.
19. Staub, N. C., *Basic respiratory physiology*. 1991, New York: Churchill Livingstone. ix, 242 p.
20. Rhoades, R. and G. A. Tanner, *Medical physiology*. 2nd ed. 2003, Philadelphia: Lippincott Williams & Wilkins. x, 781 p.
21. Weibel, E. R., *The pathway for oxygen : structure and function in the mammalian respiratory system*. 1984, Cambridge, Mass.: Harvard University Press. xv, 425 p.
22. Tyler, W. S. and M. D. Julian, *Gross and subgross anatomy of lungs, pleura, connective tissue, septa, distal airways, and structural units*, in *Treatise on pulmonary toxicology: Comparative Biology of the Normal Lung*, Parent, R. A., Editor. 1992, CRC Press: Boca Raton. p. v. <1 >.
23. Rackley, C. R. and B. R. Stripp, *Building and maintaining the epithelium of the lung*. J Clin Invest, 2012. **122**(8): p. 2724-30.
24. Franks, T. J., T. V. Colby, W. D. Travis, R. M. Tuder, H. Y. Reynolds, A. R. Brody, W. V. Cardoso, R. G. Crystal, C. J. Drake, J. Engelhardt, M. Frid, E. Herzog, R. Mason, S. H. Phan, S. H. Randell, M. C. Rose, T. Stevens, J. Serge, M. E. Sunday, J. A. Voynow, B. M. Weinstein, J. Whitsett, and M. C. Williams, *Resident cellular components of the human lung: current knowledge and goals for research on cell phenotyping and function*. Proc Am Thorac Soc, 2008. **5**(7): p. 763-6.
25. Basbaum, C. B., B. Jany, and W. E. Finkbeiner, *The serous cell*. Annu Rev Physiol, 1990. **52**: p. 97-113.
26. Rock, J. R., M. W. Onaitis, E. L. Rawlins, Y. Lu, C. P. Clark, Y. Xue, S. H. Randell, and B. L. Hogan, *Basal cells as stem cells of the mouse trachea and human airway epithelium*. Proc Natl Acad Sci U S A, 2009. **106**(31): p. 12771-5.
27. Hong, K. U., S. D. Reynolds, S. Watkins, E. Fuchs, and B. R. Stripp, *Basal cells are a multipotent progenitor capable of renewing the bronchial epithelium*. Am J Pathol, 2004. **164**(2): p. 577-88.

28. Linnoila, R. I., *Functional facets of the pulmonary neuroendocrine system*. Lab Invest, 2006. **86**(5): p. 425-44.
29. Song, H., E. Yao, C. Lin, R. Gacayan, M. H. Chen, and P. T. Chuang, *Functional characterization of pulmonary neuroendocrine cells in lung development, injury, and tumorigenesis*. Proc Natl Acad Sci U S A, 2012. **109**(43): p. 17531-6.
30. Reynolds, S. D. and A. M. Malkinson, *Clara cell: progenitor for the bronchiolar epithelium*. Int J Biochem Cell Biol, 2010. **42**(1): p. 1-4.
31. Irwin, R. S., N. Augustyn, C. T. French, J. Rice, V. Tedeschi, S. J. Welch, and T. Editorial Leadership, *Spread the word about the journal in 2013: from citation manipulation to invalidation of patient-reported outcomes measures to renaming the Clara cell to new journal features*. Chest, 2013. **143**(1): p. 1-4.
32. Winkelmann, A. and T. Noack, *The Clara cell: a "Third Reich eponym"?* Eur Respir J, 2010. **36**(4): p. 722-7.
33. Jobe, A. H. and M. Ikegami, *Biology of surfactant*. Clin Perinatol, 2001. **28**(3): p. 655-69, vii-viii.
34. Fehrenbach, H., *Alveolar epithelial type II cell: defender of the alveolus revisited*. Respir Res, 2001. **2**(1): p. 33-46.
35. Lyons, C. R. and M. F. Lipscomb, *Alveolar macrophages in pulmonary immune responses. I. Role in the initiation of primary immune responses and in the selective recruitment of T lymphocytes to the lung*. J Immunol, 1983. **130**(3): p. 1113-9.
36. Fels, A. O. and Z. A. Cohn, *The alveolar macrophage*. J Appl Physiol, 1986. **60**(2): p. 353-69.
37. Reynolds, H. Y., *Lung inflammation and fibrosis: an alveolar macrophage-centered perspective from the 1970s to 1980s*. Am J Respir Crit Care Med, 2005. **171**(2): p. 98-102.
38. Cardoso, W. V., *Lung morphogenesis, role of growth factors and transcription factors*, in *The lung : development, aging, and environment*, Harding, R., P. K.E., and C. G. Plopper, Editors. 2003, Academic Press: San Diego, CA. p.3-11.
39. Maeda, Y., V. Dave, and J. A. Whitsett, *Transcriptional control of lung morphogenesis*. Physiol Rev, 2007. **87**(1): p. 219-44.
40. Burri, P. H., *Structural aspects of postnatal lung development - alveolar formation and growth*. Biol Neonate, 2006. **89**(4): p. 313-22.
41. Zeltner, T. B. and P. H. Burri, *The postnatal development and growth of the human lung. II. Morphology*. Respir Physiol, 1987. **67**(3): p. 269-82.

42. Narayanan, M., J. Owers-Bradley, C. S. Beardsmore, M. Mada, I. Ball, R. Garipov, K. S. Panesar, C. E. Kuehni, B. D. Spycher, S. E. Williams, and M. Silverman, *Alveolarization continues during childhood and adolescence: new evidence from helium-3 magnetic resonance*. *Am J Respir Crit Care Med*, 2012. **185**(2): p. 186-91.
43. Kuczmarski, R. J., C. L. Ogden, S. S. Guo, L. M. Grummer-Strawn, K. M. Flegal, Z. Mei, R. Wei, L. R. Curtin, A. F. Roche, and C. L. Johnson, *2000 CDC Growth Charts for the United States: methods and development*. *Vital Health Stat 11*, 2002(246): p. 1-190.
44. Network, S. S. G. o. t. E. K. S. N. N. R., W. A. Carlo, N. N. Finer, M. C. Walsh, W. Rich, M. G. Gantz, A. R. Lupton, B. A. Yoder, R. G. Faix, A. Das, W. K. Poole, K. Schibler, N. S. Newman, N. Ambalavanan, I. D. Frantz, 3rd, A. J. Piazza, P. J. Sanchez, B. H. Morris, N. Laroia, D. L. Phelps, B. B. Poindexter, C. M. Cotten, K. P. Van Meurs, S. Duara, V. Narendran, B. G. Sood, T. M. O'Shea, E. F. Bell, R. A. Ehrenkranz, K. L. Watterberg, and R. D. Higgins, *Target ranges of oxygen saturation in extremely preterm infants*. *N Engl J Med*, 2010. **362**(21): p. 1959-69.
45. Tschudy, M. M., K. M. Arcara, and Johns Hopkins Hospital. Children's Medical and Surgical Center., *The Harriet Lane handbook : a manual for pediatric house officers*. 19th ed. 2012, Philadelphia, PA: Mosby Elsevier. xvi, 1132 p., 10 p. of plates.
46. Martin, R. J. and A. A. Fanaroff, *The Preterm Lung and Airway: Past, Present, and Future*. *Pediatr Neonatol*, 2013.
47. Crump, C., M. A. Winkleby, J. Sundquist, and K. Sundquist, *Risk of asthma in young adults who were born preterm: a Swedish national cohort study*. *Pediatrics*, 2011. **127**(4): p. e913-20.
48. Baraldi, E. and M. Filippone, *Chronic lung disease after premature birth*. *N Engl J Med*, 2007. **357**(19): p. 1946-55.
49. Jaakkola, J. J., P. Ahmed, A. Ieromnimon, P. Goepfert, E. Laiou, R. Quansah, and M. S. Jaakkola, *Preterm delivery and asthma: a systematic review and meta-analysis*. *J Allergy Clin Immunol*, 2006. **118**(4): p. 823-30.
50. Asikainen, T. M. and C. W. White, *Antioxidant defenses in the preterm lung: role for hypoxia-inducible factors in BPD?* *Toxicol Appl Pharmacol*, 2005. **203**(2): p. 177-88.
51. Greenwood, K. K., S. P. Proper, Y. Saini, L. A. Bramble, D. N. Jackson-Humbles, J. G. Wagner, J. R. Harkema, and J. J. LaPres, *Neonatal epithelial hypoxia inducible factor-1alpha expression regulates the response of the lung to experimental asthma*. *Am J Physiol Lung Cell Mol Physiol*, 2012. **302**(5): p. L455-62.
52. Christensen, T. G., *The distribution and function of peroxidases in the respiratory tract*. *Surv Synth Pathol Res*, 1984. **3**(3): p. 201-18.

53. Travis, S. M., B. A. Conway, J. Zabner, J. J. Smith, N. N. Anderson, P. K. Singh, E. P. Greenberg, and M. J. Welsh, *Activity of abundant antimicrobials of the human airway*. *Am J Respir Cell Mol Biol*, 1999. **20**(5): p. 872-9.
54. Zhang, P., W. R. Summer, G. J. Bagby, and S. Nelson, *Innate immunity and pulmonary host defense*. *Immunol Rev*, 2000. **173**: p. 39-51.
55. Wanner, A., M. Salathe, and T. G. O'Riordan, *Mucociliary clearance in the airways*. *Am J Respir Crit Care Med*, 1996. **154**(6 Pt 1): p. 1868-902.
56. Chilvers, M. A. and C. O'Callaghan, *Local mucociliary defence mechanisms*. *Paediatr Respir Rev*, 2000. **1**(1): p. 27-34.
57. Mizgerd, J. P., *Acute lower respiratory tract infection*. *N Engl J Med*, 2008. **358**(7): p. 716-27.
58. Akira, S., S. Uematsu, and O. Takeuchi, *Pathogen recognition and innate immunity*. *Cell*, 2006. **124**(4): p. 783-801.
59. Poltorak, A., X. He, I. Smirnova, M. Y. Liu, C. Van Huffel, X. Du, D. Birdwell, E. Alejos, M. Silva, C. Galanos, M. Freudenberg, P. Ricciardi-Castagnoli, B. Layton, and B. Beutler, *Defective LPS signaling in C3H/HeJ and C57BL/10ScCr mice: mutations in Tlr4 gene*. *Science*, 1998. **282**(5396): p. 2085-8.
60. Kato, A. and R. P. Schleimer, *Beyond inflammation: airway epithelial cells are at the interface of innate and adaptive immunity*. *Curr Opin Immunol*, 2007. **19**(6): p. 711-20.
61. Diamond, G., D. Legarda, and L. K. Ryan, *The innate immune response of the respiratory epithelium*. *Immunol Rev*, 2000. **173**: p. 27-38.
62. Hammad, H. and B. N. Lambrecht, *Dendritic cells and airway epithelial cells at the interface between innate and adaptive immune responses*. *Allergy*, 2011. **66**(5): p. 579-87.
63. Holgate, S. T., *The sentinel role of the airway epithelium in asthma pathogenesis*. *Immunol Rev*, 2011. **242**(1): p. 205-19.
64. Gordon, S. B. and R. C. Read, *Macrophage defences against respiratory tract infections*. *Br Med Bull*, 2002. **61**: p. 45-61.
65. Abbas, A. K., A. H. Lichtman, and S. Pillai, *Cellular and molecular immunology*. 6th ed. 2010, Philadelphia: Saunders/Elsevier. viii, 566 p.
66. Mills, C. D., K. Kincaid, J. M. Alt, M. J. Heilman, and A. M. Hill, *M-1/M-2 macrophages and the Th1/Th2 paradigm*. *J Immunol*, 2000. **164**(12): p. 6166-73.

67. Mosser, D. M. and J. P. Edwards, *Exploring the full spectrum of macrophage activation*. Nat Rev Immunol, 2008. **8**(12): p. 958-69.
68. Dasgupta, P. and A. D. Keegan, *Contribution of alternatively activated macrophages to allergic lung inflammation: a tale of mice and men*. J Innate Immun, 2012. **4**(5-6): p. 478-88.
69. Byers, D. E. and M. J. Holtzman, *Alternatively activated macrophages and airway disease*. Chest, 2011. **140**(3): p. 768-74.
70. Gordon, S. and P. R. Taylor, *Monocyte and macrophage heterogeneity*. Nat Rev Immunol, 2005. **5**(12): p. 953-64.
71. Sica, A. and A. Mantovani, *Macrophage plasticity and polarization: in vivo veritas*. J Clin Invest, 2012. **122**(3): p. 787-95.
72. Sibille, Y. and H. Y. Reynolds, *Macrophages and polymorphonuclear neutrophils in lung defense and injury*. Am Rev Respir Dis, 1990. **141**(2): p. 471-501.
73. Kobayashi, S. D., J. M. Voyich, C. Burlak, and F. R. DeLeo, *Neutrophils in the innate immune response*. Arch Immunol Ther Exp (Warsz), 2005. **53**(6): p. 505-17.
74. Lehrer, R. I., T. Ganz, M. E. Selsted, B. M. Babior, and J. T. Curnutte, *Neutrophils and host defense*. Ann Intern Med, 1988. **109**(2): p. 127-42.
75. Marcinkiewicz, J., *Neutrophil chloramines: missing links between innate and acquired immunity*. Immunol Today, 1997. **18**(12): p. 577-80.
76. Nelson, S., C. M. Mason, J. Kolls, and W. R. Summer, *Pathophysiology of pneumonia*. Clin Chest Med, 1995. **16**(1): p. 1-12.
77. Nelson, S., G. J. Bagby, B. G. Bainton, L. A. Wilson, J. J. Thompson, and W. R. Summer, *Compartmentalization of intraalveolar and systemic lipopolysaccharide-induced tumor necrosis factor and the pulmonary inflammatory response*. J Infect Dis, 1989. **159**(2): p. 189-94.
78. Lekstrom-Himes, J. A. and J. I. Gallin, *Immunodeficiency diseases caused by defects in phagocytes*. N Engl J Med, 2000. **343**(23): p. 1703-14.
79. Rosenzweig, S. D. and S. M. Holland, *Phagocyte immunodeficiencies and their infections*. J Allergy Clin Immunol, 2004. **113**(4): p. 620-6.
80. Lee, J. J., E. A. Jacobsen, M. P. McGarry, R. P. Schleimer, and N. A. Lee, *Eosinophils in health and disease: the LIAR hypothesis*. Clin Exp Allergy, 2010. **40**(4): p. 563-75.

81. Hogan, S. P., H. F. Rosenberg, R. Moqbel, S. Phipps, P. S. Foster, P. Lacy, A. B. Kay, and M. E. Rothenberg, *Eosinophils: biological properties and role in health and disease*. Clin Exp Allergy, 2008. **38**(5): p. 709-50.
82. Jacobsen, E. A., R. A. Helmers, J. J. Lee, and N. A. Lee, *The expanding role(s) of eosinophils in health and disease*. Blood, 2012. **120**(19): p. 3882-90.
83. Abu-Ghazaleh, R. I., S. L. Dunnette, D. A. Loegering, J. L. Checkel, H. Kita, L. L. Thomas, and G. J. Gleich, *Eosinophil granule proteins in peripheral blood granulocytes*. J Leukoc Biol, 1992. **52**(6): p. 611-8.
84. Gleich, G. J., C. R. Adolphson, and K. M. Leiferman, *The biology of the eosinophilic leukocyte*. Annu Rev Med, 1993. **44**: p. 85-101.
85. Malik, A. and J. K. Batra, *Antimicrobial activity of human eosinophil granule proteins: involvement in host defence against pathogens*. Crit Rev Microbiol, 2012. **38**(2): p. 168-81.
86. Rothenberg, M. E. and S. P. Hogan, *The eosinophil*. Annu Rev Immunol, 2006. **24**: p. 147-74.
87. Lacy, P., S. Mahmudi-Azer, B. Bablitz, S. C. Hagen, J. R. Velazquez, S. F. Man, and R. Moqbel, *Rapid mobilization of intracellularly stored RANTES in response to interferon-gamma in human eosinophils*. Blood, 1999. **94**(1): p. 23-32.
88. Guilliams, M., B. N. Lambrecht, and H. Hammad, *Division of labor between lung dendritic cells and macrophages in the defense against pulmonary infections*. Mucosal Immunol, 2013.
89. Merad, M., P. Sathe, J. Helft, J. Miller, and A. Mortha, *The dendritic cell lineage: ontogeny and function of dendritic cells and their subsets in the steady state and the inflamed setting*. Annu Rev Immunol, 2013. **31**: p. 563-604.
90. Hammad, H. and B. N. Lambrecht, *Lung dendritic cell migration*. Adv Immunol, 2007. **93**: p. 265-78.
91. Murphy, K., P. Travers, M. Walport, and C. Janeway, *Janeway's immunobiology*. 8th ed. 2012, New York: Garland Science. xix, 868 p.
92. Moore, B. B., T. A. Moore, and G. B. Toews, *Role of T- and B-lymphocytes in pulmonary host defences*. Eur Respir J, 2001. **18**(5): p. 846-56.
93. Zhu, J. and W. E. Paul, *CD4 T cells: fates, functions, and faults*. Blood, 2008. **112**(5): p. 1557-69.

94. Trinchieri, G. and A. Sher, *Cooperation of Toll-like receptor signals in innate immune defence*. Nat Rev Immunol, 2007. **7**(3): p. 179-90.
95. Hiscott, J., *Convergence of the NF-kappaB and IRF pathways in the regulation of the innate antiviral response*. Cytokine Growth Factor Rev, 2007. **18**(5-6): p. 483-90.
96. Dela Cruz, C. S., M. J. Kang, W. K. Cho, and C. G. Lee, *Transgenic modelling of cytokine polarization in the lung*. Immunology, 2011. **132**(1): p. 9-17.
97. Scanlon, S. T. and A. N. McKenzie, *Type 2 innate lymphoid cells: new players in asthma and allergy*. Curr Opin Immunol, 2012. **24**(6): p. 707-12.
98. Paul, W. E. and J. Zhu, *How are T(H)2-type immune responses initiated and amplified?* Nat Rev Immunol, 2010. **10**(4): p. 225-35.
99. Doerschuk, C. M., J. P. Mizgerd, H. Kubo, L. Qin, and T. Kumasaka, *Adhesion molecules and cellular biomechanical changes in acute lung injury: Giles F. Filley Lecture*. Chest, 1999. **116**(1 Suppl): p. 37S-43S.
100. Mizgerd, J. P., *Molecular mechanisms of neutrophil recruitment elicited by bacteria in the lungs*. Semin Immunol, 2002. **14**(2): p. 123-32.
101. Mukaida, N., *Pathophysiological roles of interleukin-8/CXCL8 in pulmonary diseases*. Am J Physiol Lung Cell Mol Physiol, 2003. **284**(4): p. L566-77.
102. Menten, P., A. Wuyts, and J. Van Damme, *Macrophage inflammatory protein-1*. Cytokine Growth Factor Rev, 2002. **13**(6): p. 455-81.
103. Chuquimia, O. D., D. H. Petursdottir, M. J. Rahman, K. Hartl, M. Singh, and C. Fernandez, *The role of alveolar epithelial cells in initiating and shaping pulmonary immune responses: communication between innate and adaptive immune systems*. PLoS One, 2012. **7**(2): p. e32125.
104. Becker, S., J. Quay, H. S. Koren, and J. S. Haskill, *Constitutive and stimulated MCP-1, GRO alpha, beta, and gamma expression in human airway epithelium and bronchoalveolar macrophages*. Am J Physiol, 1994. **266**(3 Pt 1): p. L278-86.
105. Van Coillie, E., J. Van Damme, and G. Opdenakker, *The MCP/eotaxin subfamily of CC chemokines*. Cytokine Growth Factor Rev, 1999. **10**(1): p. 61-86.
106. Petrek, M., P. Pantelidis, A. M. Southcott, P. Lympny, P. Safranek, C. M. Black, V. Kolek, E. Weigl, and R. M. du Bois, *The source and role of RANTES in interstitial lung disease*. Eur Respir J, 1997. **10**(6): p. 1207-16.
107. Robays, L. J., T. Maes, S. Lebecque, S. A. Lira, W. A. Kuziel, G. G. Brusselle, G. F. Joos, and K. V. Vermaelen, *Chemokine receptor CCR2 but not CCR5 or CCR6 mediates the increase*

- in pulmonary dendritic cells during allergic airway inflammation.* J Immunol, 2007. **178**(8): p. 5305-11.
108. Lee, H. C. and S. F. Ziegler, *Inducible expression of the proallergic cytokine thymic stromal lymphopoietin in airway epithelial cells is controlled by NFkappaB.* Proc Natl Acad Sci U S A, 2007. **104**(3): p. 914-9.
109. Angkasekwinai, P., H. Park, Y. H. Wang, Y. H. Wang, S. H. Chang, D. B. Corry, Y. J. Liu, Z. Zhu, and C. Dong, *Interleukin 25 promotes the initiation of proallergic type 2 responses.* J Exp Med, 2007. **204**(7): p. 1509-17.
110. Nakae, S., H. Morita, T. Ohno, K. Arae, K. Matsumoto, and H. Saito, *Role of interleukin-33 in innate-type immune cells in allergy.* Allergol Int, 2013. **62**(1): p. 13-20.
111. Stampfli, M. R., R. E. Wiley, G. S. Neigh, B. U. Gajewska, X. F. Lei, D. P. Snider, Z. Xing, and M. Jordana, *GM-CSF transgene expression in the airway allows aerosolized ovalbumin to induce allergic sensitization in mice.* J Clin Invest, 1998. **102**(9): p. 1704-14.
112. Xanthou, G., T. Alissafi, M. Semitekolou, D. C. Simoes, E. Economidou, M. Gaga, B. N. Lambrecht, C. M. Lloyd, and V. Panoutsakopoulou, *Osteopontin has a crucial role in allergic airway disease through regulation of dendritic cell subsets.* Nat Med, 2007. **13**(5): p. 570-8.
113. Vermaelen, K. Y., D. Cataldo, K. Tournoy, T. Maes, A. Dhulst, R. Louis, J. M. Foidart, A. Noel, and R. Pauwels, *Matrix metalloproteinase-9-mediated dendritic cell recruitment into the airways is a critical step in a mouse model of asthma.* J Immunol, 2003. **171**(2): p. 1016-22.
114. Romagnani, S., *Regulation of the T cell response.* Clin Exp Allergy, 2006. **36**(11): p. 1357-66.
115. Hammad, H., H. H. Smits, C. Ratajczak, A. Nithiananthan, E. A. Wierenga, G. A. Stewart, A. Jacquet, A. B. Tonnel, and J. Pestel, *Monocyte-derived dendritic cells exposed to Der p 1 allergen enhance the recruitment of Th2 cells: major involvement of the chemokines TARC/CCL17 and MDC/CCL22.* Eur Cytokine Netw, 2003. **14**(4): p. 219-28.
116. Lloyd, C., *Chemokines in allergic lung inflammation.* Immunology, 2002. **105**(2): p. 144-54.
117. Lloyd, C. M. and S. Saglani, *Asthma and allergy: the emerging epithelium.* Nat Med, 2010. **16**(3): p. 273-4.
118. Lambrecht, B. N. and H. Hammad, *The airway epithelium in asthma.* Nat Med, 2012. **18**(5): p. 684-92.

119. Ramakrishna, L., V. C. de Vries, and M. A. Curotto de Lafaille, *Cross-roads in the lung: immune cells and tissue interactions as determinants of allergic asthma*. Immunol Res, 2012. **53**(1-3): p. 213-28.
120. Fritz, J. H., L. Le Bourhis, J. G. Magalhaes, and D. J. Philpott, *Innate immune recognition at the epithelial barrier drives adaptive immunity: APCs take the back seat*. Trends Immunol, 2008. **29**(1): p. 41-9.
121. Mariathasan, S. and D. M. Monack, *Inflammasome adaptors and sensors: intracellular regulators of infection and inflammation*. Nat Rev Immunol, 2007. **7**(1): p. 31-40.
122. Gereke, M., S. Jung, J. Buer, and D. Bruder, *Alveolar type II epithelial cells present antigen to CD4(+) T cells and induce Foxp3(+) regulatory T cells*. Am J Respir Crit Care Med, 2009. **179**(5): p. 344-55.
123. Tosiek, M. J., A. D. Gruber, S. R. Bader, S. Mael, H. G. Hoymann, S. Prettin, T. Tschernig, J. Buer, M. Gereke, and D. Bruder, *CD4+CD25+Foxp3+ regulatory T cells are dispensable for controlling CD8+ T cell-mediated lung inflammation*. J Immunol, 2011. **186**(11): p. 6106-18.
124. Beck, J. M., V. B. Young, and G. B. Huffnagle, *The microbiome of the lung*. Transl Res, 2012. **160**(4): p. 258-66.
125. Charlson, E. S., K. Bittinger, A. R. Haas, A. S. Fitzgerald, I. Frank, A. Yadav, F. D. Bushman, and R. G. Collman, *Topographical continuity of bacterial populations in the healthy human respiratory tract*. Am J Respir Crit Care Med, 2011. **184**(8): p. 957-63.
126. Strachan, D. P., *Hay fever, hygiene, and household size*. BMJ, 1989. **299**(6710): p. 1259-60.
127. Bufford, J. D. and J. E. Gern, *The hygiene hypothesis revisited*. Immunol Allergy Clin North Am, 2005. **25**(2): p. 247-62, v-vi.
128. Jensen, F. B., *Red blood cell pH, the Bohr effect, and other oxygenation-linked phenomena in blood O₂ and CO₂ transport*. Acta Physiol Scand, 2004. **182**(3): p. 215-27.
129. Leach, R. M. and D. F. Treacher, *Oxygen transport-2. Tissue hypoxia*. BMJ, 1998. **317**(7169): p. 1370-3.
130. Birol, G., S. Wang, E. Budzynski, N. D. Wangsa-Wirawan, and R. A. Linsenmeier, *Oxygen distribution and consumption in the macaque retina*. Am J Physiol Heart Circ Physiol, 2007. **293**(3): p. H1696-704.
131. Kiaer, T. and K. D. Kristensen, *Intracompartmental pressure, PO₂, PCO₂ and blood flow in the human skeletal muscle*. Arch Orthop Trauma Surg, 1988. **107**(2): p. 114-6.

132. Duong, T. Q., C. Iadecola, and S. G. Kim, *Effect of hyperoxia, hypercapnia, and hypoxia on cerebral interstitial oxygen tension and cerebral blood flow*. Magn Reson Med, 2001. **45**(1): p. 61-70.
133. Lee, K. A., R. A. Roth, and J. J. LaPres, *Hypoxia, drug therapy and toxicity*. Pharmacol Ther, 2007. **113**(2): p. 229-46.
134. Taylor, C. T., *Mitochondria and cellular oxygen sensing in the HIF pathway*. Biochem J, 2008. **409**(1): p. 19-26.
135. Jain, M. and J. I. Sznajder, *Effects of hypoxia on the alveolar epithelium*. Proc Am Thorac Soc, 2005. **2**(3): p. 202-5.
136. Ward, J. P., *Oxygen sensors in context*. Biochim Biophys Acta, 2008. **1777**(1): p. 1-14.
137. Lopez-Barneo, J., P. Ortega-Saenz, R. Pardal, A. Pascual, and J. I. Piruat, *Carotid body oxygen sensing*. Eur Respir J, 2008. **32**(5): p. 1386-98.
138. Sommer, N., A. Dietrich, R. T. Schermuly, H. A. Ghofrani, T. Gudermann, R. Schulz, W. Seeger, F. Grimminger, and N. Weissmann, *Regulation of hypoxic pulmonary vasoconstriction: basic mechanisms*. Eur Respir J, 2008. **32**(6): p. 1639-51.
139. Kemp, P. J., V. Telezhkin, W. J. Wilkinson, R. Mears, S. B. Hanmer, H. C. Gadeberg, C. T. Muller, D. Riccardi, and S. P. Brazier, *Enzyme-linked oxygen sensing by potassium channels*. Ann N Y Acad Sci, 2009. **1177**: p. 112-8.
140. Michiels, C., *Physiological and pathological responses to hypoxia*. Am J Pathol, 2004. **164**(6): p. 1875-82.
141. Wang, G. L. and G. L. Semenza, *Characterization of hypoxia-inducible factor 1 and regulation of DNA binding activity by hypoxia*. J Biol Chem, 1993. **268**(29): p. 21513-8.
142. Wang, G. L., B. H. Jiang, E. A. Rue, and G. L. Semenza, *Hypoxia-inducible factor 1 is a basic-helix-loop-helix-PAS heterodimer regulated by cellular O₂ tension*. Proc Natl Acad Sci U S A, 1995. **92**(12): p. 5510-4.
143. Tian, H., S. L. McKnight, and D. W. Russell, *Endothelial PAS domain protein 1 (EPAS1), a transcription factor selectively expressed in endothelial cells*. Genes Dev, 1997. **11**(1): p. 72-82.
144. Gu, Y. Z., S. M. Moran, J. B. Hogenesch, L. Wartman, and C. A. Bradfield, *Molecular characterization and chromosomal localization of a third alpha-class hypoxia inducible factor subunit, HIF3alpha*. Gene Expr, 1998. **7**(3): p. 205-13.

145. Scheuermann, T. H., J. Yang, L. Zhang, K. H. Gardner, and R. K. Bruick, *Hypoxia-inducible factors Per/ARNT/Sim domains: structure and function*. Methods Enzymol, 2007. **435**: p. 3-24.
146. Kewley, R. J., M. L. Whitelaw, and A. Chapman-Smith, *The mammalian basic helix-loop-helix/PAS family of transcriptional regulators*. Int J Biochem Cell Biol, 2004. **36**(2): p. 189-204.
147. Lieb, M. E., K. Menzies, M. C. Moschella, R. Ni, and M. B. Taubman, *Mammalian EGLN genes have distinct patterns of mRNA expression and regulation*. Biochem Cell Biol, 2002. **80**(4): p. 421-6.
148. Metzen, E., U. Berchner-Pfannschmidt, P. Stengel, J. H. Marxsen, I. Stolze, M. Klinger, W. Q. Huang, C. Wotzlaw, T. Hellwig-Burgel, W. Jelkmann, H. Acker, and J. Fandrey, *Intracellular localisation of human HIF-1 alpha hydroxylases: implications for oxygen sensing*. J Cell Sci, 2003. **116**(Pt 7): p. 1319-26.
149. Ivan, M., K. Kondo, H. Yang, W. Kim, J. Valiando, M. Ohh, A. Salic, J. M. Asara, W. S. Lane, and W. G. Kaelin, Jr., *HIFalpha targeted for VHL-mediated destruction by proline hydroxylation: implications for O2 sensing*. Science, 2001. **292**(5516): p. 464-8.
150. Bruick, R. K. and S. L. McKnight, *A conserved family of prolyl-4-hydroxylases that modify HIF*. Science, 2001. **294**(5545): p. 1337-40.
151. Epstein, A. C., J. M. Gleadle, L. A. McNeill, K. S. Hewitson, J. O'Rourke, D. R. Mole, M. Mukherji, E. Metzen, M. I. Wilson, A. Dhanda, Y. M. Tian, N. Masson, D. L. Hamilton, P. Jaakkola, R. Barstead, J. Hodgkin, P. H. Maxwell, C. W. Pugh, C. J. Schofield, and P. J. Ratcliffe, *C. elegans EGL-9 and mammalian homologs define a family of dioxygenases that regulate HIF by prolyl hydroxylation*. Cell, 2001. **107**(1): p. 43-54.
152. Maxwell, P. H., M. S. Wiesener, G. W. Chang, S. C. Clifford, E. C. Vaux, M. E. Cockman, C. C. Wykoff, C. W. Pugh, E. R. Maher, and P. J. Ratcliffe, *The tumour suppressor protein VHL targets hypoxia-inducible factors for oxygen-dependent proteolysis*. Nature, 1999. **399**(6733): p. 271-5.
153. Ohh, M., C. W. Park, M. Ivan, M. A. Hoffman, T. Y. Kim, L. E. Huang, N. Pavletich, V. Chau, and W. G. Kaelin, *Ubiquitination of hypoxia-inducible factor requires direct binding to the beta-domain of the von Hippel-Lindau protein*. Nat Cell Biol, 2000. **2**(7): p. 423-7.
154. Jaakkola, P., D. R. Mole, Y. M. Tian, M. I. Wilson, J. Gielbert, S. J. Gaskell, A. von Kriegsheim, H. F. Hebestreit, M. Mukherji, C. J. Schofield, P. H. Maxwell, C. W. Pugh, and P. J. Ratcliffe, *Targeting of HIF-alpha to the von Hippel-Lindau ubiquitylation complex by O2-regulated prolyl hydroxylation*. Science, 2001. **292**(5516): p. 468-72.
155. Greer, S. N., J. L. Metcalf, Y. Wang, and M. Ohh, *The updated biology of hypoxia-inducible factor*. EMBO J, 2012. **31**(11): p. 2448-60.

156. Kaluz, S., M. Kaluzova, and E. J. Stanbridge, *Regulation of gene expression by hypoxia: integration of the HIF-transduced hypoxic signal at the hypoxia-responsive element*. Clin Chim Acta, 2008. **395**(1-2): p. 6-13.
157. Hagen, T., *Oxygen versus Reactive Oxygen in the Regulation of HIF-1alpha: The Balance Tips*. Biochem Res Int, 2012. **2012**: p. 436981.
158. Semenza, G. L., P. H. Roth, H. M. Fang, and G. L. Wang, *Transcriptional regulation of genes encoding glycolytic enzymes by hypoxia-inducible factor 1*. J Biol Chem, 1994. **269**(38): p. 23757-63.
159. Wenger, R. H., D. P. Stiehl, and G. Camenisch, *Integration of oxygen signaling at the consensus HRE*. Sci STKE, 2005. **2005**(306): p. re12.
160. Sowter, H. M., P. J. Ratcliffe, P. Watson, A. H. Greenberg, and A. L. Harris, *HIF-1-dependent regulation of hypoxic induction of the cell death factors BNIP3 and NIX in human tumors*. Cancer Res, 2001. **61**(18): p. 6669-73.
161. Kim, J. Y., H. J. Ahn, J. H. Ryu, K. Suk, and J. H. Park, *BH3-only protein Noxa is a mediator of hypoxic cell death induced by hypoxia-inducible factor 1alpha*. J Exp Med, 2004. **199**(1): p. 113-24.
162. Schmid, T., J. Zhou, and B. Brune, *HIF-1 and p53: communication of transcription factors under hypoxia*. J Cell Mol Med, 2004. **8**(4): p. 423-31.
163. Shimoda, L. A. and G. L. Semenza, *HIF and the lung: role of hypoxia-inducible factors in pulmonary development and disease*. Am J Respir Crit Care Med, 2012. **183**(2): p. 152-6.
164. Patel, S. A. and M. C. Simon, *Biology of hypoxia-inducible factor-2alpha in development and disease*. Cell Death Differ, 2008. **15**(4): p. 628-34.
165. Dunwoodie, S. L., *The role of hypoxia in development of the Mammalian embryo*. Dev Cell, 2009. **17**(6): p. 755-73.
166. Ryan, H. E., J. Lo, and R. S. Johnson, *HIF-1 alpha is required for solid tumor formation and embryonic vascularization*. EMBO J, 1998. **17**(11): p. 3005-15.
167. Iyer, N. V., L. E. Kotch, F. Agani, S. W. Leung, E. Laughner, R. H. Wenger, M. Gassmann, J. D. Gearhart, A. M. Lawler, A. Y. Yu, and G. L. Semenza, *Cellular and developmental control of O₂ homeostasis by hypoxia-inducible factor 1 alpha*. Genes Dev, 1998. **12**(2): p. 149-62.
168. Compernelle, V., K. Brusselmans, D. Franco, A. Moorman, M. Dewerchin, D. Collen, and P. Carmeliet, *Cardia bifida, defective heart development and abnormal neural crest migration in embryos lacking hypoxia-inducible factor-1alpha*. Cardiovasc Res, 2003. **60**(3): p. 569-79.

169. Tian, H., R. E. Hammer, A. M. Matsumoto, D. W. Russell, and S. L. McKnight, *The hypoxia-responsive transcription factor EPAS1 is essential for catecholamine homeostasis and protection against heart failure during embryonic development*. *Genes Dev*, 1998. **12**(21): p. 3320-4.
170. Peng, J., L. Zhang, L. Drysdale, and G. H. Fong, *The transcription factor EPAS-1/hypoxia-inducible factor 2alpha plays an important role in vascular remodeling*. *Proc Natl Acad Sci U S A*, 2000. **97**(15): p. 8386-91.
171. Compernelle, V., K. Brusselmans, T. Acker, P. Hoet, M. Tjwa, H. Beck, S. Plaisance, Y. Dor, E. Keshet, F. Lupu, B. Nemery, M. Dewerchin, P. Van Veldhoven, K. Plate, L. Moons, D. Collen, and P. Carmeliet, *Loss of HIF-2alpha and inhibition of VEGF impair fetal lung maturation, whereas treatment with VEGF prevents fatal respiratory distress in premature mice*. *Nat Med*, 2002. **8**(7): p. 702-10.
172. Scortegagna, M., K. Ding, Y. Oktay, A. Gaur, F. Thurmond, L. J. Yan, B. T. Marck, A. M. Matsumoto, J. M. Shelton, J. A. Richardson, M. J. Bennett, and J. A. Garcia, *Multiple organ pathology, metabolic abnormalities and impaired homeostasis of reactive oxygen species in Epas1-/- mice*. *Nat Genet*, 2003. **35**(4): p. 331-40.
173. Hu, C. J., A. Sataur, L. Wang, H. Chen, and M. C. Simon, *The N-terminal transactivation domain confers target gene specificity of hypoxia-inducible factors HIF-1alpha and HIF-2alpha*. *Mol Biol Cell*, 2007. **18**(11): p. 4528-42.
174. Hu, C. J., L. Y. Wang, L. A. Chodosh, B. Keith, and M. C. Simon, *Differential roles of hypoxia-inducible factor 1alpha (HIF-1alpha) and HIF-2alpha in hypoxic gene regulation*. *Mol Cell Biol*, 2003. **23**(24): p. 9361-74.
175. Wang, V., D. A. Davis, M. Haque, L. E. Huang, and R. Yarchoan, *Differential gene up-regulation by hypoxia-inducible factor-1alpha and hypoxia-inducible factor-2alpha in HEK293T cells*. *Cancer Res*, 2005. **65**(8): p. 3299-306.
176. Gordan, J. D., J. A. Bertout, C. J. Hu, J. A. Diehl, and M. C. Simon, *HIF-2alpha promotes hypoxic cell proliferation by enhancing c-myc transcriptional activity*. *Cancer Cell*, 2007. **11**(4): p. 335-47.
177. Covello, K. L., J. Kehler, H. Yu, J. D. Gordan, A. M. Arsham, C. J. Hu, P. A. Labosky, M. C. Simon, and B. Keith, *HIF-2alpha regulates Oct-4: effects of hypoxia on stem cell function, embryonic development, and tumor growth*. *Genes Dev*, 2006. **20**(5): p. 557-70.
178. Mole, D. R., C. Blancher, R. R. Copley, P. J. Pollard, J. M. Gleadle, J. Ragoussis, and P. J. Ratcliffe, *Genome-wide association of hypoxia-inducible factor (HIF)-1alpha and HIF-2alpha DNA binding with expression profiling of hypoxia-inducible transcripts*. *J Biol Chem*, 2009. **284**(25): p. 16767-75.

179. Makino, Y., R. Cao, K. Svensson, G. Bertilsson, M. Asman, H. Tanaka, Y. Cao, A. Berkenstam, and L. Poellinger, *Inhibitory PAS domain protein is a negative regulator of hypoxia-inducible gene expression*. *Nature*, 2001. **414**(6863): p. 550-4.
180. Makino, Y., A. Kanopka, W. J. Wilson, H. Tanaka, and L. Poellinger, *Inhibitory PAS domain protein (IPAS) is a hypoxia-inducible splicing variant of the hypoxia-inducible factor-3alpha locus*. *J Biol Chem*, 2002. **277**(36): p. 32405-8.
181. Jang, M. S., J. E. Park, J. A. Lee, S. G. Park, P. K. Myung, D. H. Lee, B. C. Park, and S. Cho, *Binding and regulation of hypoxia-inducible factor-1 by the inhibitory PAS proteins*. *Biochem Biophys Res Commun*, 2005. **337**(1): p. 209-15.
182. Hara, S., J. Hamada, C. Kobayashi, Y. Kondo, and N. Imura, *Expression and characterization of hypoxia-inducible factor (HIF)-3alpha in human kidney: suppression of HIF-mediated gene expression by HIF-3alpha*. *Biochem Biophys Res Commun*, 2001. **287**(4): p. 808-13.
183. Li, Q. F., X. R. Wang, Y. W. Yang, and H. Lin, *Hypoxia upregulates hypoxia inducible factor (HIF)-3alpha expression in lung epithelial cells: characterization and comparison with HIF-1alpha*. *Cell Res*, 2006. **16**(6): p. 548-58.
184. Maynard, M. A., A. J. Evans, T. Hosomi, S. Hara, M. A. Jewett, and M. Ohh, *Human HIF-3alpha4 is a dominant-negative regulator of HIF-1 and is down-regulated in renal cell carcinoma*. *FASEB J*, 2005. **19**(11): p. 1396-406.
185. Maynard, M. A., A. J. Evans, W. Shi, W. Y. Kim, F. F. Liu, and M. Ohh, *Dominant-negative HIF-3 alpha 4 suppresses VHL-null renal cell carcinoma progression*. *Cell Cycle*, 2007. **6**(22): p. 2810-6.
186. Augstein, A., D. M. Poitz, R. C. Braun-Dullaeus, R. H. Strasser, and A. Schmeisser, *Cell-specific and hypoxia-dependent regulation of human HIF-3alpha: inhibition of the expression of HIF target genes in vascular cells*. *Cell Mol Life Sci*, 2011. **68**(15): p. 2627-42.
187. Tanaka, T., M. Wiesener, W. Bernhardt, K. U. Eckardt, and C. Warnecke, *The human HIF (hypoxia-inducible factor)-3alpha gene is a HIF-1 target gene and may modulate hypoxic gene induction*. *Biochem J*, 2009. **424**(1): p. 143-51.
188. Stroka, D. M., T. Burkhardt, I. Desbaillets, R. H. Wenger, D. A. Neil, C. Bauer, M. Gassmann, and D. Candinas, *HIF-1 is expressed in normoxic tissue and displays an organ-specific regulation under systemic hypoxia*. *FASEB J*, 2001. **15**(13): p. 2445-53.
189. Wiesener, M. S., H. Turley, W. E. Allen, C. Willam, K. U. Eckardt, K. L. Talks, S. M. Wood, K. C. Gatter, A. L. Harris, C. W. Pugh, P. J. Ratcliffe, and P. H. Maxwell, *Induction of endothelial PAS domain protein-1 by hypoxia: characterization and comparison with hypoxia-inducible factor-1alpha*. *Blood*, 1998. **92**(7): p. 2260-8.

190. Wiesener, M. S., J. S. Jurgensen, C. Rosenberger, C. K. Scholze, J. H. Horstrup, C. Warnecke, S. Mandriota, I. Bechmann, U. A. Frei, C. W. Pugh, P. J. Ratcliffe, S. Bachmann, P. H. Maxwell, and K. U. Eckardt, *Widespread hypoxia-inducible expression of HIF-2alpha in distinct cell populations of different organs*. FASEB J, 2003. **17**(2): p. 271-3.
191. Groenman, F., M. Rutter, I. Caniggia, D. Tibboel, and M. Post, *Hypoxia-inducible factors in the first trimester human lung*. J Histochem Cytochem, 2007. **55**(4): p. 355-63.
192. Wagner, K. F., A. K. Hellberg, S. Balenger, R. Depping, O. J. Dodd, R. A. Johns, and D. Li, *Hypoxia-induced mitogenic factor has antiapoptotic action and is upregulated in the developing lung: coexpression with hypoxia-inducible factor-2alpha*. Am J Respir Cell Mol Biol, 2004. **31**(3): p. 276-82.
193. Bridges, J. P., S. Lin, M. Ikegami, and J. M. Shannon, *Conditional hypoxia inducible factor-1alpha induction in embryonic pulmonary epithelium impairs maturation and augments lymphangiogenesis*. Dev Biol, 2011. **362**(1): p. 24-41.
194. Xu, Y., Y. Wang, V. Besnard, M. Ikegami, S. E. Wert, C. Heffner, S. A. Murray, L. R. Donahue, and J. A. Whitsett, *Transcriptional programs controlling perinatal lung maturation*. PLoS One, 2012. **7**(8): p. e37046.
195. Yu, A. Y., M. G. Frid, L. A. Shimoda, C. M. Wiener, K. Stenmark, and G. L. Semenza, *Temporal, spatial, and oxygen-regulated expression of hypoxia-inducible factor-1 in the lung*. Am J Physiol, 1998. **275**(4 Pt 1): p. L818-26.
196. Roos, D. and J. A. Loos, *Changes in the carbohydrate metabolism of mitogenically stimulated human peripheral lymphocytes. II. Relative importance of glycolysis and oxidative phosphorylation on phytohaemagglutinin stimulation*. Exp Cell Res, 1973. **77**(1): p. 127-35.
197. Eltzschig, H. K. and P. Carmeliet, *Hypoxia and inflammation*. N Engl J Med, 2011. **364**(7): p. 656-65.
198. Nizet, V. and R. S. Johnson, *Interdependence of hypoxic and innate immune responses*. Nat Rev Immunol, 2009. **9**(9): p. 609-17.
199. Cramer, T., Y. Yamanishi, B. E. Clausen, I. Forster, R. Pawlinski, N. Mackman, V. H. Haase, R. Jaenisch, M. Corr, V. Nizet, G. S. Firestein, H. P. Gerber, N. Ferrara, and R. S. Johnson, *HIF-1alpha is essential for myeloid cell-mediated inflammation*. Cell, 2003. **112**(5): p. 645-57.
200. Crotty Alexander, L. E., K. Akong, and V. Nizet, *Analysis Of The Role Of Hypoxia Inducible Factor-1alpha In Eosinophil Function And Allergic Inflammatory Airways Disease*, in American Thoracic Society. 2012: San Francisco, CA, Area E (Hall D, North Building, Lower Level), Moscone Center.

201. Peyssonnaud, C., V. Datta, T. Cramer, A. Doedens, E. A. Theodorakis, R. L. Gallo, N. Hurtado-Ziola, V. Nizet, and R. S. Johnson, *HIF-1alpha expression regulates the bactericidal capacity of phagocytes*. J Clin Invest, 2005. **115**(7): p. 1806-15.
202. Takeda, N., E. L. O'Dea, A. Doedens, J. W. Kim, A. Weidemann, C. Stockmann, M. Asagiri, M. C. Simon, A. Hoffmann, and R. S. Johnson, *Differential activation and antagonistic function of HIF- α isoforms in macrophages are essential for NO homeostasis*. Genes Dev, 2010. **24**(5): p. 491-501.
203. Kuhlicke, J., J. S. Frick, J. C. Morote-Garcia, P. Rosenberger, and H. K. Eltzschig, *Hypoxia inducible factor (HIF)-1 coordinates induction of Toll-like receptors TLR2 and TLR6 during hypoxia*. PLoS One, 2007. **2**(12): p. e1364.
204. Moreira, A. P., K. A. Cavassani, U. B. Ismailoglu, R. Hullinger, M. P. Dunleavy, D. A. Knight, S. L. Kunkel, S. Uematsu, S. Akira, and C. M. Hogaboam, *The protective role of TLR6 in a mouse model of asthma is mediated by IL-23 and IL-17A*. J Clin Invest, 2011. **121**(11): p. 4420-32.
205. Ben-Shoshan, J., S. Maysel-Auslender, A. Mor, G. Keren, and J. George, *Hypoxia controls CD4+CD25+ regulatory T-cell homeostasis via hypoxia-inducible factor-1alpha*. Eur J Immunol, 2008. **38**(9): p. 2412-8.
206. D'Alessio, F. R., K. Tsushima, N. R. Aggarwal, E. E. West, M. H. Willett, M. F. Britos, M. R. Pipeling, R. G. Brower, R. M. Tuder, J. F. McDyer, and L. S. King, *CD4+CD25+Foxp3+ Tregs resolve experimental lung injury in mice and are present in humans with acute lung injury*. J Clin Invest, 2009. **119**(10): p. 2898-913.
207. Makino, Y., H. Nakamura, E. Ikeda, K. Ohnuma, K. Yamauchi, Y. Yabe, L. Poellinger, Y. Okada, C. Morimoto, and H. Tanaka, *Hypoxia-inducible factor regulates survival of antigen receptor-driven T cells*. J Immunol, 2003. **171**(12): p. 6534-40.
208. Biju, M. P., A. K. Neumann, S. J. Bensinger, R. S. Johnson, L. A. Turka, and V. H. Haase, *Vhlh gene deletion induces Hif-1-mediated cell death in thymocytes*. Mol Cell Biol, 2004. **24**(20): p. 9038-47.
209. Zuckerberg, A. L., L. I. Goldberg, and H. M. Lederman, *Effects of hypoxia on interleukin-2 mRNA expression by T lymphocytes*. Crit Care Med, 1994. **22**(2): p. 197-203.
210. Lederer, J. A., M. L. Rodrick, and J. A. Mannick, *The effects of injury on the adaptive immune response*. Shock, 1999. **11**(3): p. 153-9.
211. Ahmad, T., M. Kumar, U. Mabalirajan, B. Pattnaik, S. Aggarwal, R. Singh, S. Singh, M. Mukerji, B. Ghosh, and A. Agrawal, *Hypoxia response in asthma: differential modulation on inflammation and epithelial injury*. Am J Respir Cell Mol Biol, 2012. **47**(1): p. 1-10.

212. Huerta-Yeppez, S., G. J. Baay-Guzman, I. G. Bebenek, R. Hernandez-Pando, M. I. Vega, L. Chi, M. Riedl, D. Diaz-Sanchez, E. Kleerup, D. P. Tashkin, F. J. Gonzalez, B. Bonavida, M. Zeidler, and O. Hankinson, *Hypoxia inducible factor promotes murine allergic airway inflammation and is increased in asthma and rhinitis*. *Allergy*, 2011. **66**(7): p. 909-18.
213. Clerici, C. and C. Planes, *Gene regulation in the adaptive process to hypoxia in lung epithelial cells*. *Am J Physiol Lung Cell Mol Physiol*, 2009. **296**(3): p. L267-74.
214. Saini, Y., K. K. Greenwood, C. Merrill, K. Y. Kim, S. Patial, N. Parameswaran, J. R. Harkema, and J. J. LaPres, *Acute cobalt-induced lung injury and the role of hypoxia-inducible factor 1alpha in modulating inflammation*. *Toxicol Sci*, 2010. **116**(2): p. 673-81.
215. Saini, Y., K. Y. Kim, R. Lewandowski, L. A. Bramble, J. R. Harkema, and J. J. Lapres, *Role of hypoxia-inducible factor 1{alpha} in modulating cobalt-induced lung inflammation*. *Am J Physiol Lung Cell Mol Physiol*, 2010. **298**(2): p. L139-47.
216. Cummins, E. P. and C. T. Taylor, *Hypoxia-responsive transcription factors*. *Pflugers Arch*, 2005. **450**(6): p. 363-71.
217. Kenneth, N. S. and S. Rocha, *Regulation of gene expression by hypoxia*. *Biochem J*, 2008. **414**(1): p. 19-29.
218. Tsai, Y. P. and K. J. Wu, *Epigenetic regulation of hypoxia-responsive gene expression: Focusing on chromatin and DNA modifications*. *Int J Cancer*, 2013.
219. Barnes, P. J., *Biochemical basis of asthma therapy*. *J Biol Chem*, 2011. **286**(38): p. 32899-905.
220. Perkins, N. D., *Integrating cell-signalling pathways with NF-kappaB and IKK function*. *Nat Rev Mol Cell Biol*, 2007. **8**(1): p. 49-62.
221. Hayden, M. S. and S. Ghosh, *Signaling to NF-kappaB*. *Genes Dev*, 2004. **18**(18): p. 2195-224.
222. Vallabhapurapu, S. and M. Karin, *Regulation and function of NF-kappaB transcription factors in the immune system*. *Annu Rev Immunol*, 2009. **27**: p. 693-733.
223. Perkins, N. D. and T. D. Gilmore, *Good cop, bad cop: the different faces of NF-kappaB*. *Cell Death Differ*, 2006. **13**(5): p. 759-72.
224. Laderoute, K. R., *The interaction between HIF-1 and AP-1 transcription factors in response to low oxygen*. *Semin Cell Dev Biol*, 2005. **16**(4-5): p. 502-13.
225. Minet, E., G. Michel, D. Mottet, J. P. Piret, A. Barbieux, M. Raes, and C. Michiels, *c-JUN gene induction and AP-1 activity is regulated by a JNK-dependent pathway in hypoxic HepG2 cells*. *Exp Cell Res*, 2001. **265**(1): p. 114-24.

226. Fantozzi, I., S. Zhang, O. Platoshyn, C. V. Remillard, R. T. Cowling, and J. X. Yuan, *Hypoxia increases AP-1 binding activity by enhancing capacitative Ca²⁺ entry in human pulmonary artery endothelial cells*. *Am J Physiol Lung Cell Mol Physiol*, 2003. **285**(6): p. L1233-45.
227. Premkumar, D. R., G. Adhikary, J. L. Overholt, M. S. Simonson, N. S. Cherniack, and N. R. Prabhakar, *Intracellular pathways linking hypoxia to activation of c-fos and AP-1*. *Adv Exp Med Biol*, 2000. **475**: p. 101-9.
228. Salnikow, K., T. Kluz, M. Costa, D. Piquemal, Z. N. Demidenko, K. Xie, and M. V. Blagosklonny, *The regulation of hypoxic genes by calcium involves c-Jun/AP-1, which cooperates with hypoxia-inducible factor 1 in response to hypoxia*. *Mol Cell Biol*, 2002. **22**(6): p. 1734-41.
229. Suzuki, H., A. Tomida, and T. Tsuruo, *Dephosphorylated hypoxia-inducible factor 1alpha as a mediator of p53-dependent apoptosis during hypoxia*. *Oncogene*, 2001. **20**(41): p. 5779-88.
230. Zheng, X., S. Linke, J. M. Dias, X. Zheng, K. Gradin, T. P. Wallis, B. R. Hamilton, M. Gustafsson, J. L. Ruas, S. Wilkins, R. L. Bilton, K. Brismar, M. L. Whitelaw, T. Pereira, J. J. Gorman, J. Ericson, D. J. Peet, U. Lendahl, and L. Poellinger, *Interaction with factor inhibiting HIF-1 defines an additional mode of cross-coupling between the Notch and hypoxia signaling pathways*. *Proc Natl Acad Sci U S A*, 2008. **105**(9): p. 3368-73.
231. Beitner-Johnson, D. and D. E. Millhorn, *Hypoxia induces phosphorylation of the cyclic AMP response element-binding protein by a novel signaling mechanism*. *J Biol Chem*, 1998. **273**(31): p. 19834-9.
232. Taylor, C. T., G. T. Furuta, K. Synnestvedt, and S. P. Colgan, *Phosphorylation-dependent targeting of cAMP response element binding protein to the ubiquitin/proteasome pathway in hypoxia*. *Proc Natl Acad Sci U S A*, 2000. **97**(22): p. 12091-6.
233. Comerford, K. M., M. O. Leonard, J. Karhausen, R. Carey, S. P. Colgan, and C. T. Taylor, *Small ubiquitin-related modifier-1 modification mediates resolution of CREB-dependent responses to hypoxia*. *Proc Natl Acad Sci U S A*, 2003. **100**(3): p. 986-91.
234. Takiguchi, M., *The C/EBP family of transcription factors in the liver and other organs*. *Int J Exp Pathol*, 1998. **79**(6): p. 369-91.
235. Sanchez-Elsner, T., J. R. Ramirez, F. Sanz-Rodriguez, E. Varela, C. Bernabeu, and L. M. Botella, *A cross-talk between hypoxia and TGF-beta orchestrates erythropoietin gene regulation through SP1 and Smads*. *J Mol Biol*, 2004. **336**(1): p. 9-24.
236. Kaluz, S., M. Kaluzova, and E. J. Stanbridge, *Expression of the hypoxia marker carbonic anhydrase IX is critically dependent on SP1 activity. Identification of a novel type of hypoxia-responsive enhancer*. *Cancer Res*, 2003. **63**(5): p. 917-22.

237. Yan, S. F., J. Lu, Y. S. Zou, W. Kisiel, N. Mackman, M. Leitges, S. Steinberg, D. Pinsky, and D. Stern, *Protein kinase C-beta and oxygen deprivation. A novel Egr-1-dependent pathway for fibrin deposition in hypoxemic vasculature*. J Biol Chem, 2000. **275**(16): p. 11921-8.
238. Lo, L. W., J. J. Cheng, J. J. Chiu, B. S. Wung, Y. C. Liu, and D. L. Wang, *Endothelial exposure to hypoxia induces Egr-1 expression involving PKCalpha-mediated Ras/Raf-1/ERK1/2 pathway*. J Cell Physiol, 2001. **188**(3): p. 304-12.
239. Koong, A. C., E. Y. Chen, and A. J. Giaccia, *Hypoxia causes the activation of nuclear factor kappa B through the phosphorylation of I kappa B alpha on tyrosine residues*. Cancer Res, 1994. **54**(6): p. 1425-30.
240. Batra, S., G. Balamayooran, and M. K. Sahoo, *Nuclear factor-kappaB: a key regulator in health and disease of lungs*. Arch Immunol Ther Exp (Warsz), 2011. **59**(5): p. 335-51.
241. Koong, A. C., E. Y. Chen, N. F. Mivechi, N. C. Denko, P. Stambrook, and A. J. Giaccia, *Hypoxic activation of nuclear factor-kappa B is mediated by a Ras and Raf signaling pathway and does not involve MAP kinase (ERK1 or ERK2)*. Cancer Res, 1994. **54**(20): p. 5273-9.
242. Cummins, E. P., E. Berra, K. M. Comerford, A. Ginouves, K. T. Fitzgerald, F. Seeballuck, C. Godson, J. E. Nielsen, P. Moynagh, J. Pouyssegur, and C. T. Taylor, *Prolyl hydroxylase-1 negatively regulates I kappa B kinase-beta, giving insight into hypoxia-induced NFkappaB activity*. Proc Natl Acad Sci U S A, 2006. **103**(48): p. 18154-9.
243. Cockman, M. E., D. E. Lancaster, I. P. Stolze, K. S. Hewitson, M. A. McDonough, M. L. Coleman, C. H. Coles, X. Yu, R. T. Hay, S. C. Ley, C. W. Pugh, N. J. Oldham, N. Masson, C. J. Schofield, and P. J. Ratcliffe, *Posttranslational hydroxylation of ankyrin repeats in I kappa B proteins by the hypoxia-inducible factor (HIF) asparaginyl hydroxylase, factor inhibiting HIF (FIH)*. Proc Natl Acad Sci U S A, 2006. **103**(40): p. 14767-72.
244. Rius, J., M. Guma, C. Schachtrup, K. Akassoglou, A. S. Zinkernagel, V. Nizet, R. S. Johnson, G. G. Haddad, and M. Karin, *NF-kappaB links innate immunity to the hypoxic response through transcriptional regulation of HIF-1alpha*. Nature, 2008. **453**(7196): p. 807-11.
245. van Uden, P., N. S. Kenneth, and S. Rocha, *Regulation of hypoxia-inducible factor-1alpha by NF-kappaB*. Biochem J, 2008. **412**(3): p. 477-84.
246. Zhang, W., J. M. Petrovic, D. Callaghan, A. Jones, H. Cui, C. Howlett, and D. Stanimirovic, *Evidence that hypoxia-inducible factor-1 (HIF-1) mediates transcriptional activation of interleukin-1beta (IL-1beta) in astrocyte cultures*. J Neuroimmunol, 2006. **174**(1-2): p. 63-73.

247. Kim, H. Y., Y. H. Kim, B. H. Nam, H. J. Kong, H. H. Kim, Y. J. Kim, W. G. An, and J. Cheong, *HIF-1 α expression in response to lipopolysaccharide mediates induction of hepatic inflammatory cytokine TNF α* . *Exp Cell Res*, 2007. **313**(9): p. 1866-76.
248. Eltzschig, H. K., *Adenosine: an old drug newly discovered*. *Anesthesiology*, 2009. **111**(4): p. 904-15.
249. Eltzschig, H. K., J. C. Ibla, G. T. Furuta, M. O. Leonard, K. A. Jacobson, K. Enjyoji, S. C. Robson, and S. P. Colgan, *Coordinated adenosine nucleotide phosphohydrolysis and nucleoside signaling in posthypoxic endothelium: role of ectonucleotidases and adenosine A2B receptors*. *J Exp Med*, 2003. **198**(5): p. 783-96.
250. Eckle, T., A. Grenz, S. Laucher, and H. K. Eltzschig, *A2B adenosine receptor signaling attenuates acute lung injury by enhancing alveolar fluid clearance in mice*. *J Clin Invest*, 2008. **118**(10): p. 3301-15.
251. Eckle, T., M. Faigle, A. Grenz, S. Laucher, L. F. Thompson, and H. K. Eltzschig, *A2B adenosine receptor dampens hypoxia-induced vascular leak*. *Blood*, 2008. **111**(4): p. 2024-35.
252. Cagnina, R. E., S. I. Ramos, M. A. Marshall, G. Wang, C. R. Frazier, and J. Linden, *Adenosine A2B receptors are highly expressed on murine type II alveolar epithelial cells*. *Am J Physiol Lung Cell Mol Physiol*, 2009. **297**(3): p. L467-74.
253. Morote-Garcia, J. C., P. Rosenberger, J. Kuhlicke, and H. K. Eltzschig, *HIF-1-dependent repression of adenosine kinase attenuates hypoxia-induced vascular leak*. *Blood*, 2008. **111**(12): p. 5571-80.
254. Synnestvedt, K., G. T. Furuta, K. M. Comerford, N. Louis, J. Karhausen, H. K. Eltzschig, K. R. Hansen, L. F. Thompson, and S. P. Colgan, *Ecto-5'-nucleotidase (CD73) regulation by hypoxia-inducible factor-1 mediates permeability changes in intestinal epithelia*. *J Clin Invest*, 2002. **110**(7): p. 993-1002.
255. Kong, T., K. A. Westerman, M. Faigle, H. K. Eltzschig, and S. P. Colgan, *HIF-dependent induction of adenosine A2B receptor in hypoxia*. *FASEB J*, 2006. **20**(13): p. 2242-50.
256. Koepfen, M., T. Eckle, and H. K. Eltzschig, *Interplay of hypoxia and A2B adenosine receptors in tissue protection*. *Adv Pharmacol*, 2011. **61**: p. 145-86.
257. Sitkovsky, M. V., *T regulatory cells: hypoxia-adenosinergic suppression and re-direction of the immune response*. *Trends Immunol*, 2009. **30**(3): p. 102-8.
258. Colgan, S. P. and H. K. Eltzschig, *Adenosine and hypoxia-inducible factor signaling in intestinal injury and recovery*. *Annu Rev Physiol*, 2012. **74**: p. 153-75.

259. Whittemore, C. R., *Cobalt*, in *The Encyclopedia of the Chemical Elements*, Hampel, C. A., Editor. 1968, Reinhold Book Corporation: New York. p. 154-163.
260. Survey, U. G., *Rare Earth Elements—Critical Resources for High Technology*, US Geological Survey (USGS).
261. *Cobalt*. 2012, Cobalt Development Institute.
262. Delpeux, S., K. Szostak, E. Frackowiak, S. Bonnamy, and F. Beguin, *High yield of pure multiwalled carbon nanotubes from the catalytic decomposition of acetylene on in-situ formed cobalt nanoparticles*. *J Nanosci Nanotechnol*, 2002. **2**(5): p. 481-4.
263. Coles, B. L., *The use of cobalt in some common anaemias of childhood*. *Arch Dis Child*, 1955. **30**(150): p. 121-6.
264. Coles, B. L. and U. James, *Use of cobalt and iron in the treatment and prevention of anemia of prematurity*. *J Lancet*, 1955. **75**(3): p. 79-82; passim.
265. Schirmacher, U. O., *Case of cobalt poisoning*. *Br Med J*, 1967. **1**(5539): p. 544-5.
266. Alexander, C. S., *Cobalt-beer cardiomyopathy. A clinical and pathologic study of twenty-eight cases*. *Am J Med*, 1972. **53**(4): p. 395-417.
267. Gheysens, B., J. Auwerx, A. Van den Eeckhout, and M. Demedts, *Cobalt-induced bronchial asthma in diamond polishers*. *Chest*, 1985. **88**(5): p. 740-4.
268. Nordberg, G., *Handbook on the toxicology of metals*. 3rd ed. 2007, Amsterdam ; Boston: Academic Press. xlvii, 975 p.
269. Simonsen, L. O., H. Harbak, and P. Bennekou, *Cobalt metabolism and toxicology-A brief update*. *Sci Total Environ*. **432**: p. 210-5.
270. Lison, D., *Human toxicity of cobalt-containing dust and experimental studies on the mechanism of interstitial lung disease (hard metal disease)*. *Crit Rev Toxicol*, 1996. **26**(6): p. 585-616.
271. Cugell, D. W., *The hard metal diseases*. *Clin Chest Med*, 1992. **13**(2): p. 269-79.
272. Coates, E. O., Jr. and J. H. Watson, *Diffuse interstitial lung disease in tungsten carbide workers*. *Ann Intern Med*, 1971. **75**(5): p. 709-16.
273. Bech, A. O., *Hard Metal Disease and Tool Room Grinding*. *J. Soc. Occup. Med.*, 1974. **24**(1): p. 11-16.
274. Scherrer, M. and J. M. Maillard, [*Hard metal pneumopathies*]. *Schweiz Med Wochenschr*, 1982. **112**(6): p. 198-207.

275. Shirakawa, T., Y. Kusaka, N. Fujimura, S. Goto, and K. Morimoto, *The existence of specific antibodies to cobalt in hard metal asthma*. Clin Allergy, 1988. **18**(5): p. 451-60.
276. Rona, G., *Experimental aspects of cobalt cardiomyopathy*. Br Heart J, 1971. **33**: p. Suppl:171-4.
277. Kadiiska, M. B., K. R. Maples, and R. P. Mason, *A comparison of cobalt(II) and iron(II) hydroxyl and superoxide free radical formation*. Arch Biochem Biophys, 1989. **275**(1): p. 98-111.
278. Simonsen, L. O., H. Harbak, and P. Bennekou, *Passive transport pathways for Ca(2+) and Co(2+) in human red blood cells. (57)Co(2+) as a tracer for Ca(2+) influx*. Blood Cells Mol Dis. **47**(4): p. 214-25.
279. Batie, C. J., E. LaHaie, and D. P. Ballou, *Purification and characterization of phthalate oxygenase and phthalate oxygenase reductase from Pseudomonas cepacia*. J Biol Chem, 1987. **262**(4): p. 1510-8.
280. Maxwell, P. and K. Salnikow, *HIF-1: an oxygen and metal responsive transcription factor*. Cancer Biol Ther, 2004. **3**(1): p. 29-35.
281. Salnikow, K., S. P. Donald, R. K. Bruick, A. Zhitkovich, J. M. Phang, and K. S. Kasprzak, *Depletion of intracellular ascorbate by the carcinogenic metals nickel and cobalt results in the induction of hypoxic stress*. J Biol Chem, 2004. **279**(39): p. 40337-44.
282. Fisher, J. W., *A quest for erythropoietin over nine decades*. Annu Rev Pharmacol Toxicol, 1998. **38**: p. 1-20.
283. Vengellur, A., B. G. Woods, H. E. Ryan, R. S. Johnson, and J. J. LaPres, *Gene expression profiling of the hypoxia signaling pathway in hypoxia-inducible factor 1alpha null mouse embryonic fibroblasts*. Gene Expr, 2003. **11**(3-4): p. 181-97.
284. Gleadle, J. M., B. L. Ebert, J. D. Firth, and P. J. Ratcliffe, *Regulation of angiogenic growth factor expression by hypoxia, transition metals, and chelating agents*. Am J Physiol, 1995. **268**(6 Pt 1): p. C1362-8.
285. Vengellur, A. and J. J. LaPres, *The role of hypoxia inducible factor 1alpha in cobalt chloride induced cell death in mouse embryonic fibroblasts*. Toxicol Sci, 2004. **82**(2): p. 638-46.
286. Saini, Y., J. R. Harkema, and J. J. LaPres, *HIF1alpha is essential for normal intrauterine differentiation of alveolar epithelium and surfactant production in the newborn lung of mice*. J Biol Chem, 2008. **283**(48): p. 33650-7.

287. Perl, A. K., S. E. Wert, A. Nagy, C. G. Lobe, and J. A. Whitsett, *Early restriction of peripheral and proximal cell lineages during formation of the lung*. Proc Natl Acad Sci U S A, 2002. **99**(16): p. 10482-7.
288. Whitsett, J. A. and A. K. Perl, *Conditional control of gene expression in the respiratory epithelium: A cautionary note*. Am J Respir Cell Mol Biol, 2006. **34**(5): p. 519-20.
289. Lansdell, T. A., S. O'Reilly, T. Woolliscroft, L. M. Azevedo, D. K. Kahlon, S. Hovde, J. J. McCormick, R. W. Henry, J. A. Cornicelli, and J. J. Tepe, *Attenuation of collagen-induced arthritis by orally available imidazoline-based NF-kappaB inhibitors*. Bioorg Med Chem Lett, 2012. **22**(14): p. 4816-9.
290. Bradford, M. M., *A rapid and sensitive method for the quantitation of microgram quantities of protein utilizing the principle of protein-dye binding*. Anal Biochem, 1976. **72**: p. 248-54.
291. Kahlon, D. K., T. A. Lansdell, J. S. Fisk, C. D. Hupp, T. L. Friebe, S. Hovde, A. D. Jones, R. D. Dyer, R. W. Henry, and J. J. Tepe, *Nuclear factor-kappaB mediated inhibition of cytokine production by imidazoline scaffolds*. J Med Chem, 2009. **52**(5): p. 1302-9.
292. Kallet, R. H. and M. A. Matthay, *Hyperoxic acute lung injury*. Respir Care, 2013. **58**(1): p. 123-41.
293. Cho, H. Y. and S. R. Kleeberger, *Nrf2 protects against airway disorders*. Toxicol Appl Pharmacol, 2010. **244**(1): p. 43-56.
294. Ganter, M. T., J. Roux, B. Miyazawa, M. Howard, J. A. Frank, G. Su, D. Sheppard, S. M. Violette, P. H. Weinreb, G. S. Horan, M. A. Matthay, and J. F. Pittet, *Interleukin-1beta causes acute lung injury via alphavbeta5 and alphavbeta6 integrin-dependent mechanisms*. Circ Res, 2008. **102**(7): p. 804-12.
295. Ogawa, Y., S. Tasaka, W. Yamada, F. Saito, N. Hasegawa, T. Miyasho, and A. Ishizaka, *Role of Toll-like receptor 4 in hyperoxia-induced lung inflammation in mice*. Inflamm Res, 2007. **56**(8): p. 334-8.
296. Diehl, S. and M. Rincon, *The two faces of IL-6 on Th1/Th2 differentiation*. Mol Immunol, 2002. **39**(9): p. 531-6.
297. Karovic, O., I. Tonazzini, N. Rebola, E. Edstrom, C. Lovdahl, B. B. Fredholm, and E. Dare, *Toxic effects of cobalt in primary cultures of mouse astrocytes. Similarities with hypoxia and role of HIF-1alpha*. Biochem Pharmacol, 2007. **73**(5): p. 694-708.